

**Context-dependent regulation of P-body
composition and mRNA turnover in
*Saccharomyces cerevisiae***

Inauguraldissertation
zur
Erlangung der Würde eines Doktors der Philosophie
vorgelegt der
Philosophisch-Naturwissenschaftlichen Fakultät
der Universität Basel

von
Congwei Wang
aus Peking
V.R.China

Basel, 2017

Genehmigt von der Philosophisch-Naturwissenschaftlichen Fakultät
auf Antrag von

Prof. Dr. Anne Spang
Prof. Dr. Ralf Jansen

Basel, den. 24. Mai. 2016

Prof. Dr. Jörg Schibler
Dekan der Philosophisch-Naturwissenschaftlichen Fakultät

Statement of my thesis

This work has been performed in the group of Prof. Dr. Anne Spang at the Biozentrum of University of Basel in Switzerland.

My Ph.D committee members are:

Prof. Dr. Anne Spang
Prof. Dr. Ralf Jansen
Prof. Dr. Mihaela Zavolan

My Ph.D thesis consists of a synopsis and an introduction covering a variety of aspects related to my work and result sections including a submitted manuscript, a scientific publication and additional unpublished data. Finally, I discuss various aspects of my major findings.

The figure numbering within the result sections has been adapted to each subchapter.

| | |
|---|-----------|
| SUMMARY | 6 |
| <hr/> | |
| 1. INTRODUCTION | 7 |
| 1.1 Cellular stress responses in <i>Saccharomyces cerevisiae</i> | 8 |
| 1.2 Post-transcriptional regulation | 9 |
| mRNA processing, localization and translation | 9 |
| mRNA degradation | 10 |
| 1.3 mRNP granules | 12 |
| 1.4 RNA binding proteins | 13 |
| 1.5 Processing bodies (P-bodies) | 15 |
| Components of P-bodies and stress granules | 16 |
| P-body assembly | 18 |
| P-bodies in mRNA turnover | 20 |
| P-bodies under different stress conditions | 22 |
| Subcellular localization of P-bodies | 23 |
| <hr/> | |
| 2. AIMS OF THE STUDY | 25 |
| <hr/> | |
| 3. RESULTS | 27 |
| 3.1 To be, or not to be: Context-dependent deposition and regulation of mRNAs in P-bodies | 28 |
| Summary | 30 |
| Introduction | 31 |
| Results | 33 |
| Discussion | 39 |
| Experimental Procedures | 42 |
| Supplemental Materials | 52 |
| 3.2 The polysome-associated proteins Scp160 and Bfr1 prevent P-body formation under normal growth conditions | 82 |

| | |
|---|------------|
| Supplementary Material | 96 |
| 3.3 Pby1p, a stress-dependent P-body component | 100 |
| Summary | 100 |
| Introduction | 100 |
| Results | 101 |
| Discussion and Outlook | 104 |
| Materials and Methods..... | 106 |

| | |
|---|------------|
| 4. FURTHER DISCUSSION AND OUTLOOK..... | 109 |
|---|------------|

| | |
|---|------------|
| 5. APPENDIX | 117 |
| 5.1 Additional Materials and Methods | 118 |
| Media | 118 |
| Commonly used solutions and buffers | 120 |
| Web Resources and Tools..... | 122 |
| Additional methods | 122 |
| 5.2 Abbreviations | 128 |
| 5.3 References | 130 |
| 5.4 Acknowledgments | 146 |
| 5.5 Curriculum Vitae | 147 |

Summary

Control of gene expression is crucial for cells surviving in a changing environment. In eukaryotes, gene expression can be regulated at different levels, among which post-transcriptional control is of special importance, as it can rapidly modulate the level of gene products. It typically includes mRNA processing, export, translation, decay as well as protein degradation. One type of cytoplasmic granules, which is involved in repression of translation, mRNA decay, mRNA surveillance/quality control and mRNA storage are P-bodies. They consist of mRNP aggregates, constitute the 5' to 3' mRNA decay machinery in yeast cells and can be induced in response to various stress conditions. This thesis contains three studies carried out in *S. cerevisiae* aimed to uncover the mRNA contents of P-bodies, their role in mRNA turnover, as well as to better understand how P-body formation and function are regulated.

Unlike protein components, the mRNA species sequestered by P-bodies are poorly characterized. In the first part of this thesis, an approach to isolate P-body localized transcripts was established. This method was used to identify, subsequently, common and stress-specific mRNA subsets associated with P-bodies. We further examined the fates of these transcripts, and discovered two major types of transcripts. One type was decayed within P-bodies, yet the decay occurred with different kinetics. The second type remained stable for at least 1 h after stress induction. Moreover, we identified transcript-specific *cis*- and *trans*-elements that affect P-body targeting and/or degradation including the 3'UTR and RNA binding protein Puf5p.

In yeast, P-bodies were observed in close proximity to the ER, implying that the ER may play a role in mRNA regulation (Kilchert et al., 2010). In the second study, we identified Scp160p and Bfr1p as polysome-associated ER localized proteins. Loss of either Bfr1p or Scp160p led to numerous Dcp2p positive foci under normal growth condition. Dcp2p is a core constituent of P-bodies, and served as a marker in this study. Therefore, this observation suggests that they might serve as inhibitors preventing P-body formation under unstressed condition. However, general translation was unaffected, indicating that P-body formation and translation attenuation were uncoupled in the absence of Bfr1p and Scp160p.

In the third part of this thesis, we identified Pby1p as a facultative P-body component, Pby1p P-body localization was observed under glucose starvation but not when hyper osmotic shock was applied. Interestingly, loss of Pby1p caused a great reduction of cellular Dcp2p concentration without preventing P-body formation. Furthermore, the decay of particular P-body associated transcripts was slightly delayed in a $\Delta pby1$ strain, suggesting its possible role in regulating mRNA stability and P-body function.

1. INTRODUCTION

1.1 Cellular stress responses in *Saccharomyces cerevisiae*

Cells are often subjected to external fluctuations, such as nutrient deficiency, osmotic shock and temperature change. To adapt to and survive under those environmental changes, cells have evolved a variety of cellular stress responses including alterations at RNA and protein levels. Strikingly, the majority of these alterations occur at the level of mRNA transcription, translation, localization and stability, since it can lead to rapid changes in the amount and distribution of specific protein products. Interestingly, in response to various stresses, gene expression is not always modulated following the same program; many genes are regulated in a stress-specific manner. In yeast, several specialized genomic responses were studied under specific stress conditions (Gasch et al., 2000; Gasch and Werner-Washburne, 2002).

Two typical stress conditions are glucose starvation and hyperosmotic shock. In both wild and lab strains, *S. cerevisiae* preferentially utilizes glucose as primary fermentable carbon source. Therefore, yeast has developed sophisticated regulatory mechanisms to deal with glucose availability. Glucose deprivation, similar to other nutrient starvations, is one of the harshest stresses that yeasts face. During starvation, cells exit the mitotic cycle and enter a quiescent state as long as no replenishment of carbon source (Gray et al., 2004). At the cellular level, as one of the distinct characteristics of the quiescent state, bulk translation in the cell is arrested, leading to a dramatic translation attenuation (Ashe et al., 2000). After glucose withdraw, cells slow down their growth rate to reduce the energy consumption, and switch their major energy production mode from fermentation to aerobic respiration (Otterstedt et al., 2004). Functional studies of the genes required for survival under glucose starvation uncover approximately 300 genes whose deletion reduced cellular viability, among which 128 genes belonged to mitochondrion organization and cellular respiration. Maintaining functional mitochondria seems to be a predominant task for yeast survival during glucose starvation, as there is no other common process shared by the remaining genes (Klosinska et al., 2011).

Unlike glucose depletion, hyperosmotic shock, typically induces milder and transient responses. Previous study has shown exposure of 0.6 M NaCl to yeasts can result in inhibition of uracil uptake, protein synthesis, and stimulation of glucose uptake (Uesono and Toh, 2002). However, those responses are rather transient, and the resumption of those processes represents cellular adaption, which determines hyperosmotic shock as adaptive stress. Such adaptations are typically achieved by regulating the activity of the solute transporter (Tamas et al., 1999), and the expression of genes involved in solute accumulation and the organization of actin and tubulin, (Albertyn et al., 1994; Chowdhury et al., 1992; Slaninova et al., 2000). On one hand, hyperosmotic responses triggered by most ions share several common features, like activation of the high osmolarity glycerol (HOG) pathway (Schuller et al., 1994). On the other hand, some gene classes are regulated specifically in responses to elevation of

particular ions. For instance, 125 genes that are transcriptionally regulated by calcineurin/Crz1p signaling pathway are activated following treatment of yeast cells with Ca^{2+} but not with Na^+ (Yoshimoto et al., 2002), reflecting the ability of cells to fine tune cellular response to particular stresses with specialized programs.

1.2 Post-transcriptional regulation

Regulation in gene expression can take place at different levels: transcriptional, post-transcriptional and post-translational. As the most efficient way to modify the cellular proteome in a quantitative and/or localized manner, post-transcriptional control is of special importance, which normally comprises mRNA processing, export and localization, translation as well as degradation.

mRNA processing, localization and translation

A newly synthesized mRNA transcript must undergo processing, including capping, polyadenylation and splicing, which is indispensable for protecting eukaryotic nascent mRNAs (pre-mRNAs) and ensure proper export and translation. Pre-mRNAs in human cells contain up to 90% non-coding sequence that are subjected to splicing (de Almeida and Carmo-Fonseca, 2008). In contrast, splicing in *S. cerevisiae* is much less prominent, since only 283 of the 6000 genes contain introns (Parenteau et al., 2008). After being processed, mature mRNAs are exported from the nucleus to the cytoplasm where the vast majority of them is localized at specific sites within the cell. mRNA localization is important for the cell to establish a spatial and temporal gene expression pattern. One of the best-known examples in yeast is the *ASH1* mRNA. *ASH1* encodes for a transcriptional repressor of the *HO* endonuclease, which ensures the specificity of mating-type switching. *ASH1* mRNA localizes to the tip of the yeast daughter cell during mitosis (Jansen, 2001; Maxon and Herskowitz, 2001). Following cytokinesis, Ash1p enters the nucleus where it represses the transcription of the *HO* endonuclease gene.

Specific localization of mRNAs is generally dependent on the recognition between *trans*-acting RNA-binding proteins and the endogenous *cis*-acting elements or so called “zip codes”. Typically, *cis*-acting elements can be either primary mRNA sequence or higher-order structural motifs, usually stem loops. These “zip codes” can range in length from five or six to several hundred nucleotides, and function mostly in a combinatorial manner. Binding of *trans*-acting protein to RNA *cis*-element leads to messenger ribonucleoprotein (mRNP) formation, which is crucial for directing and regulating mRNA localization (Martin and Ephrussi, 2009). After the transcript arrive at its destination, the final step in the gene expression pathway is

mediated through translational control, directly modulating the proteome. The transcript contains promoter and multiple regulatory elements, allowing the recruitment of translation machinery and other factors to promote, suppress or adjust the level of translation. Translational control may be coordinated with mRNA cytoplasmic localization. For example, while *ASH1* mRNA is transported to the bud tip, binding of the translational repressor Puf6p prevents its premature translation (Du et al., 2008). Mutations in fragile X mental retardation protein (FMRP) is another example of *trans*-acting protein playing dual roles in mRNA localization and translational repression, which transports several known localized transcripts in mammalian oligodendrocytes (Bassell and Warren, 2008; Martin and Ephrussi, 2009).

mRNA degradation

mRNA degradation is another imperative aspect in post-transcriptional regulation that has been extensively studied both in yeast and metazoan. For a long time, the steady-state level of mRNAs was considered to be determined predominantly by changing the synthesis rates. However, some evidences indicate that mRNA decay is closely controlled and can directly regulate transcript levels (Wang et al., 2002).

Several routes can lead to the elimination of mRNA molecules in the cell. In yeast, two general mRNA decay pathways exist (Figure 1.1). Both are initiated by deadenylation of the poly(A) tail by the deadenylase Ccr4-Not complex (Tucker et al., 2001). After the poly(A) tail has been shortened to 10-15 residues, the transcript becomes a substrate for further decay. In the 5' to 3' degradation decapping-dependent pathway, first the 5' cap is removed by the decapping enzyme, which consists of Dcp1p and Dcp2p (Steiger et al., 2003). Dcp2 is the catalytic subunit, while Dcp1p largely enhances the efficiency of the process (Schwartz and Parker, 2000; She et al., 2008). Following decapping, transcripts are degraded by the Xrn1 exonuclease in 5' to 3' direction (Balagopal et al., 2012). Alternatively, in the 3' to 5' degradation exosome-mediated pathway the transcripts are directly subject to decay from 3' end by the exosome complex, which exhibits both exonuclease and RNA helicase activities (Houseley et al., 2006). In yeast, it has been suggested that the bulk of mRNAs is decayed from 5' to 3' through the decapping-dependent pathway (Parker and Sheth, 2007; Parker and Song, 2004). Nevertheless, the coordination between the two decay pathway, in particular under stress conditions, needs to be determined.

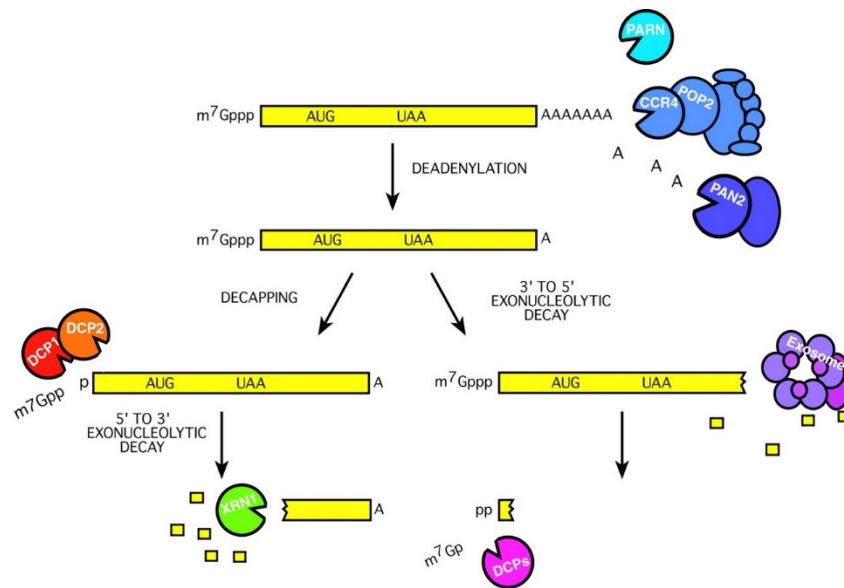


Figure 1.1. General cytoplasmic mRNA decay pathways: Decapping-dependent pathway and Exosome-mediated pathway.

The general degradation pathways are initiated by deadenylation through the Ccr4-Not deadenylase complex. Once the poly(A) length is reduced to 10-15 adenosines, mRNA can be degraded in a 5' to 3' decapping-dependent or 3' to 5' exosome-mediated pathway. Taken from Decker and Parker (2002).

In addition to the general decay machineries, mRNA can also be degraded by several quality control or specialized pathways. Nonsense Mediated Decay (NMD) can destroy mRNAs with aberrant translation termination, such as premature translation-termination codons (PTCs), which are recognized by the Upf-protein family (Upf1, Upf2, and Upf3) and in yeast generally targeted for decapping and 5' to 3' mRNA degradation by exonuclease Xrn1 (Baker and Parker, 2004; Garre et al., 2013). Besides elimination of aberrant transcripts, it has been proposed that NMD is routinely employed by both mammalian and yeast cells to adjust proper gene expression levels (Isken and Maquat, 2008; Neu-Yilik and Kulozik, 2008). Another quality control system is the No-go decay pathway, which functions primarily, when ribosomes are stalled during translational elongation caused by strong RNA stem loops, rare codons, polyLys or polyArg stretches and sites of depurination (Chen et al., 2010; Doma and Parker, 2006; Gandhi et al., 2008). mRNA is then subjected to endonucleolytic cleavage triggered by Dom34p and Hbs1p. The resultant 5' RNA fragment is degraded by exosome mediated pathway and the uncapped 3' fragment becomes a substrate of Xrn1p (Doma and Parker, 2006). Moreover, mRNAs that do not contain translation termination codons can also be removed by non-stop decay, which requires the exosome and the Ski proteins (Frischmeyer et al., 2002; van Hoof et al., 2002).

1.3 mRNP granules

Messenger ribonucleoprotein (mRNP) granules are compartments consisting of translationally inactive mRNPs. Increasing evidences have revealed their key roles in controlling mRNA localization and turnover (Anderson and Kedersha, 2009; Buchan, 2014; Erickson and Lykke-Andersen, 2011).

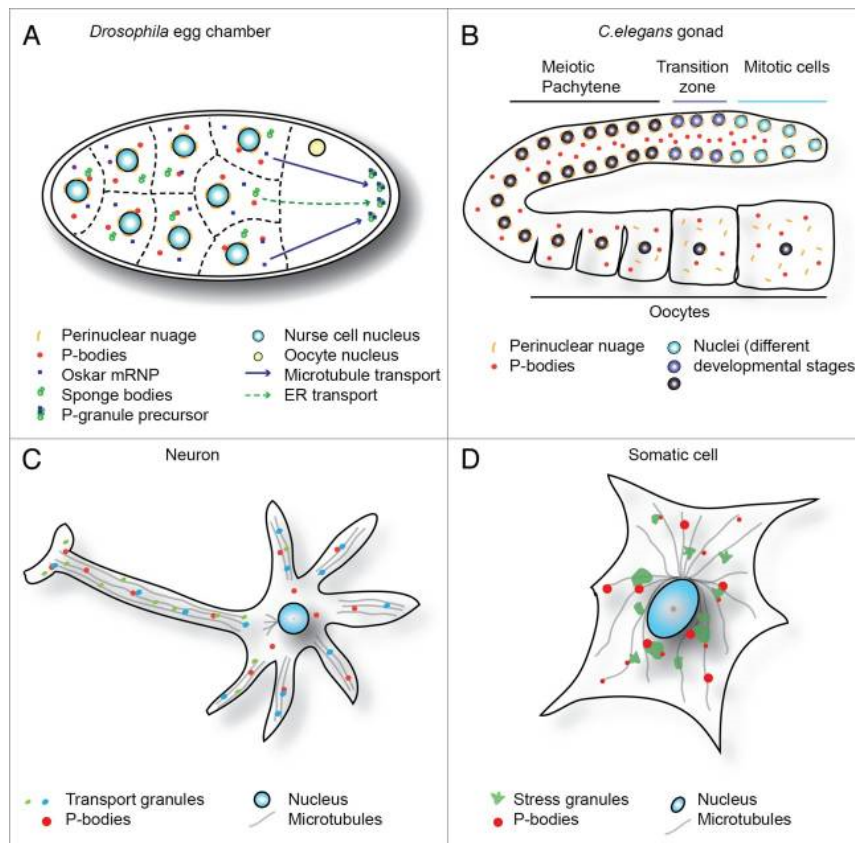


Figure 1.2. Eukaryotic mRNP granules in different species and cell types.

(A) *Drosophila* egg chamber. (B) Gonad of a *C.elegans*. (C) Simplified neuronal cell. (D) Stressed somatic cell. Taken from Buchan (2014).

So far, several cellular mRNP granules have been characterized over the last years. Sponge bodies distributed throughout the nurse cells and oocytes of the *Drosophila* ovary, and contains endoplasmic reticulum (ER)-like cisternae or vesicles (Wilsch-Brauninger et al., 1997). It has been implicated that sponge bodies have been implicated in mRNA traffic and translational repression (Jaglarz et al., 2011; Snee and Macdonald, 2009). In the early *C.elegans* embryo, P granules asymmetrically localize to germline precursors (P-blastomeres) during the first embryonic divisions to store the determinants that specify the germline fate (Brangwynne et al., 2009; Gallo et al., 2010; Updike and Strome, 2010). Neuronal granules transport translationally silenced mRNAs to dendritic synapses that enables synaptic activity to promote their localized translation (Anderson and Kedersha, 2006; Batish et al., 2012). Furthermore, another group of mRNP granules is highly conserved and known to sequester transcripts under diverse stress conditions, which is represented by processing bodies (P-bodies) and stress granules (SGs) (Balagopal and Parker, 2009;

Although some RBPs have been shown to bind mRNA generally, like the cytoplasmic poly(A) binding protein, which associates with poly(A) tails of the mRNAs (Kuhn and Wahle, 2004), the majority of the RBPs recognize only a subset of transcripts by specific *cis*-acting elements within the transcripts. *cis*-acting elements can exist in the form of sequence elements, structural motifs, or a combination of both. Examples containing primary sequence elements include most binding targets of AU-rich elements (ARE), Argonaute1-4 and some Pumillo family proteins (Gruber et al., 2011; Kishore et al., 2011; Li et al., 2014). Instead of interacting with specific base sequences, some RBDs identify their RNA targets primarily by their shape and geometry. For instance, the dsRBD domain, which is present in many protein factors within the RNAi silencing pathway, can distinguish dsRNA by probing 2'-OH groups on the ribose and A-U base pair in the minor groove (Li et al., 2014; Masliah et al., 2013). Some RBPs require a combination of sequence and structural features for mRNA recognition. For example, the coat proteins of three different RNA phages, MS2, Q β and PP7 distinguish both stem-loop structure and bases on the stems of their targets (Lim and Peabody, 2002).

To study the binding targets of RBPs in a large-scale, several *in vitro* approaches have been developed, like systematic evolution of ligands by exponential enrichment (SELEX) and RNAcompete. Both techniques are based on incubating an affinity-tagged RBP with a RNA sequence pool, and followed by microarray or high-throughput sequencing (Campbell et al., 2012; Ellington and Szostak, 1990; Ray et al., 2009). In contrast to the 20 to 80 nucleotide (nt) random sequence used in SELEX, RNAcompete pools were designed to contain less RNA fragments with 30 to 40 nt in length, and predicted to be only weakly structured (Gerstberger et al., 2013). Although *in vitro* SELEX and RNAcompete enable the discovery of a broad range of RNA targets, *in vivo* experiments are essential to elucidate and understand *bona fide* RBP-RNA interactions. *In vivo* immunoprecipitation based techniques using an antibody to the endogenous protein or epitope tag followed by microarray or high-throughput sequencing, like RNA immunoprecipitation-microarray (RIP-chip) and RNA immunoprecipitation-high-throughput sequencing (RIP-Seq) have been established (Cook et al., 2015; Tenenbaum et al., 2000). Although RIP allows identification of target RNA molecules binding to an RBP, the exact binding site on the target mRNA may be difficult to determine as indirectly bound sequences are also present and are not easily separated from the binding sequences. Furthermore, RIP conditions must be calibrated to minimize re-association of RBP with mRNA after cell lysis (Mili and Steitz, 2004). To circumvent these drawbacks, cross-linking was introduced, and is performed prior to immunoprecipitation (CLIP). UV cross-linking is mostly used as it stabilizes the contacts between RBP and RNA (Ule et al., 2003). To date, several UV cross-linking based CLIP protocols have been developed for different applications, for example, photoactivatable ribonucleoside-enhanced crosslinking and immunoprecipitation (PAR-CLIP) and individual-nucleotide resolution UV crosslinking and immunoprecipitation

(iCLIP). PAR-CLIP utilizes modification of RNA with photoactivatable nucleoside analogs instead of natural nucleic acids, while iCLIP enables PCR amplification of truncated cDNAs by employing a random barcode to the DNA adapter, and thereby identifying protein-RNA crosslink sites with precise nucleotide resolution (Figure 1.4) (Ascano et al., 2012; Cheong and Hall, 2006; Kishore et al., 2011; Konig et al., 2010). Apart from UV cross-linking based CLIP, formaldehyde cross-linking followed by quenching with glycine was shown to be practical in yeast, in particular to capture transient interactions when applying different treatments, due to its ease of use and capability of rapid penetrating the yeast cell wall (Tanaka, 2001; Weidner et al., 2014). However, both RIP and CLIP are approaches primarily used for identification of the RNAs bound to a given RBP. To discover novel RBPs for a specific RNA molecule or sequence, proteome-wide approaches based on mass spectrometry have been applied, and a number of RBPs without canonical RNA-binding domains, some of these novel RBPs have been annotated previously for RNA-independent functions were identified using proteomics approaches (Scherrer et al., 2010; Tsvetanova et al., 2010).

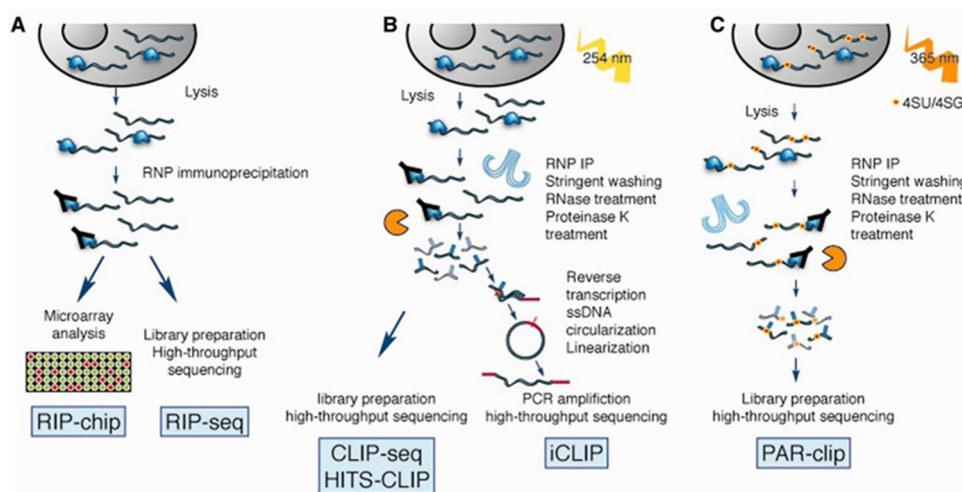


Figure 1.4. *In vivo* methods for determining RBP targets.

(A) RIP-chip and RIP-Seq identify RBP targets by performing immunoprecipitation and analyzing RNA species with microarrays or high-throughput sequencing. (B) CLIP-Seq combine UV cross-linking and immunoprecipitation. iCLIP identifies binding sites more precisely by taking advantage of the fact that the amino acid tag left by proteinase K treatment terminates reverse transcription. (C) PAR-CLIP is another variant of CLIP-Seq using modified nucleoside (4SU or 6SG). Taken from Cook et al. (2015).

1.5 Processing bodies (P-bodies)

As one of the best characterized type of cytoplasmic granules, P-bodies have been reported to participate in translation repression, mRNA decay, surveillance and storage (Arribere et al., 2011; Decker and Parker, 2012; Eulalio et al., 2007a; Sheth and Parker, 2006). P-bodies are composed predominantly of different decay factors and translationally inactive mRNAs. Under normal growth condition, P-bodies exist mostly in monomers, and are responsible for routine

decapping-dependent 5' to 3' degradation. Under certain cellular conditions these monomers can recruit additional P-body components to aggregate into microscopically visible P-bodies, which are believed to be involved in the regulation of various cellular activities. In yeast, the formation of P-body aggregates can be induced by a variety of stress conditions, including nutrient starvation, oxidative stress, changing of temperatures or hyper-/hypo-osmotic shocks (Teixeira and Parker, 2007), and such aggregates are generally proposed to be part of the stress response mechanisms. In neurons, P-bodies are found to localize in close proximity to synapses, and disappear from dendrites when neurons are stimulated, implying a potential role in synaptic plasticity (Zeitelhofer et al., 2008). In mammalian cells, miRNA mediated silencing pathway has been suggested to be in a tight relationship with P-bodies. This finding is supported by the discovery of RNA interference (RNAi) effector complex, RISC, in P-bodies, and reporter mRNAs that are targeted for translational repression by miRNAs are found enriched in P-bodies in a miRNA-dependent manner (Liu et al., 2005a; Liu et al., 2005b).

The composition and assembly of P-bodies has been extensively studied in yeast, and several recent experiments also provide information on localization, function and dynamics of P-bodies (Decker et al., 2007; Eystathioy et al., 2003; Ingelfinger et al., 2002; Kilchert et al., 2010; Mazzoni et al., 2007; van Dijk et al., 2002). However, several aspects, for example, mechanism that delivering mRNAs to P-bodies, the content and fates of P-body sequestered transcripts, and pathways that leading to P-body formation remain to be elucidated.

Components of P-bodies and stress granules

The core protein components of P-bodies are mainly enzymes and regulators that are involved in decapping and the 5' to 3' mRNA decay pathway. As a prerequisite for degradation, the poly(A) tail of the mRNA needs to be removed by Ccr4-Not deadenylation complex, which locates inside P-bodies (Chen and Shyu, 2011, 2013). Following deadenylation, the decapping enzyme complex Dcp2/1 binds to the 5' end of transcripts, while at the 3' end, a heptameric ring complex, composed of Lsm1-7p, surrounds the mRNA, acting as a scaffold to mediate interactions between Dcp2/1p, Xrn1p and Pat1p as well as to promote P-body aggregate formation (Decker et al., 2007; Tharun et al., 2000; Tharun and Parker, 2001). Both *in vivo* and *in vitro* assays suggest Pat1p and Lsm1-7p form a tight complex at the 3' end, which can protect the mRNA from further trimming (Boeck et al., 1998; He and Parker, 2001). Pat1p itself exhibits dual activities in activating decapping and repressing translation, and it was shown to bind Dhh1p, Scd6p and Edc3p (Buchan et al., 2010; Sheth and Parker, 2003). Dhh1p is a DEAD box RNA helicase that unwinds the RNA molecule, while Edc3p and Scd6p are both RNA-binding proteins, responsible for P-body assembly and repression of translation initiation, respectively (Buchan, 2014; Rajyaguru et al., 2012; Walters et al., 2014). After

decapping, the mRNA is degraded by the exonuclease Xrn1p from 5' to 3' end (Buchan et al., 2010) (Table 1.1). Moreover, additional factors involved in nonsense mediated decay, miRNA silencing machinery, viral replication and spreading inhibition might also be found inside P-bodies depending on the species (Jakymiw et al., 2005; Liu et al., 2005b; Lloyd, 2013; Parker and Sheth, 2007; Pillai et al., 2005).

Although the dynamic equilibrium model demonstrates a close link between translation and P-body formation, translation initiation factors and ribosome subunits are generally absent in P-bodies, except eIF4E in mammalian P-bodies (Andrei et al., 2005; Ferraiuolo et al., 2005). In contrast, SGs contain a subset of translation initiation factors eIF4E, eIF4G, eIF4A, eIF4B, eIF3, eIF2, Pab1p and 40S ribosome subunits (Grousl et al., 2009; Kedersha et al., 2005). Additionally, several factors are shared by both granules (Buchan and Parker, 2009), suggesting SGs act as intermediate compartments which connect translation and decay pools.

Table 1. 1: Protein components of P-bodies. Adapted from Eulalio et al. (2007a).

| Name | Function | Organisms |
|---|---|---|
| XRN1, Sc Kem1 | 5'→3' exonuclease | Human, mouse, Sc |
| GW182, Ce AIN-1 | In the miRNA pathway | Human, <i>Dm</i> , <i>Ce</i> |
| DCP2, Ce DCAP-2 | Decapping enzyme | Human, <i>Dm</i> , <i>Ce</i> , <i>Sc</i> |
| DCP1, Ce DCAP-1 | Decapping-enzyme subunit | Human, <i>Dm</i> , <i>Ce</i> , <i>Sc</i> |
| Hedls, Ge-1 | Decapping co-activator | Human, <i>Dm</i> |
| <i>Dm</i> CG5208, Pat1 | Decapping co-activator | <i>Dm</i> , <i>Sc</i> |
| EDC3 (LSm16) | Decapping co-activator | Human, <i>Dm</i> , <i>Sc</i> |
| LSm1-7 | Decapping co-activator complex | Human, <i>Sc</i> |
| RAP55 (LSm14) | Predicted decapping co-activator | Human |
| RCK/p54, <i>Dm</i> Me31B, Ce CGH-1, <i>Sc</i> Dhh1 | Decapping co-activator, translation regulator | Human, <i>Dm</i> , <i>Ce</i> , <i>Sc</i> |
| eIF4E | Translation-initiation factor | Human, rat |
| eIF4E-T | Translational repression | Human |
| SMG7 | NMD | Human |
| SMG5 | NMD | Human (when co-expressed with SMG7) |
| UPF1, Sc Nam7 | NMD | Human (when co-expressed with SMG7), <i>Sc</i> (on depletion of DCP2, DCP1, XRN1, UPF2 or UPF3) |
| UPF2 | NMD | <i>Sc</i> (on depletion of DCP2, DCP1 or XRN1) |
| UPF3 | NMD | <i>Sc</i> (on depletion of DCP2 DCP1 or XRN1) |
| Argonaute proteins | In the siRNA and miRNA pathways | Human, <i>Dm</i> , <i>Ce</i> |
| CCR4-CAF1-NOT complex | Deadenylation | Human, <i>Sc</i> |
| CPEB | Translation regulator | Human |
| FAST | Fas-activated serine/threonine phosphoprotein | Human |
| TTP | ARE-mediated mRNA decay | Human |
| Staufen | Double-stranded RNA-binding protein, mRNA localization | <i>Dm</i> |
| Rbp1 | RNA-binding protein, mediates decay of mitochondrial porin mRNA | <i>Sc</i> (under stress conditions) |
| Rpb4 | Subunit of RNA polymerase II | <i>Sc</i> |
| Sbp1 | Suppressor of decapping defects | <i>Sc</i> |
| Gemin5 | Component of the SMN protein complex involved in assembly of U snRNPs | Human |

| | | |
|--|--|-------|
| Dcs2 | Stress-induced regulatory subunit of the scavenger decapping enzyme Dcs1 | Sc |
| APOBEC3G, APOBEC3F | Deoxycytidine deaminase with antiviral activity | Human |
| <i>Ce</i> , <i>Caenorhabditis elegans</i> ; CPEB , cytoplasmic polyadenylation element-binding protein; <i>Dm</i> , <i>Drosophila melanogaster</i> ; EDC3 , enhancer of decapping-3; eIF4E , eukaryotic translation-initiation factor-4E; eIF4E-T , eIF4E-transporter; miRNA , microRNA; NMD , nonsense-mediated mRNA decay; <i>Sc</i> , <i>Saccharomyces cerevisiae</i> ; siRNA , small interfering RNA; SMN , survival of motor neurons; snRNP , small nuclear ribonucleoprotein; TTP , tristetraprolin. | | |

P-bodies are highly dynamic structures. Fluorescence recovery after photobleaching (FRAP) experiments revealed that many components shuttle in and out of P-bodies (Aizer et al., 2008; Guil et al., 2006; Kedersha et al., 2005). Furthermore, an increasing number of auxiliary and transient P-body components have been discovered recently (Cai and Fletcher, 2013; Hey et al., 2012a; Ling et al., 2014b; Weidner et al., 2014; Zayat et al., 2015). Among these newly identified P-body proteins, some were not shown to be directly involved in mRNA degradation previously (Hey et al., 2012b; Zayat et al., 2015), which might expand current knowledge regarding the role of P-bodies. As an example, DEF6 is a Rho-family guanine nucleotide exchange factor (GEF), localized to the immune synapse, which has been shown to be involved in T cell signaling. Upon cellular stress, DEF6 proteins aggregates into cytoplasmic granules that co-localize with P-bodies. Although the role of DEF6 inside P-bodies is not fully understood, this finding provides a potential link between T cell receptor-mediated signaling and translation regulation in P-bodies (Hey et al., 2012b).

Another essential constituent of P-bodies is mRNA, RNase A treatment disrupts P-body integrity (Teixeira et al., 2005). In addition, P-body formation is inhibited when transcripts are trapped at polysomes by cycloheximide treatment, suggesting translation competent pool is the source of P-body sequestered mRNAs (Teixeira et al., 2005). However, to date, which mRNAs are present in P-bodies, particularly, under specific stress conditions remains to be uncovered, and in yeast only a handful mRNAs have been shown to ever be present in P-bodies (Bregues et al., 2005; Cai and Fletcher, 2013; Lavut and Raveh, 2012; Simpson et al., 2014). Therefore, a global analysis of mRNAs present in P-bodies is necessary to determine the different species as well as to understand the physiology of these transcripts and their products.

P-body assembly

Evidences in budding yeast have suggested three steps in the formation of P-body aggregates. First, two groups consisting of Dcp1p, Dcp2p, Dhh1p, and Edc3p/Scd6p as well as Pat1p, Xrn1p, and Lsm1-7p, assemble independently from each other, and are loaded onto the 5' and 3' ends of the mRNA, respectively. Next, Pat1p serves as a platform to join both complexes together, forming a "closed-loop", which is typically considered as P-body mRNP

or P-body monomer (Chowdhury and Tharun, 2009; Fromm et al., 2012; Pilkington and Parker, 2008). Lacking Pat1p, P-body formation was reduced (Buchan et al., 2008; Kilchert et al., 2010). Finally, P-bodies further aggregates from monomer mRNPs into larger structures, that can be visualized under the microscope upon stress conditions (Figure 1.5).

The aggregation of P-bodies has been demonstrated to be largely dependent on specific protein domains, like the prion-like glutamine and asparagine (Q/N)-rich domain and the self-interacting (Yjef-N) domain (Decker et al., 2007). These domains locate at the carboxyl terminus of Lsm4p and Edc3p, respectively, and in double deletion strain the P-body assembly is dramatically impaired (Decker et al., 2007; Ling et al., 2008; Reijns et al., 2008) (Figure 1.5). To date, approximately 170 to 200 proteins in yeast are predicted to harbor prion-like domains (Alberti et al., 2009; Harrison and Gerstein, 2003). Many of them are involved in mRNA transport, translation, degradation and particularly mRNP aggregation (Decker et al., 2007). For instance, the assembly of SG is also regulated through the Q/N-rich domains in the RNA binding proteins TIA-1 and TIA-R, and their orthologues (Gilks et al., 2004; Kedersha et al., 2000; Kedersha et al., 1999). Interestingly, the aggregation of Q/N-rich domains can be reversed by specific heat shock proteins, like Hsp104, Hsp70 and Hsp40 (Rikhvanov et al., 2007). Therefore, one mechanism of P-body or SG assembly is that owing to accumulation of unfolded proteins following stresses, which may titrate heat shock proteins, driving Q/N-rich domains towards aggregation (Decker and Parker, 2012). Moreover, Dcp2p and Pat1p are shown to comprise phosphorylation sites that modulate P-body formation (Ramachandran et al., 2011; Yoon et al., 2010). Therefore, another possible mechanism is that post-translational

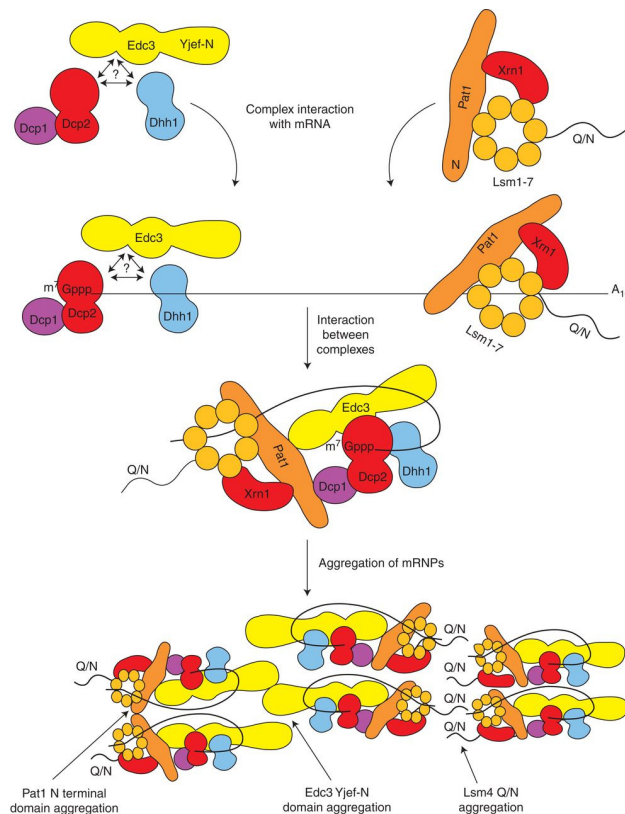


Figure 1.5. Model for P-body assembly in yeast.

Initially, two complexes form independently, and assemble onto mRNA through a series of direct interactions between their components and with the mRNA. Next, Pat1p serves as a platform bringing two complexes together leading to a “closed-loop” structure. These P-body mRNP or monomers can further assemble into larger aggregates via prion-like (Q/N)-rich domain and other self-interacting (Yjef-N) domain located in Lsm4p and Edc3p, respectively. Taken from Decker et al. (2007).

modification might mask or unmask Q/N-rich and Yjef-N domains, preventing or allowing aggregate formation.

P-bodies in mRNA turnover

Although the function of P-bodies has not yet been fully elucidated, their important role in transcript turnover is undisputed. As mentioned above, the dynamic equilibrium model describes the inverse relationship between P-bodies and translation (Coller and Parker, 2005). Under normal growth conditions, transcripts are bound by ribosomes and engaged in translation. On one hand, upon stress, cells typically reduce the bulk translation as an immediate stress response, which is typically accompanied by occurrence of P-bodies (Cougot et al., 2004; Eulalio et al., 2007a; Teixeira et al., 2005). On the other hand, cells restore translation after removal of the stressor, leading to clearance of existing P-bodies through disassembly and/or autophagy (Buchan et al., 2013; Coller and Parker, 2005). The dynamic equilibrium model essentially refers to the balance between these two states, suggesting transcripts may shuttle between P-body and translation competent pools.

The core constituents of P-bodies are involved in translational repression and mRNA decay. Few transcripts were observed to be cleared within P-bodies by time-lapse imaging after 40-100 min stress application (Aizer et al., 2014). Therefore, P-bodies are generally considered as decay compartments. However, recent observations in yeast implied that degradation is likely not the only fate for P-body sequestered transcripts. Upon glucose deprivation, the reporter mRNA MFA2pG was recruited to P-bodies, and released back to translation pool following alleviation of the stress (Bregues et al., 2005). Genome-wide measurements of mRNA abundance, translation, and ribosome occupancy upon glucose starvation have shown that a part of non-translating transcripts can reenter translation after glucose replenishment (Arribere et al., 2011), likely through release from P-bodies. Nevertheless, no direct evidence on non-reporter transcripts was reported demonstrating the storage of P-body-associated mRNAs thus far. Another possibility might be that mRNA degradation or storage are not two independent events, rather being a time-dependent decision as an integrative part of cellular stress responses.

A prevailing view in the field is that, as part of stress responses, specific mRNAs may preferentially accumulate in P-bodies under different stresses, which promotes cell adaption and survival (Decker and Parker, 2012), the different morphologies, half-lives and assembly pathways, can support this idea. However, lacking a global picture of mRNA species nevertheless greatly hinders the study into the functional role of P-bodies in stress induced mRNA regulation as well as mRNA turnover. A major hurdle in universal identification of mRNAs present in P-bodies is that part of the transcripts is likely deadenylated and partially

degraded, and widely-used oligo-dT purification is not applicable in such case. Therefore, alternative methods to isolate P-body-associated mRNAs are necessary.

SGs are another type of mRNP granules that harbor stalled translation initiation complexes, similar to P-bodies, their formation can also be triggered upon a variety of stresses (Buchan et al., 2008; Hoyle et al., 2007; Kedersha et al., 2000; Kedersha et al., 1999). In contrast to P-bodies, the protein components associated with SGs are primarily translation initiation factors, translational activators and ribosomal subunits (Buchan and Parker, 2009). Both the protein and RNA components of SGs are in equilibrium with polysomes, as translational inhibitor cycloheximide prevents SG formation, while puromycin treatment that promote premature termination induces SG assembly (Kedersha et al., 2000). SGs are highly dynamic, their composition appears to be stress-dependent and alter over time (Grousl et al., 2009; Serman et al., 2007; Stoecklin et al., 2004), for example, SGs induced by NaN_3 contained additional translation factors Prt1p and Rpg1p which are not typically seen in SGs under glucose starvation (Buchan et al., 2011).

SGs are frequently observed to dock and fuse with P-bodies, and they share some common protein factors, such as yeast Dhh1p, Scd6p and Xrn1p (Kedersha et al., 2005; Stoecklin and Kedersha, 2013; Wilczynska et al., 2005). Transcripts sequestered by SGs are not subject to immediate degradation in both yeast and mammalian cells (Kedersha et al., 2000; Kedersha et al., 1999; Stoecklin and Kedersha, 2013). These findings suggest an mRNP cycle in which transcripts can be exchanged between P-bodies, SGs and polysomes. In this scenario, SGs are likely to be the intermediated sites that transfer mRNAs from polysome to P-bodies or vice versa (Figure 1.6) (Buchan et al., 2008). Since mRNAs in polysomes and SGs are polyadenylated, whereas deadenylation is a prerequisite for mRNAs targeting for P-bodies (Stoecklin and Kedersha, 2013; Tucker et al., 2001), one hypothesis is that transitions between the three compartments might be controlled by the length of the poly(A) tail. Interestingly, SG assembly upon glucose starvation was shown to depend on the formation of P-bodies, while following NaN_3 , its formation is independent, suggesting this cycle might be complex and vary according to the stress (Buchan et al., 2008; Buchan et al., 2011). Moreover, the signaling pathways required for P-body and SG formation are not identical in yeast (Shah et al., 2013; Yoon et al., 2010), and SGs are not always exist in close proximity with P-bodies, indicating SGs can be independently regulated and may also play other role(s) in mRNA regulation, independent of P-bodies (Erickson and Lykke-Andersen, 2011; Kedersha et al., 2005).

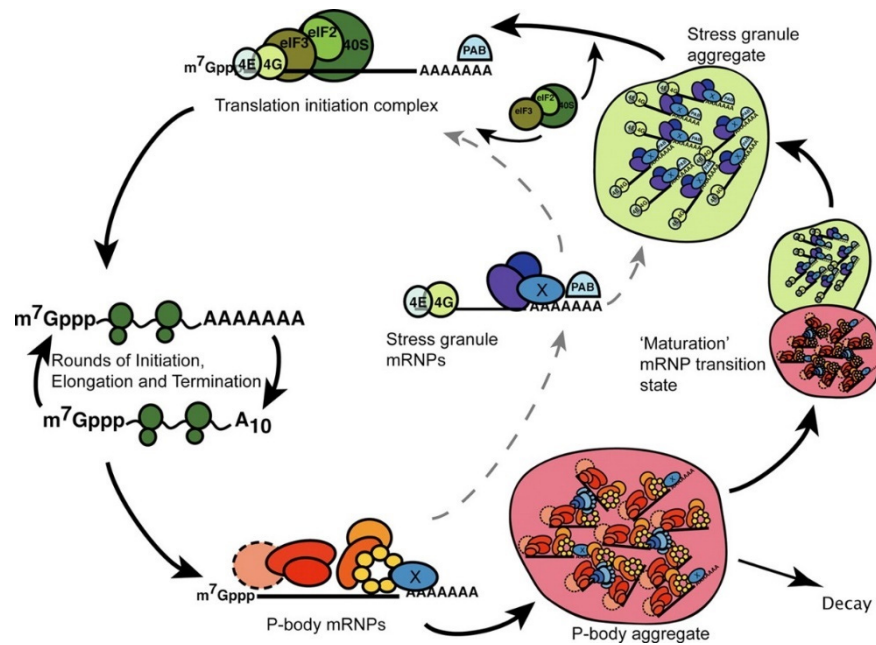


Figure 1.6. Model for cytoplasmic flow of mRNAs through P-body and stress granule.

This model shows transcripts can exist in several states associating with different complexes. Following stress, translation is largely inhibited in the cell, mRNAs dissociate from ribosomes and assemble with P-body or SGs factors. mRNAs sequestered by P-bodies can be targeted for decay, or return to translation via transition to SGs. Taken from Buchan et al. (2008).

P-bodies under different stress conditions

Interestingly, P-body morphologies, half-lives and signaling molecules that affect their formation vary depending on the particular stress (Kilchert et al., 2010). Upon hyper-osmotic stress yeast cells form more than 10 P-bodies per cell, while glucose depletion induces larger-sized P-bodies, but less in terms of numbers (2-5 per cell). Additionally, the half-lives of these P-bodies are also variable, since the ones appearing during glucose starvation persist as long as no carbon source replenished, while under hyper-osmotic stress, the existence of P-bodies is rather transient (20-40 min) (Kilchert et al., 2010; Romero-Santacreu et al., 2009).

Since hyper-osmotic stresses belong to adaptive stress, cells can then initialize numerous mechanisms to protect and adapt to the current condition. Depending the hyper-osmolarity, after certain period, cells resume the majority of gene expression and proliferation following adaptation (Burg et al., 2007), which likely leads to the disappearance of P-bodies. In contrast, following glucose starvation, cells have no other routes to circumvent the condition apart from re-addition of glucose, therefore the half-life of P-bodies is dramatically expanded (Figure 1.7).

The cAMP-dependent protein kinase (PKA) has been demonstrated to be a key regulator of the assembly of yeast P-bodies in several tested conditions, which can repress the formation of the P-body aggregates by directly phosphorylating Pat1p (Ramachandran et al., 2011; Shah et al., 2013). In secretory mutants, numerous P-bodies were induced upon shifting to non-permissive temperature, which mimicked the P-bodies observed by Ca^{2+} (Kilchert et al., 2010). Interestingly, these P-bodies required the presence of calcium binding protein calmodulin, P-body components Scd6p, but not upon glucose starvation and other osmotic stress, like Na^+ (Kilchert et al., 2010), which indicates there are common and stress-specific pathways in triggering P-body assembly.

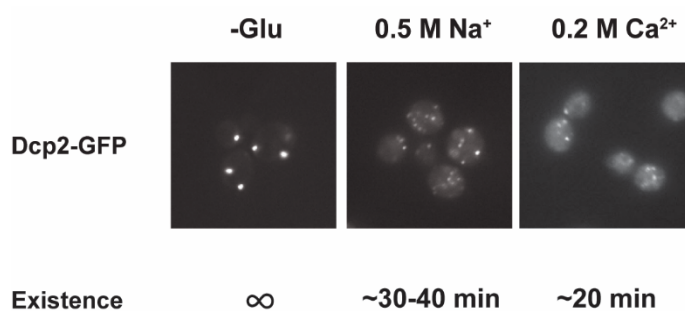


Figure 1.7. Morphology and half-lives of P-bodies vary under different stresses.

In comparison with P-bodies formed upon glucose depletion, Na^+ or Ca^{2+} hyper-osmotic shock induces numerous, smaller and much short-lived P-bodies. Adapted from Kilchert et al. (2010).

Subcellular localization of P-bodies

Many mRNPs are localized to specific cellular locations. In fibroblasts, β -actin mRNA was found in lamellipodia, and its translation is required for cytoskeletal-mediated motility (Condeelis and Singer, 2005), while in the mRNA encoding the T-box transcription factor VegT localizes to the vegetal pole and induces endodermal and mesodermal cell fates in the *Xenopus* embryo (King et al., 2005). The subcellular localization of P-bodies seems to be more complex. Observations in mammalian cells and *Arabidopsis* showed that P-bodies are motile structures and associate with cytoskeleton (Aizer et al., 2008; Kedersha et al., 2005; Loschi et al., 2009; Steffens et al., 2014). Although, alpha-tubulin co-localizes with P-bodies upon microtubule destabilization, and class V myosin Myo2p partially overlaps with the P-body marker Dcp2p in stationary yeast culture (Chang et al., 2008; Sweet et al., 2007), no data demonstrating the direct interaction between P-bodies and cytoskeleton in yeast has been obtained to date. In addition to be associated with the cytoskeleton, P-bodies have also been reported to dock at diverse membrane-bound organelles in different species. In *Drosophila*, P-body like granules (Balbiani body) were observed to be associated with the endoplasmic reticulum (ER) membranes (Voronina et al., 2011). In yeast, immuno-electron microscopy showed P-bodies are also localized in close proximity with the ER, and P-body marker

co-fractionated with ER membranes, further indicating P-bodies are physically associated with the ER (Kilchert et al., 2010). Interestingly, in a recent study, P-bodies were found to interact with two polysome-associated ER localized proteins, suggesting the ER might serve as a platform to mediate the transcripts shuttling between translational machinery and P-bodies (Weidner et al., 2014). Furthermore, P-bodies were discovered to interact with multivesicular bodies (MVBs) and transport vesicles destined for lysosomal degradation in *Drosophila* and mammals (Gibbins et al., 2009; Lee et al., 2009). To date, it is not yet fully understood the rationale behind the association P-bodies with membrane trafficking organelle. One speculation is that these organelles may exchange materials with P-bodies that providing the basis for P-body dynamics.

2. AIMS OF THE STUDY

The overall aim of this thesis was to gain a broader and deeper knowledge in cytoplasmic P-body aggregates, particularly with respect to mRNA content, P-body formation as well as its role in regulating mRNA turnover.

P-bodies consist of non-translating mRNAs and primarily proteins that are involved in the 5' to 3' mRNA decay pathway. To date, much knowledge has been obtained with respect to the protein constituents of P-bodies and their dynamics, function in P-body assembly and general mRNA decay. In contrast, the knowledge about the mRNA content, whether and how mRNA localization with P-bodies is stress specifically regulated remain largely undiscovered. Consequently, lacking this information hinders the study of the functional role of P-bodies in mRNA turnover and stress response. A major obstacle in identifying P-body associated transcripts is that no robust technique has been developed thus far, and the widely-used oligo-dT method is biased, as mRNAs might be deadenylated and degraded inside P-bodies. Therefore, we first established an approach that allowed us to isolate P-body sequestered transcripts, and characterize their transport and fates. In the first part of this thesis we would like to answer the following questions:

1. What is the mRNA composition within P-bodies under different stress conditions?
2. What are the fates of P-body associated mRNAs?
3. How transcripts are targeted to P-bodies?

Recent work demonstrated that P-bodies localize in close proximity to the ER in *S. cerevisiae*. This finding raises the possibility that the ER acts as a platform to link mRNA translation and decay. In the second part of this thesis, we aimed to investigate this potential connection and wanted to answer the following questions:

1. Whether there were proteins at the ER that regulate P-body formation?
2. How P-bodies are localized to the ER and whether there is a protein that tethers P-bodies, keeping them at the ER.

Although the core P-body protein components are conserved and extensively studied across various stress conditions, little is known about stress-specific factors and their function. In the third part of this thesis, we tried to solve the following questions:

1. What is the protein composition of P-bodies under various stress conditions?
2. What is the role of stress-specific associated P-body components?

3. RESULTS

3.1 To be, or not to be: Context-dependent deposition and regulation of mRNAs in P-bodies

The following manuscript is currently submitted.

Statement of contributions: The project was performed in collaboration with Fabian Schmich from the group of Prof. Niko Beerenwinkel in Department of Biosystems Science and Engineering at ETH Zürich. In this study, all experimental work was performed by me, including the creation and assembly of all figures unless otherwise noted. Fabian Schmich conducted processing of the RNA-Seq data and further computational analysis, including Figure 1B, 1C, 1D, S1 and S5A. Julie Weidner was involved in establishing the cCLAP protocol applied in this study. Finally, the manuscript was written by Prof. Anne Spang and by me.

To be, or not to be: Context-dependent deposition and regulation of mRNAs in P-bodies

Congwei Wang¹, Fabian Schmich^{2,3}, Julie Weidner¹, Niko Beerenwinkel^{2,3} and Anne Spang¹

¹Growth & Development, Biozentrum, University of Basel, Klingelbergstrasse 70, CH-4056 Basel, Switzerland

²Department of Biosystems Science and Engineering, ETH Zürich, Mattenstrasse 26, CH-4058 Basel, Switzerland

³SIB, Swiss Institute of Bioinformatics, Mattenstrasse 26, CH-4058 Basel, Switzerland

Address of correspondence:

Anne Spang

Biozentrum

University of Basel

Klingelbergstrasse 70

4056 Basel

Switzerland

Phone: + 41 61 267 2380

FAX: + 41 61 267 0759

email: anne.spang@unibas.ch

Summary

Cells respond to stress by remodeling of their transcriptome through transcription and degradation. Most mRNA decay in *S. cerevisiae* occurs in processing bodies (P-bodies), which have also been proposed to store mRNA. However how mRNAs are selected into P-bodies remains largely unknown. Here, we identified both common and stress-specific mRNA subsets associated with P-bodies under different stress conditions. We found that mRNAs targeted for degradation to P-bodies, decayed with different kinetics. Moreover, the localization of a specific set of mRNAs stabilized in P-bodies under glucose deprivation was obligatory to prevent decay. The 3'UTR is essential but not sufficient to determine the fate and localization of specific mRNAs under stress. Depending on its client mRNA, Puf5p either promoted or inhibited decay. We propose that mRNAs can be sent P-bodies through different pathways and that their fate is determined by intrinsic mRNA properties and *trans*-acting factors.

Introduction

Cells are often subjected to environmental fluctuations, such as nutrient deficiency, osmotic shock and temperature change. Therefore, cells have evolved a variety of cellular mechanisms to adapt and survive under those conditions, which are generally referred to as stress responses (Mager and Ferreira, 1993). Regulation of transport, translation and stability of messenger RNAs (mRNAs) are among the first acute responses contributing to the rapid adjustment of the proteome. In response to stress, protein synthesis is globally attenuated, but a subset of mRNAs, necessary to cope with the stress, is still subject to efficient translation (Ashe et al., 2000). Non-translating mRNAs are mostly deposited into processing bodies (P-bodies) and stress granules (SGs), which are two types of ribonucleoprotein particles (RNP), conserved from yeast to mammals. As the formation of both granules is induced under diverse stress conditions and a number of components appear to be shared, their precise role in stress response is still a matter of debate (Kulkarni et al., 2010; Mitchell et al., 2013).

P-bodies have been reported to participate in repression of translation, mRNA decay, mRNA surveillance and mRNA storage (Decker and Parker, 2012). The composition of P-bodies have been extensively studied in both yeast and metazoan (Kulkarni et al., 2010), yet, Numerous auxiliary and transient components are still being discovered (Hey et al., 2012a; Ling et al., 2014b; Weidner et al., 2014) contributing to the debate of P-body function. The P-body core proteins are highly conserved and contain mostly enzymes and regulators that are involved in translational repression and the decapping-dependent mRNA decay pathway. In budding yeast, the major mRNA degradation pathway is through decapping by Dcp1p/Dcp2p, followed by deadenylation and 5' to 3' degradation by the exonuclease Xrn1p. Besides the general decay machinery, P-bodies accommodate additional factors of specific degradation pathways, e.g. nonsense-mediated decay (NMD) and AU-rich element (ARE)-mediated mRNA decay (Stoecklin and Anderson, 2007). In addition, factors involved in microRNA (miRNA)-mediated regulation such as Argonaute proteins are present in P-bodies at least in *Drosophila* and mammalian cells, where they function to translational silence miRNA (Hillebrand et al., 2007; Liu et al., 2005a). Moreover, P-body assembly has been demonstrated to be largely dependent on proteins containing prion-like glutamine and asparagine (Q/N)-rich domains or other self-interacting domains, such as Lsm4 and Edc3 in yeast (Decker et al., 2007; Reijns et al., 2008).

mRNAs are essential constituents of P-bodies, as RNase A treatment disrupts P-body integrity (Teixeira et al., 2005). To date, however, the RNA inventory in P-bodies under particular stress remains unclear, and in yeast only a handful of mRNAs have been confirmed to localize to P-bodies (Bregues et al., 2005; Cai and Fletcher, 2013; Lavut and Raveh, 2012). Several studies have proposed P-bodies to act not only as decay compartments but also to

store and later release RNAs back into the translation pool, particularly upon stress removal. This notion is primarily supported by an observed dynamic equilibrium of mRNA localization between polysomes and P-bodies (Bregues et al., 2005; Kedersha et al., 2005; Teixeira et al., 2005). A prevailing hypothesis in the field is that specific mRNAs preferentially accumulate in P-bodies under different stresses promoting cell adaptation and survival (Decker and Parker, 2012). In support of this concept, the number, morphology and half-life of P-bodies vary depending on the particular stress. For example, under glucose starvation only a few, large, long-lived P-bodies are observed, whereas Ca^{2+} stress produces numerous, small P-bodies that disappear within 30 to 45 min after the initial induction (Kilchert et al., 2010). Lacking a global picture of mRNA species in P-bodies greatly hinders the study of the functional role of P-bodies in mRNA turnover and stress response.

A major obstacle in the universal identification of mRNAs present in P-bodies is that at least a portion of the transcripts are likely engaged in deadenylation or degradation, and, hence, widely-used oligo-dT purification provides an incomplete and biased picture of the mRNAs present in P-bodies. We overcame this obstacle by employing a modified crosslinking affinity purification protocol (Weidner et al., 2014) to globally isolate P-body associated transcripts. We show that P-bodies contain functionally distinct mRNA species in response to specific stresses. The sequestered transcripts underwent different fates depending on their function, for example: mRNAs involved in overcoming stress were stabilized while others were degraded. Similarly, mRNA decay kinetics differed depending on the mRNA examined. Our observations are consistent with a dual role of P-bodies in mRNA degradation and storage. Under glucose starvation, the RNA-binding protein Puf5p plays a central role as it regulates the decay of a set of mRNAs and is also responsible for the localization and stability of another set. The mRNA fate seems to be partially encoded in its 3' untranslated region (UTR) as it is necessary but not sufficient to determine stability or degradation.

Results

A novel method to isolate RNAs sequestered into P-bodies

To determine the mRNA species sequestered into P-bodies upon different stress conditions, we modified and adapted a method based on *in vivo* chemical crosslinking and affinity purification, which we had previously used to purify P-bodies as well as to identify a regulator and facultative component of P-bodies (Weidner et al., 2014). Hitherto, we showed that most P-bodies in yeast are in very close proximity to the endoplasmic reticulum (ER) and that they fractionate with ER membranes (Kilchert et al., 2010; Weidner et al., 2014). To explore the mRNA content of P-bodies, either Dcp2p or Scd6p, which are part of the 5' and the 3'UTR-associated complex of P-bodies, respectively, were chromosomally tagged with a His₆-biotinylation sequence-His₆ tandem tag (HBH) (Tagwerker et al., 2006; Weidner et al., 2014). After P-body purification, commonly used techniques were employed enabling us to generate RNA libraries for subsequent RNA-Seq (Hafner et al., 2010; Kishore et al., 2011) (Fig. 1A). P-bodies were either induced through glucose starvation or through the addition of CaCl₂ or NaCl. We have previously shown that secretory pathway mutants induce P-bodies through a Ca²⁺/calmodulin-dependent pathway, which is mimicked by the addition of Ca²⁺ to the medium (Kilchert et al., 2010). Notably, this induction pathway is different from the one employed by the cell upon glucose starvation. Yeast cells were exposed to stress for 10 min, cross-linked and, after lysis, P-bodies were purified from the membrane fraction through the HBH-tag present on either Dcp2p or Scd6p. Libraries for RNA-Seq were prepared in two ways: either using PAGE purification with radiolabeled mRNAs or using a column-based purification method.

Principal Component Analysis (PCA) performed on the read count profile for each condition from the aligned RNA-Seq data of the five independent biological replicates generated four clusters, corresponding perfectly to the three stress conditions plus the unstressed control (Fig. S1). Neither the tagged P-body component nor the purification method used for RNA-Seq sample preparation perturbs the clustering pattern, indicating a high degree of reproducibility of our method. Given that we used two types of hyperosmotic stress, it is not surprising that the Ca²⁺ and Na⁺ datasets cluster more closely than the ones derived from glucose starvation conditions. Yet, being able to detect differences between the two osmotic shock conditions further exemplifies the robustness of our approach. Therefore, chemical Cross-Linking coupled to Affinity Purification (cCLAP) is a valid method to determine the RNA content of RNPs.

The nature of P-body sequestered RNAs is stress-dependent

In total, we identified 1544 mRNAs statistically significantly enriched in P-bodies under glucose depletion and Na⁺ and Ca²⁺ stresses, relative to the unstressed condition (Fig. 1B and Table S1). While about 65% of the detected mRNAs were common between stresses, approximately 35% of the RNAs were specific to an individual stress (Fig. 1B). Reads on stress-specific targets were distributed over the entire length without any preferential accumulation or depletion at the 5' or 3' UTRs as exemplified by the selected transcripts (Fig. 1C).

If mRNA deposition in P-bodies was context-dependent, one would expect an enrichment of mRNAs belonging to the same pathways/processes. To test this notion, we employed Gene Ontology (GO) enrichment analysis (biological process) (Fig. 1D). Consistent with the Venn diagram (Fig. 1B), a number of biological processes were shared by all three stress conditions, yet many GO terms were specific to one particular stress, suggesting that mRNA sequestration in P-bodies is, in general, context-dependent. For example, within the glucose specific set, we found a group of processes related to mitochondrial oxidative phosphorylation (herein referred to as mitochondria-related mRNAs). This group is of particular interest, as mitochondria respiration genes are generally up-regulated upon glucose starvation (Wu et al., 2004). Taken together, our data suggest that a subset of mRNAs is sequestered in P-bodies in a stress-dependent manner.

mRNAs localize to P-bodies in a context-dependent manner

Thus far, we have shown that mRNAs can be cross-linked to P-body components in a stress-dependent manner. To demonstrate that these mRNAs indeed localize to P-bodies, we employed fluorescence *in situ* hybridization coupled to immunofluorescence (FISH-IF; Fig. 2A). We used Dcp2p as P-body marker for immunofluorescence. Since P-bodies exhibit a compact, dense structure (Souquere et al., 2009), the commonly employed long probes (around 1000 nt) are not suitable for detection of mRNA in P-bodies. However, using multiple 50-100 nt FISH probes (4-8 per transcript) allowed us to detect specific mRNAs in P-bodies, as the no probe control only exhibited background staining (Fig. 2, S2A). Regardless, we may not be able to detect all mRNA molecules and are likely underestimating the extent of localization of mRNAs within P-bodies. Moreover, transcripts in yeast are often present in less than 10 copies per cell (Zenklusen et al., 2008), which may hinder detection by this method. Finally, most mRNAs are degraded in P-bodies (Sheth and Parker, 2003), therefore any given mRNA may be detected in P-bodies at any given time. Taken these constraints into consideration, we set the threshold at ≥ 1.5 fold enrichment over control mRNAs to determine P-body association.

We selected a set of mRNAs from each stress condition and determined their subcellular localization. Upon glucose depletion, seven mRNAs including both non-mitochondria-related (*BSC1*, *TPI1*, *RLM1*) and mitochondria-related (*ATP11*, *ILM1*, *MRPL38*, *AIM2*) groups, based on the GO pathways, showed significant co-localization with P-bodies (Fig. 2B, 2C) relative to background (Fig. S2B, S2C). To validate that the mRNA localization to P-bodies is stress-specific, we repeated the FISH-IF under osmotic stresses for three mRNAs (Fig. 2D). None were significantly enriched in P-bodies under these stress conditions (Fig. 2E). Similarly, we found mRNAs that were specifically enriched in P-bodies under a unique osmotic condition but not under the other stresses (data not shown). We conclude that at least a subset of mRNAs must be selected for or spared from transport to P-bodies in a context-dependent manner.

mRNAs experience divergent fates inside P-bodies

It has been proposed that mRNAs are not only decayed in P-bodies, but may be stored there and re-enter translation after stress subsides (Bregues et al., 2005). We found mRNAs that were potentially excellent candidates for storage in P-bodies. The mitochondria-related genes were transcriptionally upregulated following glucose starvation (Fig. S3B), while at the same time transcripts were sequestered in P-bodies. To investigate the fate of P-body associated mRNAs further, we employed the 4-TU non-invasive pulse-chase RNA labeling technique followed by qRT-PCR. With this technique we can specifically label RNA before stress application and determine its decay rate (Munchel et al., 2011) (Fig. 3A). To differentiate P-body specific degradation from the second decay pathway mediated by the exosome, we analyzed mRNA half-life in the presence and absence of the P-body 5'-3' exonuclease Xrn1p (Fig. 3B). *ACT1* was used as endogenous reference gene due to its high stability during glucose starvation (Fig. S3A). No significant reduction in mRNA levels was observed for group II mRNAs (*ATP11*, *ILM1*, *MRPL38* and *AIM2*) for up to one-hour of glucose withdrawal, suggesting that those transcripts were stabilized inside P-bodies (Fig. 3B, Group II). Consistently, after a rapid initial increase, the total transcript levels remained constant over the time course (Fig. S3B Group II). Conversely, the transcripts within group I (*BSC1*, *TPI1*, and *RLM1*) underwent Xrn1-dependent decay (Fig. 3B, Group I). Intriguingly, the onset and the kinetic of the decay varied from mRNA to mRNA, indicating that individual intrinsic properties of the mRNAs may determine their half-lives within P-bodies. Likewise, the total mRNA levels were modulated in a similar way (Fig. S3B, Group I), hinting towards coordination between P-body specific decay and transcription. Our data provide strong evidence that the decay kinetics and stability of mRNAs within P-bodies depend on individual properties, and that mRNAs acting in the same process might be co-regulated.

Next we asked whether the fate of an mRNA has an impact on its translation product. Therefore, we assessed the protein level of Tpi1p (Group I) and Atp11p (Group II) upon glucose depletion over time (Fig. 3C). Consistent with the changes in mRNA levels, Tpi1p levels dropped while the levels of Atp11p increased during the glucose starvation time course. Our results reveal distinct and separable roles of P-bodies in regulating mRNA stabilities. On one hand, P-bodies contain transcripts undergoing decay in an individually regulated time-dependent manner. On the other hand, another group of mRNAs, whose protein product contributes to stress response, are protected by P-bodies.

Puf5p contributes to both recruitment and decay of P-body mRNAs

Next, we aimed to record the transport of mRNAs into P-bodies by live-cell imaging using the well-established MS2 and U1A systems (Chung and Takizawa, 2011; Zenklusen et al., 2007). Tagging transcripts with U1A stem loops massively induced P-body formation under non-stress conditions (data not shown). Similarly, appending candidate transcripts with MS2 loops increased the co-localization of mRNA and P-body components to almost 100% (Fig. S2D), which is in marked contrast to the FISH data. This high degree of co-localization can be explained by the recent finding that highly repetitive stem-loops can lead to non-degradable 3' mRNA fragments causing mislocalization of tagged mRNAs (Garcia and Parker, 2015). Considering the strong discrepancy between the FISH and MS2 localization data in terms of extent of P-body localization, and the recently published potential aberrant localization of MS2-tagged mRNAs, it would be extremely difficult to identify determinants of P-body localization and interpret live-cell imaging data.

Due to the abovementioned obstacles, we had to rely again on FISH-IF to identify factors required for the localization and/or fate of mRNAs in P-bodies. We explored several known protein factors, which may contribute to this process with a candidate approach using *BSC1* (Group I) and *ATP11* (Group II) probes (Fig. S4A). We deleted known P-body components or factors associating with P-bodies upon glucose deprivation (Sbp1p, Khd1p, Ngr1p and Whi3p) (Cai and Fletcher, 2013; Mitchell et al., 2013). However, none of the deletion strains showed a reduction of co-localization between the two tested mRNAs and P-bodies (Fig. S4). Therefore, we further expanded our analysis to candidates known to promote mRNA decay or repress mRNA translation, including poly(A)-binding protein II (Pbp2p), two PUF family proteins (Puf3p and Puf5p) and one non-canonical PUF protein (Puf6p) (Chritton and Wickens, 2010; Wickens et al., 2002). Remarkably, the loss of Puf5p efficiently inhibited the recruitment of *ATP11* to P-bodies as the co-localization dropped to background levels (Fig. 4A, 4B). In contrast, *BSC1* localization was unaffected (Fig. 4A, 4B). The observed lack of *ATP11* P-body localization in $\Delta puf5$ cells was specific, since none of the other deletion strains showed a targeting defect (Fig. S4A). To investigate the consequence of the inability of *ATP11*

to be protected in P-bodies in $\Delta puf5$, we determined the *ATP11* mRNA levels. Indeed, *ATP11* mRNA levels declined, when no longer associated with P-bodies (Fig. 4C). These data confirm that *ATP11* mRNA is protected from decay in P-bodies.

Conversely, the localization of *BSC1* mRNA to P-bodies was not altered in cells lacking Puf5p and the mRNA seemed to be stabilized to a certain degree, consistent with Puf5p's role in mRNA decay (Goldstrohm et al., 2006). Recent data suggest that Puf5p binds to both *BSC1* and *TP11* mRNA, but not to any of the candidates of group II (Wilinski et al., 2015). In contrast, *ATP11* has been reported to be a target of Puf3p (Gerber et al., 2004). However, in $\Delta puf3$ neither the localization to P-bodies nor *ATP11* stability was affected, suggesting Puf3p is presumably not essential for P-body related *ATP11* regulation upon glucose deprivation (Fig. S4B). As previously observed (Goldstrohm et al., 2006), we were unable to detect Puf5p in P-bodies (Fig. S4C). Our data suggest that Puf5p directly controls *BSC1* mRNA stability and indirectly *ATP11* mRNA localization.

The 3'UTR is necessary but not sufficient for mRNA targeting to P-bodies

Considering that the 3'UTR of mRNAs contains most regulatory elements, which often have an important role in determining mRNA localization (Andreassi and Riccio, 2009; Vuppalanchi et al., 2010), we next investigated whether 3'UTRs play a role in mRNA targeting to P-bodies. We replaced the endogenous 3'UTR of *BSC1* and *ATP11* with the 3'UTR of *K. lactis TRP1* (*klTRP1*) and examined the localization of the chimera by FISH-IF after glucose starvation (Fig. 5A). Replacement of the 3'UTR abolished recruitment of both mRNAs to P-bodies (Fig. 5B, 5C), suggesting that even though the localization signal must be different between *ATP11* and *BSC1*, the necessary sequences are present in the 3'UTR. Consistent with the mislocalization, *BSC1* and *ATP11* transcripts were stabilized and degraded, respectively (Fig. 5D). The destabilization of the *ATP11* mRNA is also reflected in the reduction of Atp11 protein levels under the same conditions. Thus, the 3'UTR is essential for the fate and P-body localization under glucose starvation for both transcripts.

Since the 3'UTR was essential for both mRNAs, we investigated whether common primary sequence motifs between all mRNAs, which were specifically enriched in P-bodies under a unique stress, exist using the MEME Suite (Bailey et al., 2009). We could not find any significant primary sequence conservations or enrichment, however, of any particular motif. This may not be surprising considering the different requirements of group I and group II mRNAs for P-body localization. Next, we clustered stress-dependent P-body mRNAs based on secondary structures within the 3'UTR using NoFold (Middleton and Kim, 2014). In comparison to non-candidate mRNAs, each stress-specific candidate set contained 10-20 clusters of transcripts that were differentially enriched in certain structure motifs (Table S2). Interestingly, enriched motifs exhibited strong similarities (Z-score > 3) to known miRNA motifs

from RFAM, in line with the observation that at least in mammalian cells and *Drosophila*, P-bodies were shown to contain miRNA silencing complex components (Liu et al., 2005b; Sen and Blau, 2005). Although *S. cerevisiae* is not believed to possess the machinery for miRNA-mediated silencing, it is tempting to speculate that those miRNA motifs likely share a similar mechanism in directing mRNAs to P-bodies. Alternatively, general stem-loop structures may favor P-body localization under stress.

To determine whether 3'UTRs are sufficient to guide mRNAs into P-bodies, we transplanted the 3'UTR of *BSC1* or *ATP11* to a non-P-body associated transcript *SEC59* and a sodium specific P-body-associated transcript *YLR042C* (Fig. S5A). None of the four chimaeras recapitulated the localization of native *BSC1* and *ATP11* transcripts under stress (Fig. S5B, S5C). Thus, although the 3'UTRs are essential, they are not sufficient by themselves to drive mRNA transport into P-bodies. Most likely other elements in the coding sequence and/or 5'UTR act cooperatively.

Discussion

Here we demonstrate that the mRNA content present in P-bodies and the fate of mRNA is stress dependent, varying from decay to stabilization. We furthermore provide evidence that different mRNA classes use different mechanisms to be P-body localized. The localization and fate of these mRNAs are dependent on interactions with RNA binding proteins such as Puf5p and essential information present in the 3'UTR of the mRNA. miRNA-like structures or stem loops in the 3'UTR may facilitate recruitment to P-bodies.

To enable this analysis, we first adapted a method to enrich RNPs based on *in vivo* chemical cross-linking followed by streptavidin affinity purification. This method allows the identification and global analysis of P-body associated mRNAs. We previously used a similar approach to successfully discover a novel exomer-dependent cargo (Ritz et al., 2014) and a novel facultative P-body component (Weidner et al., 2014). We modified the procedure to allow for the reliable enrichment and detection of mRNAs associated with P-bodies under a variety of stress conditions. Moreover, our method works independently, regardless of poly(A) tail length or partial transcript degradation and hence could be applied for the identification of many types of RNA.

We mostly concentrated our further analysis on the hits from the glucose starvation experiments but it is very likely that these findings can be generalized to other stresses. We identified three classes of mRNAs in P-bodies. The first class consists of mRNAs that are generally deposited into P-bodies, independent of the stressor. We did not investigate their fate further in this study, but we assume that most of those transcripts would be prone to decay. The second class contains mRNAs that are stressor-dependent and decayed. It is important to note that the decay rate of mRNAs in this class is very variable and could represent an intrinsic property of the mRNA or a subset of mRNAs. Some transcripts will be decayed almost immediately after arrival in P-bodies, while others are initially excluded from degradation. The kinetics of the decay also appear to vary, indicating that even within P-bodies the decay of client RNAs is highly regulated. Finally, the third class corresponds to mRNAs that are also stress-specific, but stabilized, rather than degraded, in P-bodies. It appears as if this class is enriched for transcripts whose products would be beneficial for survival under stress. This hypothesis is based on the stabilization of transcripts involved in mitochondrial function under glucose starvation, a condition under which mitochondria are up-regulated (Wu et al., 2004). Thus, P-bodies emerge as context-dependent regulator in stress responses. Although the P-bodies have been proposed previously as mRNA decay and storage organelles (Sheth and Parker, 2003), the studies on which this model was based had either been performed on very few selected transcripts or artificial transcripts with extended G-tracts driving P-body localization through imaging or genome-wide analyses, taking all the mRNAs

present in a lysate into account (Arribere et al., 2011; Brengues et al., 2005; Sun et al., 2013). Our approach is different in that we enrich first for P-bodies and then extract the RNA specifically from the P-body fraction. Therefore, our data provide an unprecedented wealth of information on the mRNA content and fate within P-bodies.

Since the fate of an mRNA is stressor-dependent, it is tempting to speculate that the different mRNA classes are recruited to P-bodies through different pathways. In support of this hypothesis, we identified the RNA binding protein Puf5 as a protein regulating both the localization of on transcript as well as the degradation of another (Fig. 6). The latter function is easily explained by the established role of Puf5p as interactor of the Crr4/Not deadenylation complex, which shortens the poly(A)-tail independent of the subsequent route of destruction through P-bodies or exosomes (Balagopal et al., 2012). In fact, *BSC1* mRNA was recently identified as Puf5p target (Wilinski et al., 2015). The role of Puf5p in the localization of *ATP11* to P-bodies is not so straightforwardly explained. In the absence of Puf5p, *ATP11* is no longer P-body localized and is destabilized. Hence, in this case P-bodies protect an mRNA from degradation in a Puf5p-dependent manner. Whether this protection is through direct or indirect binding of Puf5p to *ATP11* mRNA, remains to be determined. However, *ATP11* does not contain any consensus Puf5p-binding site and was not detected in any Puf5p interaction studies (Gerber et al., 2004; Hogan et al., 2015). One possibility is that Puf5p protects *ATP11* from being attacked by the Crr4/Not complex and *ATP11* becomes stabilized. In the absence of Puf5p, this protection would be lost, the poly(A)-tail shortened, and *ATP11* prone for degradation. It is striking, however, that Puf5p possesses this dual role of protection and destruction depending on the mRNA, as well as being involved in the localization of mRNAs to P-bodies.

The 3'UTR of mRNAs appears to contain key information about their fate as the replacement of the 3'UTR in our candidate mRNAs reversed their fates under stress: the destabilized mRNA became stabilized and the stable one was degraded. Although the 3'UTR might be essential in fate determination, it was insufficient as sole determinant for mRNA fate. Our data are consistent with previous studies showing that mRNA stability could be governed by multiple factors such as the length of poly(A) tails, 5'-cap, and most importantly sequence or structural elements that can be recognized by specific RNA-binding proteins (Wiederhold and Passmore, 2010). A structural determinant in stress dependent P-body localized mRNA might be a concentration of hairpins and stem loops in client RNAs. We and others observed that appending mRNAs with loops that recognized by the MS2 coat protein or contain a U1A tag are prone to localize to P-bodies and can even induce P-bodies in the absence of stress dependent on the RNA (Garcia and Parker, 2015) (Fig. S2D and unpublished observation). In mammalian cells, P-bodies also contain the RISC complex, which is a major part of the miRNA machinery (Chan and Slack, 2006). In fact, we found an enrichment of structural elements

similar to miRNA structure in client RNAs deposited into P-bodies dependent on a specific stressor. Thus the secondary structure element may sensitize mRNAs to be brought to P-bodies. Even though *S. cerevisiae* does not contain the miRNA silencing machinery, expression of only three human components Ago2, Dicer and TRBP were sufficient to provide RISC-dependent silencing (Suk et al., 2011). The correlation is intriguing and needs further investigation.

Our findings demonstrate that P-body associated mRNA can follow different fates, namely decay or stabilization. Whether these two functions are performed by the same or different P-bodies remains unclear. We favor the possibility, however, that both functions can be provided by the same P-body. Recent data from *Drosophila* sponge bodies, which might be the equivalent of P-bodies in embryos, suggest that the degradation and decay may happen in the same compartment (Weil et al., 2012). Likewise, there is no evidence thus far for differential protein composition of P-bodies formed under the same stress condition (Kulkarni et al., 2010). Although, it is possible that the transient protein components may vary from one another, we expect the major factors would be discriminative to fulfill opposing functions and mRNA selectivity.

The stabilized mRNAs may return into the translation competent pool. Whether this re-initiation would be through diffusion of the mRNA from the P-body into the cytoplasm or through another organelle, such as stress granules (SG), remains to be established. SGs harbor stalled translation initiation complexes, whose formation can also be triggered upon a variety of stresses. Additionally, at least in mammalian cells, SGs frequently dock and fuse with P-bodies, and they share some common protein factors (Kedersha et al., 2005; Stoecklin and Kedersha, 2013). As mRNAs in SGs are polyadenylated, they are not subject to immediate degradation (Kedersha et al., 1999; Stoecklin and Kedersha, 2013). Based on those evidences, we speculate that the re-engagement of stable transcripts into translation is likely mediated via SGs.

A number of genome-wide studies detailing responses to stress have been performed (Miller et al., 2011; Munchel et al., 2011). Most of the studies deal with global RNA synthesis and decay, but do not provide any insights into the regulated storage of mRNA. We demonstrate here that P-bodies act as storage and decay compartment and that the fate of a P-body associated mRNA depends on its 3'UTR and the interaction with *trans*-acting factors. Moreover, classes of mRNAs are protected from decay in a stress-dependent manner.

Experimental Procedures

Yeast strains and growth conditions

Standard genetic techniques were employed throughout (Sherman, 1991). Unless otherwise noted, all genetic modifications were carried out chromosomally. Chromosomal tagging and deletions were performed as described (Janke et al., 2004; Knop et al., 1999). For C-terminal tagging with 3xHA, the plasmid pYM-3HA (*kitRP1*) was used. The plasmid pFA6a-natNT2 was used for construction of all deletion strains, except for $\Delta puf3$ (pUG73). 3'UTR transplantation experiments were carried out with the *Delitto Perfetto* method using the pCORE plasmid (*kanMX4-URA3*) (Storici and Resnick, 2006). Primers and strains used in this study are listed in Table S3 and S4.

Unless otherwise noted, yeast cells were grown in YPD (1% yeast extract, 2% peptone, 2% dextrose) at 30°C. For glucose deprivation, cultures were further grown in YP media without dextrose for indicated times. For mild osmotic stress, YPD growth medium was supplemented with 0.5 M NaCl or 0.2 M CaCl₂ for indicated times. Generally, yeast cells were harvested at mid-log phase with an OD₆₀₀ of 0.4-0.8.

RNA-Seq sample preparation, processing and analysis

RNA-Seq libraries were constructed according to (Hafner et al., 2010) and (Kishore et al., 2011) with modifications and sequenced on Illumina HiSeq2000 with single 50 bp reads. We aligned reads to the *Saccharomyces cerevisiae* genome EF4.72 from ENSEMBL using Bowtie version 1.0.0 (Langmead et al., 2009). Reads were subsequently counted per exon using htseq-count (Anders et al., 2015) against ENSEMBL's matching GTF file for EF4.72 and aggregated on the gene-level. To identify significant ($p < 0.05$) P-body enriched genes, we employed edgeR version 3.0 (Robinson et al., 2010) for count normalization and estimation of dispersion. For glucose depletion stress, genes previously shown to be significantly enriched in polysomes (Arribere et al., 2011) for the same stress were excluded from our analysis. Detailed procedures and parameters see Extended Experimental Procedures.

Gene Ontology (GO) term enrichment analysis

GO biological processes (BP) enrichment analysis was performed using hypergeometric tests as detailed in the Extended Experimental Procedures.

Combined Fluorescence in situ Hybridization (FISH) and immunofluorescence (IF)

Combined FISH and IF was performed as described previously (Kilchert and Spang, 2011; Takizawa et al., 1997). Antibodies and solutions used for detection see Extended Experimental Procedures. Images were acquired with an Axiocam MRm camera mounted on

an Axioplan 2 fluorescence microscope using a Plan Achromat 63x/NA1.40 objective and filters for eqFP611 and GFP. Axiovision software 3.1 to 4.8 was used to process images (Carl Zeiss).

Co-localization analysis

Signals of P-bodies and mRNA were identified using the spots tools in Imaris software package (Bitplane). For co-localization determination, the MATLAB (MathWorks)-Imaris plug-in “co-localize spots” function was used with a threshold of 50% of the distance between centers of two spots. The percentage of mRNA co-localization with P-bodies was calculated by dividing co-localized FISH spots by total FISH spots. Approximately 200 cells from at least three biologically independent experiments were counted per mRNA per condition.

Pulse-chase labeling with 4TU and RNA purification

The pulse-chase labeling experiments were carried out according to (Zeiner et al., 2008) with modifications as described in Extended Experimental Procedures.

Quantitative RT-PCR

0.5-1 µg of 4-TU labeled RNA or total RNA was reverse transcribed with the Transcriptor reverse transcriptase kit (Roche), oligo-dTs and random hexamers. The mRNA levels were analyzed by SYBR green incorporation using ABI StepOne Plus real-time PCR system (Applied Biosystems). Primers used in qRT-PCR are listed in Table S3.

Western Blotting

Glucose deprived cells were harvested at indicated times ($t = 0, 10, 20, 30,$ and 60 min). For each time point, 9 ml of culture was taken, immediately treated with cold trichloroacetic acid (10% final concentration), and incubated on ice for 5 min. Yeast extracts were prepared as described (Stracka et al., 2014). The protein concentration was determined using the DC Protein Assay (Bio-Rad), and the total lysate was analyzed by SDS-PAGE and immunoblotting. The following antibodies were used for immunoblotting: anti-Tpi1 (LSBio LS-C147665; 1:5,000); anti-Atp11 (a gift from Sharon H. Ackerman, Wayne State University, Detroit, MI); anti-HA (Eurogentec HA11; 1:1,000); anti-Pgk1 (Invitrogen #A-6457; 1:1,000). Enhanced Chemiluminescence (ECL; GE Healthcare) was used for detection.

Accession Numbers

The RNA-Seq data reported in this study is deposited in Gene Expression Omnibus (GEO) database, and the accession number is GSE76444.

Author Contributions

AS and CW conceived the project and experiments. Most experiments were performed by CW. JW was involved in initial experiments. FS, CW, NB and AS performed data analysis. AS, CW and FS wrote the manuscript with input from all authors.

Acknowledgements

We thank C. Brown, M. Zavolan and J. Guimaraes for help with the data analysis and discussions, and M. Zavolan, I. G. Macara and T. Gross for critical comments on the manuscript. S. Ackerman is acknowledged for providing the Atp11 antibody. This work was supported through grants from HFSP (RGP0031), the Swiss National Science Foundation (31003A_141207, 310030B_163480) and the University of Basel to AS. CW and JW were supported by Werner Siemens Fellowships and FS by SystemsX.ch (2009/025), the Swiss Initiative in Systems Biology.

Wang et al., Figure 1

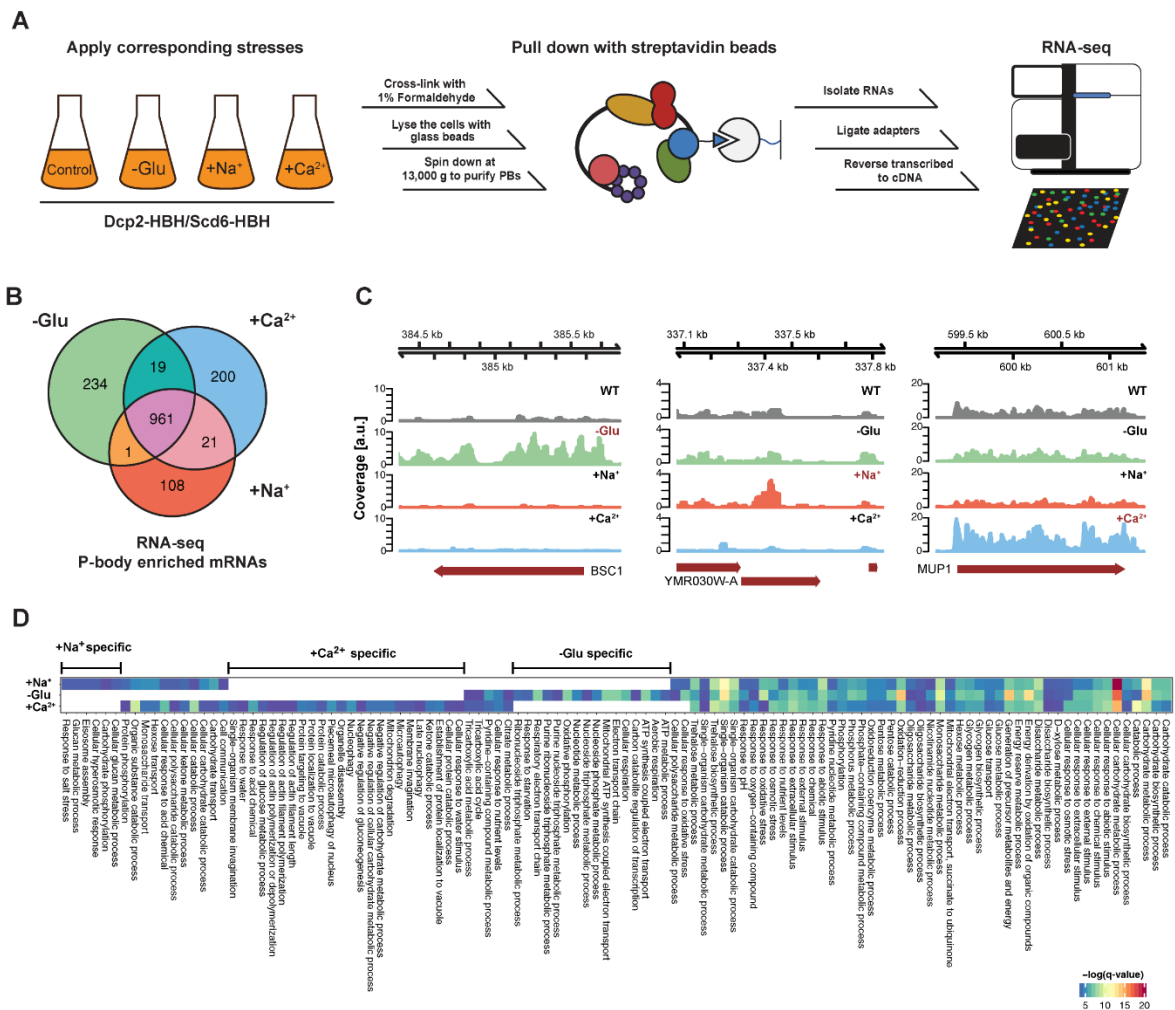


Figure 1. RNA-Seq reveals stress-specific mRNA subsets enriched in P-bodies.

(A) RNA-Seq library preparation workflow. Cells expressing Dcp2-HBH or Scd6-HBH were stressed for 10 min, followed by cross-linking with formaldehyde. After cell lysis, centrifugation was performed to enrich membrane fractions. Cross-linked complexes were subsequently purified via streptavidin affinity purification. mRNAs were isolated and ligated with adapters. cDNA libraries were prepared by reverse transcription and sequenced using single-read RNA-Seq. (B) Venn diagram illustrating the intersections among mRNAs enriched in P-bodies ($p < 0.05$) under glucose depletion and osmotic stress conditions with Na⁺ or Ca²⁺, relative to the no stress condition as determined by RNA-Seq. (C) Read coverage plots (average over five biological replicates) of RNA-Seq data mapped to P-body enriched genes under specific stress conditions. (D) Enrichment analysis of P-body associated genes under different stress conditions against Gene Ontology's (GO) biological processes (BP). Significantly enriched pathways (q -value < 0.05) from hypergeometric tests are presented in a clustered heatmap. Rows and columns correspond to stress conditions and pathways, respectively, and the negative logarithms of q -values are color-coded from blue (low) to red (high).

Wang et al., Figure 2

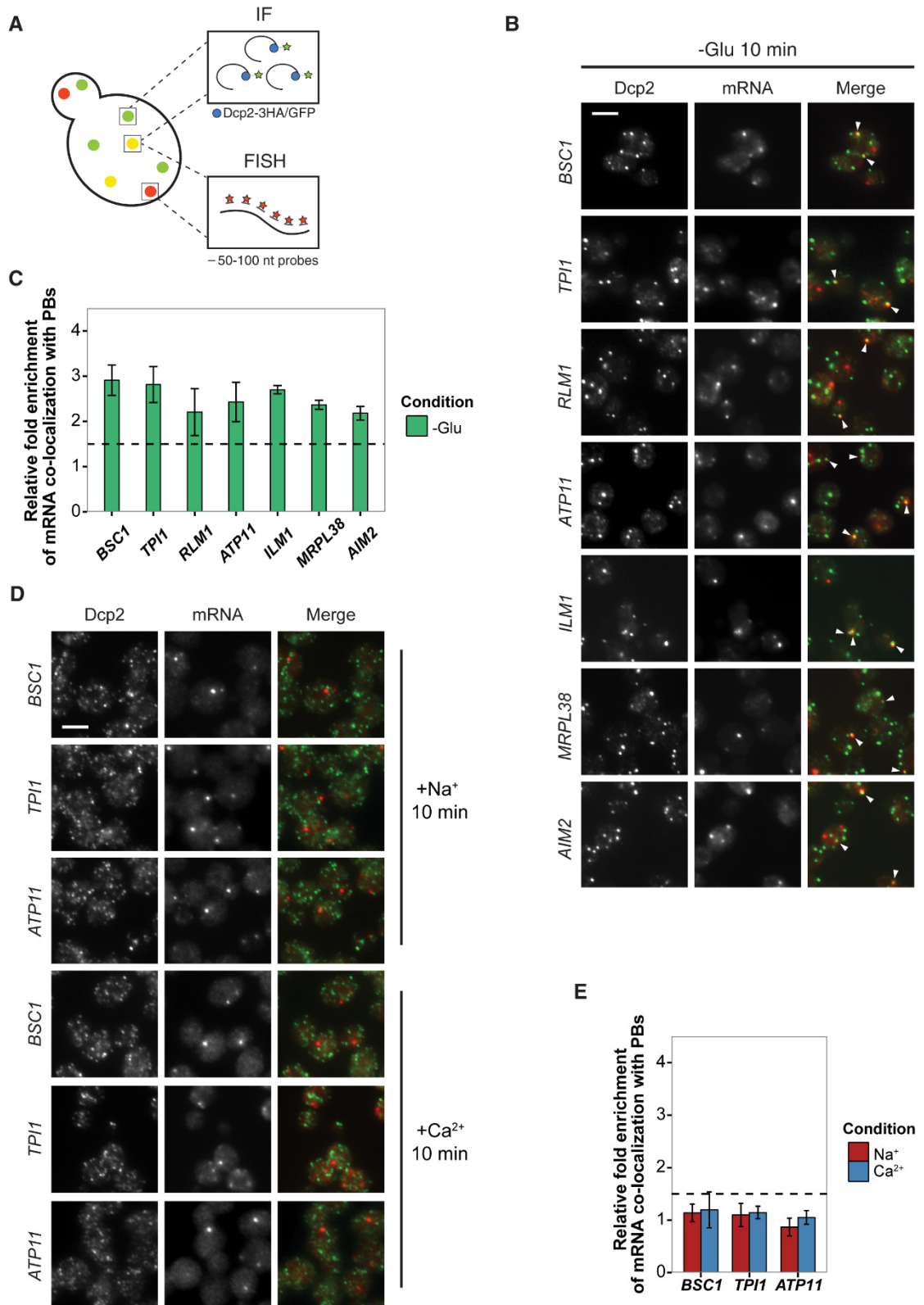


Figure 2. Validation of glucose-specific candidates by combined fluorescence *in situ* hybridization and immunofluorescence (FISH-IF).

(A) Schematic representation of combined FISH-IF technique. Immunofluorescence staining was performed against P-body marker Dcp2 chromosomally tagged with 3HA or GFP. To detect mRNAs accumulating in P-bodies, multiple short probes (50-100 nt) against the open reading frame (ORF) of each gene were used for FISH. (B) Fluorescence images of P-bodies and glucose-starvation-specific candidate mRNAs after glucose depletion. Cells expressing Dcp2-3HA were first grown in YPD media to mid-log phase and shifted to YP media lacking glucose for 10 min. Scale bar, 5 μm . Error bars, $\pm\text{SEM}$. (C) Bar plot depicting the quantification of co-localization between candidate mRNAs and P-bodies. The percentage of co-localization was quantified as described in Experimental procedures. The relative fold enrichment was subsequently calculated by normalizing the percentage of candidate mRNAs against the percentage of control mRNAs (Figure. S2C). The dashed line represents an arbitrarily fixed threshold of 1.5 for determining significant P-body association. (D) Fluorescence images of P-bodies and glucose-specific candidate mRNAs under mild osmotic stress with Na^+ or Ca^{2+} . Cells expressing Dcp2-3HA were first grown in YPD media to mid-log phase and shifted to YPD media containing 0.5 M NaCl or 0.2 M CaCl_2 for 10 min. Scale bars, 5 μm . Error bars, $\pm\text{SEM}$. (E) Same as (C) except stress conditions. Scale bar, 5 μm . Error bars, $\pm\text{SEM}$.

Wang et al., Figure 3

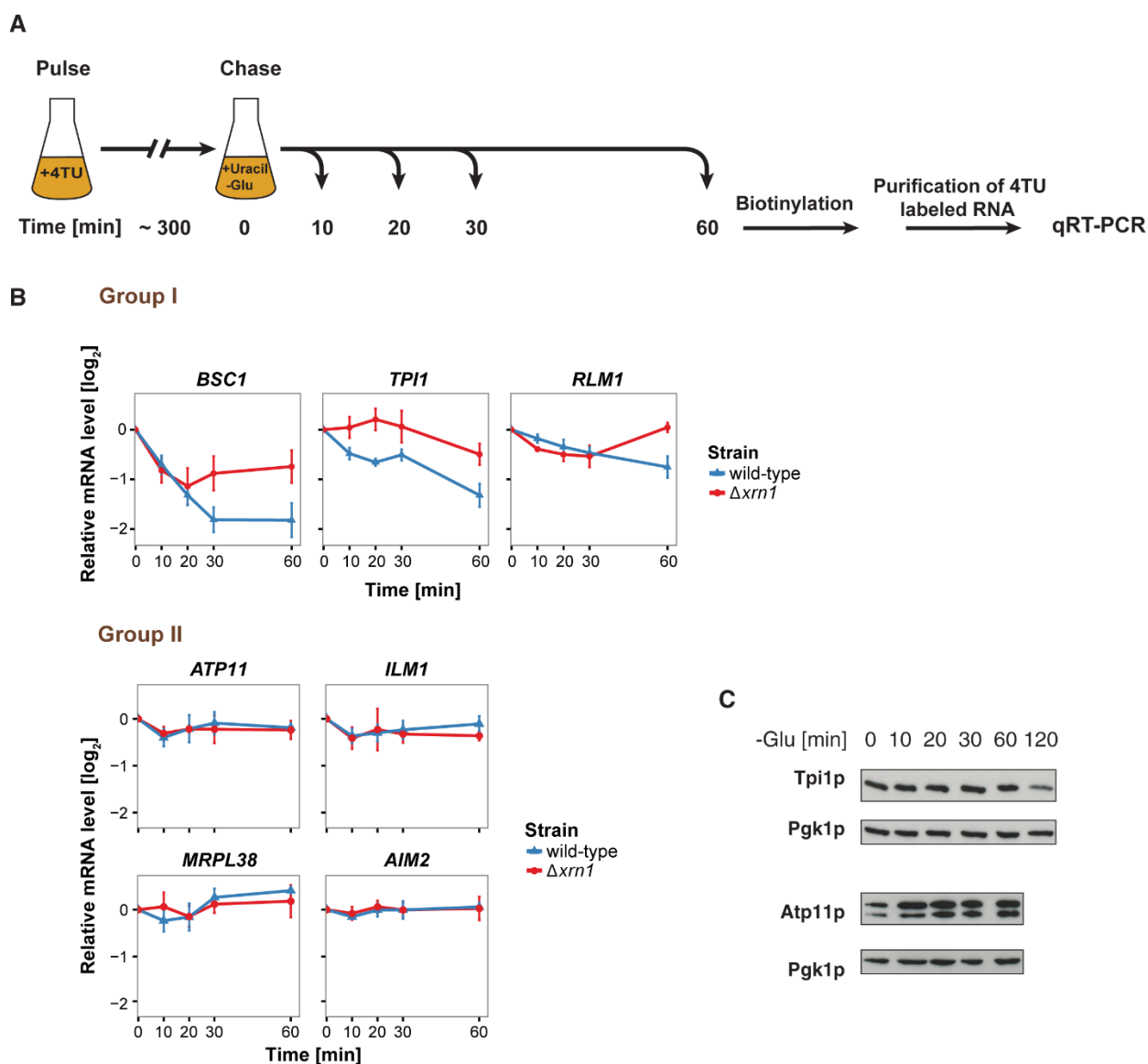


Figure 3. The stability of P-body enriched mRNAs varies and can be categorized according to their GO terms.

(A) Schematic illustration of pulse-chase protocol. Cells were grown in the presence of 0.2 mM 4TU and shifted into media lacking glucose but containing 20 mM uracil. Cells were harvested at indicated time points after the shift. Total RNA was extracted and biotinylated. 4TU labeled RNA was purified and subsequently analyzed by qRT-PCR. (B) The stability of 4TU labeled candidate mRNAs was determined by qRT-PCR in wild-type and $\Delta xrn1$ strains at indicated time points following a shift to glucose-depleted media. Transcription levels were normalized using *ACT1* gene as an endogenous reference. Group I: non-mitochondria-related candidates. Group II: mitochondria-related candidates. Error bars, \pm SEM. (C) Western blot analysis of Tpi1p and Atp11p at indicated time points after glucose deprivation. Pgk1p was used as a loading control. Anti-Tpi1p, anti-Atp11p and anti-Pgk1p were used for detection.

Wang et al., Figure 4

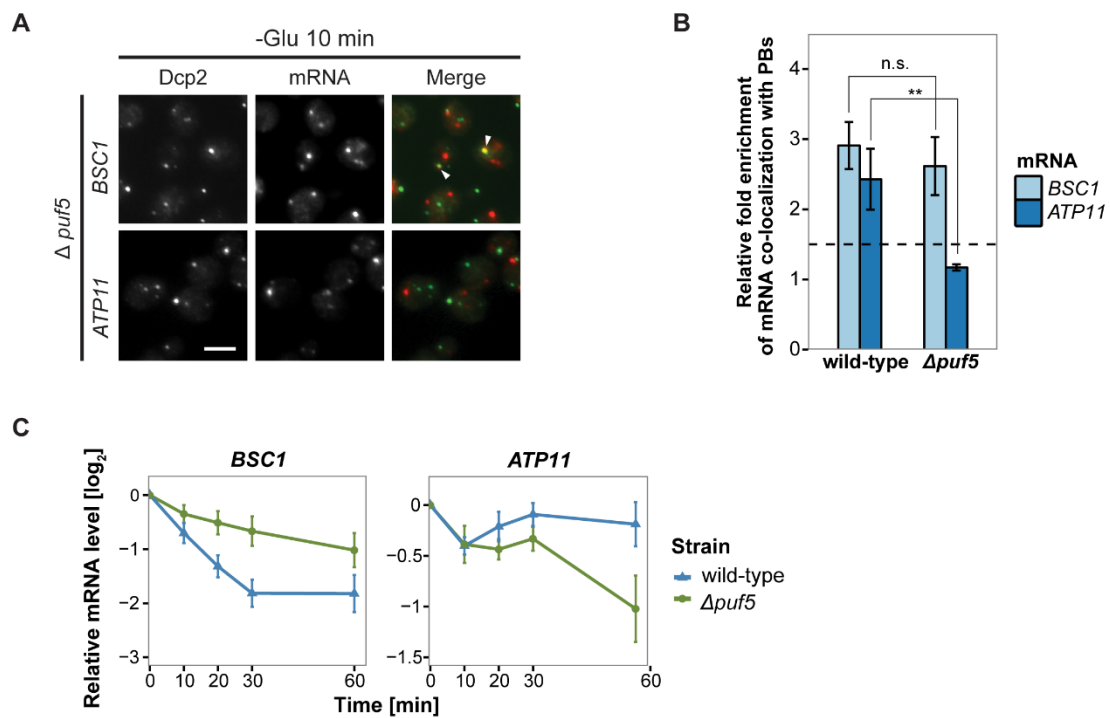


Figure 4. Puf5p is required for both mRNA recruitment and regulation of mRNA decay in P-bodies.

(A) Fluorescence images of P-bodies and *BSC1* (Group I) or *ATP11* (Group II) mRNAs following glucose depletion on $\Delta puf5$ cells expressing Dcp2-GFP. Scale bar, 5 μ m. (B) Bar plot showing the relative fold enrichment of co-localization between *BSC1*, *ATP11* and P-bodies in $\Delta puf5$ strain 10 min after switched to glucose-free media. Wild-type is plotted as in Figure 2C. The dashed line represents a fixed threshold of 1.5 for determining significant enrichment. Error bars, \pm SEM. Asterisks (**) indicate $p < 0.01$ and n.s. indicates $p > 0.05$ (A one-tailed, non-paired Student's *t*-test was used to determine *p* values). (C) The stability of 4TU labeled *BSC1* and *ATP11* mRNAs was measured by qRT-PCR in $\Delta puf5$ strain at indicated time points following glucose depletion. Wild type is plotted as in Figure 3B. Error bars, \pm SEM.

Wang et al., Figure 5

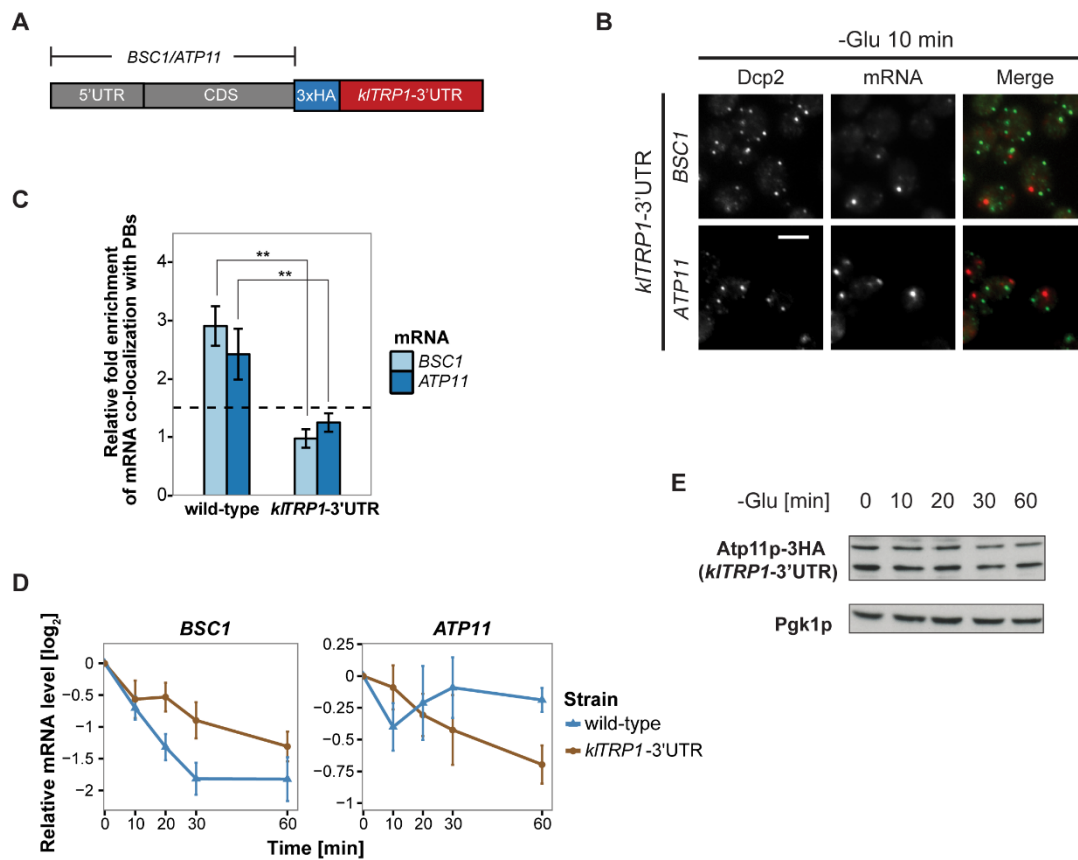


Figure 5. 3'UTR is necessary for mRNA localization to P-bodies.

(A) A schematic representation of C-terminal tagging with 3x HA. The endogenous 3'UTR was simultaneously replaced by the 3'UTR of *kITRP1*. (B) Fluorescence images of P-bodies and *BSC1*, *ATP11* mRNAs following glucose depletion on corresponding 3'UTR replaced strains. Scale bar, 5 μ m. (C) Bar plot depicting the relative fold enrichment of co-localization between *BSC1*, *ATP11* and P-bodies in corresponding 3'UTR replaced strains 10 min after glucose starvation. Wild type is plotted as in Figure 2C. The dashed line represents a fixed threshold of 1.5 for determining significant enrichment. Error bars, \pm SEM. Asterisks (**) indicate $p < 0.01$ (A one-tailed, non-paired Student's *t*-test was used to determine *p* values). (D) The stability of 4TU labeled *BSC1* and *ATP11* mRNAs was determined by qRT-PCR in corresponding 3'UTR replaced strains at indicated time points following glucose depletion. Wild type is plotted as in Figure 3B. Error bars, \pm SEM. (E) Western blot analysis of Atp11-HA (*kITRP1* 3'UTR) at indicated time points after glucose deprivation. Pgk1 was used as a loading control. Anti-HA and anti-Pgk1p were used for detection.

Wang et al., Figure 6

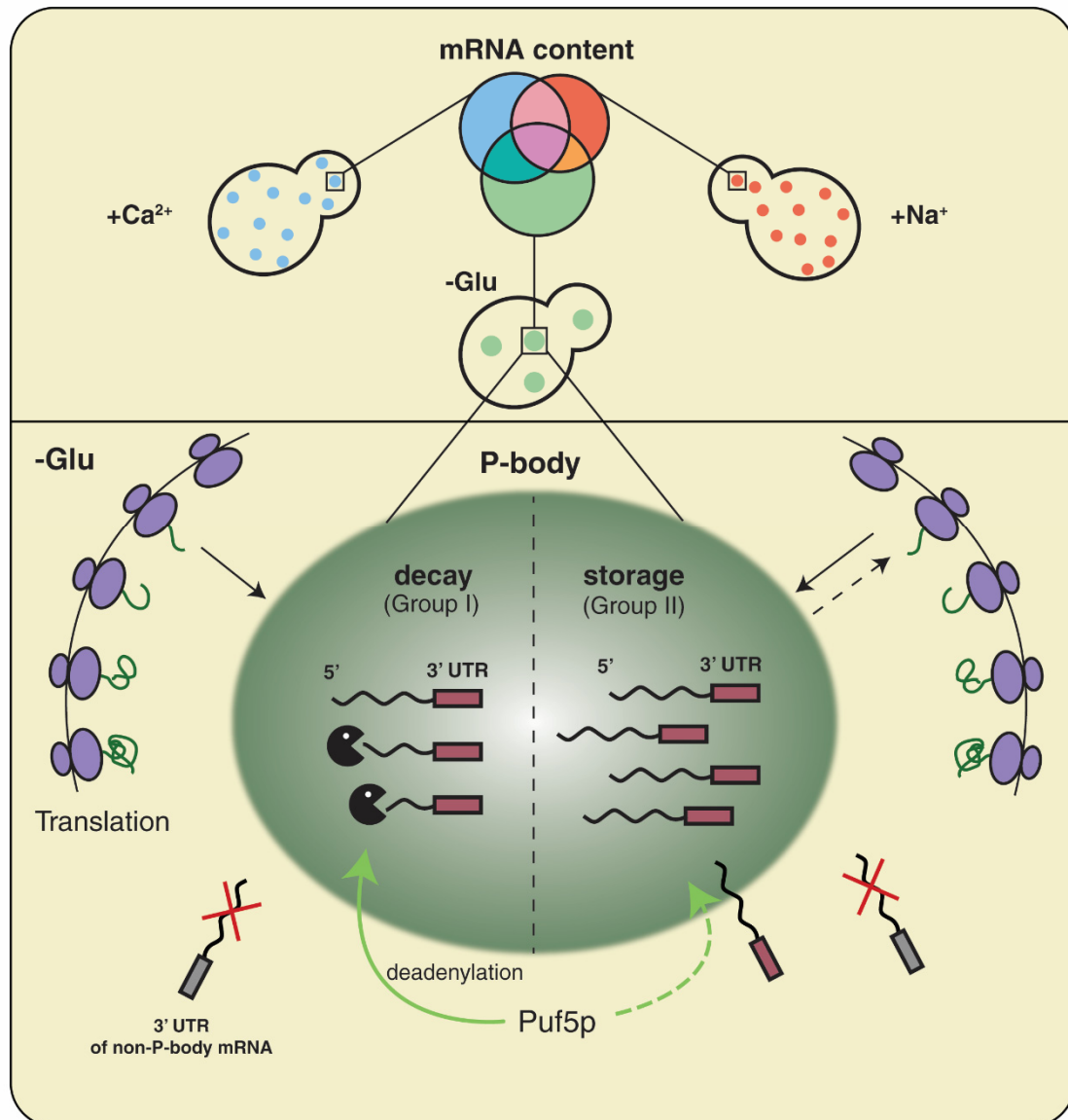
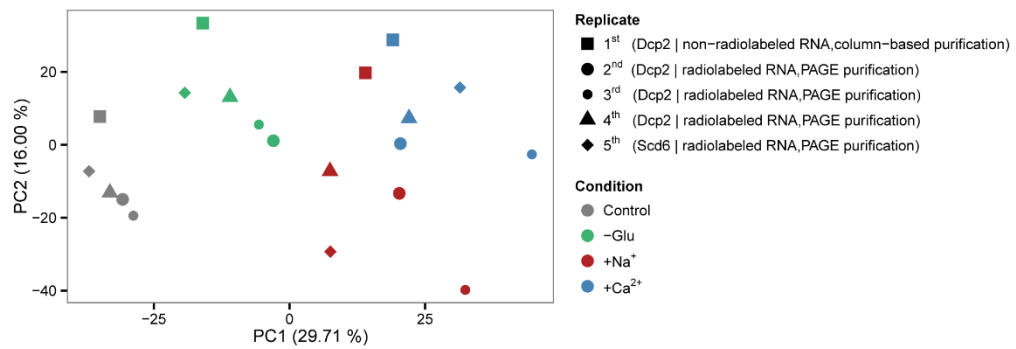


Figure 6. Schematic model summarizing our findings.

Supplemental Materials

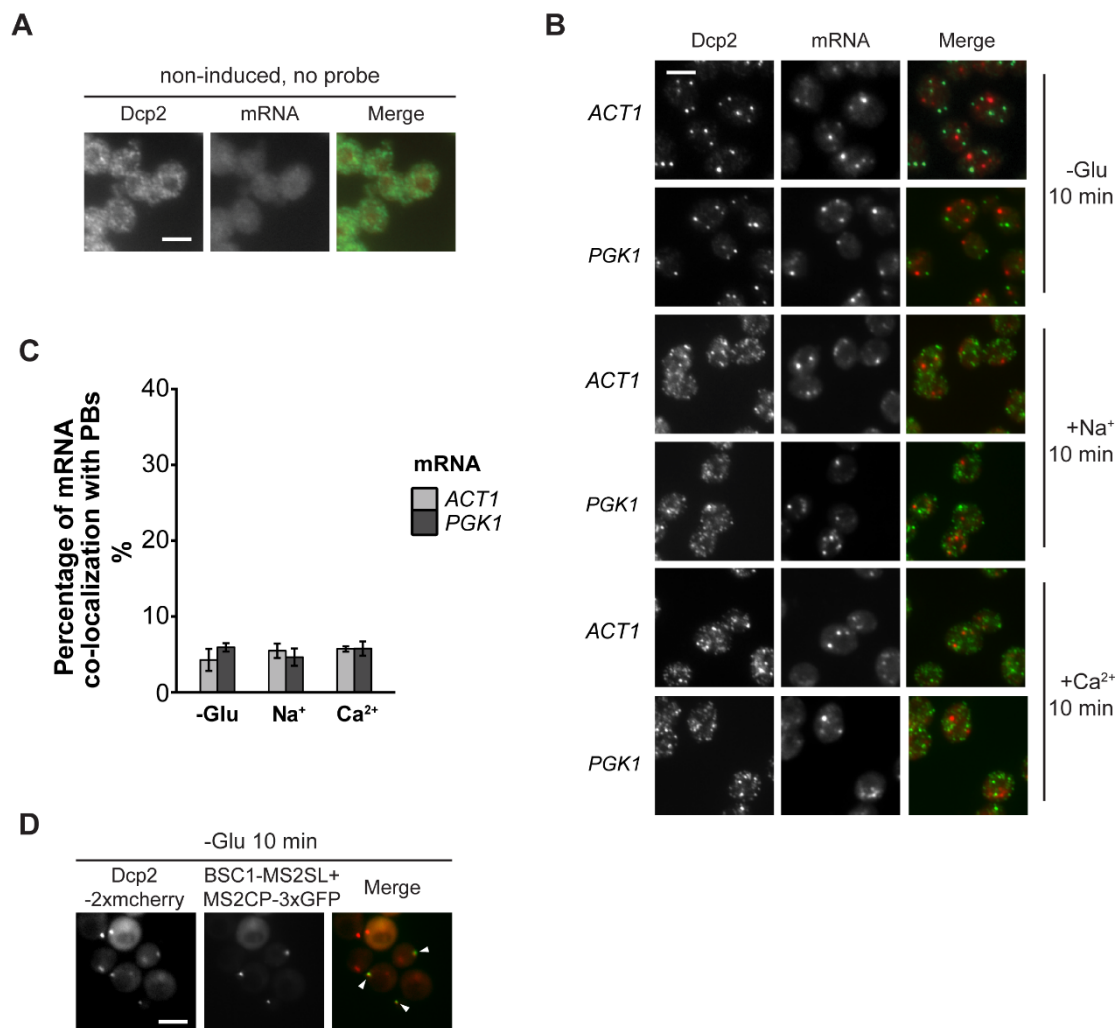
Supplemental figures

Wang et al., Figure S1

**Figure S1. Reproducibility of datasets derived from RNA-Seq.**

Principal component analysis (PCA) plot based on the read count profile from aligned RNA-Seq data of five biological replicates for each condition. The two first principal components are plotted with the proportion of variance explained, indicated by each component next to the axes labels.

Wang et al., Figure S2

**Figure S2. Evaluation of non-candidate mRNAs by FISH-IF.**

(A) FISH-IF controls. Combined FISH-IF was performed without probes with cells expressing Dcp2-3HA under non-induced condition. Scale bar, 5 μ m. (B) Fluorescence images of P-bodies and two non-candidate mRNAs, *ACT1* and *PGK1*. Cells expressing Dcp2-3HA were treated with indicated stresses. Scale bar, 5 μ m. (C) Bar plot depicting the percentage of co-localization between non-candidate mRNAs and P-bodies. The average of the percentages of *ACT1* and *PGK1* under each condition served as a control level in calculating the fold enrichment in Figure 2C, 2E, 4B, 5C and S5C. Error bars, \pm SEM. Scale bar, 5 μ m. (D) Live-cell detection of P-bodies (Dcp2-2xmcherry) and *BSC1* mRNA molecules using the MS2 system. Scale bar, 5 μ m.

Wang et al., Figure S3

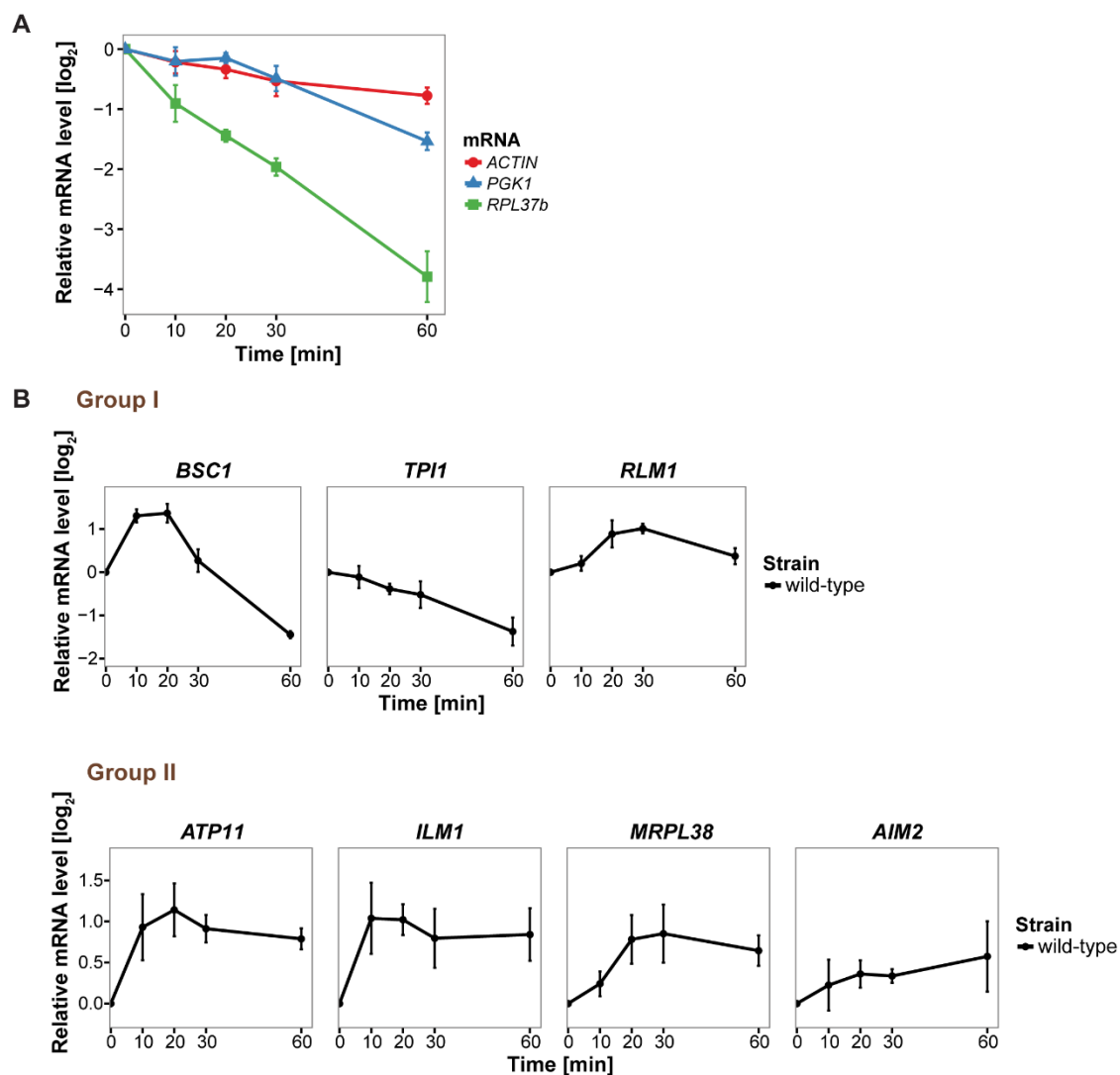


Figure S3. Changes in total candidate mRNA levels corresponding to Xrn1-dependent degradation.

(A) Evaluation of qRT-PCR reference genes stability after glucose depletion. The total mRNA levels of three commonly used reference genes were measured by qRT-PCR and normalized to spike-in RNA control as described in Experimental procedures. Error bars, \pm SEM. (B) Fold changes of total candidate mRNA levels after glucose depletion were determined by qRT-PCR using *ACT1* as reference. Group I: non-mitochondria-related candidates. Group II: mitochondria-related candidates. Error bars, \pm SEM.

Wang et al., Figure S4

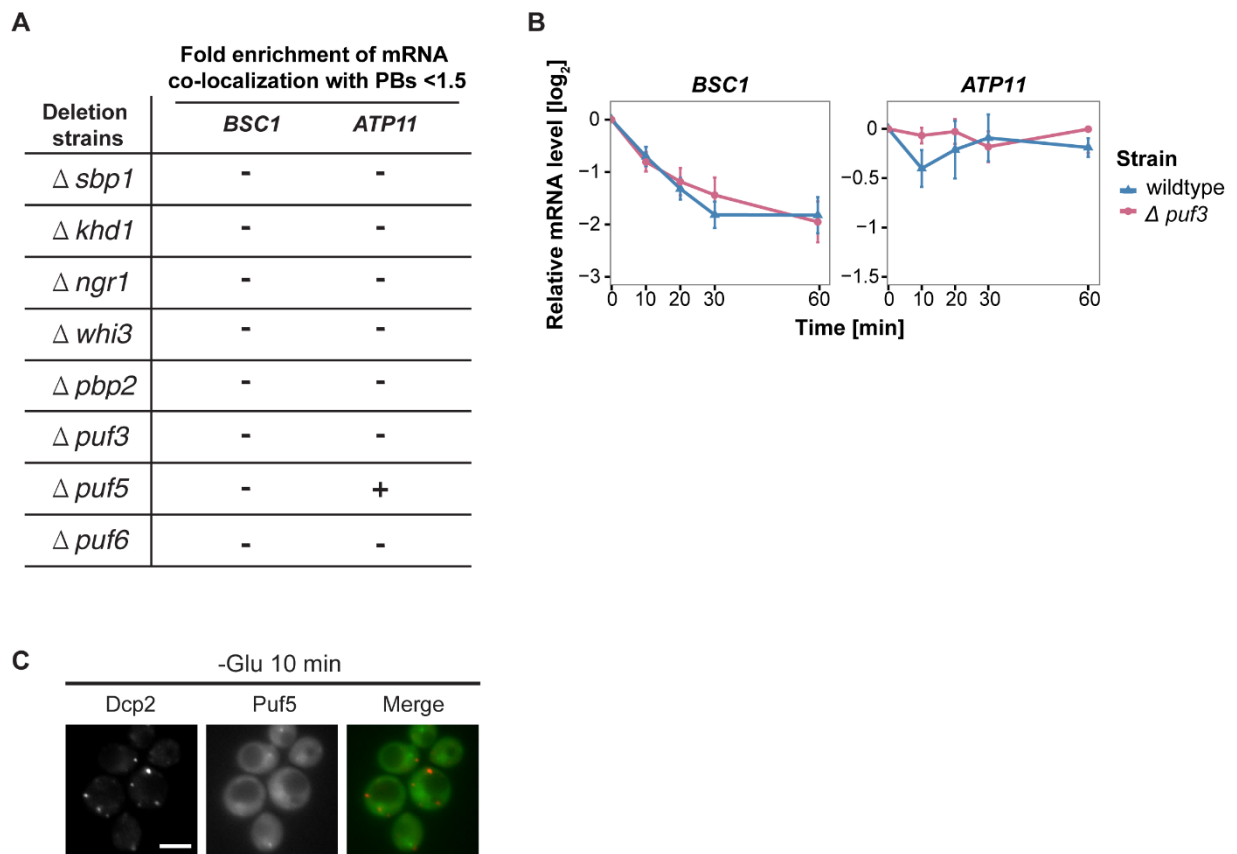


Figure S4. A screen for RNA-binding proteins required for mRNA recruitment to P-bodies.

(A) A screen to identify RNA-binding proteins affecting mRNA recruitment to P-bodies by FISH-IF. *BSC1* and *ATP11* were selected for screening performed with the deletion strains as listed. A fold enrichment value above 1.5 was classified as not required (-), below as required (+). (B) The stability of 4TU labeled *BSC1* and *ATP11* mRNAs was measured by qRT-PCR in $\Delta puf3$ strain at indicated time points following glucose depletion. Wild type is plotted as in Figure 3B. Error bars, \pm SEM. (C) Live-cell detection of P-bodies (Dcp2-2xmcherry) and Puf5p (GFP) following glucose withdrawal. Scale bar, 5 μ m.

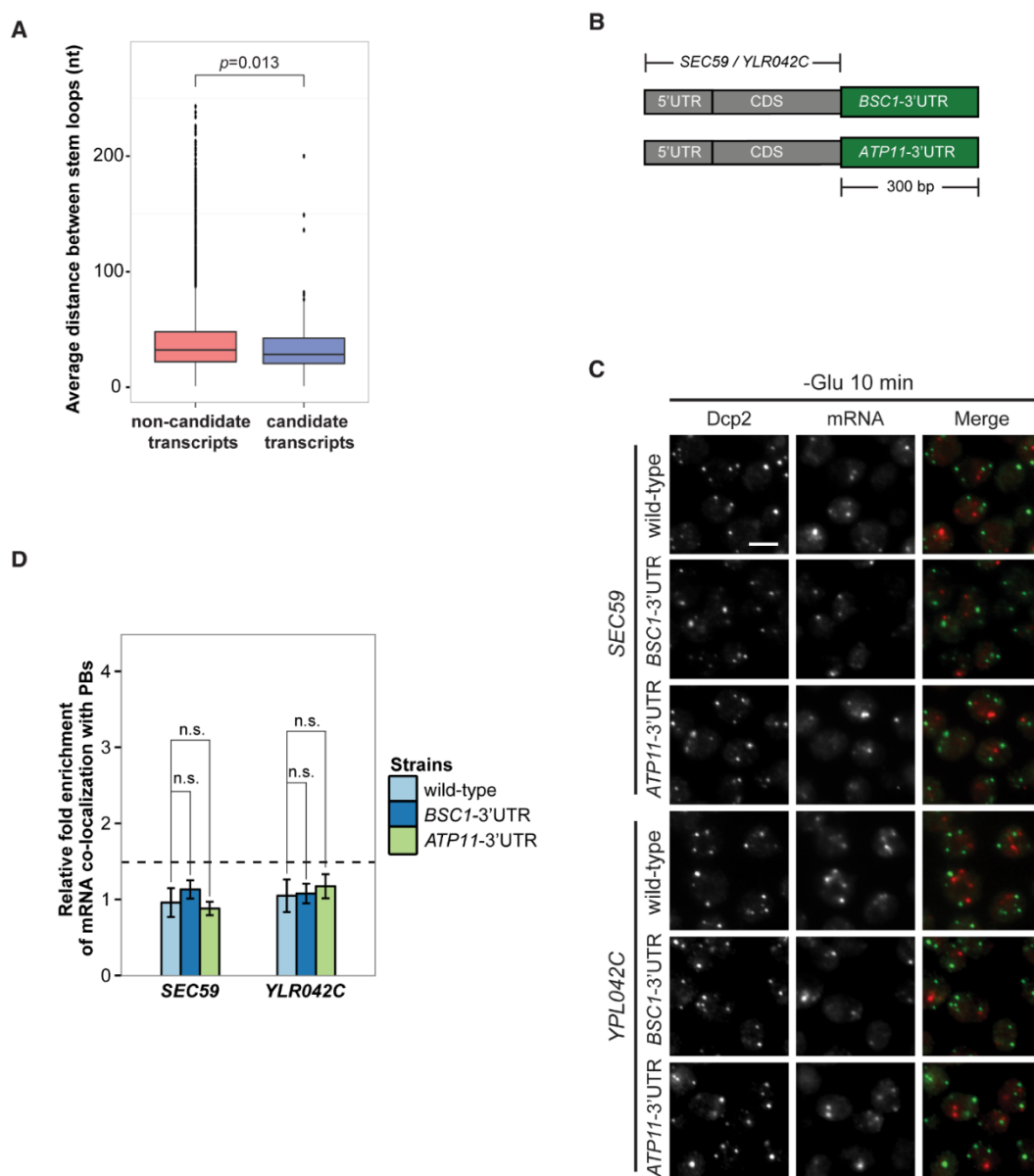


Figure S5. 3'UTR is insufficient for mRNA localization to P-bodies.

(A) Box plot of average distances between stem loops among the 3'UTRs of candidate transcripts versus non-candidate transcripts, $p=0.013$ (A non-parametric, one-sided Wilcoxon rank-sum test was used). (B) A schematic representation of 3'UTR transplantation chimeras. The endogenous 3'UTRs (300 bp downstream from stop codon) of *SEC59* and *YLR042C* (300 bp downstream from stop codon) were replaced by the 3'UTRs of *BSC1* and *ATP11*, respectively. (C) Fluorescence images of P-bodies and *SEC59* and *YLR042C* mRNAs following glucose depletion. Scale bar, 5 μm . (D) Bar plot showing the relative fold enrichment of co-localization between *SEC59*, *YLR042C* and P-bodies in indicated chimeric strains 10 min after glucose withdrawal. Wild type is plotted as in Figure 2C. The dashed line represents a fixed threshold of 1.5 for determining significant enrichment. Error bars, $\pm\text{SEM}$. n.s. indicates $p>0.05$ (A one-tailed, non-paired Student's *t*-test was used to determine *p* values).

Supplemental tables

Table S1: P-body enriched mRNA candidates.

| Glucose starvation specific hits (non-polysome enriched) | Na ⁺ specific hits | Common hits _triple | | |
|--|-------------------------------|---------------------|---------|-----------|
| BSC1 | CIN1 | GPD1 | SDH1 | PDI1 |
| PRM7 | YBR099C | FMP48 | PDR10 | PAR32 |
| YOR338W | RRM3 | CMK2 | CYC7 | ECI1 |
| PRM5 | PTP3 | RTC3 | PTK2 | ZIP1 |
| DAP1 | SIP1 | BDH2 | KHA1 | GUD1 |
| YER158C | ATF1 | CTT1 | YDL206W | YKR005C |
| PHD1 | THI21 | YNL194C | UGA1 | YPR1 |
| YHR145C | MGA2 | HSP12 | DOA4 | ADY2 |
| YPL088W | TOS3 | DDR2 | TAX4 | YPL277C |
| SPS19 | YOL024W | PHM7 | YLR152C | CYT1 |
| CRG1 | VMR1 | SPI1 | RIM4 | PKH2 |
| ERG28 | ATG26 | HXT5 | UBP9 | COQ4 |
| MRPL38 | SPR1 | TPS2 | JID1 | YPR160W-A |
| HMS1 | YMR1 | MGA1 | GAL2 | NPR1 |
| PST1 | SIP18 | CYB2 | YMR265C | HAP2 |
| RLM1 | MEI4 | YOR385W | MCR1 | HPA2 |
| ECM13 | WSC3 | FMP43 | YLR108C | LSB1 |
| BAP2 | IZH3 | GLC3 | MTL1 | SCS22 |
| YCL049C | YDR333C | HSP42 | PPT2 | YGR201C |
| MIG1 | CIK1 | XBP1 | DDR48 | CYC3 |
| SUS1 | UME6 | YLR194C | YDL233W | RAD4 |
| ATP14 | EUG1 | PGM2 | CRZ1 | YOR214C |
| OPI3 | ADY4 | BAG7 | MDG1 | MAM3 |
| POG1 | FRE2 | TMA10 | YBR139W | YDR018C |
| SNA3 | YMR030W-A | HSP26 | YKL100C | DUR3 |
| ZPR1 | CRF1 | MSC1 | STF1 | ATG34 |
| TPH1 | HXT9 | YLR149C | POX1 | RFX1 |
| PCD1 | YRO2 | DIA1 | EIS1 | YGR066C |
| COA2 | YDL109C | RG11 | FLC1 | YPL260W |
| PET100 | MET1 | GAD1 | ATG23 | ECM21 |
| FPR2 | RED1 | AIM17 | MPM1 | DNL4 |
| REE1 | SSL2 | PRR2 | FHN1 | PUT1 |
| YIR035C | YDR222W | EMI2 | FYV10 | LAS17 |
| COX2 | NTH2 | RCN2 | UIP3 | ECL1 |
| YPR010C-A | KRE5 | YJL171C | YJR087W | YJL132W |
| COX14 | YLR030W | YHR097C | YNL011C | YIP5 |
| YDR319C | YOR192C-B | YPS1 | SUC2 | MAC1 |
| YDR282C | ECM3 | PRM10 | GPT2 | RPN4 |
| TVP18 | YML053C | HOR2 | BOP3 | IMP2 |
| YSA1 | YLR042C | HSP104 | SUB1 | ICY2 |
| AIM19 | RPH1 | STL1 | LSB6 | HSE1 |
| MTR2 | YLR352W | PUN1 | RTC2 | NCA2 |
| ECM14 | PLM2 | GSY1 | MAL11 | TEX1 |
| UTR4 | URN1 | YJL144W | REG2 | RAD16 |
| PCP1 | IMA5 | ALD3 | QCR8 | GAL4 |
| ASR1 | SLU7 | TSL1 | VPS27 | COS9 |
| FTH1 | PLB3 | NQM1 | GSM1 | YGL081W |
| ACA1 | RRN6 | YNL195C | ARI1 | RMR1 |
| SEC11 | SER3 | GYP7 | GPI12 | NSG2 |
| YBR137W | YNL284C-B | PRM8 | FBP26 | VPS62 |
| QRI5 | YPL245W | TPO4 | TBS1 | PRE4 |
| SPL2 | TRR2 | HXK1 | YNL208W | COS8 |
| YHL008C | TIR3 | YJL107C | UBX5 | SSN8 |
| YHR210C | ULP2 | HXT1 | GRH1 | YMR181C |
| SNF11 | YJR098C | PUT4 | HRK1 | GSH1 |
| YAR1 | GUF1 | IGD1 | AGX1 | SIP2 |
| PEX10 | YDR261W-B | TPS1 | ERO1 | TGL3 |
| ERD2 | SFP1 | PNC1 | SIP5 | CET1 |
| ZRT1 | DFG16 | GLK1 | MSS11 | CDC7 |
| CDC36 | APP1 | PNS1 | RHR2 | MUP3 |
| MSF1 | YEL023C | DCS2 | HFD1 | FIS1 |
| YNL228W | PPZ1 | ENA1 | RIM101 | YLR173W |
| ILM1 | HOT1 | YMR196W | GID8 | SNG1 |
| HYR1 | DIN7 | OM45 | FAA2 | COQ1 |
| LDB7 | RMD9 | TKL2 | YBR016W | STE11 |
| PRE8 | LCL1 | YAK1 | VHS3 | RVS161 |
| YIL029C | BUD25 | TDA1 | SDH2 | MSP1 |
| YGL177W | SWC4 | JEN1 | YIM1 | DAK2 |
| YJL133C-A | MUM3 | FRT2 | HAL1 | PEX28 |
| YCH1 | HNT2 | PIC2 | SLZ1 | FMP46 |
| OLI1 | FUR4 | HXT2 | YDR306C | VNX1 |

Results, Part I

| | | | | |
|-----------|--------------------------------------|-----------|-----------|-----------|
| IES6 | YIL001W | STF2 | GAL7 | BSC5 |
| SHR3 | YNR068C | YNR014W | PCL8 | NAB2 |
| ARC15 | TSC11 | YLR345W | YET3 | URA8 |
| HCH1 | SNM1 | YOR062C | YOL107W | YMR102C |
| YPL222C-A | RFT1 | YPL247C | THI4 | MDH1 |
| ENV7 | EAR1 | RIM8 | TDA10 | EDS1 |
| ROT1 | YHL019W-A | FMP45 | HUL4 | SCS3 |
| DIF1 | SNU23 | MEP1 | YSC83 | CTL1 |
| COX3 | SRX1 | RCR1 | TGL4 | IRS4 |
| IZH2 | PTA1 | YOR019W | PRM4 | CBP3 |
| MDM35 | ISC1 | ALD4 | YAP1801 | YPL109C |
| PET494 | BYE1 | YPC1 | MSN2 | NBP35 |
| CTA1 | BCH2 | SOL4 | PCK1 | BLI1 |
| MBA1 | RGM1 | SSE2 | ARA1 | DIT2 |
| YER134C | PAN3 | YDL124W | MDM34 | BET2 |
| LIP1 | TPO1 | NCE103 | MBR1 | SRL3 |
| DFG5 | YPL272C | YIL055C | YIR016W | YFR039C |
| CYC2 | UBA4 | GPA2 | ALD6 | RPR2 |
| OYE3 | RIT1 | CHS1 | RFS1 | PEX22 |
| MHR1 | PAD1 | ORM2 | SDH4 | RGA2 |
| YBR126W-B | USA1 | SDS24 | UGA2 | YDR338C |
| STP2 | ARA2 | YBR056W-A | FMP33 | RPN11 |
| GPM1 | YJR061W | NRG1 | CCP1 | PCL6 |
| YOR228C | YCL048W-A | USV1 | YRR1 | HUL5 |
| CMC4 | PDE2 | CAT8 | ROD1 | GTS1 |
| UPS1 | NRD1 | HOR7 | RCK1 | ENO1 |
| YDR056C | COG6 | EDC2 | FES1 | IRC19 |
| YMR013W-A | CYR1 | YLR252W | FAA1 | YMR317W |
| COA4 | MDM31 | SUR1 | YGR237C | YDR476C |
| YPT35 | HOS1 | YOR052C | SIS1 | STR3 |
| COB | SOG2 | HAL5 | FUS2 | TMT1 |
| YOP1 | YSP3 | YJR115W | NEO1 | RIB1 |
| YLR036C | PUF2 | SSA4 | TAM41 | YKU70 |
| IGO2 | CWC23 | ICT1 | UGX2 | YOR186W |
| ATP11 | GLG2 | GIP2 | PUT2 | PGA1 |
| AIM23 | LAC1 | YKL091C | CSG2 | AIM39 |
| CMC1 | SRF1 | SYM1 | SAP4 | ECM38 |
| MXR2 | SPT3 | GPH1 | SHE4 | THP1 |
| YMR134W | YER097W | YBR085C-A | YMR114C | ARG82 |
| AME1 | GRX7 | IKS1 | ATG8 | JLP1 |
| ALT2 | SRC1 | XKS1 | YNL134C | RRG8 |
| VTC1 | AKR2 | YMR084W | SAC6 | MID2 |
| COX19 | FIT3 | GOR1 | PIR3 | MEF2 |
| CUE4 | VID22 | YGR250C | YHR033W | YHR022C |
| GFD1 | RUP1 | CSR2 | SOH1 | KGD2 |
| IRA2 | ZRT3 | OPI10 | SHY1 | NCA3 |
| RPN14 | GPI16 | YPS3 | ROX1 | SNF6 |
| PIN2 | KRE29 | DCS1 | YOL085C | NNK1 |
| COX18 | ARN2 | ADR1 | PGC1 | PYC1 |
| YKL162C | ENT5 | TMA17 | RRT8 | IST1 |
| MTQ1 | YFL032W | OM14 | YKL133C | SNA4 |
| VOA1 | YJL113W | FMP16 | CST6 | COA1 |
| AAC1 | VPS33 | YML131W | KNS1 | NYV1 |
| FPR1 | YPK9 | VPS36 | BDH1 | MON1 |
| QCR7 | DAL1 | BOP2 | PAM1 | COQ9 |
| EEB1 | ECM30 | HSP78 | IMA1 | PDC6 |
| ERP1 | ATG32 | ATH1 | YUR1 | GAT1 |
| DSF2 | SWD1 | YPT53 | MTH1 | GTT1 |
| CDC42 | MLH2 | IPT1 | TYE7 | AFG1 |
| YKR047W | Ca²⁺ specific hits | CLD1 | ART10 | CUR1 |
| AIM7 | MUP1 | TFS1 | LSB5 | YER053C-A |
| COA3 | MET2 | PRB1 | YGL052W | ASI2 |
| LCL2 | DUR1,2 | PMC1 | IML2 | BCY1 |
| TRS23 | MCA1 | YER184C | YGL036W | HDA2 |
| NKP1 | MET10 | UGP1 | ARO10 | UBS1 |
| YGL117W | VAM6 | GSY2 | YOR139C | YGR053C |
| YOL073C | VPS35 | AMS1 | CAR2 | SSP120 |
| COX13 | PAH1 | ATO2 | RRI2 | ICS2 |
| VMA11 | CRR1 | YDC1 | FMS1 | YMR103C |
| CRC1 | MEP2 | HBT1 | YGR240C-A | YHR080C |
| CHS7 | MVP1 | IRC15 | GPX1 | LAP2 |
| TOA2 | MMP1 | YGR067C | YGR127W | OTU1 |
| FSH2 | NTH2 | BX11 | RAS2 | CUE5 |
| AHP1 | ECM3 | YLR257W | YCR007C | RTA1 |
| YSF3 | SLD7 | AFR1 | YIR007W | ATG7 |
| QCR10 | YGL185C | GRE3 | GPI18 | PKH1 |
| VAB2 | YJR107W | PEP12 | ASI3 | YPR145C-A |
| YNL320W | YDR535C | TPK1 | YNL092W | OXR1 |
| SUR2 | NSL1 | GAP1 | BNA3 | PPG1 |
| YAP6 | NPL4 | GAC1 | SSK1 | CMP2 |
| YBR071W | UME6 | RTS3 | ZTA1 | HSV2 |

| | | | | |
|-----------|-----------|-----------|-----------|-----------|
| GPD2 | CDC37 | YHR138C | RDL1 | PRE7 |
| VAR1 | EAF3 | YBR287W | ARE2 | LSC2 |
| BET4 | PUG1 | GGA1 | SOL1 | XDJ1 |
| DFM1 | COY1 | RSB1 | ATG14 | POF1 |
| COQ2 | GAL83 | RTN2 | AGP1 | BDF2 |
| YKL187C | YER134C | CUP2 | MSS1 | DOG2 |
| NHP10 | DAP2 | PHO89 | REX3 | OPY2 |
| YRO2 | PAP1 | HUA1 | PET20 | NDL1 |
| AIM4 | VPS29 | PHM8 | YNR034W-A | SNX4 |
| TVP15 | YHR202W | YMR034C | ULA1 | TSC13 |
| ULP1 | ARC18 | UBX6 | NGR1 | SPO1 |
| SPO73 | MET12 | GRE2 | MYO3 | FLC2 |
| BGL2 | MHT1 | NDI1 | DGA1 | RPL15B |
| RGS2 | ECM29 | YJL185C | MNN4 | SKM1 |
| GRX3 | DSD1 | GSC2 | YNL193W | YNK1 |
| OMA1 | YGK3 | YJR008W | YDR379C-A | UBC5 |
| MIG3 | SKG3 | GIS1 | YAP1802 | ZWF1 |
| AIM27 | DCR2 | OSW2 | YOR223W | VPS68 |
| YIR024C | YMR160W | SLM1 | ROG3 | YJL016W |
| TRX1 | TIS11 | YDR034W-B | GRX6 | PCT1 |
| BNA1 | PSK1 | HMX1 | MOT3 | ECM4 |
| PUP3 | YIL166C | GSP2 | YPL113C | YML002W |
| LEU2 | YIP3 | NGL3 | MAL31 | DCC1 |
| YHC1 | RPT3 | PRX1 | YBR053C | YMR111C |
| VPS25 | UBP6 | GCY1 | MND2 | AEP3 |
| MSS2 | UBX7 | BTN2 | AZF1 | SNZ1 |
| INO2 | UBP15 | CIN5 | PEX29 | PDE1 |
| YDL086W | FCJ1 | GLG1 | YDL012C | AVO2 |
| YTH1 | YMR052C-A | YGP1 | PIG2 | GYP1 |
| COS6 | LSB3 | SDP1 | GIP4 | NPT1 |
| RSM19 | GPI16 | PFK26 | YGR126W | YGR111W |
| ARL3 | KGD1 | AGP2 | YIR014W | ERV41 |
| YDL119C | ICL2 | SAF1 | MFM1 | UPS3 |
| YOL014W | YOR097C | MNT4 | YDR387C | YOL159C |
| PFY1 | MET17 | POM33 | GRX1 | UBA3 |
| URA10 | NUS1 | YNL144C | MPT5 | YOL162W |
| CPD1 | EMP46 | TDH1 | OSH2 | MND1 |
| YER034W | PDR1 | YGR149W | DOA1 | YJL070C |
| IRC24 | YML116W-A | HSP82 | CAK1 | CLN3 |
| AIM2 | GD11 | KIN82 | HEM15 | YNL155W |
| TDA6 | YOR152C | ISF1 | CSE2 | KTR4 |
| FMP41 | SKO1 | ATG20 | BNA2 | SHC1 |
| RIM21 | UFD1 | YKR011C | SNF3 | PPE1 |
| CRD1 | RPT5 | PXA1 | PKP1 | MPC54 |
| CDC31 | PTC6 | YLR415C | YKL023W | MLH3 |
| MRPL31 | RPN3 | YDL199C | INO1 | AGE2 |
| RBD2 | RPT2 | YFR052C-A | YFL042C | YGR109W-B |
| BI2 | RPN2 | ROM1 | MLS1 | TPP1 |
| GLC8 | SAP1 | LST8 | RSF1 | ADH5 |
| PBI2 | RTG3 | MRP8 | YIP4 | REH1 |
| PHO8 | PST2 | RTK1 | GTO3 | KSP1 |
| CPR2 | YDR319C | YMR090W | TDP1 | YLR001C |
| MOS2 | ARP3 | PIN3 | CAR1 | SPG1 |
| REC107 | QCR7 | PYK2 | RIM20 | ARC35 |
| YAR023C | BDS1 | HSP30 | RSM10 | STI1 |
| PDR8 | ALF1 | SFK1 | MRK1 | YHR180W |
| YIP3 | PSP1 | STE13 | YIL108W | MUK1 |
| KTR1 | YNR048W | COS111 | UBP11 | HAP1 |
| YPL191C | GDH2 | FRE4 | CIT1 | YKR017C |
| TSA2 | AIM21 | MDJ1 | VPS21 | MIH1 |
| FMC1 | SAS5 | GAT2 | YEL057C | ERG9 |
| YGL082W | BTS1 | PDR15 | MAL33 | KKQ8 |
| YOR097C | HRD1 | YMR262W | PET8 | PMA2 |
| PEX7 | DUG2 | UBP5 | SDH3 | DOT6 |
| APC11 | SNU23 | RCR2 | YMR295C | YPL014W |
| YNL217W | YMR226C | FIT1 | RRI1 | TVP38 |
| SPC3 | OCT1 | ADI1 | AIM18 | YOL159C-A |
| TRX2 | YPL191C | YBR284W | MPD1 | PRE10 |
| GPX2 | WTM1 | CPS1 | IMP2' | YBR062C |
| PRP46 | HXT9 | YJL213W | JSN1 | PEP8 |
| YOR072W-A | SOD2 | APJ1 | ISN1 | ISU1 |
| ATP20 | DNM1 | FUN19 | YBR225W | MRS4 |
| YLR050C | IRC24 | YER079W | VTI1 | YCP4 |
| TOM7 | RPN5 | YLR225C | IGO1 | BNA5 |
| MDH3 | FMP27 | ATG5 | INO4 | DDI1 |
| CIT2 | CKI1 | YET1 | AIM6 | YCL042W |
| PEX18 | LYS5 | ATG19 | DGR2 | YER076C |
| OST2 | KIN1 | YLR177W | EMI5 | THO1 |
| GDH3 | TDA11 | CMK1 | YNL097W-A | YDR042C |
| HLJ1 | ATE1 | VHS1 | AHC1 | VCX1 |
| CPR5 | YPT35 | YJL163C | LDH1 | YIA6 |

Results, Part I

| | | | | |
|--|-----------|-----------|-----------|-----------|
| YJL068C | MIA40 | SIA1 | TWF1 | YBR126W-A |
| ALG13 | YBL039W-B | GND2 | YLR349W | YHR140W |
| Glucose starvation specific (polysome enriched) | KRE1 | YET2 | GIP1 | ATG18 |
| | VPS5 | SPG4 | CAD1 | PCL5 |
| | YPL150W | DIA3 | SCO2 | JIP4 |
| YGR035C | CWC21 | PIL1 | SSH4 | CDC15 |
| HAP4 | YNR064C | STB2 | DON1 | MSB3 |
| TPQ2 | AIM2 | VID30 | RRD1 | ADE2 |
| YKL044W | YGR266W | GRX2 | APM1 | MDY2 |
| OLE1 | CAJ1 | LSP1 | AVT3 | SKS1 |
| MSN4 | MGA2 | MET14 | HBN1 | CPR4 |
| HXT3 | PBN1 | GDB1 | ATG29 | RNR3 |
| CTH1 | ASI1 | PTP2 | PEX30 | HAL9 |
| HXT7 | IRC4 | SGA1 | RCK2 | YJR079W |
| ATP6 | UBC7 | RNY1 | YLR164W | YPR013C |
| MRP20 | LDB17 | YMR173W-A | NRG2 | CBT1 |
| ICY1 | STB3 | UBI4 | HVG1 | STE50 |
| ADH1 | YPR172W | VPS73 | DBP1 | NCR1 |
| SUT1 | RPN6 | YPK2 | YLR241W | YMR31 |
| TOS8 | YMR294W-A | YPR036W-A | YDL027C | MST27 |
| YHR162W | SNM1 | YBR056W | ATG4 | RRT6 |
| RPM2 | YOL014W | YMR085W | FOX2 | VPS17 |
| RPS12 | YOR300W | YDR391C | YCR061W | NEM1 |
| SNQ2 | YSR3 | ATG1 | AIM37 | MHP1 |
| Common_glucose and Na ⁺ | PMR1 | FPK1 | MRL1 | FAD1 |
| | PBI2 | TPS3 | PCA1 | TIP41 |
| YRO2 | GLC8 | PXA2 | YMR210W | COQ3 |
| Common_glucose and Ca²⁺ | YGR125W | YKL151C | MLF3 | PCI8 |
| | MSL1 | GPM2 | YBR285W | CWC27 |
| SNA3 | YBP1 | CSH1 | QCR9 | YOR376W-A |
| YDR319C | SIP1 | PTP1 | YGR161W-C | PIB1 |
| ASR1 | FAR8 | YLR312C | APE4 | YOR352W |
| YER134C | ROT2 | PLB1 | GID7 | ABM1 |
| COA4 | CAP2 | SMP1 | KTR2 | ERF2 |
| YPT35 | RAD59 | DAK1 | YBR116C | YIL059C |
| QCR7 | PRM1 | TPK2 | MNR2 | NIT2 |
| YOL073C | APP1 | NTH1 | GPG1 | ACS1 |
| YSF3 | HOS2 | SLT2 | YJR085C | MCH1 |
| COS6 | SEC18 | YGR130C | YPL119C-A | DAL7 |
| YOL014W | ORT1 | RIM11 | CBP4 | RBK1 |
| IRC24 | BEM4 | SPS100 | AVT6 | DAS1 |
| AIM2 | VPS41 | ARO9 | IDP3 | NDE2 |
| GLC8 | CRF1 | YKR075C | YOR292C | YER163C |
| PBI2 | YGR115C | GLO1 | NAB6 | YLL056C |
| YIP3 | SEC9 | GRE1 | YOR131C | MET28 |
| YPL191C | RRD2 | YPS6 | HNT1 | YFL052W |
| YOR097C | COA4 | IME2 | SNX41 | COQ6 |
| MDH3 | TRE2 | YIL077C | YBL029C-A | YPI1 |
| Common_Na⁺ and Ca²⁺ | ENT3 | PHR1 | YCR100C | PEX17 |
| | VPS33 | PPM1 | VID28 | YJR039W |
| YDL109C | YOL163W | STP4 | GYP5 | SUL2 |
| YLR352W | BBC1 | YSC84 | ACH1 | YMR178W |
| | YKL066W | RSC9 | RMD5 | DAL3 |
| | CYR1 | DLD1 | YMR253C | FUN14 |
| | VPS13 | UIP4 | YPK1 | PUS5 |
| | MIC17 | TES1 | YLR446W | ESBP6 |
| | YGR137W | NCE102 | PEP4 | LEU5 |
| | APE3 | YBR241C | ATG15 | ATG9 |
| | MRM2 | YMR315W | RAD2 | RGT2 |
| | ENT2 | SGE1 | MET16 | PEX32 |
| | INH1 | UBC8 | YJU3 | MIG2 |
| | APL1 | SDS22 | PTH1 | AIM3 |
| | BRO1 | LAP4 | BUD7 | CAF120 |
| | HCS1 | ECM27 | SIP4 | AIM41 |
| | ARP2 | FMP40 | VBA2 | RIB4 |
| | FMP37 | SSA1 | HAA1 | HER1 |
| | RUP1 | ARK1 | UBX3 | CPR1 |
| | SSY1 | SOL2 | PPZ2 | SPR3 |
| | YHR112C | BSD2 | MSC3 | |
| | YDR131C | MAL13 | YIL100W | |
| | THI6 | MBF1 | YOL087C | |
| | AMD2 | YER130C | MSK1 | |
| | GDH1 | VHR1 | YIL169C | |
| | YIL067C | SUE1 | RIP1 | |
| | SHR5 | TUL1 | PEX3 | |
| | THO2 | SRY1 | IRC10 | |
| | ATG2 | COX20 | STP3 | |
| | YMR087W | YGR122W | CYT2 | |
| | SED5 | APA2 | YNL200C | |
| | RTG2 | PKP2 | CWP1 | |
| | COS6 | YNL115C | HSP31 | |

| | | | | |
|--|-----------|-----------|---------|--|
| | YOS9 | RCN1 | YTP1 | |
| | AIP1 | YOR289W | ETP1 | |
| | IMA5 | YJR096W | FMP21 | |
| | HSF1 | YMR206W | ZRG8 | |
| | TGL1 | YDR119W-A | NVJ1 | |
| | ERG26 | COX5B | ATG3 | |
| | YOL073C | YBL086C | TGL2 | |
| | PRP4 | LEE1 | IRC3 | |
| | CAP1 | ENB1 | AVT7 | |
| | VRP1 | YLL058W | AIM14 | |
| | ARC40 | YFL054C | YEL020C | |
| | EAR1 | HXT4 | YGL010W | |
| | SRV2 | GUT2 | AIM11 | |
| | YMR316C-B | LUC7 | GLO4 | |
| | CTI6 | SYP1 | MMT2 | |
| | ERG10 | ATG21 | PET10 | |
| | YEF1 | | | |
| | CDC28 | | | |
| | SPO14 | | | |
| | COX23 | | | |
| | XRS2 | | | |
| | YNL260C | | | |
| | SNA3 | | | |
| | CEF1 | | | |
| | SGF73 | | | |
| | RME1 | | | |
| | TPD3 | | | |
| | RPT6 | | | |
| | YLR352W | | | |
| | TOK1 | | | |
| | CHS5 | | | |
| | AKL1 | | | |
| | YMR027W | | | |
| | YHL044W | | | |
| | MDH3 | | | |
| | CAT2 | | | |
| | DAL1 | | | |
| | RIT1 | | | |
| | COS10 | | | |
| | RAV1 | | | |
| | YSF3 | | | |
| | COX15 | | | |
| | TIM21 | | | |
| | SPG3 | | | |
| | KRE2 | | | |
| | PIG1 | | | |
| | PRM9 | | | |
| | ASR1 | | | |
| | YLR099W-A | | | |
| | PRC1 | | | |
| | GLO2 | | | |
| | SPT3 | | | |
| | YNL295W | | | |
| | SEC8 | | | |
| | IOC4 | | | |
| | FYV8 | | | |
| | YDL109C | | | |

Table S2: 3'UTR secondary structure prediction of glucose starvation, Na⁺ and Ca²⁺ candidates.

| glucose starvation candidates | | | | |
|-------------------------------|---|----------------|----------------------------------|--|
| Cluster | Transcripts | ID | Name | Score [Z] |
| | | | | Top 3 cluster motifs (by avg z-score): |
| 1 | YIL059C, YER158C, YDR519W, YBR006W | U5 | U5_spliceosomal_RNA | 3.17 |
| | | MIR821 | RNA_MIR821 | 3.14 |
| | | snR10 | Small_nucleolar_RNA_snR10 | 3.06 |
| 2 | YPL014W, YKR009C, YOR292C | MIR476 | microRNA_MIR476 | 3.13 |
| | | Mir-624 | microRNA_mir-624 | 2.64 |
| | | MIR397 | microRNA_MIR397 | 2.56 |
| | | GEMM_RNA_motif | GEMM_cis-regulatory_element | 4.32 |
| 3 | YGL035C, YOR327C, YMR030W | MIR821 | microRNA_MIR821 | 4.14 |
| | | IS102 | IS102_RNA | 4.11 |
| | | NrrF_RNA | NrrF_RNA | 3.34 |
| 4 | YBR007C, YNL315C, YCL051W, YCL049C | Mir-137 | microRNA_mir-137 | 3.16 |
| | | MIR821 | microRNA_MIR821 | 3.09 |
| | | KCNQ1DN | KCNQ1_downstream_neighbour | 2.25 |
| 5 | YDR313C, YNL265C, YOL159C, YGL082W, YBR165W, YIR035C, YOR223W, YER093C-A, YDR319C | InvR | Invasion_gene-associated_RNA | 2.18 |
| | | CRISPR-DR52 | CRISPR_RNA_direct_repeat_element | 2.17 |
| | | Mir-200 | microRNA_mir-200 | 3.03 |
| 6 | YBR185C, YDL091C, YGR043C, YPL170W, YNL217W | Mir-350 | microRNA_mir-350 | 2.88 |
| | | Mir-450 | microRNA_mir-450 | 2.74 |
| | | Rox2 | Drosophila_rox2_ncRNA | 4.22 |
| 7 | YDL047W, YGR062C, YBL043W | Mir-583 | microRNA_mir-583 | 3.92 |
| | | Mir-764 | microRNA_mir-764 | 3.70 |
| | | Mir-340 | microRNA_mir-340 | 2.89 |
| 8 | YEL038W, YNL135C, YIL117C, YPL088W, YMR071C, YPL026C | SraD | SraD_RNA | 2.70 |
| | | Chlorobi-RRM | Chlorobi-RRM_RNA | 2.68 |

| | | | | |
|----------------|--|---|--|------------------|
| 9 | YLR204W, YOL084W, YER045C | CRISPR-DR42 | CRISPR_RNA_direct_repeat_element | 2.68 |
| | | Rli45 | Listeria_snRNA_rli45 | 2.63 |
| 10 | YKR046C, YFR003C, YGR146C | SnR190 | Small_nucleolar_RNA_snR190 | 2.58 |
| | | Rox2 | Drosophila_rox2_ncRNA | 3.69 |
| 11 | YBR207W, YGL255W, YOL059W | Plasmodium_snoR11 | small_nucleolar_RNA_snoR11 | 3.15 |
| | | CeN115 | C_elegans_sRNA_ceN115 | 3.06 |
| 12 | YHR132C, YDR079W, YJL210W, YMR298W, YJL031C, YGR174C | Mir-556 | microRNA_mir-556 | 3.15 |
| | | Mir-233 | microRNA_mir-233 | 3.06 |
| 13 | YKL043W, YER088C, YOR215C | Alpha_tmRNA | Alphaproteobacteria_transfer-messenger_RNA | 2.81 |
| | | MIR1122 | microRNA_MIR1122 | 2.51 |
| 13 | YKL043W, YER088C, YOR215C | P14 | Pseudomonas_sRNA_P14 | 2.50 |
| | | Mir-556 | MicroRNA_mir-556 | 2.46 |
| 13 | YKL043W, YER088C, YOR215C | Rli24 | Listeria_sRNA_rli22 | 3.37 |
| | | Mycoplasma_FSE | mycoplasma_ribosomal_frameshift_element | 3.30 |
| 13 | YKL043W, YER088C, YOR215C | Bacteroid-tp | Bacteroidete_ryptophan_peptide_leader_RNA | 3.30 |
| | | Na⁺ candidates | | |
| Cluster | Transcripts | ID | Name | Score [Z] |
| | | Top 3 cluster motifs (by avg z-score): | | |
| 1 | YML002W, YIL134W, YLR289W, YPL258C, YNL156C | T-box | T-box_leader | 3.11 |
| | | Mir-764 | microRNA_mir-764 | 3.10 |
| 2 | YLR023C, YLR166C, YDL034W, YBR099C, YLR263W, YKR050W | NrrF | NrrF_RNA | 3.08 |
| | | rydB | rydB_RNA | 2.26 |
| 3 | YLR320W, YDR501W, YHR131C, YDR422C | MIR2118 | microRNA_MIR2118 | 2.22 |
| | | MicF | MicF_RNA | 2.20 |
| 4 | YEL023C, YMR019W, YDL020C | snR85 | Small_nucleolar_RNA_snR85 | 2.73 |
| | | SNORA30 | Small_nucleolar_RNA_SNORA30/SNORA37_family | 2.57 |
| 4 | YEL023C, YMR019W, YDL020C | snoR98 | Small_nucleolar_RNA_snoR98 | 2.56 |
| | | traJ_5 | traJ_5'_UTR | 3.71 |
| 4 | YEL023C, YMR019W, YDL020C | STnc150 | STnc150_Hfq_binding_RNA | 3.04 |
| | | snoR98 | Small_nucleolar_RNA_snoR98 | 2.88 |

| | | | | |
|-----------|---|---|--|--|
| 5 | YGR023W, YJL106W, YHR116W | mir-787 rli32 mir-2780 mir-3 mir-126 mir-605 tRNA | microRNA_mir-787 Listeria_sRNA_rli32 microRNA_mir-2780 microRNA_mir-3 microRNA_mir-126 microRNA_mir-605 tRNA | 4.50 3.40 3.26 5.02 4.94 4.92 3.41 |
| 6 | YDL230W, YLR082C, YBR128C | | | |
| 7 | YKR090W, YNL012W, YOR377W, YOL106W, YNL125C, YNL094W, YPL137C | RsaB snR190 SNORD73 | RNA_Staph_aureus_A Small_nucleolar_RNA_snR190 Small_nucleolar_RNA_SNORD73 | 2.49 2.17 3.60 |
| 8 | YML053C, YIR041W, YIL143C | rli38 MIR403 | Listeria_sRNA_rli38 microRNA_MIR403 | 3.48 3.41 |
| 9 | YGL075C, YOL036W, YBL014C, YDL247W | snoZ107_R87 RyhB | Small_nucleolar_RNA_Z107/R87 RyhB_RNA | 2.84 2.61 |
| 10 | YGR030C, YER040W, YAL005C, YNL082W | snoZ5 SNORA53 SCARNA24 mir-787 | Small_nucleolar_RNA_Z5 Small_nucleolar_RNA_SNORA53 Small_Cajal_body_specific_RNA_24 microRNA_mir-787 | 2.36 3.15 2.94 2.86 |
| 11 | YDR170W-A, YDR210W-A, YNL284C-A, YGR038C-A | MIR403 H19_3 PVX_3 CRISPR-DR40 U5 InvR | microRNA_MIR403 H19_conserved_region_3 Potato_virus_X_cis-acting_regulatory_element CRISPR_RNA_direct_repeat_element U5_spliceosomal_RNA Invasion_gene-associated_RNA | 2.99 2.98 2.96 3.98 3.09 2.78 |
| 12 | YFR040W, YJL132W, YMR180C | mir-249 mir-240 mir-1287 | microRNA_mir-249 microRNA_mir-240 microRNA_mir-1287 | 2.90 2.82 2.57 |
| 14 | YCL019W, YDR210W-B, YPR158W-B, YDR210C-D, YOR192C-B, YLR410W-B, YPR158C-D, YBL005W-B, YOR142W-B, YNL284C-B, YFL002W-A | iscRS T-box StraD | iscR_stability_element T-box_leader StraD_RNA | 3.93 3.83 3.82 |

| | | | | |
|---|------------------------------------|--------------------|--|------------------|
| 15 | YLL028W, YMR182C, YOL011W | SAM_V | SAM-V_riboswitch | 2.98 |
| | | yjF | yjF_RNA | 2.94 |
| | | snR50 | Small_nucleolar_RNA_snR50 | 2.93 |
| 16 | YHL043W, YLR176C, YER081W, YJR079W | rli53 | Listeria_sRNA_rli53 | 3.80 |
| | | snoZ155 | Small_nucleolar_RNA_Z155 | 3.43 |
| | | GAIT | GAIT_element | 3.38 |
| | | Bacteria_small_SRP | Bacterial_small_signal_recognition_particle_RNA | 3.86 |
| 17 | YPL054W, YMR040W, YMR244W | CAESAR | ctgf/hcs24_CAESAR | 3.78 |
| | | BTE | Luteovirus_cap-independent_translation_element_(BTE) | 3.53 |
| | | GadY | GadY | 3.28 |
| 18 | YIR013C, YOR306C, YFR032C | PyrR | PyrR_binding_site | 3.15 |
| | | rli53 | Listeria_sRNA_rli53 | 3.12 |
| | | bxd_6 | Bithoraxoid_conserved_region_6 | 2.55 |
| 19 | YJR061W, YHR096C, YDR222W | snoU18 | Small_nucleolar_RNA_U18 | 2.35 |
| | | CRISPR-DR57 | CRISPR_RNA_direct_repeat_element | 2.35 |
| | | mir-2780 | microRNA_mir-2780 | 2.56 |
| 20 | YOR214C, YER157W, YOR181W, YKR069W | SraD | SraD_RNA | 2.40 |
| | | STnc150 | STnc150_Hfq_binding_RNA | 2.33 |
| Ca²⁺ candidates | | | | |
| Top 3 cluster motifs (by avg z-score): | | | | |
| Cluster | Transcripts | ID | Name | Score [Z] |
| 1 | YDR466W, YKR076W, YDL215C, YPR075C | CRISPR-DR52 | CRISPR_RNA_direct_repeat_element | 2.58 |
| | | MicF | MicF_RNA | 2.53 |
| | | Phe_leader | Phenylalanine_leader_peptide | 2.44 |
| 2 | YLR001C, YJL070C, YJL036W | traJ_5 | traJ_5_UTR | 3.58 |
| | | mir-217 | microRNA_mir-217 | 3.57 |
| | | rli53 | Listeria_sRNA_rli53 | 3.36 |
| 3 | YDR173C, YCL034W, YPL161C | CRISPR-DR40 | CRISPR_RNA_direct_repeat_element | 3.86 |
| | | C0299 | C0299_RNA | 3.62 |
| | | Plasmid_RNAIII | Plasmid_RNAIII | 3.6 |

| | | | | |
|-----------|---|--------------------|---|------|
| 4 | YGL181W, YFR050C, YOR152C | rox2 | Drosophila_ rox2_ncRNA | 2.93 |
| | | AMV_RNA1_SL | Alfalfa_mosaic_virus_RNA_1_5'_UTR_stem-loop | 2.78 |
| 5 | YMR004W, YOR197W, YOR138C | snoR72 | Small_nucleolar_RNA_R72 | 2.65 |
| | | mir-6 | mir-6_microRNA_precursor | 3.78 |
| | | mir-350 | microRNA_mir-350 | 3.74 |
| | | mir-71 | microRNA_mir-71 | 3.55 |
| | | mir-316 | microRNA_mir-316 | 5.16 |
| | | mir-135 | mir-135_microRNA_precursor_family | 4.58 |
| | | mir-651 | microRNA_mir-651 | 4.27 |
| | | mir-3 | microRNA_mir-3 | 3.76 |
| | | mir-126 | microRNA_mir-126 | 3.71 |
| | | MIR1428 | microRNA_MIR1428 | 3.55 |
| 8 | YLR107W, YMR266W, YNL020C, YDR032C, YOR128C | snR85 | Small_nucleolar_RNA_snR85 | 2.85 |
| | | mir-384 | microRNA_mir-384 | 2.8 |
| | | mir-983 | microRNA_mir-983 | 2.79 |
| | | snoR29 | small_nucleolar_RNA_snoR29 | 3.11 |
| | | snoR20 | Small_nucleolar_RNA_R20 | 2.89 |
| 9 | YCL047C, YKL195W, YDR058C, YPL150W | ceN84 | C._elegans_snoRNA_ceN84 | 2.85 |
| | | Bacteria_small_SRP | Bacterial_small_signal_recognition_particle_RNA | 3.13 |
| | | ceN101 | C._elegans_snoRNA_ceN101 | 3.07 |
| | | PK-PYVV | 3-terminal_pseudoknot_in_PYVV | 2.83 |
| | | mir-787 | microRNA_mir-787 | 3.54 |
| | | snoZ266 | Small_nucleolar_RNA_Z266 | 3.47 |
| | | traJ-II | traJ-II_RNA | 3.46 |
| | | mir-5 | microRNA_mir-5 | 4.55 |
| | | MIR473 | microRNA_MIR473 | 4.37 |
| | | STnc290 | -STnc290_Hfq_binding_RNA | 3.78 |
| 12 | YOL151W, YLR026C | MIR444 | microRNA_MIR444 | 4.59 |
| | | MIR2118 | microRNA_MIR2118 | 4.14 |
| | | mir-32 | microRNA_mir-32 | 3.81 |
| 13 | YGL084C, YFR004W, YLR370C | | | |
| | | | | |
| | | | | |
| | | | | |
| | | | | |
| | | | | |
| | | | | |
| | | | | |
| | | | | |
| | | | | |
| | | | | |

| | | | | |
|-----------|--|--|--|-----------------------------|
| 14 | YOL164W, YDL193W, YNL183C, YMR020W, YPL109C, YDR210W | HOTAIR_1 RsaB | HOTAIR conserved region_1 RNA_Staph._aureus_A | 2.55 |
| 15 | YLR324W, YNL277W | GIR1 mir-351 mir-200 mycoplasma_FSE | GIR1_branching_ribozyme microRNA_mir-351 microRNA_mir-200 mycoplasma_ribosomal_frameshift_element | 2.28 4.36 4.28 4.1 |
| 16 | YER143W, YML057W, YOR209C | snR35 MIR1444 RNA-OUT | Small_nucleolar_RNA_snR35 microRNA_MIR1444 RNA-OUT | 3.57 3.46 3.4 |
| 17 | YLR187W, YDR379C-A, YJL149W, YER068W, YHL048W | ceN54 MIR403 CRISPR-DR44 | C._elegans_snoRNA_ceN54 microRNA_MIR403 CRISPR_RNA_direct_repeat_element | 2.84 2.57 2.34 |
| 18 | YFR021W, YBR229C, YGL013C | mir-2778 mir-318 mir-126 mir-981 | microRNA_mir-2778 microRNA_mir-318 microRNA_mir-126 microRNA_mir-981 | 3.19 3.1 3.09 3.71 |
| 19 | YIL034C, YKR016W, YBR237W | snoU6-47 HOTAIR_4 | Small_nucleolar_RNA_U6-47 HOTAIR_intron_conserved_region_4 | 3.43 3.36 |
| 20 | YOR352W, YHR180W, YGL126W | mir-583 mir-624 Chlorobi-RRM | microRNA_mir-583 microRNA_mir-624 Chlorobi-RRM_RNA | 6.83 6.52 6.26 |
| 21 | YGL062W, YDR368W, YFR024C-A | MIR473 Thr_leader Leu_leader | microRNA_MIR473 Threonine_operon_leader Leucine_operon_leader | 4.27 4.08 3.86 |
| 22 | YAL016W, YFR039C, YPL028W | Entero_CRE TB11Cs2H1 ctfRNA_pND324 | Enterovirus_cis-acting_replication_element Trypanosomatid_snoRNA_TB11Cs2H1 ctfRNA | 2.76 2.55 2.51 |
| 23 | YPR117W, YLL062C, YKR031C, YOR069W, YDR475C, YNR001C | rli32 RsaB CRISPR-DR44 | Listeria_sRNA_rli32 RNA_Staph._aureus_A CRISPR_RNA_direct_repeat_element | 2.96 2.65 2.63 |

| | | | | |
|-----------|------------------------------------|----------------|---|------|
| 24 | YOR213C, YBR016W, YKL145W, YKR098C | rfi32 | Listeria_sRNA_rfi32 | 3.34 |
| | | MIR807 | microRNA_MIR807 | 3.33 |
| 25 | YDL045C, YKL105C, YPL228W | mir-556 | microRNA_mir-556 | 3.24 |
| | | mir-787 | microRNA_mir-787 | 4.44 |
| | | SBWMV2_UPD-PKI | Pseudoknot_of_upstream_pseudoknot_domain_(UPD)_of_the_3'UTR | 3.87 |
| | | SNORA36 | Small_nucleolar_RNA_SNORA36_family | 3.69 |

Table S3. List of primers used in this study.

| Primer ID | Designation | Sequence |
|-----------|---------------------------------|--|
| CK059 | Dcp2 S2 C-tagging-forward | TTCAATTACAGTGTGCTATAAAAACGTATAACACTTATCTTTCAATCGATGAATTCGAGCTCG |
| CK060 | Dcp2 S3 C-tagging-reverse | GGAACTTCAGGGTCTAATGAATTTAAGCAATTTGCATAGGAAGCGGTACGCTGCAGGGTCGAC |
| CW156 | 3' adapter (RA3) | TGGAATTCGGGTGCCAAGG |
| SH138 | 5' adapter (RA5) | GUUCAGAGUUCUACAGUCCGACGAUC |
| CW157 | Illumina Indexing Primer (RPI1) | CAAGCAGAAGACGGGCATACGAGATCGTGACTGGAGTTCCCTTGGCACCCCGAGAAATTCCA |
| CW158 | Illumina Indexing Primer (RPI2) | CAAGCAGAAGACGGGCATACGAGATACATCGGTGACTGGAGTTCCCTTGGCACCCCGAGAAATTCCA |
| CW159 | Illumina Indexing Primer (RPI3) | CAAGCAGAAGACGGGCATACGAGATGCCTAAGTGACTGGAGTTCCCTTGGCACCCCGAGAAATTCCA |
| CW160 | Illumina Indexing Primer (RPI4) | CAAGCAGAAGACGGGCATACGAGATTTGGTCAAGTACTGGAGTTCCCTTGGCACCCCGAGAAATTCCA |
| CW244 | PGK1_1 FISH-forward | TTTGGAACACACCCCAAGAT |
| CW245 | PGK1_1 FISH-reverse | TAATACGACTCACTATAGGGAGCGTTCTTTCACCCGTTTGGT |
| CW246 | PGK1_2 FISH-forward | TGCGTTACCACATCGAAGAA |
| CW247 | PGK1_2 FISH-reverse | TAATACGACTCACTATAGGGAGCATCTTCCCTTGGAAAGCCTTG |
| CW248 | PGK1_3 FISH-forward | GGTGGTGGTATGGCTTTTCAC |
| CW249 | PGK1_3 FISH-reverse | TAATACGACTCACTATAGGGAGCGAAGATGGAGTCAACCAGATT |
| CW250 | PGK1_4 FISH-forward | TTCTCTGCTGATGCCAACAC |
| CW251 | PGK1_4 FISH-reverse | TAATACGACTCACTATAGGGAGCGCCAGCTGGAATACCTTC |
| CW252 | PGK1_5 FISH-forward | ACTGGTGGTGGTCTTCTTT |
| CW253 | PGK1_5 FISH-reverse | TAATACGACTCACTATAGGGAGAGAAAACAACACCTGGCAATTC |
| CW963 | PGK1 qPCR-forward | TTGATTGACAACTTGTGGGA |
| CW964 | PGK1 qPCR-reverse | CAGTGACAGTCTTGGTGTTG |
| CW278 | ACT1_1 FISH-forward | CTGAGGTTGCTGCTTTGGTT |
| CW279 | ACT1_1 FISH-reverse | TAATACGACTCACTATAGGGAG GCAAAAACCGGCTTTACACAT |
| CW280 | ACT1_2 FISH-forward | TGTCACCAACTGGGACGATA |
| CW281 | ACT1_2 FISH-reverse | TAATACGACTCACTATAGGGAG TGTTCCTTCTGGGGCAACTCT |
| CW282 | ACT1_3 FISH-forward | CGTTCCAAATTTACGCTGGTT |
| CW283 | ACT1_3 FISH-reverse | TAATACGACTCACTATAGGGAG GGCCAAAATCGATTCTCAAAA |
| CW284 | ACT1_4 FISH-forward | TCCACCACTGCTGAAAGAGA |
| CW285 | ACT1_4 FISH-reverse | TAATACGACTCACTATAGGGAG GAAGTCCAAGGGGACGCTAAC |

| | | |
|-------|------------------------------------|---|
| CW286 | ACT1_5 FISH-forward | ACATCGTTATGTCCGGTGGT |
| CW287 | ACT1_5 FISH-reverse | TAATACGACTCACTATAGGGGAG CGGTGATTCCTTTTGCATT |
| CW288 | ACT1_6 FISH-forward | TCCATCTCCATGAAGGTCA |
| CW289 | ACT1_6 FISH-reverse | TAATACGACTCACTATAGGGGAG CCACCAATCCAGACGGGAGTA |
| CW961 | ACT1 qPCR-forward | AGGTTGCTGCTTTGGTTATTG |
| CW962 | ACT1 qPCR-reverse | CCGACGATAGATGGGAAGAC |
| CW560 | BSC1_1 FISH-forward | TCCGTATCATGGGTCAAGGA |
| CW561 | BSC1_1 FISH-reverse | TAATACGACTCACTATAGGGGAGGAGCCGTTGACACCAA |
| CW562 | BSC1_2 FISH-forward & qPCR-forward | TCTGACGGTTGCACAGTTTG |
| CW563 | BSC1_2 FISH-reverse | TAATACGACTCACTATAGGGGAGTGCCAAAGTTTGCCAGTACTG |
| CW564 | BSC1_3 FISH-forward | CCTGGATTTTATTGGACCTACC |
| CW565 | BSC1_3 FISH-reverse | TAATACGACTCACTATAGGGGAGGTAGTAATGATGAAAGACGAGGCTTT |
| CW566 | BSC1_4 FISH-forward | TTCATCAAGCGTAGCCGATA |
| CW567 | BSC1_4 FISH-reverse | TAATACGACTCACTATAGGGGAGTGAAGTGAAGTGAAGTGAAGGCTGAAAGGA |
| CW729 | BSC1 qPCR-reverse | TGCCAAGTTTGCCAGTACTG |
| CW584 | TPI1_1 FISH-forward | AAACGGTTCCAAACAATCCA |
| CW585 | TPI1_1 FISH-reverse | TAATACGACTCACTATAGGGGAGTGAGGACAGATAACAACCTTCG |
| CW586 | TPI1_2 FISH-forward | CGCCTACTTGAAGGCTCTG |
| CW587 | TPI1_2 FISH-reverse | TAATACGACTCACTATAGGGGAGGAGTGACCCCAAAATAACC |
| CW588 | TPI1_3 FISH-forward & qPCR-forward | CAATTGAACCGCTGCTTTGGA |
| CW589 | TPI1_3 FISH-reverse | TAATACGACTCACTATAGGGGAGTCTGGAGTAGCAGGACGACCCAAACC |
| CW590 | TPI1_4 FISH-forward | GCCAGCGAATTGAGAATCTT |
| CW591 | TPI1_4 FISH-reverse | TAATACGACTCACTATAGGGGAGATCGACATCAGCCTTGTCCT |
| CW734 | TPI1 qPCR-reverse | TCTGGAGTAGCAGCCAAACC |
| CW766 | RLM1_1 FISH-forward | AAGAAGGCCCATGAACTATCC |
| CW767 | RLM1_1 FISH-reverse | TAATACGACTCACTATAGGGGAGACGTTATTGGACCCCCAGT |
| CW768 | RLM1_2 FISH-forward | CCGAGTGCACACATGAAGTT |
| CW769 | RLM1_2 FISH-reverse | TAATACGACTCACTATAGGGGAGGCTTCTCAGGATGACGTTT |
| CW770 | RLM1_3 FISH-forward | CCTTTAATGGTCGCTCCCA |
| CW771 | RLM1_3 FISH-reverse | TAATACGACTCACTATAGGGGAGGTCCTTGAGGATGCATTTG |

| | | |
|--------|-------------------------------------|--|
| CW772 | RLM1_4 FISH-forward & qPCR-forward | AGGCCCTTAACTCTCCAAA |
| CW773 | RLM1_4 FISH-reverse | TAATACGACTCACTATAGGGAGTAGAACCGTTAGGCGCATT |
| CW774 | RLM1_5 FISH-forward | AATATTCCTGGCGGACCTTT |
| CW775 | RLM1_5 FISH-reverse | TAATACGACTCACTATAGGGAGTGTGGTATTGCTGGGTTTG |
| CW776 | RLM1_6 FISH-forward | CGGAAACACAAACAATCCT |
| CW777 | RLM1_6 FISH-reverse | TAATACGACTCACTATAGGGAGGTGCTGCTGATAATTGCTGGA |
| CW1178 | RLM1 qPCR-reverse | TAGAACCGTTAGGGCATT |
| CW1027 | ATP11_1 FISH-forward | CTAATCAGCTGTCGCCCAT |
| CW1028 | ATP11_1 FISH-reverse | TAATACGACTCACTATAGGGAGGGGCTGGAAGAATAAAAAACG |
| CW1029 | ATP11_2 FISH-forward | GGAAGAGGCTCAAAAAACAAGG |
| CW1030 | ATP11_2 FISH-reverse | TAATACGACTCACTATAGGGAGAGTCTTTTCAGGGGGTTCGAT |
| CW1031 | ATP11_3 FISH-forward | TGGATGTTGGAAAACTGAAGG |
| CW1032 | ATP11_3 FISH-reverse | TAATACGACTCACTATAGGGAGCTTTTGTGCCCATCTTGTCT |
| CW1033 | ATP11_4 FISH-forward | ATGGCAAAATGCCAGGAATAA |
| CW1034 | ATP11_4 FISH-reverse | TAATACGACTCACTATAGGGAGGTCGGTTTTGCATCCTCAG |
| CW1035 | ATP11_5 FISH-forward | GGAATTTGCAAGGCCACATA |
| CW1036 | ATP11_5 FISH-reverse | TAATACGACTCACTATAGGGAGGTTCAACATGGCCATTTCAT |
| CW1037 | ATP11_6 FISH-forward & qPCR-forward | TATGGTGCATGGGTGAAGA |
| CW1038 | ATP11_6 FISH-reverse | TAATACGACTCACTATAGGGAGCCCGGAGAGGCCCTTAGAGAAA |
| CW976 | ATP11 qPCR-reverse | TCAATTTCTCGACGGTGAATC |
| CW995 | ILM1_1 FISH-forward | CAAGCCTTGAACCTCCACCAA |
| CW996 | ILM1_1 FISH-reverse | TAATACGACTCACTATAGGGAGACAAAAGAAGCGCATCGTGA |
| CW997 | ILM1_2 FISH-forward | GCAAGCGATGAATTTACCCG |
| CW998 | ILM1_2 FISH-reverse | TAATACGACTCACTATAGGGAGCAGAAGAGCGAAAAGACCCCA |
| CW999 | ILM1_3 FISH-forward | TTCCAACTGTTGTGCCAGT |
| CW1000 | ILM1_3 FISH-reverse | TAATACGACTCACTATAGGGAGTTGACTCCCAAAAGGTACGAGA |
| CW1001 | ILM1_4 FISH-forward | TGCCATTAGGGAGGAGAAAA |
| CW1002 | ILM1_4 FISH-reverse | TAATACGACTCACTATAGGGAGTGGGTTCTTCAATATCCTCAT |
| CW1003 | ILM1_5 FISH-forward | CCGTGAAGACTGAAACCACA |
| CW1004 | ILM1_5 FISH-reverse | TAATACGACTCACTATAGGGAGCTTTCCCATCTTCATCGTCA |

| | | |
|---------------|--------------------------------|--|
| CW969 | ILM1 qPCR-forward | CAATGGGCTCTTTTCGCTCT |
| CW970 | ILM1 qPCR-reverse | CTGGCAACACAGATTGGAAG |
| CW1107 | MRPL38_1 FISH-forward | CGACAAATTCAGGGTGCACAAT |
| CW1108 | MRPL38_1 FISH-reverse | TAATAGCACTCACTATAGGGAGCCAAACCATTGCAGGACTCTT |
| CW1109 | MRPL38_2 FISH-forward | GCAAAGCCCTTGACTCAAAA |
| CW1110 | MRPL38_2 FISH-reverse | TAATAGCACTCACTATAGGGAGACGACAAATTCGGTGACAAAAT |
| CW1111 | MRPL38_3 FISH-forward | ACCGTTGCATTGGAGATAC |
| CW1112 | MRPL38_3 FISH-reverse | TAATAGCACTCACTATAGGGAGTCTTGTCCCCAGAGGTTCCAC |
| CW1113 | MRPL38_4 FISH-forward | TGGCTAATGATGGTTGTGTAGA |
| CW1114 | MRPL38_4 FISH-reverse | TAATAGCACTCACTATAGGGAGACCCTACTTGGCCAAAAGAGCA |
| CW993 | MRPL38 qPCR-forward | GTGAACCTCTGGGGACAAGA |
| CW994 | MRPL38 qPCR-reverse | ACCCTACTTGCCAAAAGAGCA |
| CW880 | AIM2_1 FISH-forward | AGTTTGTACAGATGGAACACC |
| CW881 | AIM2_1 FISH-reverse | TAATAGCACTCACTATAGGGAGGGGAGATGTAGAGCCTGCTG |
| CW882 | AIM2_2 FISH-forward | TGTGTATGGCAATAAATTCACAAA |
| CW883 | AIM2_2 FISH-reverse | TAATAGCACTCACTATAGGGAGCCCATGTACCCAGCACTAGCA |
| CW884 | AIM2_3 FISH-forward | CGATGCTATCTCATCGGACA |
| CW885 | AIM2_3 FISH-reverse | TAATAGCACTCACTATAGGGAGTCTTGGTGACTTCAGGAGAATG |
| CW886 | AIM2_4 FISH-forward | TTTGCCGTCCAACACATTAG |
| CW887 | AIM2_4 FISH-reverse | TAATAGCACTCACTATAGGGAGCGAAAGATGGATGTGCAATG |
| CW888 | AIM2_5 FISH-forward | GCAATTGATAGCAAGAAACCCAA |
| CW889 | AIM2_5 FISH-reverse | TAATAGCACTCACTATAGGGAGGTTTGGCCGGAAAGATGTGAT |
| CW890 | AIM2_6 FISH-forward | CTCTTCAGTGGTGTGGCTCA |
| CW1179 | AIM2 qPCR-forward | TTTGCCGTCCAACACATTAG |
| CW1180 | AIM2 qPCR-reverse | CGAAAGATGGATGTGCAATG |
| JW270 | RPL37b qPCR-forward | ATTCGGTAAGCGTCACAA |
| JW271 | RPL37b qPCR-reverse | CCACAAGAGGAAACAGGTC |
| SH809 | hRLuc qPCR-forward | TCATATCGCCTCCTGGAT |
| SH810 | hRLuc qPCR-reverse | CTTGTCTTGGTGTCTCGTA |
| SH732 | Xm1 S1 deletion-forward | TCAACACTTGTAACAACAGCAGCAACAATAATATACAGTACGGTCAGCTGAAGCTTCGTACGC |
| SH733 | Xm1 S2 deletion-reverse | ACTATTAAAGTAACTCGAATACTCTCGTTTTTAGTCGTATGTTGCATAGGCCACTAGTGGATCTG |

| | | |
|---------------|----------------------------------|--|
| CW1149 | Puf5 S1 deletion-forward | TCTAC GCAAAATTTAT AAATCAATTA CGATTTTCC AGTTTCTCTT ATG CGTACGCTGCAGGTCGAC |
| CW1150 | Puf5 S2 deletion/tagging-reverse | TTTGTACAGTAGAAGGAAAGAAAAGAAAAGAAAAGAAAAGTATTA ATCGATGAATTCGAGCTCG |
| CW1151 | Puf5 S2 tagging-forward | CCATGAATAC CGCTAGAACA TCTGATGAAC TTCAATTCAC TTTGCCA CGTACGCTGCAGGTCGAC |
| CK504 | Puf3 pUG deletion-forward | TACGCATTTTAAA TTTCTTCTGAATAACGCAATATTGCGGGTATAACAGCTGAAGCTTCGTACG |
| CK505 | Puf3 pUG deletion-reverse | AAAAAAAATAGTAAAAAGTGAAGGAGAACGATGATAACACTAAGCATAGGCCACTAGTGGATCTG |
| CW1152 | Puf6 S1 deletion-forward | AGTA CTGAAATAAA GCACAAATCAG GAAATAACAAA TTAAC TGACA ATG CGTACGCTGCAGGTCGAC |
| CW1153 | Puf6 S2 deletion-reverse | CAGATGCTTATATACCAAAATTTGACTTTATCGTAGAAAAATTTAATCGATGAATTCGAGCTCG |
| CW1342 | Sbp1 S1 deletion-forward | GAAGTTTCCCCAAAAG AAAGAAGAAA ACCCTCAAAAC GAAGAAAAAT ATGCGTACGCTGCAGGTCGAC |
| CW1343 | Sbp1 S2 deletion-reverse | AACTTAGCAAAAACCTCAAGTTAGAAATAGGGATGTTGGTAAAGAAATAAATCGATGAATTCGAGCTCG |
| CW1330 | Khd1 S1 deletion-forward | GCATCAACTTACGGGTAAC TTAGAGACAG CATTAGTATA TATACCAGCC ATGCGTACGCTGCAGGTCGAC |
| CW1331 | Khd1 S2 deletion-reverse | GATAGTTGTTTTGCTGTGTTGGACGTCGCGCACGACACGATATACTAATACTGATGAATTCGAGCTCG |
| CW1333 | Pbp2 S1 deletion-forward | TCCAGCGGGCATTAAAT AATCTTTCTG TAATACTCTT TAGCTCAATT ATGCGTACGCTGCAGGTCGAC |
| CW1334 | Pbp2 S2 deletion-reverse | GTTTTGTTTTTATTTCTATGTGTTTTTATTGACTAGCAGTATATTTAATCGATGAATTCGAGCTCG |
| CW1339 | Ngr1 S1 deletion-forward | AGCTTTTTCATATCC TTCGC CATCGATTTT TGCC TGAAAA ATTTACACAA ATGCGTACGCTGCAGGTCGAC |
| CW1340 | Ngr1 S2 deletion-reverse | GATAAACTGCGGACAAGATTAAAAATTTCTTTTTTGTCTTTGTAATCAATCGATGAATTCGAGCTCG |
| JW17 | Whi3 S1 deletion-forward | GCC TTT ATC GAT CAA TAT TTC AGA GGG AAA AAC CTG TAT CTC TTA GCA TGC GTA CGC TGC AGG TCG AC |
| JW16 | Whi3 S2 deletion-reverse | TAT AAT GTG ATA CAT GCA AGG AAA TCA GGT TTT TGC GGA ACC ATT TTT TTA ATC GAT GAA TTC GAG CTC G |
| CW1303 | Bsc1 S2 C-tagging-forward | GTAGTCACAGCGCTTGAACACTAGTTGGGCTCTTGAACCTTGAACCTTACTACTTAATCGATGAATTCGAGCTCG |
| CW1304 | Bsc1 S3 C-tagging-reverse | CGATG TAACCAGTTC AACCATCAA ACTACTCTG TTGATCCAAC CACTCGTACGCTGCAGGTCGAC |
| CW1257 | Atp11 S2 C-tagging-forward | TGTCATTAATATATATATATATATATATACGTATACGGAAGTAAATTCCTCGTTAAATCGATGAATTCGAGCTCG |
| CW1256 | Atp11 S3 C-tagging-reverse | GGAT TCACCGTCGA GAAATTGATT TCGCTATCAC AGTCCATGGA AAA TCGTACGG TCGCAGGTCGAC |
| CW1394 | HSP42 3'UTR repl-forward | GAC GAAAGAA TTGG AGTTTGAAGAAAATCCCAAC CCTACGGTAG AAAAT TGAGAGCTCGTTTTTCACACTGG |
| CW1395 | HSP42 3'UTR repl-reverse | TTATCCGAGCAAGTCGATGAAGAAAACCGCTTTTGTACAGTACAATGGTCCCTACCATAAGTTGATC |
| CW1396 | SEC59 3'UTR repl-forward | TTTTGATACC TGCATTTATG ATGAT TTGTG AAAAAATTAAT TACTCTTTGAGAGCTCGTTTTTCGACACTGG |
| CW1397 | SEC59 3'UTR repl-reverse | CCGTCAAAAAGAAGGATGACGTTAAACCTGAAATGGCTAACAAAAGTGGGAGCTCGTTTTTCGACACTGG |
| CW1399 | YLR042C 3'UTR repl-forward | GTCT TTACTTCGTT TTAATGTTAG AAACAATCGC TTATTTGTTT TCTTAAGAGCTCGTTTTTCGACACTGG |
| CW1400 | YLR042C 3'UTR repl-reverse | TAAAACTCCATGAAGAA TGCCATGTCTGCATCTGCAGCTGCGGACCTGGTCCCTACCATAAGTTGATC |
| CW1382 | ATP11-SEC59 3'UTR repl-forward | TTTTGATACC TGCATTTATG ATGAT TTGTG AAAAAATTAAT TACTCTTTGACGA AGAATTTACTT CCGTATACGT |
| CW1383 | ATP11-SEC59 3'UTR repl-reverse | CCGTCAAAAAGAAGGATGACGTTAAACCTGAAATGGCTAACAAAAGTGGAAATACGTACCTTTGGGACCCAGA |
| CW1386 | ATP11-YLR042C 3'UTR repl-forward | GTCT TTACTTCGTT TTAATGTTAG AAACAATCGC TTATTTGTTT TCTTAACGA AGAATTTACTT CCGTATACGT |
| CW1387 | ATP11-YLR042C 3'UTR repl-reverse | GTTTCGTAACGGATATCGAAATCACTTTGATTAGAAAACAAATACGCCCGGAATAA TACGTACCTTTGGGACCCAGA |

| | | |
|---------------|---|---|
| CW1388 | BSC1-SEC59_3 UTR repli-forward | TTTTGATACC TGCATTTATG ATGATTTTGTG AAAAAATTAAT TACTCTTTGAGTA GTAAGTTCAA GTTCAGAAG |
| CW1389 | BSC1-SEC59_3 UTR repli-reverse | CCGTAAAAAGAGGATGACGTTAAACCTGAATTTGGCTAACAAAAAGTGTGGCTACTTTAGATCAGCTGAACCTTG |
| CW1392 | BSC1-YLR042C_3 UTR repli-forward | GTCT TTACTTCGTT TTAATGTTAG AAACAATCGC TTATTTGTTT TCITTAAGTA GTAAGTTCAA GTTCAGAAG |
| CW1393 | BSC1-YLR042C_3 UTR repli-reverse | GTTTCGTAACCTGGATATCGAAATCAGTTGATTAGAAACAATACGCCGGAATGCTACTTAGATCAGCTGAACCTTG |
| CW1407 | YLR042C_1 FISH-forward | CGCCCCAATTGTGCTACTAC |
| CW1408 | YLR042C_1 FISH-reverse | TAATACGACTCACTATAGGGAGCAGCTTTCTGTCCAAGGGCAG |
| CW1409 | YLR042C_2 FISH-forward | TCATCTTCCAAGCACCACCT |
| CW1410 | YLR042C_2 FISH-reverse | TAATACGACTCACTATAGGGAGACGACGATGATGAAAAGCCG |
| CW1411 | YLR042C_3 FISH-forward | CCAAAAAGTCACTTCCAGCGT |
| CW1412 | YLR042C_3 FISH-reverse | TAATACGACTCACTATAGGGAGCTCGACGAAGAAGGCAA TGG |
| CW1413 | YLR042C_4 FISH-forward | GTTCAAGTACAAGCACAGGAGG |
| CW1414 | YLR042C_4 FISH-reverse | TAATACGACTCACTATAGGGAGACAAAGTAAAGACATGGCTTGAC |
| CW190 | SEC59_1 FISH-forward | GAAGCCAAATGCCAACTGAG |
| CW191 | SEC59_1 FISH-reverse | TAATACGACTCACTATAGGGAGGCCCCACATCAAA TTTACGA |
| CW192 | SEC59_2 FISH-forward | TGGTGTGTTTGATAATGGTTGG |
| CW193 | SEC59_2 FISH-reverse | TAATACGACTCACTATAGGGAGCGCAACTTGGGTAGGCTTTTG |
| CW194 | SEC59_3 FISH-forward | GATGGCGAACTCAGTTGGTAG |
| CW195 | SEC59_3 FISH-reverse | TAATACGACTCACTATAGGGAGCCTGTCAACCAGCCTCAAAAT |
| CW196 | SEC59_4 FISH-forward | TTTCAGAGGCTGGCACAGTA |
| CW197 | SEC59_4 FISH-reverse | TAATACGACTCACTATAGGGAGGCAAGGATAATGCCCTTCAA |
| CW198 | SEC59_5 FISH-forward | CATCGGGCTTCCACTTTT |
| CW199 | SEC59_5 FISH-reverse | TAATACGACTCACTATAGGGAGGCCAAAAGTAGCGGATTTTCA |
| CW200 | SEC59_6 FISH-forward | AACACCTCCGAAAAATTGTG |
| CW201 | SEC59_6 FISH-reverse | TAATACGACTCACTATAGGGAGTGAATCCA TTTTGGAA TGACG |
| CW202 | SEC59_7 FISH-forward | TGCTGATGATAGGGACCACA |
| CW203 | SEC59_7 FISH-reverse | TAATACGACTCACTATAGGGAGAAAGGTGTTGATATTTCCGAAGAG |
| CW204 | SEC59_8 FISH-forward | TCGTTGAAAAAGGTACACAAAAA |
| CW205 | SEC59_8 FISH-reverse | TAATACGACTCACTATAGGGAGCCAAAACAACGATAAAAACCTCG |
| CW1396 | SEC59_pCore_forward | TTTTGATACCTGCATTTATG ATGATTTGTG AAAAA TTAATTACTCTTTGAGAGCTCGTTTTCCGACACTGG |
| CW1397 | SEC59_pCore_reverse | CCGTAAAAAGAGGATGACGTTAAACCTGAATTTGGCTAACAAAAAGTGTGGTCTTACCATTAAAGTTGATC |
| CW1399 | YLR042C_pCore_forward | GTCTTTACTTCGTT TTAATGTTAG AAACAATCGCTTATTTGTTT TCITTAAGAGCTCGTTTTCCGACACTGG |

| | | |
|---------------|--|---|
| CW1401 | YLR042C_pCore_reverse | GTTTCGTAAGTGGATATCGAAATCAGTGGATTAGAAACAATACGCCGGAAATTCCTTACCATTAAGTTGATC |
| CW1388 | <i>BSC1-SEC59 300 3'_repl_forward</i> | TTTTGATACC TGCATTTATG ATGATTTGTG AAAAAATTAAT TACTCTTTGAGTA GTAAGTTCAA GTTCAGAAAG |
| CW1389 | <i>BSC1-SEC59 300 3'_repl_reverse</i> | CCGTCAAAAAGGAGGATGACGTTAAACCTGAATTTGGCTAACAAAAAGTGGGCTACTTTAGATCAGCTGAAC TTG |
| CW1382 | <i>ATP11-SEC59 300 3'_repl_forward</i> | TTTTGATACC TGCATTTATG ATGATTTGTG AAAAAATTAAT TACTCTTTGACCGA AGAATTACTT CCGTATACGT |
| CW1383 | <i>ATP11-SEC59 300 3'_repl_reverse</i> | CCGTCAAAAAGGAGGATGACGTTAAACCTGAATTTGGCTAACAAAAAGTGGAAATACGTACCTTTGGGACCCACAGA |
| CW1392 | <i>BSC1-YLR042C 300 3'_repl_forward</i> | GTCCTTACTTCGTTTTAATGTTAG AAACAATCGCTTATTTGTTTTCTTAAAGTAGTAAGTTCAAGTTCAGAAAG |
| CW1393 | <i>BSC1-YLR042C 300 3'_repl_reverse</i> | GTTTCGTAAGTGGATATCGAAATCAGTGGATTAGAAACAATACGCCGGAAATGCTACTTAGATCAGCTGAAC TTG |
| CW1386 | <i>ATP11-YLR042C 300 3'_repl_forward</i> | GTCCTTACTTCGTTTTAATGTTAGAAACAATCGC TTATTTGTTTTCTTAAACGAAAGAAATTACTT CCGTATACGT |
| CW1387 | <i>ATP11-YLR042C 300 3'_repl_reverse</i> | GTTTCGTAAGTGGATATCGAAATCAGTGGATTAGAAACAATACGCCGGAAATTAATACGTACCTTTGGGACCCACAGA |
| CW546 | <i>BSC1 MS2 forward</i> | TAACCAGTTCAACCATTCAAACTACTTCTGTTGATCCAAACCACTTAAGCCGCTCTAGAACTAGTGGATCC |
| CW547 | <i>BSC1 MS2 reverse</i> | AGTCACAGCGCTTGAAC TAGTTGGGCTCTCTGAACTTGAAC TTACTACGCATAGGCCACTAGTGGATCTG |

Table S4. List of strains used in this study.

| Strain ID | Designation | Genotype | Reference |
|-----------|-------------------------------|--|-----------------------|
| NY0-1 | ARF1 | MAT a ade2::ARF1::ADE2 arf1::HIS3 ura3 lys2 trp1 his3 leu2 | Yahara et al., 2001 |
| YAS2501 | Dcp2-HBH | MAT a ade2::ARF1::ADE2 arf1::HIS3 ura3 lys2 trp1 his3 leu2 DCP2::DCP2-HBH-kanMX4 | Weidner et al., 2014 |
| YAS3240 | Scd6-HBH | MAT a ade2::ARF1::ADE2 arf1::HIS3 ura3 lys2 trp1 his3 leu2 SCD6::SCD6-HBH-TRP1 | Weidner et al., 2014 |
| YAS1031A | Dcp2-GFP | MAT a ade2::ARF1::ADE2 arf1::HIS3 ura3 lys2 trp1 his3 leu2 DCP2::DCP2-yEGFP-kanMX4 | Kilchert et al., 2010 |
| YAS2789 | Dcp2-3HA | MAT a ade2::ARF1::ADE2 arf1::HIS3 ura3 lys2 trp1 his3 leu2 DCP2::DCP2-3HA-kITRP1 | This study |
| YAS4381 | $\Delta xrr1$ | MAT a ade2::ARF1::ADE2 arf1::HIS3 ura3 lys2 trp1 his3 leu2 xrr1::natNT2 | This study |
| YAS4469 | Dcp2-GFP $\Delta puf5$ | MAT a ade2::ARF1::ADE2 arf1::HIS3 ura3 lys2 trp1 his3 leu2 DCP2::DCP2-yEGFP-kanMX4 puf5::natNT2 | This study |
| YAS4610 | Dcp2-GFP $\Delta puf3$ | MAT a ade2::ARF1::ADE2 arf1::HIS3 ura3 lys2 trp1 his3 leu2 DCP2::DCP2-yEGFP-kanMX4 puf3::kLEU2 | This study |
| YAS4470 | Dcp2-GFP $\Delta puf6$ | MAT a ade2::ARF1::ADE2 arf1::HIS3 ura3 lys2 trp1 his3 leu2 DCP2::DCP2-yEGFP-kanMX4 puf6::natNT2 | This study |
| YAS4543 | Dcp2-GFP $\Delta sbp1$ | MAT a ade2::ARF1::ADE2 arf1::HIS3 ura3 lys2 trp1 his3 leu2 DCP2::DCP2-yEGFP-kanMX4 sbp1::natNT2 | This study |
| YAS4544 | Dcp2-GFP $\Delta khd1$ | MAT a ade2::ARF1::ADE2 arf1::HIS3 ura3 lys2 trp1 his3 leu2 DCP2::DCP2-yEGFP-kanMX4 khd1::natNT2 | This study |
| YAS4546 | Dcp2-GFP $\Delta pbb2$ | MAT a ade2::ARF1::ADE2 arf1::HIS3 ura3 lys2 trp1 his3 leu2 DCP2::DCP2-yEGFP-kanMX4 pbb2::natNT2 | This study |
| YAS4843 | Dcp2-GFP $\Delta ngr1$ | MAT a ade2::ARF1::ADE2 arf1::HIS3 ura3 lys2 trp1 his3 leu2 DCP2::DCP2-yEGFP-kanMX4 ngr1::natNT2 | This study |
| YAS4472 | Dcp2-GFP $\Delta whi3$ | MAT a ade2::ARF1::ADE2 arf1::HIS3 ura3 lys2 trp1 his3 leu2 DCP2::DCP2-yEGFP-kanMX4 whi3::natNT2 | This study |
| YAS4547 | Dcp2-GFP Bsc1-3HA | MAT a ade2::ARF1::ADE2 arf1::HIS3 ura3 lys2 trp1 his3 leu2 DCP2::DCP2-yEGFP-kanMX4 BSC1::BSC1-3HA-kITRP1 | This study |
| YAS4551 | Dcp2-GFP Alp11-3HA | MAT a ade2::ARF1::ADE2 arf1::HIS3 ura3 lys2 trp1 his3 leu2 DCP2::DCP2-yEGFP-kanMX4 | This study |
| YAS4650 | Dcp2-3HA SEC59-BSC1(3'UTR) | MAT a ade2::ARF1::ADE2 arf1::HIS3 ura3 lys2 trp1 his3 leu2 DCP2::DCP2-3HA-kITRP1 SEC59::SEC59-BSC1(3'UTR) | This study |
| YAS4651 | Dcp2-3HA SEC59-ATP11(3'UTR) | MAT a ade2::ARF1::ADE2 arf1::HIS3 ura3 lys2 trp1 his3 leu2 DCP2::DCP2-3HA-kITRP1 SEC59::SEC59-ATP11(3'UTR) | This study |
| YAS4659 | Dcp2-3HA YLR042C-BSC1(3'UTR) | MAT a ade2::ARF1::ADE2 arf1::HIS3 ura3 lys2 trp1 his3 leu2 DCP2::DCP2-3HA-kITRP1 YLR042C::YLR042C-BSC1(3'UTR) | This study |
| YAS4660 | Dcp2-3HA YLR042C-ATP11(3'UTR) | MAT a ade2::ARF1::ADE2 arf1::HIS3 ura3 lys2 trp1 his3 leu2 DCP2::DCP2-3HA-kITRP1 YLR042C::YLR042C-ATP11(3'UTR) | This study |
| YAS4163 | Dcp2-2mcherry | MAT a ade2::ARF1::ADE2 arf1::HIS3 ura3 lys2 trp1 his3 leu2 DCP2::DCP2-2xyemcherry-hphNT1 | This study |
| YAS4457 | Dcp2-2mcherry Puf5-GFP | MAT a ade2::ARF1::ADE2 arf1::HIS3 ura3 lys2 trp1 his3 leu2 DCP2::DCP2-2xyemcherry-hphNT1 PUF5::PUF5-yEGFP-kITRP1 | This study |
| YAS4675 | Dcp2-2mcherry BSC1-24xMS2SL | MAT a ade2::ARF1::ADE2 arf1::HIS3 ura3 lys2 trp1 his3 leu2 DCP2::DCP2-2xyemcherry-hphNT1 BSC1::BSC1-24xMS2SL | This study |

Table S5. Experimental Design.

| Condition | Gel Label | Batch | Replicate |
|------------------------|-------------------|---------|-----------|
| Unstressed control | non-radiolabeling | March | R1 |
| Glucose Depletion | non-radiolabeling | March | R1 |
| Sodium Osmotic Stress | non-radiolabeling | March | R1 |
| Calcium Osmotic Stress | non-radiolabeling | March | R1 |
| Unstressed control | radiolabeling | March | R2 |
| Glucose Depletion | radiolabeling | March | R2 |
| Sodium Osmotic Stress | radiolabeling | March | R2 |
| Calcium Osmotic Stress | radiolabeling | March | R2 |
| Unstressed control | radiolabeling | May | R3 |
| Glucose Depletion | radiolabeling | May | R3 |
| Sodium Osmotic Stress | radiolabeling | May | R3 |
| Calcium Osmotic Stress | radiolabeling | May | R3 |
| Unstressed control | radiolabeling | August | R4 |
| Glucose Depletion | radiolabeling | August | R4 |
| Sodium Osmotic Stress | radiolabeling | August | R4 |
| Calcium Osmotic Stress | radiolabeling | August | R4 |
| Unstressed control | radiolabeling | October | R5 |
| Glucose Depletion | radiolabeling | October | R5 |
| Sodium Osmotic Stress | radiolabeling | October | R5 |
| Calcium Osmotic Stress | radiolabeling | October | R5 |

Supplemental Experimental Procedures

Yeast strains

For C-terminal tagging Puf5p with GFP, the plasmid pYM26 (*kITRP1*) was used. pFA6a-3xmcherry (*hphNT1*) plasmid was used in tagging Dcp2p with mcherry (Maeder et al., 2007). For live-cell mRNA imaging, MS2SL tagged strains were constructed using pDZ415 (24MS2SL loxP-Kan-loxP). To remove selection marker and visualize the transcripts, the Cre recombinase-containing plasmid pSH47 (URA3) and MS2SL coat protein expressing plasmid pDZ274 (pLEU MET25pro MCP-2x-yeGFP) were co-transformed into cells afterwards (Hocine et al., 2013). Plasmids pDZ415 (Addgene plasmid # 45162) and pDZ274 (Addgene plasmid # 45929) were gifts from Robert Singer and Daniel Zenklusen (Albert Einstein College of Medicine, Bronx, NY, USA). Primers and strains used in this study are listed in Table S3 and S4.

Preparation of RNA-Seq Samples

The RNA-Seq sample preparation was carried out according to Tagwerker, et al. (2006), Hafner et al., (2010) and Kishore, et al. (2011) with modifications. Cells expressing Dcp2-HBH or Scd6-HBH were grown to mid-log phase, subjected to the corresponding stress and crosslinked with 1% formaldehyde for 2 min. Control cells were treated equally except stress application. Cells were lysed in RIPA buffer (50 mM Tris-HCl pH 8.0, 150 mM NaCl, 1% NP-40, 0.5% sodium deoxycholate, 0.1% SDS, supplemented with protease inhibitors) with FastPrep machine (MP Biomedicals). To dissolve large RNPs, the supernatants were treated with 50 U/ml RNase T1 (Fermentas) at 22°C for 15 min. Pull-downs were performed with streptavidin agarose beads (Thermo Fisher Scientific) in binding buffer (50 mM NaPi pH 8.0, 300 mM NaCl, 6 M GuHCl, 0.5% Tween-20). The second RNase T1 digestion was performed on the beads with a final concentration of 1 U/μl. Radiolabeling of RNA was performed by adding 0.5 μCi/μl γ-³²P-ATP (Hartmann analytic) and 1 U/μl T4 PNK (New England Biolabs). To purify RNA, proteins were digested using 1.2 mg/ml proteinase K (Roche) in 2 x proteinase K buffer (100 mM Tris-HCl pH 7.5, 200 mM NaCl, 2 mM EDTA, 1% SDS) for 30 min at 55°C. The RNA was subsequently isolated using phenol-chloroform-isoamyl alcohol (125:24:1) (Sigma-Aldrich) as described (Schmitt et al., 1990). Purified RNA was subjected to 3' and 5' adapter ligation following Illumina's TruSeq Small RNA Library Prep Guide. To reduce the rRNA species, RiboMinus transcriptome isolation kit (Invitrogen) was used according to the manufacturer's protocol. Reverse transcription using SuperScript III reverse transcriptase (Invitrogen), oligo-dT and random hexamer was performed afterwards. The cDNA libraries were generated by a final PCR amplification step with Illumina indexing primer (RPI1-4, Table S3). In this study, five library sets (from five biological replicates) were sequenced. Except the first library set, all the libraries were generated as described above. In the first library set, the

radiolabeling step was omitted and the PAGE purification steps were replaced by column-based purification with RNeasy kit (Qiagen), according to the manufacturer's instruction.

Processing of small RNA-Seq reads

RNA-Seq libraries were sequenced on Illumina HiSeq2000 with single read to 50 bp reads. We clipped adapters and trimmed low quality bases using Trimmomatic version 0.30 (Bolger et al., 2014) with parameters "SE -s phred33 ILLUMINACLIP:Illumina_smallRNA_adapters.fa:20:5:30 LEADING:30 TRAILING:30 MINLEN:10", where Illumina_smallRNA_adapters.fa contained all adapter and primer sequences from the TruSeq Small RNA Sample Preparation Kit. Subsequently, reads were aligned to *Saccharomyces cerevisiae* genome EF4.72 from ENSEMBL using Bowtie version 1.0.0 (Ben Langmead et al., 2008) with parameters "-n 0 -l 28 -e 70 -k 1 -m 1 --best --strata --sam --nomaqround". Reads were counted per exon using htseq-count (Anders et al., 2015) with default parameters against ENSEMBL's matching GTF file for EF4.72 and aggregated on the gene-level.

Analysis of P-body enriched mRNAs

Analysis of P-body enriched mRNAs was performed using edgeR version 3.0 (Robinson et al., 2010) using standard procedures for count normalization and estimation of dispersion. The gel label and batch were included as factors in the experimental design (Table S5). We identified significant ($p < 0.05$) upregulated genes exclusive for each stress condition by testing each individual stress condition against the wild type condition and removing those genes that were identified as common hits when testing the joint set of stress conditions against unstressed control. For glucose depletion stress, we additionally excluded genes previously shown to be significantly enriched in polysomes (Arribere et al., 2011) for the same stress.

Gene Ontology (GO) term enrichment analysis

P-body enriched mRNAs for each stress condition were tested for GO biological processes (BP) enrichment using hypergeometric tests as implemented in the hyperGTest function from the GOstats R/Bioconductor package version 1.7.4. The gene universe was defined for each stress condition as the set of genes with a mean enrichment level over all replicates larger than or equal to the first quartile. For GO term gene annotation, the R/Bioconductor package org.Sc.sgd.db version 3.1.2 was used. P-values from the hypergeometric tests were visualized using the ggplot2 R package version 1.0.1.

Combined Fluorescence in situ hybridization (FISH) and immunofluorescence (IF)

Combined FISH and IF was performed as described (Kilchert et al., 2010; Takizawa et al., 1997). The following antibodies and solution were used for detection: anti-DIG-POD (Roche, 1:750 in PBTB), anti-HA (Eurogentec HA11; 1:250), anti-GFP (Roche GFP clones 7.1 and

13.1, 1:250), goat anti-mouse-IgG-Alexa488 (Invitrogen, 1:400 in PBS) and tyramide solution (PerkinElmer, 1:100 in Amplification Solution supplied with kit). Primers with T7 promoter ends (Table S3) and MEGAscript T7 transcription kit (Ambion) were used for probe generation. To obtain fluorescence images, slides were mounted with Citifluor AF1 (Citifluor), supplemented with 1 µg/ml DAPI to stain the nuclei. Images were acquired with an Axiocam MRm camera mounted on an Axioplan 2 fluorescence microscope using a Plan Apochromat 63x/NA1.40 objective and filters for eqFP611 and GFP. Axiovision software 3.1 to 4.8 was used to process images (Carl Zeiss).

Live-cell imaging

For live-cell imaging with MS2 system. Yeast cells were grown in HC-Leu medium containing 2% glucose to mid-log phase. The cells were taken up in glucose-free HC-Leu medium afterwards. For live-cell imaging with Dcp2p and Puf5p, Yeast cells were grown in YPD medium to mid-log phase, and resuspended in HC-complete medium lacking glucose. Fluorescence was monitored as described in FISH-IF.

Pulse-chase labeling with 4TU and RNA purification

The pulse-chase labeling experiment was carried out as described previously (Zeiner et al., 2008). For the pulse, yeast culture was grown in HC-Ura drop-out media supplemented with 2% dextrose, 0.1 mM uracil and 0.2 mM 4-Thiouracil (Sigma-Aldrich) for 6 h. Yeast were spun down at 3,000 g for 2 min and resuspended in HC-Ura drop-out media containing 20 mM uracil (chase). Afterwards, yeast were collected by centrifugation at the following time points: t = 0, 10, 20, 30, and 60 min. Cells were lysed followed by total RNA isolation using phenol-chloroform-isoamyl alcohol (125:24:1) (Sigma-Aldrich) as described (Schmitt et al., 1990). The RNA was then subjected to biotinylation and further purification according to Zeiner et al., 2008. The same RNA purification protocol was followed to isolate total RNA. To determine the mRNA stability of *ACT1*, *PGK1* and *RPL37b* under glucose deprivation condition, 200 pg humanized Renilla luciferase (hRLuc) RNA spike-in was added per microgram total RNA as reference gene.

Identification of secondary structure motifs within the 3'UTRs of P-Body-associated mRNAs

Secondary structure motifs in the 3' untranslated regions (UTRs) of gene transcripts, overrepresented among differentially expressed genes for each stress condition, were identified using NoFold (Middleton and Kim, 2014) version 1.0. 3' UTR sequences were extracted from the biomart (<http://biomart.org>) by selecting 300 base pairs (bp) downstream of the coding sequence (CDS). The internal NoFold boundary file `bounds_300seq.txt` was used along with a file containing UTR sequences of all non-enriched genes as a background

for enrichment analysis and parameter `--rnaz`. All other parameters were used in the default setting.

3.2 The polysome-associated proteins Scp160 and Bfr1 prevent P-body formation under normal growth conditions

The following article is published on **JOURNAL OF CELL SCIENCE**, 2014; 127 (9): 1992.

Statement of contributions: In this study, Julie Weidner performed experiments represented by Table 1, Fig. 1, 2, 3B, 5, 6, 7, S2A, 2B, S3, S4. All polysome profile analysis including Fig. 4A and S1, phosphatase assay of Fig. 4B and microscopy of Fig. S2E were conducted by me. Cristina Prescianotto-Baschong did EM analysis represented by Fig. 3A. Alejandro F. Estrada contributed to Fig. S2C and S2D. Finally, the manuscript was written by Prof. Anne Spang.

RESEARCH ARTICLE

The polysome-associated proteins Scp160 and Bfr1 prevent P body formation under normal growth conditions

Julie Weidner, Congwei Wang, Cristina Prescianotto-Baschong, Alejandro F. Estrada and Anne Spang*

ABSTRACT

Numerous mRNAs are degraded in processing bodies (P bodies) in *Saccharomyces cerevisiae*. In logarithmically growing cells, only 0–1 P bodies per cell are detectable. However, the number and appearance of P bodies change once the cell encounters stress. Here, we show that the polysome-associated mRNA-binding protein Scp160 interacts with P body components, such as the decapping protein Dcp2 and the scaffold protein Pat1, presumably, on polysomes. Loss of either Scp160 or its interaction partner Bfr1 caused the formation of Dcp2-positive structures. These Dcp2-positive foci contained mRNA, because their formation was inhibited by the presence of cycloheximide. In addition, Scp160 was required for proper P body formation because only a subset of bona fide P body components could assemble into the Dcp2-positive foci in *Δscp160* cells. In either *Δbfr1* or *Δscp160* cells, P body formation was uncoupled from translational attenuation as the polysome profile remained unchanged. Collectively, our data suggest that Bfr1 and Scp160 prevent P body formation under normal growth conditions.

KEY WORDS: Processing bodies, mRNA, mRNA metabolism, Endoplasmic reticulum, Translation, *Saccharomyces cerevisiae*, mRNA-binding proteins, mRNA decay, Stress response, Ribonucleotide particles, Stress granules

INTRODUCTION

The protein content in a cell at any given time is regulated by transcription, translation and protein degradation. Transcription largely determines the number of mRNA molecules, whereas the balance of mRNA translation and protein degradation is important for the regulation of protein homeostasis. Upon encountering stress, a cell needs to quickly alter its proteome, thus, as a type of primary response to stress, translation often becomes attenuated. Consequently, mRNAs that are no longer engaged in translation are frequently stored in processing bodies (P bodies) (Parker and Sheth, 2007). P bodies consist of the decapping enzymes Dcp1 and Dcp2, the helicase Dhh1, activators of decapping – such as Pat1, Scd6, Edc3 and the Lsm1–7 complex – and the 5′–3′ exonuclease Xrn1 (Parker and Sheth, 2007). In addition to this basic assortment of P body components, an ever-growing list of proteins associated with P bodies has been reported (Jain and Parker, 2013; Mitchell et al., 2013; Parker and Sheth, 2007).

To date, P bodies have been reported to be involved in mRNA decapping, nonsense-mediated decay, translational repression, mRNA storage and other RNA related functions (Parker and Sheth, 2007). The transcripts that are stored in P bodies are in a dynamic exchange with the pool of mRNAs undergoing translation and can either be degraded or be bound by ribosomes for translation.

P bodies are not the only ribonucleoprotein (RNP) structures that are formed upon stress. Numerous stress conditions also promote the formation of stress granules. Stress granules are mainly composed of stalled translation initiation components and are sites of mRNA storage. The analysis of the different RNP structures is complicated by the fact that numerous factors are found in both types of granules, such as the exonuclease Xrn1 (Buchan and Parker, 2009). In addition, mRNA can traverse from P bodies into stress granules and vice versa (Buchan et al., 2008). Moreover, P bodies and stress granules are found in close contact to each other, which might facilitate the transfer of components and mRNA.

In yeast, 5′–to–3′ decay of mRNA appears to be the major direction of mRNA degradation (Muhlrad et al., 1995; Shoemaker and Green, 2012). Once the cell encounters stress, P bodies become visible by microscopy, which is thought to occur through the aggregation of P body components that are, presumably, bound to mRNA. These aggregates are, nevertheless, highly dynamic and can dissolve either upon adaptation of the cell to the stressor or when the stress ceases to exist (Bregues et al., 2005; Teixeira and Parker, 2007). Depending upon the stress that is encountered, the size and number of P bodies varies. For example, glucose starvation induces a few relatively large foci, whereas high salt and high Ca²⁺ cause the formation of smaller but more numerous P bodies (Bregues et al., 2005; Kilchert et al., 2010). The reason for the different responses is not clear. It has to be noted, however, that glucose starvation can only be remedied by the addition of a good carbon source, whereas cells can adapt to stresses such as high salt (Ashe et al., 2000; Bregues et al., 2005). As a consequence, P bodies that form under such stress disassemble after adaptation (Kilchert et al., 2010).

P bodies are found in close proximity to, and might even be physically linked to, the endoplasmic reticulum (ER) (Kilchert et al., 2010). To determine whether P bodies are physically linked to the ER, we aimed to identify proteins that bind to P body components. The peripheral ER proteins Scp160 and Bfr1 were identified as interacting proteins of P bodies. The association of Scp160 and Bfr1 with polysomes prompted us to test whether Scp160 and Bfr1 might play a role in P body formation. Our results suggest that Bfr1 and Scp160 act independently as negative regulators of P body formation at the ER. Moreover, our data imply that Scp160 is required for the correct assembly of P bodies.

Growth & Development, Biozentrum, University of Basel, Klingelbergstrasse 70, 4056 Basel, Switzerland.

*Author for correspondence (anne.spang@unibas.ch)

Received 2 September 2013; Accepted 4 February 2014

1992

RESULTS

Screen for novel P-body-interacting proteins at the endoplasmic reticulum

We have shown previously that P bodies are localized in close proximity to ER membranes (Kilchert et al., 2010). In order to identify potential ER-localized interaction partners of P body components, we employed tandem affinity purification after crosslinking with the P body components Dcp2 and Scd6, which are part of the 5'UTR- and the 3'UTR-associated complexes of P bodies, respectively. We chose a crosslinking approach because P bodies are highly dynamic, and their interaction with the ER could be transient (Teixeira and Parker, 2007). We also opted for a stringent method and, therefore, selected the HBH tag for the purification scheme. The HBH tag consists of a biotinylation sequence, which is flanked by two His₆ peptides, allowing tandem purification under denaturing conditions (Tagwerker et al., 2006).

The temperature-sensitive *arf1-11* mutation in the small GTPase Arf1p causes the formation of numerous P bodies at the restrictive temperature (Kilchert et al., 2010). Cultures of *arf1-11* mutants expressing chromosomally tagged Dcp2–HBH or Scd6–HBH and wild-type cells were shifted to 37°C for 1 h to induce P bodies. Protein complexes were crosslinked *in vivo*, extracted from membrane pellets that had been enriched for ER membranes, and purified over Ni-NTA and streptavidin beads under denaturing conditions. The proteins were digested, and the peptides analyzed by mass spectrometry. This approach was successful because we could identify P body components in our purification scheme (Table 1). In addition, proteins were identified that were neither present in the untagged wild-type control nor in other HBH purifications for unrelated baits that have been performed by our group (Ritz et al., 2014). Those proteins present only in the Dcp2–HBH or Scd6–HBH sample, or in both samples, were considered for further analysis (Table 1).

Bfr1 and Scp160 are newly identified P-body-interacting proteins at the ER

Three of the proteins identified in the tandem affinity purifications were ER-associated proteins – Bfr1, Scp160 and Cdc48. Cdc48 is a AAA-ATPase that is involved in homotypic membrane fusion during karyogamy, and in the extraction and retro-translocation of polypeptides from the ER that are destined

for degradation by the proteasome (Hitchcock et al., 2001; Latterich et al., 1995; Schubert and Buchberger, 2005). The function of Cdc48 in ER-associated degradation might mean that it also transmits a signal to induce P body formation under ER stress conditions. We decided, however, to focus on the two other proteins Scp160 and Bfr1. Scp160 is an mRNA-binding protein that, together with Bfr1, associates with actively translating polysomes at the ER (Lang et al., 2001). Loss of Scp160 causes mislocalization of the asymmetrically localized *ASH1* mRNA (Irie et al., 2002; Trautwein et al., 2004) and *SRO7* mRNA after pheromone treatment (Gelin-Licht et al., 2012). Bfr1 has been identified as a multicopy suppressor of brefeldinA-induced lethality (Jackson and Képès, 1994). However, the molecular function of Bfr1 is still unknown.

First, we established whether Scp160 and Bfr1 are still associated with the ER at 37°C, the temperature at which we performed the crosslink. To this end, we appended both Scp160 and Bfr1 chromosomally with a GFP tag in strains that expressed the ER marker Sec63 that had been tagged with red fluorescent protein (RFP). Both proteins remained associated with the ER, irrespective of the temperature (23°C or 37°C) or the strain background (wild-type or *arf1-11*) (Fig. 1).

Because we used a crosslinking approach to detect proteins that interact with P body components, we wanted to ensure that Scp160 and Bfr1 were not just localized in the vicinity of P bodies and therefore caught in the complex, and that Scp160 and Bfr1 were also able to interact with P body components in the absence of crosslinking agents. 3× FLAG tagged Scp160 co-immunoprecipitated Dcp2 that had been tagged with nine repeats of a Myc epitope (9Myc), irrespective of whether the cells were stressed by glucose starvation, high intracellular Ca²⁺ or unstressed (Fig. 2A,B). The association of Bfr1 with Dcp2 was detected to a lower extent, and the levels were more variable, indicating that Dcp2 might interact primarily with Scp160 rather than with Bfr1. Given that Scp160 is an RNA-binding protein and interacts with the machinery that stores and decays mRNAs, we next tested whether the interaction between Scp160 and Dcp2 was dependent on mRNA. Indeed, treatment of yeast lysates with RNase strongly reduced the amount of co-immunoprecipitated Dcp2 (Fig. 2C).

To explore the possibility that other P body components could also interact with Scp160 and/or Bfr1, we repeated the

Table 1. Proteins identified by HBH-purification

| Found only in Dcp2-HBH | Found only in Scd6-HBH | Found in both purifications |
|------------------------|------------------------|-----------------------------|
| Nog1 | Sbp1 | Dcp2 |
| Hta1 | <i>Eap1</i> | Xrn1 |
| Atp1 | <i>Not1</i> | Edc3 |
| Cdc48** | Rps12 | Scd6 |
| | Hef3 | <i>Bfr1</i> ** |
| | Hsp12 | Dhh1 |
| | Tif5 | Tef4 |
| | <i>Scp160</i> ** | Sti1 |
| | <i>Yra1</i> | <i>Pab1</i> |
| | <i>Tif3</i> | Cpr1 |
| | <i>Psp2</i> | <i>Nam7</i> |
| | Lsm5 | Pat1 |
| | Lsm2 | Def1 |
| | Dcp1 | Vma13 |
| | | Hsp26 |
| | | Mpg1 |

Bold formatting indicates P body components, italic formatting indicates RNA-related function, ** indicates ER association.

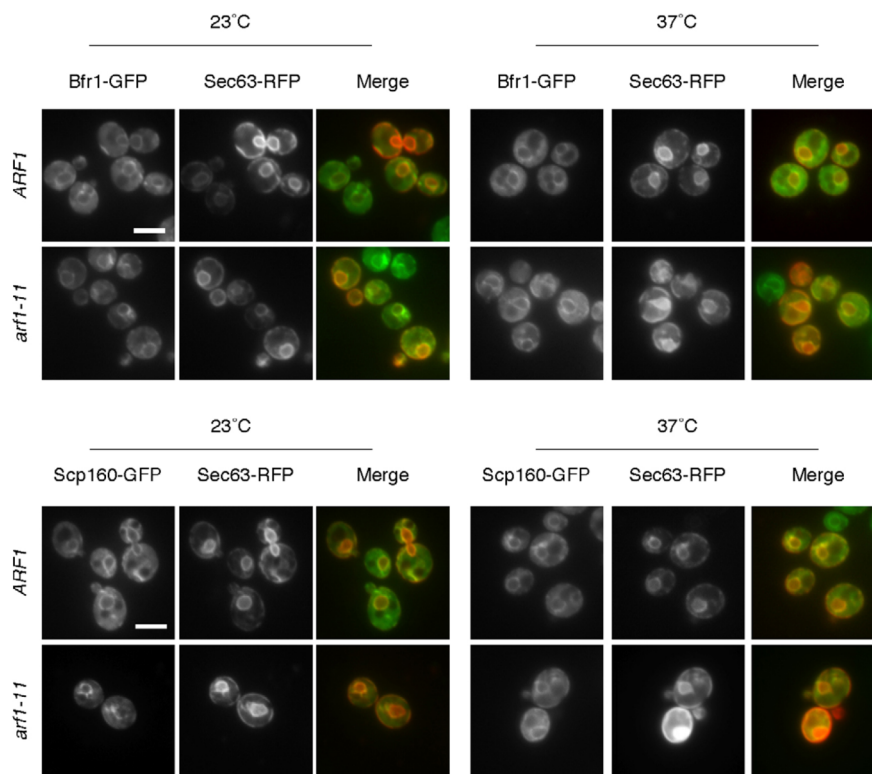


Fig. 1. Bfr1p and Scp160 are identified as potential interacting proteins of P bodies at the ER. Bfr1 and Scp160 localize to the ER. Strains were created in which Bfr1 and Scp160 were chromosomally tagged with GFP (in a background of ARF1 or *arf1-11*, the latter induces P body formation at the restrictive temperature). These strains were then transformed with a plasmid encoding Sec63-RFP (red) to label the ER. Cells were observed at 23°C and after a 1 h shift to 37°C to mimic the conditions that had been used for the HBH purification. At both temperatures, Bfr1-GFP and Scp160-GFP (green) localized to ER membranes. Scale bars: 5 μ m.

immunoprecipitations and probed for Pat1 and Edc3, both of which had been tagged with six repeats of the HA epitope (Pat1-6HA and Edc3-6HA, respectively), without stress or under glucose starvation (Fig. 2D). Similar to Dcp2, Pat1 and Edc3 were part of a complex that was associated with, at least, Scp160-FLAG. In all cases, the stress seemed to slightly, but consistently, increase the interaction of Scp160 with these P body components. By contrast, Scd6-6HA was not co-immunoprecipitated with Scp160-FLAG (Fig. 2D). The ability of Scp160 to interact with P body components appeared to be independent of stress, indicating that induction of stress is not a prerequisite for the interaction of P body components with Scp160. Because Dcp2 and Pat1 play a more prominent role in P body assembly (Teixeira and Parker, 2007), our data suggest that at least partially assembled P bodies could be present on actively translating ribosomes. We conclude that Scp160 is a newly identified mRNA-dependent protein that interacts with P body components at the ER.

Scp160 and Bfr1 are not required for the localization of P bodies to the ER

P bodies localize in close proximity to the ER (Kilchert et al., 2010). Therefore, we asked whether Scp160 and Bfr1 are required for P body localization at the ER. Dcp2-9Myc-positive structures were detected by immunoelectron microscopy as being in close proximity to the ER in both the *Abfr1* and *Ascp160* cells, or in the wild type, when shifted to 37°C (Fig. 3A). The distribution of the Dcp2-9Myc signal, which was suggestive of a ring-like globular structure, was similar in both strains. We then used a biochemical assay to investigate further the results of the ultrastructural

analysis. We have shown previously that Dcp2-9Myc co-migrates with ER membranes in a sucrose gradient (Kilchert et al., 2010); here, the association of Dcp2 with the ER was not drastically altered in either of the deletion strains (Fig. 3B) – similar amounts of Dcp2-9Myc floated at the 0% to 40% sucrose interface. Our data demonstrate that neither Scp160 nor Bfr1 are essential for the recruitment of Dcp2 to ER membranes.

P body components co-fractionate with polysomes independently of Scp160 or Bfr1

Bfr1 and Scp160 have been shown to be associated with polysomes (Lang et al., 2001), therefore, we asked whether P body components could be recruited to polysomes. We fractionated polysomes from wild-type, *Ascp160*, *Abfr1* and *Abfr1 Ascp160* cells on a sucrose gradient and subjected the polysome fractions to immunoblot analysis. As previously observed (Baum et al., 2004; Li et al., 2003), we did not find a significant change in the polysome profile or an increase in the 80S monosome fraction in any of the strains, which would be indicative of translation attenuation (Fig. 4A). In all cases, Dcp2-9Myc and Scd6-6HA were detected in the polysome fraction (Fig. 4A); thus, association of P body components with the polysomes is independent of Bfr1 and Scp160.

P bodies were not induced in the wild-type cells under the growth conditions that were used for the experiment; therefore, our data indicate that P body components are associated with polysomes during translation in normal logarithmically growing cells. We noticed that Dcp2-9Myc was detected as a double band by immunoblotting, and that, in the fractions of the *Ascp160 Abfr1* polysome profile, the upper band was strongly reduced.

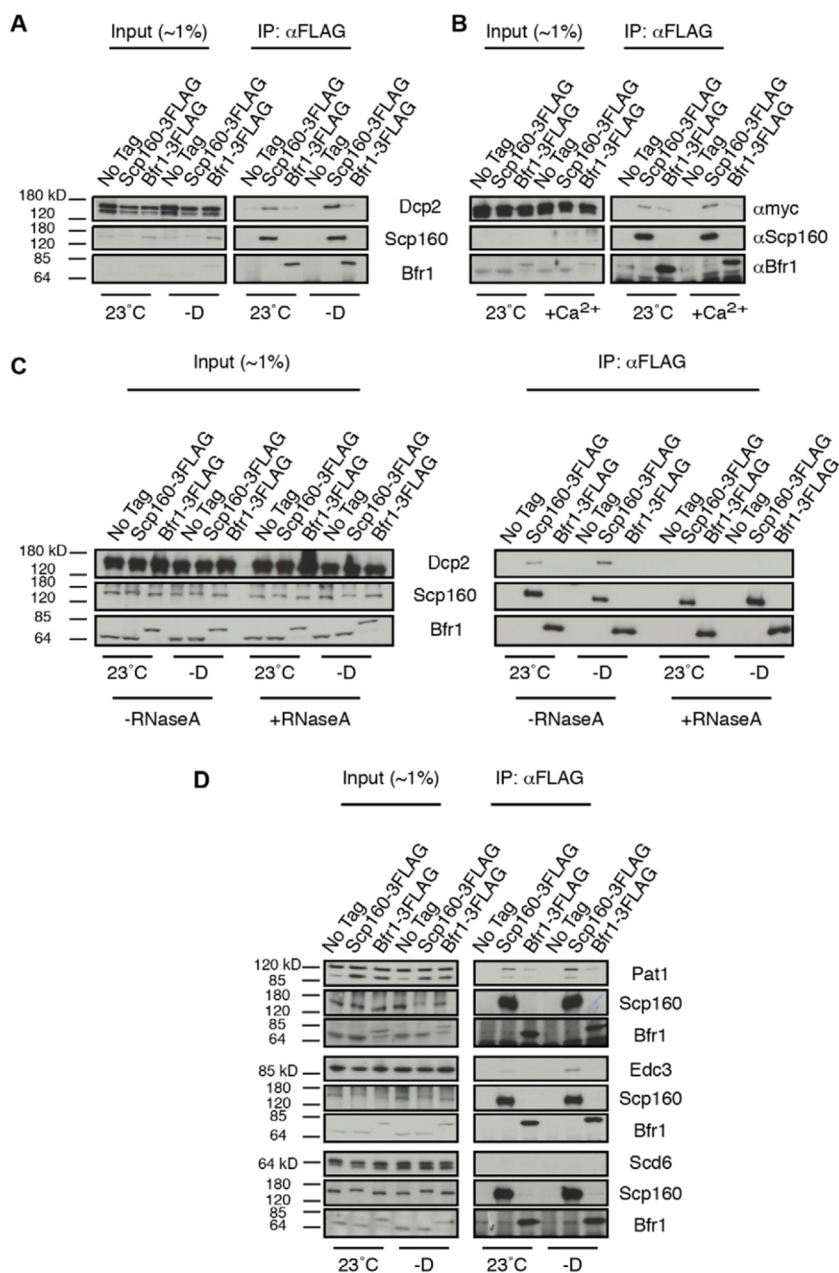


Fig. 2. Scp160 associates with P body components independently of stress. (A) Scp160 associates with Dcp2 independently of glucose starvation. Co-immunoprecipitation experiments were performed using an antibody against the FLAG peptide and lysates from strains that had been chromosomally tagged with Scp160-3FLAG or Bfr1-3FLAG. All strains also expressed Dcp2-9Myc. Where indicated, cells were subjected to starvation for 10 min (-D) before the immunoprecipitation (IP). Dcp2-9Myc co-precipitated with Scp160-3FLAG in both conditions. A weak precipitation of Dcp2-9Myc with Bfr1-3FLAG was sometimes observed. (B) Ca²⁺ stress does not affect the Scp160-Dcp2 association. Cells were treated with 200 mM CaCl₂ for 10 min (+Ca²⁺) and then a 5 min washout in rich media without CaCl₂ was performed before lysate preparation. Under stressed and unstressed conditions, Dcp2-9Myc co-immunoprecipitated with Scp160-3FLAG. (C) The association of Scp160 with Dcp2 is lost in the absence of RNA. To determine if RNA was needed for the interaction between Scp160 and Dcp2, strains were treated as in A and then subjected to treatment with RNaseA for 1 h before immunoprecipitation. Upon RNaseA treatment, the association of Dcp2-9Myc with Scp160-3FLAG was no longer observed under either condition. (D) Scp160 associates with P body components. Pat1, Edc3 or Scd6 were chromosomally appended with a 6HA tag. The strains were treated as in A. Scp160-3FLAG was able to precipitate Pat1-6HA and Edc3-6HA under both conditions but did not precipitate Scd6-6HA.

Thus, we tested whether the double band represented different phosphorylation states. Phosphorylation of Dcp2 has been previously reported, but no band shift in SDS gels had been observed (Yoon et al., 2010). Treatment of the gradient fractions with alkaline phosphatase caused the double band to collapse into the lower molecular weight band (Fig. 4B). These data suggest that phosphorylated and non-phosphorylated forms of Dcp2 are present on polysomes.

P bodies are present on ER membranes, and Scp160 and Bfr1 are enriched on ER-associated polysomes; yet, we used total yeast lysate for the polysome profiles. It is conceivable that P body

components associate with the ER-bound polysomes in an Scp160-Bfr1-dependent manner. Moreover, the phosphorylated and dephosphorylated forms of Dcp2 might segregate between membrane-bound and soluble polysomes. To test these hypotheses, we recorded the polysome profiles of membrane and soluble fractions (supplementary material Fig. S1). Immunoblotting of the gradient fractions revealed that P body components could bind to soluble and membrane-associated polysomes (Fig. 4A). Interestingly, the ER-associated polysome pool was enriched for the phosphorylated form of Dcp2 (Fig. 4A). Phosphorylation of Dcp2 has been reported to be required for its accumulation in P

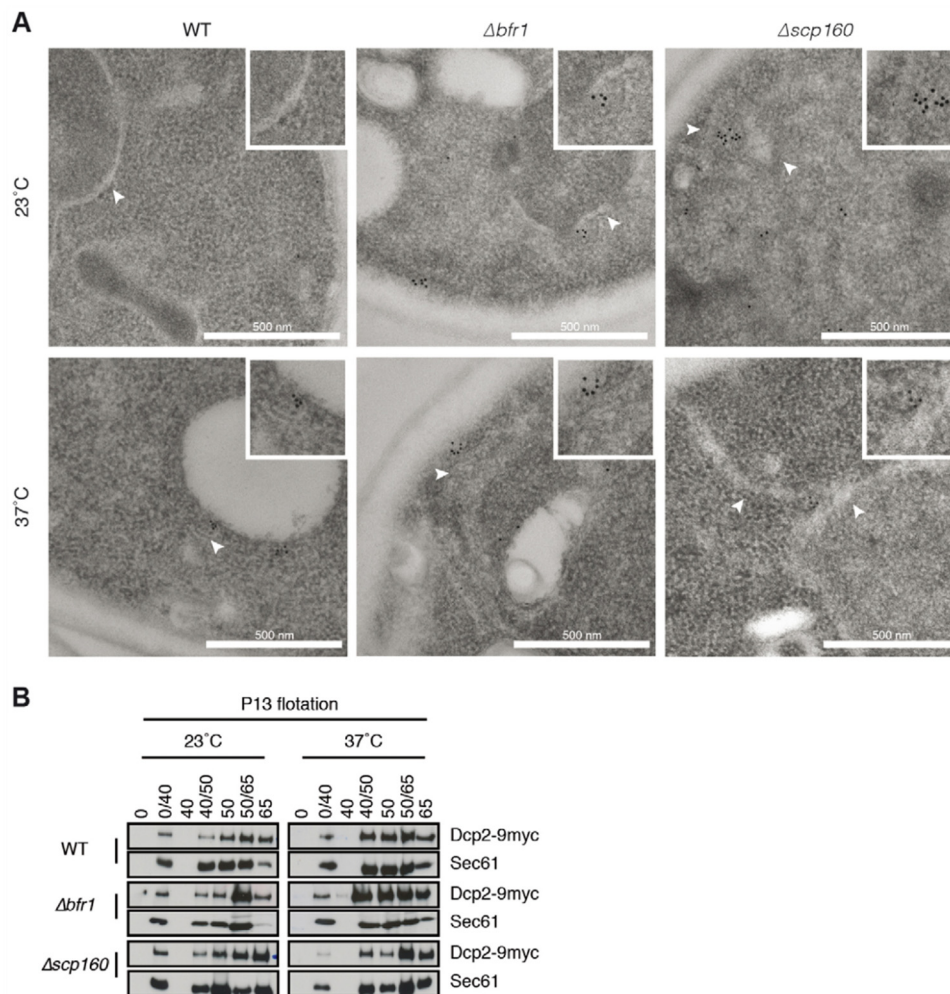


Fig. 3. Loss of *BFR1* or *SCP160* does not impair P body association with the ER. (A) P bodies remain in close proximity to ER membranes in $\Delta bfr1$ and $\Delta scp160$ cells. Cells that expressed Dcp2-9Myc, in which *BFR1* or *SCP160* had been deleted, were grown at 23°C and then shifted for 1 h to 37°C. A wild-type (WT) control is also shown. Cells were fixed and prepared for immunoelectron microscopy. Dcp2-9Myc was visualized by using gold particles. Scale bars: 500 nm. The insets are a 2 \times magnification of the area where the gold particles were found. White arrowheads indicate ER membranes. (B) Dcp2 associates with ER membranes in the absence of *BFR1* or *SCP160*. Wild-type, $\Delta bfr1$ and $\Delta scp160$ yeast cells expressing Dcp2-9Myc were shifted to 37°C for 1 h. Lysates were prepared, and a pellet was formed from a 13,000 *g* centrifugation (P13) and corresponding supernatant fraction (S13). The pellet was subjected to buoyant density centrifugation. In all conditions, a portion of Dcp2-9Myc fractionated with the ER marker Sec61p at the 0% to 40% sucrose interface (0/40).

bodies (Yoon et al., 2010), which is consistent with the notion that P bodies are associated with ER membranes (Kilchert et al., 2010). Notably, the amount of phosphorylated Dcp2 was reduced in the soluble polysome pool in $\Delta scp160 \Delta bfr1$ cells, indicating that Scp160 and Bfr1 together are required to maintain the Dcp2 phosphorylation state. Taken together, our data demonstrate that P body components are associated with polysomes and suggest that phosphorylated Dcp2 preferentially binds to membrane-associated polysomes.

Loss of Bfr1 or Scp160 induces the formation of multiple Dcp2-positive structures

The immunoelectron microscopy analysis revealed that, unlike in wild-type cells, in the $\Delta scp160$ and $\Delta bfr1$ strains, Dcp2-9Myc-positive

structures were readily observed under normal non-stress growth conditions (Fig. 3A, 23°C). This observation led us to determine whether P bodies form in the mutant strains without any stress being applied at the normal growth temperature. Indeed, when we visualized Dcp2-GFP in the $\Delta bfr1$ and $\Delta scp160$ strains, and in the $\Delta bfr1 \Delta scp160$ double mutant, we found a large increase in the number of P bodies compared with the wild-type cells, which typically contained 0–2 P bodies per cell (Fig. 5A,B; supplementary material Fig. S2A). Importantly, this increase in Dcp2-positive structures was restricted to normal growth conditions. Shifting the mutant cells to 37°C, which causes a mild temperature stress – as indicated by the small increase in P body number in wild-type cells – reduced the number of the Dcp2-positive structures in the mutant strains to below even that of the

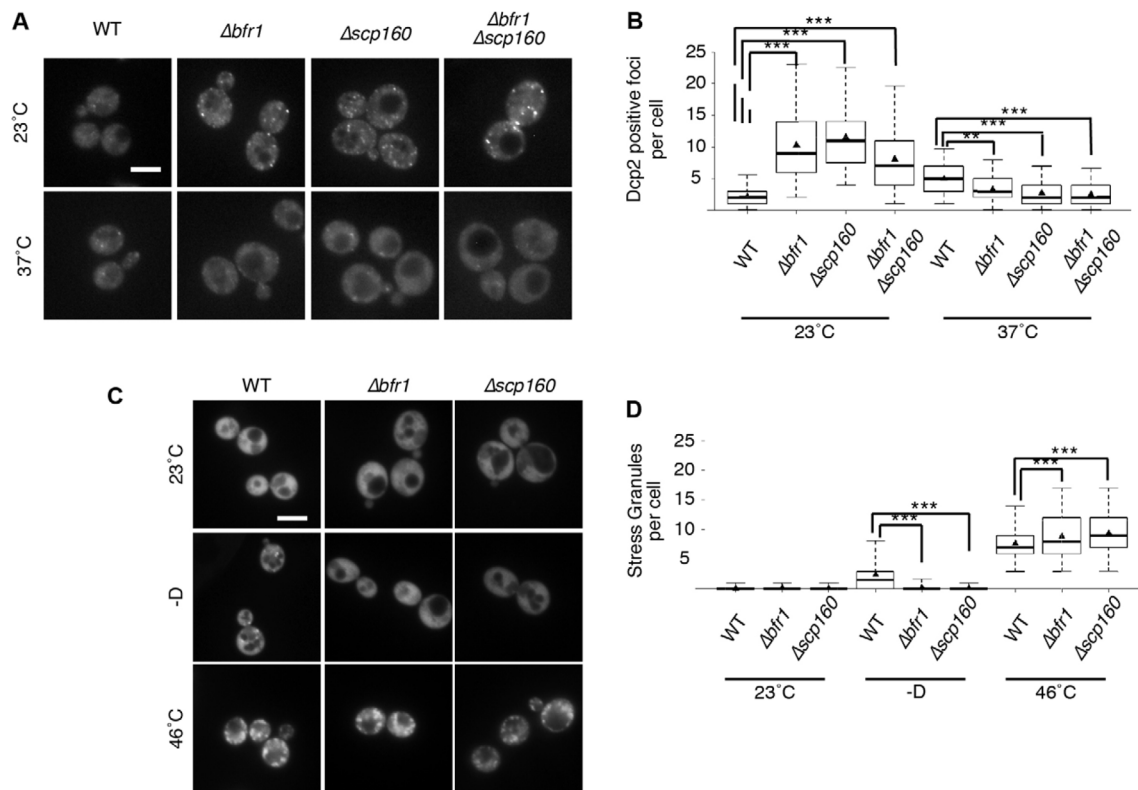


Fig. 5. Loss of *BFR1* or *SCP160* increases P body number under normal growth conditions. (A) Increased P body number was observed in $\Delta bfr1$, $\Delta scp160$ and $\Delta bfr1 \Delta scp160$ cells. Dcp2 was chromosomally tagged and used as a marker for P bodies. Under normal growth conditions at 23°C in the wild-type (WT) strain 0–2 P bodies were observed. Upon deletion of *BFR1*, *SCP160* or both from the cell, the number of P bodies increased. (B) Quantification of the P body phenotype observed in the wild-type and deletion strains upon temperature shift. A minimum of 200 cells from at least three independent experiments were counted per condition. The size of the box is determined by the 25th and 75th percentiles, the whiskers represent the 5th and 95th percentiles, the horizontal line and the triangle represent the median and mean, respectively. *** $P < 0.001$, ** $P < 0.01$. (C) Stress granules failed to form in $\Delta bfr1$ or $\Delta scp160$ cells under starvation conditions. Wild-type, $\Delta bfr1$ and $\Delta scp160$ cells were transformed with a high copy plasmid expressing the stress granule marker Pub1-mCherry. Cells were grown to mid-log phase at 23°C then shifted to 46°C or incubated in rich media lacking a carbon source (–D) for 10 min. (D) Quantification of Pub1-positive foci that were observed under various stresses. *** $P < 0.001$. Scale bars: 5 μm .

stress granule formation (Yoon et al., 2010), we next asked whether the number of stress granules is also increased under standard growth conditions in the mutant strains. Stress granule formation has been demonstrated to occur under glucose starvation and under heat stress (Buchan et al., 2008; Grousl et al., 2009). As a marker for stress granule formation, we used the polyU-binding protein Pub1p (Buchan et al., 2008). Indeed, we observed stress granule formation in wild-type cells under both conditions, whereas, in $\Delta scp160$ and $\Delta bfr1$ cells, stress granules were only visible after heat stress (Fig. 5C,D). Thus, Scp160 and Bfr1 might be required for stress granule formation only under certain stresses. Consistently, the $\Delta bfr1$ and $\Delta scp160$ strains did not induce stress granule formation under standard growth conditions (Fig. 5C,D); therefore, the phenotype of P body induction in the $\Delta bfr1$ and $\Delta scp160$ strains is not strictly coupled to stress granule formation.

Overexpression of *SCP160* or *BFR1* rescues the enhanced P body formation phenotype of $\Delta bfr1$ or $\Delta scp160$, respectively
Bfr1 and Scp160 form a complex at actively translating polysomes, and their localization at the ER is interdependent,

nevertheless, they have been shown to have distinct functions (Lang et al., 2001). For example, only Scp160 binds mRNA, and only Bfr1 causes resistance to brefeldinA when overexpressed (Jackson and Képès, 1994; Lang and Fridovich-Keil, 2000; Weber et al., 1997). Moreover, Scp160, rather than Bfr1, bound to the mRNA associated P body components. We, therefore, wondered whether the interaction of Scp160 with Bfr1 is required to prevent P body formation under normal growth conditions, or whether Bfr1 and Scp160 can act independently. To distinguish between these possibilities, we overexpressed *SCP160* and *BFR1* by using the strong *TEF1* promoter in the $\Delta bfr1$ and $\Delta scp160$ strains, respectively. Both genes were also overexpressed, individually, in the wild-type strain. In wild-type cells, the increased expression caused both proteins to also localize to the cytoplasm, indicating that the binding sites at the ER were saturable (Fig. 6A). Overexpression of *BFR1* in $\Delta scp160$ cells, or *SCP160* in $\Delta bfr1$ cells, reduced the number of Dcp2-positive foci to that found in wild-type cells (Fig. 6B,C). This reciprocal rescue was specific because overexpression of the unrelated ArfGAP *GLO3*, under the control of the *TEF1* promoter, did not

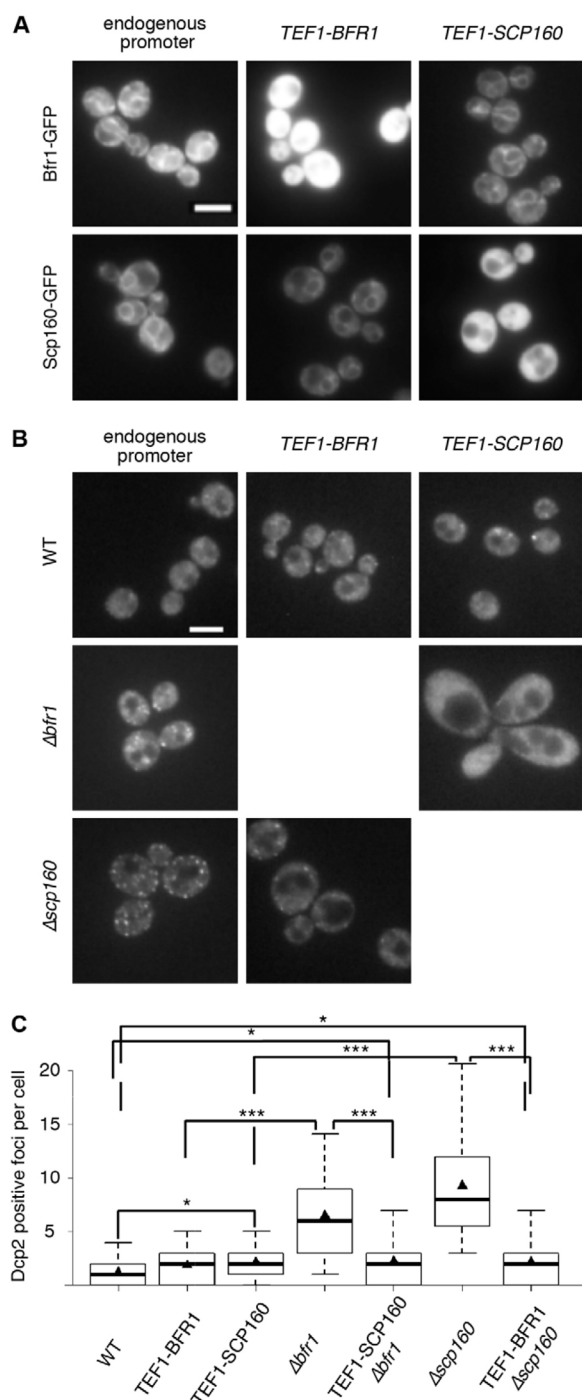


Fig. 6. Overexpression of *SCP160* or *BFR1* rescues the Dcp2-foci phenotype in the reciprocal deletion. (A) Overexpression of Bfr1-GFP or Scp160-GFP led to saturation of ER sites, whereas Bfr1-GFP or Scp160-GFP remained at the ER in *TEF1-SCP160* or *TEF1-BFR1* cells, respectively. The endogenous promoters of *BFR1* or *SCP160* were chromosomally exchanged for the constitutive *TEF1* promoter and the localization of Bfr1-GFP or Scp160-GFP was observed. (B) Dcp2-positive foci were reduced in *TEF1-SCP160 Δbfr1* or *TEF1-BFR1 Δscp160* strains compared with the deletions alone. *BFR1* or *SCP160* were overexpressed in strains expressing Dcp2-GFP in which either *SCP160* or *BFR1* had been deleted. (C) Quantification of the Dcp2-positive foci in cells shown in B. See Fig. 5B for details on the representation. *** $P < 0.001$, * $P < 0.05$. Scale bars: 5 μ m.

Loss of Scp160 generates pseudo P bodies

So far we have shown that loss of Scp160 and Bfr1 induces Dcp2-positive foci. P bodies are highly dynamic structures in which P body components assemble in an aggregate-like manner, similar to prions. In fact, a number of P body proteins contain prion-like domains (Alberti et al., 2009; Reijns et al., 2008); thus, it would be conceivable that, in the absence of Scp160 or Bfr1, proper P bodies do not form. Given that the formation of P bodies requires the presence of RNA in these structures (Coller and Parker, 2005; Teixeira et al., 2005), we treated cells with cycloheximide, which 'locks' ribosomes onto mRNA and restricts the availability of the mRNA for the formation of P bodies. As expected, treatment of cells with cycloheximide abolished the Dcp2-positive foci in the mutant strains (Fig. 7A), indicating that *Δscp160* and *Δbfr1* cause the appearance of bona fide P bodies.

To expand our results, we determined the localization of three additional P body constituents (Scd6, Edc3 and Dhh1) (Fig. 7B and C). All of the markers formed multiple foci in *Δbfr1* cells, only a few Scd6- or Edc3-positive structures were observed in *Δscp160* cells and Dhh1 did not form foci that would correspond to P-bodies. To demonstrate that the foci formed by the different P body components associated with the same structures, we co-expressed Dcp2-GFP and Edc3-mCherry (supplementary material Fig. S2E). The localizations of the P body components showed extensive overlap, indicating that they are, indeed, present on the same structure. These data indicate that, in *Δbfr1* cells, bona fide P bodies are formed in the absence of stress. By contrast, loss of Scp160 led to the formation of aggregates that lacked certain P body components, which we define as pseudo P bodies. Our results suggest that Scp160 might play a role in the assembly of P body proteins. Taken together, our data are consistent with both Bfr1 and Scp160 being negative regulators of P body formation in the absence of stress.

Scp160 and Bfr1 do not repress P body formation under stress

We hypothesized that because Bfr1 and Scp160 associate with actively translating polysomes, both proteins could prevent access of P body components to mRNA during translation. During stress conditions, under which translation is attenuated (Bregues et al., 2005; Kilchert et al., 2010), it is possible that polysomes disassemble and, therefore, that Scp160 and Bfr1 are lost from the mRNA, which means that they cannot protect mRNA and cannot be involved in the control of P body formation. Consequently, the loss of Scp160 or Bfr1 should not affect P body formation under such stress conditions. Upon withdrawal of glucose from wild-type, *Δscp160* or *Δbfr1* cultures, we observed P body induction to a similar extent in wild-type and *Δbfr1* cells (Fig. 7D and E). A small increase in the number of Dcp2-positive

rescue the multiple-P-body phenotype in *Δscp160* or *Δbfr1* strains (supplementary material Fig. S2D); thus, merely increasing the mRNA levels did not rescue the P body phenotype. These data indicate that both Scp160 and Bfr1 are able to independently prevent P body formation under normal growth conditions.

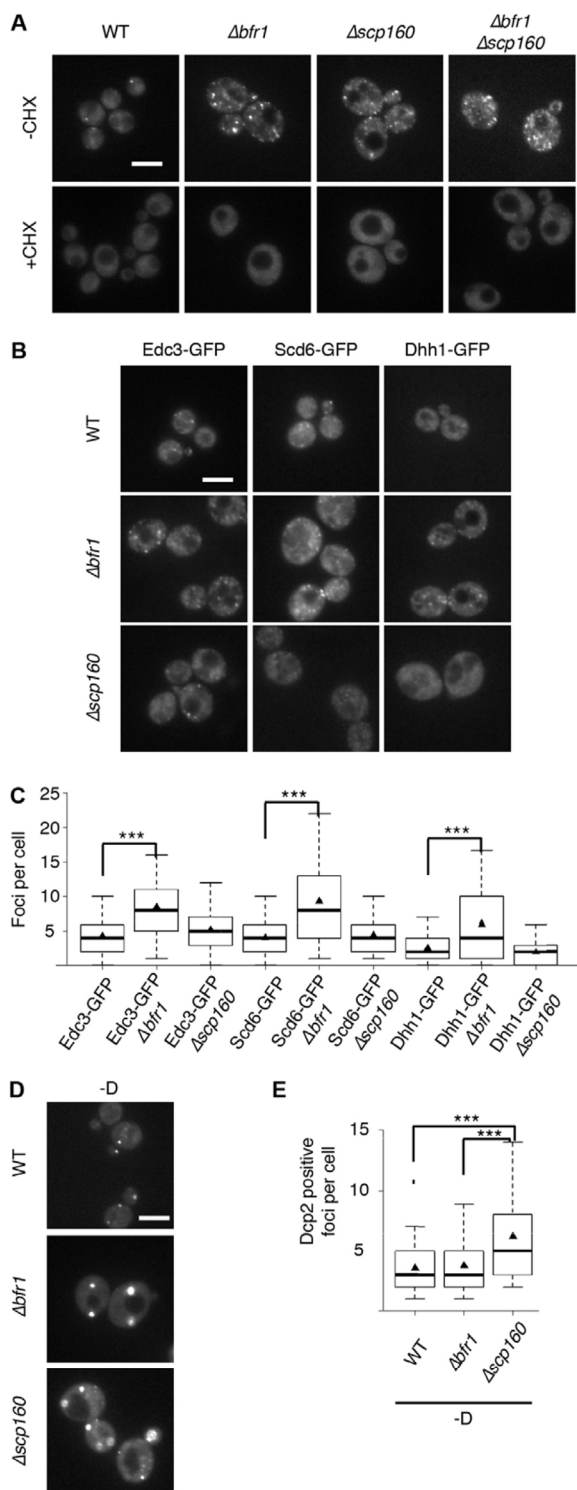


Fig. 7. Pseudo P bodies are formed in $\Delta scp160$ cells. (A) Cycloheximide inhibits the formation of Dcp2-positive foci. Dcp2-GFP expressing cells were grown at 23°C to mid-log phase and then cycloheximide was added to a final concentration of 100 $\mu\text{g/ml}$ for 10 min before imaging. In all cases, few, if any, Dcp2-positive foci were observed upon addition of cycloheximide, indicating that the Dcp2-containing foci contained RNA. (B) Pseudo P bodies are formed in $\Delta scp160$ cells. To test if the Dcp2 containing foci were bona fide P bodies, either *BFR1* or *SCP160* was deleted from strains that expressed Edc3-GFP, Scd6-GFP or Dhh1-GFP. Although multiple foci were observed in $\Delta bfr1$ cells for all markers, very few foci were observed in $\Delta scp160$ cells. (C) Quantification of the Edc3-GFP-, Scd6-GFP- and Dhh1-GFP-positive foci observed in B. $***P < 0.001$. For a description of the quantification, see Fig. 5B. (D) Starvation induces Dcp2-positive foci. Cells containing Dcp2-GFP were grown to mid-log phase and then incubated in rich medium without a carbon source (-D) for 10 min before imaging. Bright Dcp2-positive foci were observed in wild-type (WT), $\Delta bfr1$ and $\Delta scp160$ cells. In $\Delta scp160$ cells, foci of different sizes were observed. (E) Quantification of the Dcp2-GFP foci observed under conditions of starvation in D. $***P < 0.001$. Scale bars: 5 μm .

structures was observed in the $\Delta scp160$ strain, consistent with a role for Scp160 in the correct assembly of P bodies. A similar result was obtained under heat stress (supplementary material Fig. S3). Our results are consistent with Scp160 and Bfr1 having a negative role on the formation of P bodies, but only in the absence of stress.

DISCUSSION

P body formation is an important process by which eukaryotic cells respond to a plethora of stresses, such as environmental, metabolic and cellular stress. Here, we aimed to understand why P bodies are localized in close proximity to the ER membrane. We find that P body components interact with the polysome-associated mRNA-binding protein Scp160. This interaction exposes the P body components to mRNA molecules as soon as they are released from the polysomes. Thus, the function of Scp160, and its interacting protein Bfr1, is, probably, to keep the P body components in a 'waiting' position but, nevertheless, inhibit the formation of P bodies under normal growth and stress-free conditions (Fig. 8). In this model, as soon as the cell encounters stress, the protective function of Scp160 and Bfr1 is lost, and P body components have unrestricted access to mRNAs.

We find that loss of either Bfr1 or Scp160 causes the formation of multiple Dcp2-positive structures. Although both structures contain mRNA, only the Dcp2-positive foci in $\Delta bfr1$ cells appear to be fully assembled P bodies (Fig. 8). In $\Delta scp160$ cells, the Dcp2-positive structures do not contain all of the P body components and, hence, are probably not functional in terms of mRNA decay. Thus, Scp160 appears to play a, perhaps, regulatory role in the correct assembly of P bodies. We assume that this role is more involved in the regulation of the process, because P bodies formed in $\Delta scp160$ strains under glucose starvation and also because stress granules appeared under heat stress.

The association of P body components with polysomes is, perhaps, not surprising. Different laboratories have previously proposed a model of dynamic equilibrium in which P body formation is directly coupled to translation attenuation (Coller and Parker, 2005; Franks and Lykke-Andersen, 2008). The most plausible way to achieve this coupling would be through a direct interaction. In addition, influencing the phosphorylation state of Dcp2 could be a part of the regulation of the dynamic equilibrium. Dcp2 is predominantly in the phosphorylated state on membrane-associated polysomes, whereas the phosphorylated

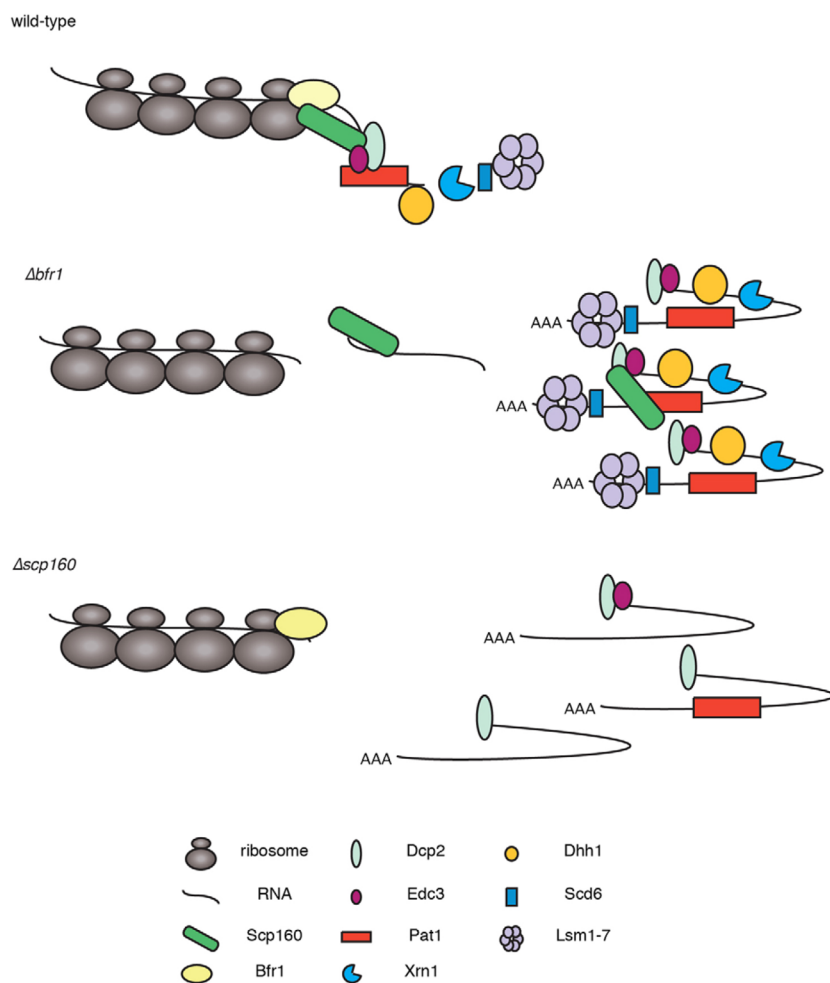


Fig. 8. Scp160 and Bfr1 inhibit P body formation under normal growth conditions. In wild-type cells under normal growth conditions, Scp160 and Bfr1 protect RNA at polysomes. Scp160 interacts with RNA and P body components and leaves P bodies in a 'waiting' position while still inhibiting P body formation. In $\Delta bfr1$ cells, Scp160 is not efficiently recruited to the polysomes and cannot properly protect the RNA, thus, allowing P body components to access RNAs. In $\Delta scp160$, Bfr1 can, to an extent, be recruited to polysomes, but without Scp160, proper P body assembly cannot occur, leading to the formation of pseudo P bodies.

and non-phosphorylated forms of Dcp2 are present in the soluble pool of polysomes. Phosphorylation of Dcp2 is required for the assembly of P bodies, which might influence the decay of some mRNAs (Yoon et al., 2010). Because P bodies are in close proximity to the ER, the phosphorylation state of Dcp2 might represent a 'primed state' for P body formation. Moreover, the P body components Dhh1 and Pat1 have been shown to be translational repressors, indicating that there might be a feedback mechanism between P bodies and ribosomes (Franks and Lykke-Andersen, 2008; Pilkington and Parker, 2008).

Scp160 and Bfr1 are, most likely, not the only proteins that can restrict the access of P body components to polysome-associated mRNA. Moreover, they are not essential for the association of P body components with polysomes, or the localization of P bodies close to the ER. Still, it is noteworthy that Scp160 is predominantly associated with membrane-bound polysomes (Weber et al., 1997). Thus, it cannot be excluded that Scp160 has some role in P body localization to the ER. It has been established that Scp160 only binds to a subset of mRNAs (Gelin-Licht et al., 2012; Hogan et al., 2008; Li et al., 2003), and a biological role for the mRNA–Scp160 interaction has been demonstrated for *ASH1* mRNA localization and pheromone

sensing (Gelin-Licht et al., 2012; Irie et al., 2002; Trautwein et al., 2004). Importantly, Scp160 has been shown to bind *DHHL1* mRNA and is required for efficient translation of this message (Li et al., 2003). Thus, Scp160 could be part of a regulatory loop that controls the translation of specific messages. In the case of Dhh1, however, we could not detect a difference in the protein levels in $\Delta scp160$ cells (supplementary material Fig. S4). This role could be regulated by phosphorylation because Scp160 is phosphorylated upon inhibition of the TOR complex by rapamycin, mimicking amino acid starvation (Soulard et al., 2010). In addition, Scp160 is part of a complex that contains Eap1, a negative regulator of translation (Cosentino et al., 2000; Mendelsohn et al., 2003). In fact, the Smy2, Eap1, Scp160, Asc1 (SESA) complex has been shown to act as a translational repressor of the *POM34* mRNA in response to spindle pole body (SPB) duplication defects (Sezen et al., 2009). Pom34 is a component of the nuclear pore complex that plays a role in the insertion of the SPB into the nuclear envelope.

Scp160 appears to have multiple cellular functions – Scp160 controls ploidy (hence the name *Saccharomyces* protein controlling ploidy) (Wintersberger et al., 1995), it is required for the asymmetric localization of mRNAs (Gelin-Licht et al.,

2012; Irie et al., 2002; Trautwein et al., 2004) and is part of a translational repressor complex (Sezen et al., 2009). Scp160 might also act as a signaling platform on ribosomes to control the translation of specific mRNAs (Baum et al., 2004), as it has been shown to act as an effector of a G-protein in the mating response pathway (Guo et al., 2003) and contributes to the regulation of telomere silencing (Marsellach et al., 2006). Furthermore, here, we show that Scp160 negatively regulates P body formation in the absence of stress and might be a novel P body component. How can all of these functions be performed by one protein? Scp160 could be part of different complexes that regulate Scp160 functions and recruit it to the correct site of function; such an adaptor function could be performed by Bfr1. Scp160 requires Bfr1 for efficient polysome association, and Bfr1 might recruit the SESA complex to the SPB (Sezen et al., 2009). However, Bfr1 must have additional functions, besides being an Scp160 interactor because overexpression of *BFR1* in the *Δscp160* strain was sufficient to alleviate the pseudo P body phenotype, and the concomitant loss of *BFR1* and *SCP160* showed a strong reduction of phosphorylated Dcp2 on soluble polysomes. Bfr1 might directly interact with P body components, although with a lower affinity than Scp160. Overexpression of *BFR1* could, potentially, increase its interaction with P body components and maintain the P body components in the ‘waiting’ position.

In addition, the localization of *ASH1* mRNA at the bud tip is not only dependent on Scp160 but also on Bfr1 and ribosomes (Irie et al., 2002; Trautwein et al., 2004). Thus, it is conceivable that Bfr1 is the adaptor for complexes that are involved in translation activation and repression. Clearly, Scp160 must have other adaptor proteins to fulfill its Bfr1-independent roles as a G protein effector or in the silencing of telomeres.

Scp160 is conserved in species up to human, and the closest homologues are vigilin (also known as HDLBP) and the fragile X syndrome protein FMRP (also known as FMR1) (Currie and Brown, 1999; Weber et al., 1997). Vigilin has been proposed to have a role in cytoplasmic mRNA metabolism in *Drosophila* and human cell lines (Goolsby and Shapiro, 2003) and to protect vitellogenin mRNA from degradation by the mRNA endonuclease PMR-1 in *Xenopus* (Cunningham et al., 2000). In addition, vigilin binds to the mRNA of the proto-oncogene *c-fms* and inhibits its translation, thereby relieving suppression of breast cancer cell proliferation (Cao et al., 2004; Woo et al., 2011). These functions might be regulated in a similar manner through binding to polysomes, because, akin to Scp160, vigilin binds to ribosomes through its C-terminal tail (Vollbrandt et al., 2004). Furthermore, the second mammalian homologue of Scp160 FMRP binds to a subset of mRNAs, and the I304N mutation, which was first described in a fragile X syndrome (FXS) patient, reduces the association of the protein with mRNAs and polysomes (Ascano et al., 2012; Feng et al., 1997; Siomi et al., 1994). Therefore, it is also conceivable that the function of Scp160 to control the translation of a subset of mRNAs is also conserved in vigilin and FMRP.

MATERIALS AND METHODS

Yeast methods

Standard genetic techniques were used throughout (Sherman, 1991). All modifications were carried out chromosomally, with the exceptions listed below. Chromosomal tagging and deletions were performed as described previously (Knop et al., 1999; Knop et al., 1999; Gueldener et al., 2002; Gueldener et al., 2002). For co-staining of the ER, the cells were transformed with the plasmid pSM1959 (with selectable marker LEU2) carrying Sec63-RFP (kindly provided by Susan Michaelis, Johns Hopkins University, Baltimore, MD), pRP1661 (with selectable marker

URA3) encoding Pub1-mCherry and pRP1575 (with selectable marker TRP1) encoding Edc3-mCherry were provided by Roy Parker (University of Colorado, Boulder, CO). The plasmid pMS449 carrying the $\Delta C4$ truncation of Scp160 was obtained from Matthias Seedorf (ZMBH Heidelberg, Germany). The plasmid pTEF-Glo3-FLAG (with selectable marker LEU2) was created through amplification of the *GLO3* gene using the primers Glo3-6F and Glo3-11R (5'-GCAATTTAGGA-TCCAC-ATAGCGACAATGAG-3' and 5'-GAGAAAATTCTCGAGATTCTTCTAAGTAG-3', respectively) and the resulting fragment was cloned using *Bam*HI and *Xho*I into pcDNA3.1 with a C-terminal FLAG tag.

The C-terminal FLAG tag was obtained through PCR of the plasmid pcDNA3.1+the Glo3-FLAG construct with the primers Glo3-6F and Glo3-10R (5'-GGCAAAGTGCAGATGGCTG-3'). The resulting PCR fragment was digested with *Bam*HI and *Pst*I, and ligated into vector p425TEF. The final plasmids were confirmed by sequencing. The strains used in this study are listed in supplementary material Table S1.

HBH-purification

The HBH purification was carried out as previously described by Tagwerker and colleagues (Tagwerker, et al., 2006) with modifications. Cells that expressed Dcp2-HBH or Scd6-HBH were grown to mid-to-late log phase at 23°C then shifted for 1 h to 37°C. The cells were fixed by adding 37% formaldehyde to a final concentration of 1% and incubating at room temperature for 2 min with gentle agitation. The formaldehyde was quenched for 5 min by the addition of glycine to a final concentration of 1.25 mM. The cells were harvested (4700 g for 3 min at 4°C), washed in 50 ml ice-cold double distilled H₂O, pooled, sedimented by centrifugation (5 min at 3000 g), flash frozen in liquid nitrogen and stored at -80°C. The cells were thawed and resuspended in 2 ml of buffer 1 (50 mM NaPi pH 8.0, 8 M urea, 300 mM NaCl, 20 mM imidazole, 0.5% Tween-20) per gram of yeast cell pellet. Per 2 ml screw capped tube containing 500 μ l glass beads, 1 ml of the cell suspension was added. Lysis was performed in a FastPrep instrument four times for 45 seconds each at 4°C. The glass beads and cell debris were cleared with a slow spin (1300 g for 10 min at 4°C), and the supernatant was removed and pooled. The supernatants were spun at 20,000 g for 15 min at 4°C and the resulting pellets were resuspended in 500 μ l buffer 1 with the addition of 1% Tween-20. 2.5 ml of Ni-NTA slurry that had been washed in buffer 1 was added to the pooled lysates and rotated overnight at room temperature. The tubes were spun at room temperature for 3 min at 2500 g and washed with 10 ml buffer 1. The tubes were spun as before and a series of 10 ml washes and spins were sequentially performed (buffer 2: 50 mM NaPi pH 6.4, 8 M urea, 300 mM NaCl, 0.5% Tween-20; buffer 3: 50 mM NaPi pH 8.0, 8 M urea, 300 mM NaCl, 0.5% Tween-20, 20 mM imidazole; buffer 4: 50 mM NaPi pH 8.0, 8 M urea, 300 mM NaCl, 0.5% Tween-20, 40 mM imidazole). After the final wash and spin, 4 ml of elution buffer (50 mM NaPi pH 6.4, 8 M urea, 300 mM NaCl, 0.5% Tween-20, 300 mM imidazole) was added and rotated with the beads for 45 min. The beads were spun down as before, the eluate was collected, and the elution step was repeated. 300 μ l streptavidin agarose that had been washed in buffer 1 was added to the 8 ml of elute and rotated for 2 h at room temperature. The slurry was then spun as before and washed with 10 ml of buffer 6 (50 mM Tris-HCl pH 8.0, 8 M urea, 300 mM NaCl, 2% SDS). This step was then repeated with 10 ml buffer 7 (50 mM Tris-HCl pH 8.0, 8 M urea, 300 mM NaCl, 0.2% SDS). The final wash was performed in buffer 8 (50 mM Tris-HCl pH 8.0, 8 M urea, 300 mM NaCl) and the streptavidin agarose was resuspended in 1 ml buffer 8. The slurry was then washed three times with 1 ml 50 mM Tris-HCl pH 8.0 with 0.1% SDS, and 50 μ l of solution was left in the tube after the final wash. To each tube, 0.25 μ l of 1 mg/ml Endoproteinase LysC (ELC) was added, and the tubes were placed at 37°C with shaking. After 2 h, a further 0.25 μ l of 1 mg/ml ELC was added and the tubes were placed at 37°C overnight with shaking. The tubes were briefly spun down and the supernatant was collected. The beads were extracted twice with 50 mM Tris-HCl pH 8.0 with 0.1% SDS (in a volume of 200 μ l followed by 100 μ l). The three samples were pooled and dried in a Speed-Vac concentrator. The peptides were

resuspended in 400 μ l BS (85% acetonitrile, 10 mM ammonium acetate with formic acid pH 3.5) and loaded twice on a HILIC TopTip PolyLC spin column (PolyLC) that had been equilibrated three times with 50 μ l ES (5% acetonitrile, 10 mM ammonium acetate with formic acid pH 3.5) and three times with 50 μ l BS. The column was washed three times with 50 μ l BS and the peptides were eluted four times with 25 μ l ES. All elutions were pooled and dried in a Speed-Vac concentrator. The peptides were then resuspended in 50 μ l of 50 mM NH_4HCO_3 and subjected to trypsin digest with 0.5 μ l 1 mg/ml trypsin (Promega) for 6 h at 37°C. Mass spectrometric analysis was performed using LC-MS/MS (Orbitrap).

Fluorescence microscopy

Cells were grown in yeast extract peptone dextrose (YPD) medium to early-log phase and then either shifted to 37°C for 1 h or subjected to various stresses, as indicated. The cells were spun at 3000 *g* for 3 min and resuspended in Hartwell's complete (HC) medium and immobilized on concanavalin-A-coated slides. For strains harboring the pTEF-Glo3-FLAG plasmid, the cells were grown in HC medium that lacked leucine. In the methionine experiments, cells were grown at 30°C in YPD containing 100 μ g/ml methionine for 72 h and maintained at an OD_{600} of between 0.2 and 1.0 through continuous dilution.

Fluorescence was monitored with an Axiocam mounted on an Axioplan 2 fluorescence microscope (Carl Zeiss, Oberkochen, Germany) by using Axiovision software. Image processing was performed using Image J and Adobe Photoshop CS5 (San Jose, CA). For counting, a minimum of 200 cells from at least three independent experiments was counted per condition. In the quantification graphs, the size of the box is determined by the 25th and 75th percentiles, the whiskers represent the 5th and 95th percentiles, the lines and the triangles mark the median and the mean, respectively.

Immunoelectron microscopy

Cells expressing Dcp2-9Myc were grown to early-log phase at 23°C and then shifted to 37°C for 1 h. The cells were fixed and treated for immunoelectron microscopy as described previously (Prescianotto-Baschong and Riezman, 2002). Secondary antibodies against goat anti-rabbit IgG that had been coupled to 10-nm gold particles (BBInternational, Cardiff, United Kingdom) were used to detect the binding of polyclonal rabbit antibodies that recognise Myc (Abcam, Cambridge, MA).

Immunoprecipitations

Immunoprecipitations were performed similarly as described previously (Sezen et al., 2009). Twenty OD_{600} units of logarithmically growing cells that had been grown in YPD and subjected to the various stresses, as indicated, were disrupted with glass beads in 300 μ l of immunoprecipitation buffer [50 mM triethanolamine pH 6.0, 150 mM KCl, 5 mM EDTA, 5 mM EGTA, protease inhibitor tablet (Roche), 1 mM PMSF and 1 mM benzimidazole]. The lysates were incubated with 1% Triton X-100 for 10 min at 4°C, and the extracts were cleared by centrifugation (3000 *g* for 10 min at 4°C). An aliquot was removed that served as the input control, and the remainder of the extract was incubated with a monoclonal antibody against FLAG peptide (M2, Invitrogen) and magnetic bead slurry (Dynal) for 2.5 h at 4°C. The beads were washed three times with immunoprecipitation buffer containing 0.1% Triton X-100. The beads were resuspended in sample buffer and analyzed by immunoblotting.

For the RNase A treated samples, after the extracts had been cleared by centrifugation, they were treated with 40 U of RNase inhibitor (Promega) or 1 μ g/ μ l RNase A and incubated for 1 h at 4°C. The extracts were then spun for 3 min at 3000 *g*, and the supernatant was used for the immunoprecipitation as described above.

Antibodies

Antibodies were used to detect the following epitope tags and proteins: Myc (9E10, 1:1000, Sigma-Aldrich), hemagglutinin (HA11, 1:1000, Covance, Princeton, NJ), Scp160 (1:1000), Bfr1 (1:1000), Rpl16a

(1:1500, a gift from Michael N. Hall, Biozentrum, Basel, Switzerland) and Sec61 (1:10,000, a gift from Martin Spiess, Biozentrum, Basel, Switzerland).

Flotation of P bodies

Flotation of ER membranes was performed as described previously (Schmid et al., 2006). The equivalent of 50 OD_{600} units was converted into spheroplasts at 37°C and lysed by Dounce homogenization in 3 ml lysis buffer [20 mM HEPES in KOH, pH 7.6, 100 mM sorbitol, 100 mM KAc, 5 mM $\text{Mg}(\text{Ac})_2$, 1 mM EDTA, 1 mM dithiothreitol, 100 μ g/ml cycloheximide, protease inhibitors]. After the removal of cellular debris (5 min, 300 *g*), the membranes were pelleted by centrifugation (10 min, 13,000 *g*), resuspended in 2 ml lysis buffer containing 50% sucrose and layered on top of 2 ml 65% sucrose in lysis buffer. Two additional 5 ml and 2 ml cushions (40% and 0% sucrose) were layered on top. The step gradient was spun in a TST41.14 rotor for 16 h at 28,000 *g*. After centrifugation, 1 ml fractions were collected from each of the cushions and the interfaces, and were then precipitated with trichloroacetic acid (TCA). The samples were analyzed by SDS-PAGE and immunoblotting.

Polysome profile analysis

Preparations of polysomes were performed as described previously (de la Cruz et al., 1997) on 4–47% sucrose gradients that had been prepared using a Gradient Master (Nycomed Pharma, Westbury, NY). Gradient analysis was performed using a gradient fractionator (Labconco, Kansas City, MO) and the Åcta FPLC system (GE Healthcare) and continuously monitored at A_{254} . Fractions were precipitated with 10% TCA, separated using SDS-PAGE and analyzed by western blotting.

Acknowledgements

We thank Cornelia Kilchert (Biozentrum, University Basel), Roy Parker, Matthias Seedorf, Michael N. Hall, Martin Spiess, Paul Jenö, Suzette Moes, Ian G Macara for reagents. Paul Jenö and Suzette Moes (Biozentrum, University of Basel) are acknowledged for the mass spectrometric analysis of the HBH purifications. Ian G. Macara is acknowledged for critically reading the manuscript.

Competing interests

The authors declare no competing interests.

Author contributions

J.W. and A.S. conceived the study; J.W., C.W., C.P.-B., A.F.E. and A.S. performed the experiments and analyzed the data; A.S. wrote the manuscript; all authors provided comments on the manuscript.

Funding

This work was supported by Werner-Siemens Fellowships (to J.W. and C.W.), the Human Frontiers Science Program [grant number RGP0031/2009-C], the Swiss National Science Foundation [grant number 31003A_141207] and the University of Basel (to A.S.).

Supplementary material

Supplementary material available online at <http://jcs.biologists.org/lookup/suppl/doi:10.1242/jcs.142083/-DC1>

References

- Alberti, S., Halfmann, R., King, O., Kapila, A. and Lindquist, S. (2009). A systematic survey identifies prions and illuminates sequence features of prionogenic proteins. *Cell* **137**, 146–158.
- Ascano, M., Jr, Mukherjee, N., Bandaru, P., Miller, J. B., Nusbaum, J. D., Corcoran, D. L., Langlois, C., Munschauer, M., Dewell, S., Hafner, M. et al. (2012). FMRP targets distinct mRNA sequence elements to regulate protein expression. *Nature* **492**, 382–386.
- Ashe, M. P., De Long, S. K. and Sachs, A. B. (2000). Glucose depletion rapidly inhibits translation initiation in yeast. *Mol. Biol. Cell* **11**, 833–848.
- Baum, S., Bittins, M., Frey, S. and Seedorf, M. (2004). Asc1p, a WD40-domain containing adaptor protein, is required for the interaction of the RNA-binding protein Scp160p with polysomes. *Biochem. J.* **380**, 823–830.
- Bregues, M., Teixeira, D. and Parker, R. (2005). Movement of eukaryotic mRNAs between polysomes and cytoplasmic processing bodies. *Science* **310**, 486–489.
- Buchan, J. R. and Parker, R. (2009). Eukaryotic stress granules: the ins and outs of translation. *Mol. Cell* **36**, 932–941.
- Buchan, J. R., Muhlrad, D. and Parker, R. (2008). P bodies promote stress granule assembly in *Saccharomyces cerevisiae*. *J. Cell Biol.* **183**, 441–455.

- Cao, W. M., Murao, K., Imachi, H., Yu, X., Abe, H., Yamauchi, A., Niimi, M., Miyauchi, A., Wong, N. C. and Ishida, T. (2004). A mutant high-density lipoprotein receptor inhibits proliferation of human breast cancer cells. *Cancer Res.* **64**, 1515–1521.
- Coller, J. and Parker, R. (2005). General translational repression by activators of mRNA decapping. *Cell* **122**, 875–886.
- Cosentino, G. P., Schmelzle, T., Haghghat, A., Helliwell, S. B., Hall, M. N. and Sonenberg, N. (2000). Eap1p, a novel eukaryotic translation initiation factor 4E-associated protein in *Saccharomyces cerevisiae*. *Mol. Cell. Biol.* **20**, 4604–4613.
- Cunningham, K. S., Dodson, R. E., Nagel, M. A., Shapiro, D. J. and Schoenberg, D. R. (2000). Vigilin binding selectively inhibits cleavage of the vitellogenin mRNA 3'-untranslated region by the mRNA endonuclease polysomal ribonuclease 1. *Proc. Natl. Acad. Sci. USA* **97**, 12498–12502.
- Currie, J. R. and Brown, W. T. (1999). KH domain-containing proteins of yeast: absence of a fragile X gene homologue. *Am. J. Med. Genet.* **84**, 272–276.
- de la Cruz, J., Iost, L., Kressler, D. and Linder, P. (1997). The p20 and Ded1 proteins have antagonistic roles in eIF4E-dependent translation in *Saccharomyces cerevisiae*. *Proc. Natl. Acad. Sci. USA* **94**, 5201–5206.
- Feng, Y., Absher, D., Eberhart, D. E., Brown, V., Malter, H. E. and Warren, S. T. (1997). FMRP associates with polyribosomes as an mRNA, and the 1304N mutation of severe fragile X syndrome abolishes this association. *Mol. Cell* **1**, 109–118.
- Franks, T. M. and Lykke-Andersen, J. (2008). The control of mRNA decapping and P-body formation. *Mol. Cell* **32**, 605–615.
- Gelin-Licht, R., Paliwal, S., Conlon, P., Levchenko, A. and Gerst, J. E. (2012). Scp160-dependent mRNA trafficking mediates pheromone gradient sensing and chemotropism in yeast. *Cell Rep.* **1**, 483–494.
- Goolsby, K. M. and Shapiro, D. J. (2003). RNAi-mediated depletion of the 15 KH domain protein, vigilin, induces death of dividing and non-dividing human cells but does not initially inhibit protein synthesis. *Nucleic Acids Res.* **31**, 5644–5653.
- Grousl, T., Ivanov, P., Frydlová, I., Vasicová, P., Janda, F., Vojtová, J., Malinská, K., Malcová, I., Nováková, L., Janosková, D. et al. (2009). Robust heat shock induces eIF2 α -phosphorylation-independent assembly of stress granules containing eIF3 and 40S ribosomal subunits in budding yeast, *Saccharomyces cerevisiae*. *J. Cell Sci.* **122**, 2078–2088.
- Gueldeger, U., Heinisch, J., Koehler, G. J., Voss, D. and Hegemann, J. H. (2002). A second set of loxP marker cassettes for Cre-mediated multiple gene knockouts in budding yeast. *Nucleic Acids Res.* **30**, e23.
- Guo, M., Aston, C., Burchett, S. A., Dyke, C., Fields, S., Rajarao, S. J., Uetz, P., Wang, Y., Young, K. and Dohlman, H. G. (2003). The yeast G protein alpha subunit Gpa1 transmits a signal through an RNA binding effector protein Scp160. *Mol. Cell* **12**, 517–524.
- Hitchcock, A. L., Krebber, H., Frieze, S., Lin, A., Latterich, M. and Silver, P. A. (2001). The conserved npl4 protein complex mediates proteasome-dependent membrane-bound transcription factor activation. *Mol. Biol. Cell* **12**, 3226–3241.
- Hogan, D. J., Riordan, D. P., Gerber, A. P., Herschlag, D. and Brown, P. O. (2008). Diverse RNA-binding proteins interact with functionally related sets of RNAs, suggesting an extensive regulatory system. *PLoS Biol.* **6**, e255.
- Irie, K., Tadauchi, T., Takizawa, P. A., Vale, R. D., Matsumoto, K. and Herskowitz, I. (2002). The Khd1 protein, which has three KH RNA-binding motifs, is required for proper localization of ASH1 mRNA in yeast. *EMBO J.* **21**, 1158–1167.
- Jackson, C. L. and Képés, F. (1994). BFR1, a multicopy suppressor of brefeldin A-induced lethality, is implicated in secretion and nuclear segregation in *Saccharomyces cerevisiae*. *Genetics* **137**, 423–437.
- Jain, S. and Parker, R. (2013). The discovery and analysis of P Bodies. *Adv. Exp. Med. Biol.* **768**, 23–43.
- Kilchert, C., Weidner, J., Prescianotto-Baschong, C. and Spang, A. (2010). Defects in the secretory pathway and high Ca²⁺ induce multiple P-bodies. *Mol. Biol. Cell* **21**, 2624–2638.
- Knop, M., Siegers, K., Pereira, G., Zachariae, W., Winsor, B., Nasmyth, K. and Schiebel, E. (1999). Epitope tagging of yeast genes using a PCR-based strategy: more tags and improved practical routines. *Yeast* **15**, 963–972.
- Lang, B. D. and Fridovich-Keil, J. L. (2000). Scp160p, a multiple KH-domain protein, is a component of mRNP complexes in yeast. *Nucleic Acids Res.* **28**, 1576–1584.
- Lang, B. D., Li Am, Black-Brewer, H. D. and Fridovich-Keil, J. L. (2001). The brefeldin A resistance protein Bfr1p is a component of polyribosome-associated mRNP complexes in yeast. *Nucleic Acids Res.* **29**, 2567–2574.
- Latterich, M., Fröhlich, K. U. and Schekman, R. (1995). Membrane fusion and the cell cycle: Cdc48p participates in the fusion of ER membranes. *Cell* **82**, 885–893.
- Li, A. M., Watson, A. and Fridovich-Keil, J. L. (2003). Scp160p associates with specific mRNAs in yeast. *Nucleic Acids Res.* **31**, 1830–1837.
- Marsellach, F. X., Huertas, D. and Azorin, F. (2006). The multi-KH domain protein of *Saccharomyces cerevisiae* Scp160p contributes to the regulation of telomeric silencing. *J. Biol. Chem.* **281**, 18227–18235.
- Mendelsohn, B. A., Li, A. M., Vargas, C. A., Riehm, K., Watson, A. and Fridovich-Keil, J. L. (2003). Genetic and biochemical interactions between SCP160 and EAP1 in yeast. *Nucleic Acids Res.* **31**, 5838–5847.
- Mitchell, S. F., Jain, S., She, M. and Parker, R. (2013). Global analysis of yeast mRNPs. *Nat. Struct. Mol. Biol.* **20**, 127–133.
- Muhrad, D., Decker, C. J. and Parker, R. (1995). Turnover mechanisms of the stable yeast PGK1 mRNA. *Mol. Cell. Biol.* **15**, 2145–2156.
- Parker, R. and Sheth, U. (2007). P bodies and the control of mRNA translation and degradation. *Mol. Cell* **25**, 635–646.
- Pilkington, G. R. and Parker, R. (2008). Pat1 contains distinct functional domains that promote P-body assembly and activation of decapping. *Mol. Cell. Biol.* **28**, 1298–1312.
- Prescianotto-Baschong, C. and Riezman, H. (2002). Ordering of compartments in the yeast endocytic pathway. *Traffic* **3**, 37–49.
- Reijms, M. A., Alexander, R. D., Spiller, M. P. and Beggs, J. D. (2008). A role for Q/N-rich aggregation-prone regions in P-body localization. *J. Cell Sci.* **121**, 2463–2472.
- Ritz, A. M., Trautwein, M., Grassinger, F. and Spang, A. (2014). The prion-like domain in the exomer-dependent cargo Pin2 serves as a trans-Golgi retention motif. *Cell Rep.* doi: 10.1016/j.celrep.2014.02.026. [Epub ahead of print].
- Schmid, M., Jaedicke, A., Du, T. G. and Jansen, R. P. (2006). Coordination of endoplasmic reticulum and mRNA localization to the yeast bud. *Curr. Biol.* **16**, 1538–1543.
- Schubert, C. and Buchberger, A. (2005). Membrane-bound Ubx2 recruits Cdc48 to ubiquitin ligases and their substrates to ensure efficient ER-associated protein degradation. *Nat. Cell Biol.* **7**, 999–1006.
- Sezen, B., Seedorf, M. and Schiebel, E. (2009). The SESA network links duplication of the yeast centrosome with the protein translation machinery. *Genes Dev.* **23**, 1559–1570.
- Sherman, F. (1991). Getting started with yeast. *Methods Enzymol.* **194**, 3–21.
- Shoemaker, C. J. and Green, R. (2012). Translation drives mRNA quality control. *Nat. Struct. Mol. Biol.* **19**, 594–601.
- Siomi, H., Choi, M., Siomi, M. C., Nussbaum, R. L. and Dreyfuss, G. (1994). Essential role for KH domains in RNA binding: impaired RNA binding by a mutation in the KH domain of FMR1 that causes fragile X syndrome. *Cell* **77**, 33–39.
- Soulard, A., Cremonesi, A., Moes, S., Schütz, F., Jenö, P. and Hall, M. N. (2010). The rapamycin-sensitive phosphoproteome reveals that TOR controls protein kinase A toward some but not all substrates. *Mol. Biol. Cell* **21**, 3475–3486.
- Tagwerker, C., Flick, K., Cui, M., Guerrero, C., Dou, Y., Auer, B., Baldi, P., Huang, L. and Kaiser, P. (2006). A tandem affinity tag for two-step purification under fully denaturing conditions: application in ubiquitin profiling and protein complex identification combined with in vivo cross-linking. *Mol. Cell. Proteomics* **5**, 737–748.
- Teixeira, D. and Parker, R. (2007). Analysis of P-body assembly in *Saccharomyces cerevisiae*. *Mol. Biol. Cell* **18**, 2274–2287.
- Teixeira, D., Sheth, U., Valencia-Sanchez, M. A., Brengues, M. and Parker, R. (2005). Processing bodies require RNA for assembly and contain nontranslating mRNAs. *RNA* **11**, 371–382.
- Trautwein, M., Dengjel, J., Schirle, M. and Spang, A. (2004). Arf1p provides an unexpected link between COPI vesicles and mRNA in *Saccharomyces cerevisiae*. *Mol. Biol. Cell* **15**, 5021–5037.
- Vollbrandt, T., Willkomm, D., Stossberg, H. and Kruse, C. (2004). Vigilin is colocalized with 80S ribosomes and binds to the ribosomal complex through its C-terminal domain. *Int. J. Biochem. Cell Biol.* **36**, 1306–1318.
- Weber, V., Wernitznig, A., Hager, G., Harata, M., Frank, P. and Wintersberger, U. (1997). Purification and nucleic-acid-binding properties of a *Saccharomyces cerevisiae* protein involved in the control of ploidy. *Eur. J. Biochem.* **249**, 309–317.
- Wintersberger, U., Kühne, C. and Karwan, A. (1995). Scp160p, a new yeast protein associated with the nuclear membrane and the endoplasmic reticulum, is necessary for maintenance of exact ploidy. *Yeast* **11**, 929–944.
- Woo, H. H., Yi, X., Lamb, T., Menzl, I., Baker, T., Shapiro, D. J. and Chambers, S. K. (2011). Posttranscriptional suppression of proto-oncogene c-fms expression by vigilin in breast cancer. *Mol. Cell. Biol.* **31**, 215–225.
- Yoon, J. H., Choi, E. J. and Parker, R. (2010). Dcp2 phosphorylation by Ste20 modulates stress granule assembly and mRNA decay in *Saccharomyces cerevisiae*. *J. Cell Biol.* **189**, 813–827.

Supplementary Material

Table S1: Yeast strains used in this study

| Strain | Designation | Genotype | Reference |
|----------|-----------------------|---|---------------------------|
| YPH499 | WT | MAT a ade2-101 his3-200 leu2-1 lys2-801 trp-63 ura3-52 | Sikorski and Hieter, 1989 |
| NY0-1 | ARF1 | MAT a ade2::ARF1::ADE2 arf1::HIS3 arf2::HIS3 ura3 lys2 trp1 his3 leu2 | Yahara et al., 2001 |
| NY11-1 | arf1-11 | MAT a ade2::arf1-11::ADE2 arf1::HIS3 arf2::HIS3 ura3 lys2 trp1 his3 leu2 | Yahara et al., 2001 |
| YAS2501 | Dcp2-HBH | MAT a ade2::ARF1::ADE2 arf1::HIS3 arf2::HIS3 ura3 lys2 trp1 his3 leu2 DCP2::DCP2-HBH-kanMX4 | This study |
| YAS2502 | arf1-11 Dcp2-HBH | MAT a ade2::arf1-11::ADE2 arf1::HIS3 arf2::HIS3 ura3 lys2 trp1 his3 leu2 DCP2::DCP2-HBH-kanMX4 | This study |
| YAS3240 | Scd6-HBH | MAT a ade2::ARF1::ADE2 arf1::HIS3 arf2::HIS3 ura3 lys2 trp1 his3 leu2 SCD6::SCD6-HBH-TRP1 | This study |
| YAS3257 | arf1-11 Scd6-HBH | MAT a ade2::arf1-11::ADE2 arf1::HIS3 arf2::HIS3 ura3 lys2 trp1 his3 leu2 SCD6::SCD6-HBH-TRP1 | This study |
| YAS1031A | Dcp2-GFP | MAT a ade2::ARF1::ADE2 arf1::HIS3 arf2::HIS3 ura3 lys2 trp1 his3 leu2 DCP2::DCP2-yEGFP-kanMX4 | This study |
| YAS1271 | Bfr1-GFP | MAT a ade2::ARF1::ADE2 arf1::HIS3 arf2::HIS3 ura3 lys2 trp1 his3 leu2 BFR1::BFR1-yEGFP-kanMX4 | This study |
| YAS1184 | Scp160-GFP | MAT a ade2::ARF1::ADE2 arf1::HIS3 arf2::HIS3 ura3 lys2 trp1 his3 leu2 SCP160::SCP160-yEGFP-kanMX4 | This study |
| YAS1272 | arf1-11 Bfr1-GFP | MAT a ade2::arf1-11::ADE2 arf1::HIS3 arf2::HIS3 ura3 lys2 trp1 his3 leu2 BFR1::BFR1-yEGFP-kanMX4 | This study |
| YAS1185 | arf1-11 Scp160-GFP | MAT a ade2::arf1-11::ADE2 arf1::HIS3 arf2::HIS3 ura3 lys2 trp1 his3 leu2 SCP160::SCP160-yEGFP-kanMX4 | This study |
| YAS3135 | Dcp2-GFP Δbfr1 | MAT a ade2::ARF1::ADE2 arf1::HIS3 arf2::HIS3 ura3 lys2 trp1 his3 DCP2::DCP2-yEGFP-kanMX4 bfr1::LEU2 | This study |
| YAS3136 | Dcp2-GFP Δscp160 | MAT a ade2::ARF1::ADE2 arf1::HIS3 arf2::HIS3 ura3 lys2 trp1 his3 leu2 DCP2::DCP2-yEGFP-kanMX4 scp160::URA3 | This study |
| YAS3137 | Dcp2-GFP Δbfr1Δscp160 | MAT a ade2::ARF1::ADE2 arf1::HIS3 arf2::HIS3 ura3 lys2 trp1 his3 leu2 DCP2::DCP2-yEGFP-kanMX4 bfr1::LEU2 scp160::URA3 | This study |
| YAS2238 | Edc3-GFP | MAT a ade2::ARF1::ADE2 arf1::HIS3 arf2::HIS3 ura3 lys2 his3 leu2 EDC3::EDC3-yEGFP-TRP1 | This study |
| YAS2867 | Edc3-GFP Δbfr1 | MAT a ade2::ARF1::ADE2 arf1::HIS3 arf2::HIS3 ura3 lys2 his3 leu2 EDC3::EDC3-yEGFP-TRP1 bfr1::URA3 | This study |
| YAS2778 | Edc3-GFP Δscp160 | MAT a ade2::ARF1::ADE2 arf1::HIS3 arf2::HIS3 ura3 lys2 his3 leu2 EDC3::EDC3-yEGFP-TRP1 scp160::URA3 | This study |
| YAS1153 | Dhh1-GFP | MAT a ade2::ARF1::ADE2 arf1::HIS3 arf2::HIS3 ura3 lys2 trp1 his3 leu2 DHH1::DHH1-yEGFP-kanMX4 | This study |
| YAS2878 | Dhh1-GFP Δbfr1 | MAT a ade2::ARF1::ADE2 arf1::HIS3 arf2::HIS3 ura3 lys2 trp1 his3 leu2 DHH1::DHH1-yEGFP-kanMX4 bfr1::URA3 | This study |
| YAS2782 | Dhh1-GFP Δscp160 | MAT a ade2::ARF1::ADE2 arf1::HIS3 arf2::HIS3 ura3 lys2 trp1 his3 leu2 DHH1::DHH1-yEGFP-kanMX4 scp160::URA3 | This study |
| YAS2315 | Scd6-GFP | MAT a ade2::ARF1::ADE2 arf1::HIS3 arf2::HIS3 ura3 lys2 trp1 his3 leu2 SCD6::SCD6-yEGFP-kanMX4 | This study |
| YAS2819 | Scd6-GFP Δbfr1 | MAT a ade2::ARF1::ADE2 arf1::HIS3 arf2::HIS3 ura3 lys2 trp1 his3 leu2 SCD6::SCD6-yEGFP-kanMX4 bfr1::URA3 | This study |
| YAS2783 | Scd6-GFP Δscp160 | MAT a ade2::ARF1::ADE2 arf1::HIS3 arf2::HIS3 ura3 lys2 trp1 his3 leu2 SCD6::SCD6-yEGFP-kanMX4 scp160::URA3 | This study |
| YAS1294 | Dcp2-9myc | MAT a ade2::ARF1::ADE2 arf1::HIS3 arf2::HIS3 ura3 lys2 trp1 his3 leu2 DCP2::DCP2-9myc-TRP1 | This study |

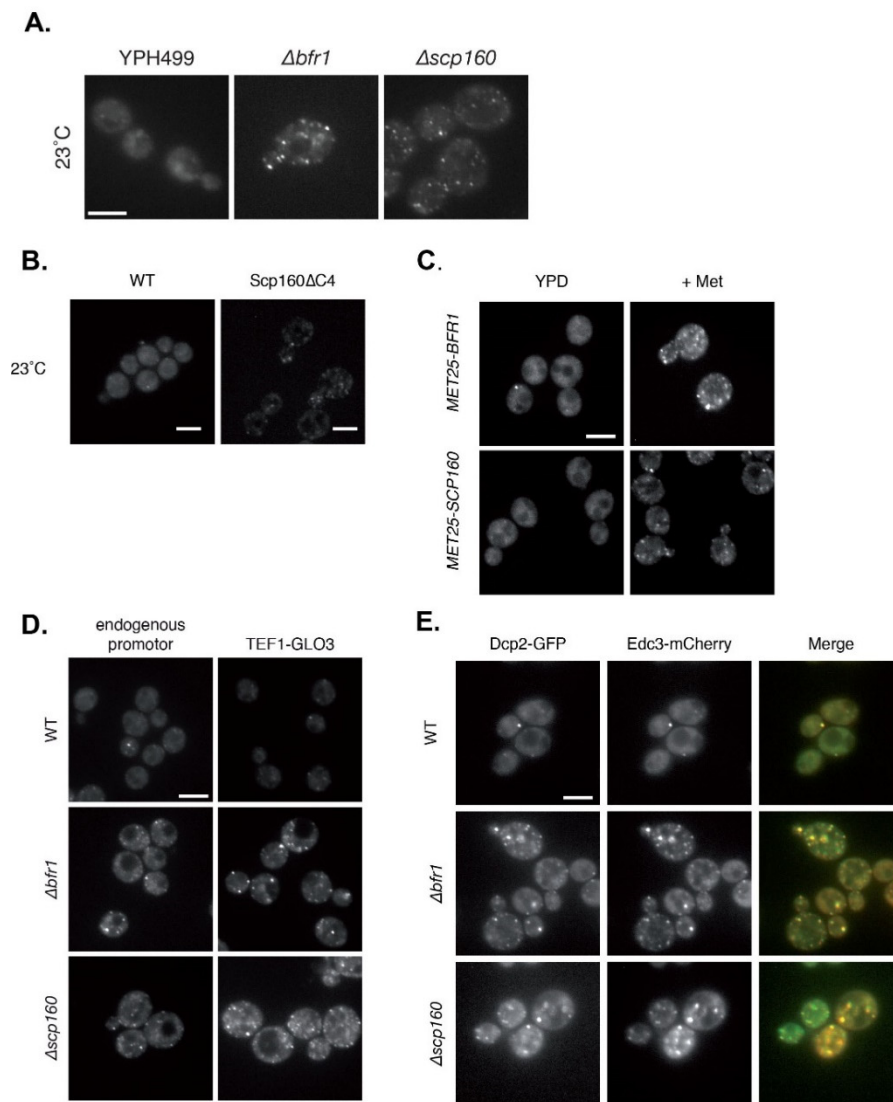


Figure S2. (A) Deletion of *SCP160* or *BFR1* led to multiple Dcp2-positive foci. *SCP160* or *BFR1* were deleted in the wild type YPH499 in which Dcp2 was tagged with GFP. (B) Deletion of the last 4 KH domains in Scp160 results in multiple P-bodies. The endogenous copy of *SCP160* was replaced through homologous recombination with the linearized plasmid pMS449, in which the 4 most C-terminally located KH domains of Scp160 had been deleted. This strain also contains Dcp2-GFP tagged. The cells were grown at 23°C and P-body formation was observed. Similarly, to the $\Delta scp160$ strain, Scp160 Δ C4 led to an increase in P-bodies under normal growth conditions. (C) Loss of *BFR1* or *SCP160* through methionine shut-off results in an increase in P-body number. Strains were made, in which the endogenous promoters of *BFR1* and *SCP160* were replaced by the inducible MET25 promoter to simulate deletion of the gene. After 72 hours of methionine treatment, the observed P-body phenotypes in the shut-off were similar to the constant gene deletions. (D) Overexpression of an unrelated gene does not rescue $\Delta bfr1$ and $\Delta scp160$ phenotypes. Wild type, $\Delta bfr1$, and $\Delta scp160$ cells expressing Dcp2-GFP and containing the ArfGAP Glo3 under the endogenous promoter or on a plasmid expressing *GLO3* from the strong TEF1 promoter were observed at 23°C. In both $\Delta bfr1$ and $\Delta scp160$ strains, the increased level of *GLO3* mRNA did not affect the number of P-bodies induced. (E) Different P-body proteins co-localize in $\Delta bfr1$ and $\Delta scp160$ cells. Wild type, $\Delta bfr1$, and $\Delta scp160$ cells expressing Dcp2-GFP and containing a plasmid expressing Edc3-mCherry were observed at 23°C. In the majority of the cases Edc3-mCherry and Dcp2-GFP were seen to co-localize.

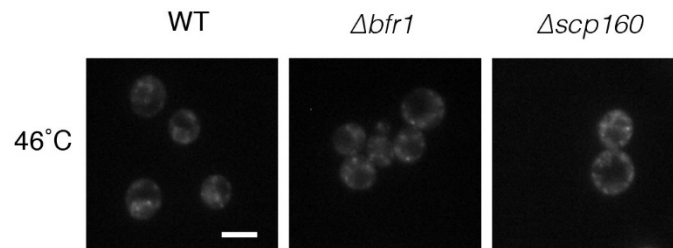


Figure S3. Heat stress induces P-bodies in $\Delta bfr1$ and $\Delta scp160$ similarly to wild type. Wild-type, $\Delta bfr1$, and $\Delta scp160$ cells expressing Dcp2-GFP were shifted to 46°C for 10 min before imaging. In all strains, P-body formation was observed.

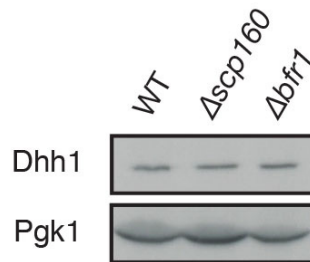


Figure S4. Dhh1 protein levels are similar in wild-type and mutant cells. Whole cell lysates were prepared from wild-type, $\Delta bfr1$, and $\Delta scp160$ cells expressing Dhh1-GFP. Lysates were separated by SDS-PAGE and Dhh1-GFP levels were assessed by immunoblot. In all strains, a similar level of Dhh1-GFP was observed. Pgk1 was used as loading control.

3.3 Pby1p, a stress-dependent P-body component

Summary

Processing bodies (P-bodies) are cytoplasmic RNP granules involved in mRNA storage, degradation and translational control. P-body formation can be triggered by a variety of stress conditions. Here, we identified Pby1p as a glucose starvation specific component of P-bodies. There it acts to stabilize specifically Dcp2p, as in $\Delta pby1$ Dcp2p but not two other major P-body components is degraded. Therefore, P-body formation still occurs but its function might be hampered. Instead, the decay of a subset of mRNAs was delayed, we propose that Pby1p is a modulator of P-body function under glucose starvation.

Introduction

P-bodies are nonmembrane-bound subcellular RNP granules, conserved from yeast to human. The formation of P-bodies can be induced by a variety of stresses, for instance, nutrient starvation, osmotic shocks, heat, acid stresses, and stationary phase of growth (Teixeira and Parker, 2007). Irrespective of the organism and the stress, the core protein components of P-bodies are always the same, which are mainly factors involved in the 5' to 3' mRNA decapping-dependent degradation pathway (Buchan et al., 2010). Recent studies revealed several novel, auxiliary or transient P-body components (Cai and Fletcher, 2013; Hey et al., 2012b; Ling et al., 2014a; Mitchell et al., 2013). For example, Whi3p is a RNA-binding protein, which inhibits several of its target mRNAs, was recently found to localize within P-bodies (Cai and Fletcher, 2013). However, some of the new constituents were not previously identified to be involved in mRNA regulation, for example, the Rho-family GEF DEF6 was known to be part of the T cell signaling for a long time and has lately been found to be involved in P-body formation through its Q rich domain (Hey et al., 2012b). Although the core P-body components appear to be identical across various stress conditions, morphology and half-life of P-bodies, as well as factors affecting P-body assembly vary depending on the particular stress (Buchan et al., 2010; Iwaki and Izawa, 2012; Kilchert et al., 2010). In addition, our previous work showed that the mRNA content sequestered in P-bodies is stress-dependent (Wang et al, unpublished), providing evidence for stress-specific factors. Those factors might play a role in P-body appearance, dynamics and/or recruitment of different subsets of transcripts depending on various stress conditions.

Here, we aimed to identify proteins that associated with P-bodies in response to a specific stress. Using a tandem affinity purification approach coupled with crosslinking, we identified Pby1p as a glucose-starvation specific component of P-bodies. Pby1p is essential for Dcp2p stability under glucose starvation and is involved in the regulation of mRNA decay.

Results

Pby1p is a P-body constituent under glucose starvation but not hyper-osmotic stresses

To determine whether the protein constituents of P-bodies vary in different stress conditions, a tandem affinity purification after crosslinking approach followed by MS using Dcp2p as a bait was employed. Glucose starvation and two hyper-osmotic stresses (0.5 M Na⁺ or 0.2 M Ca²⁺) which are rather commonly used were applied in this study. We had used a similar approach previously to identify P-body components and P-body sequestered transcripts (Weidner et al., 2014) (Wang et al., unpublished).

Table 1. Proteins identified uniquely under each stress condition by Mass Spectrometry.

(unique peptide > 1, number of peptide ≥ 3)

| | | | |
|------------------------------|-------------|-------|------|
| -Glu only | Pby1 | Hrr25 | Rpb2 |
| | Rpl26a | Cdc39 | Hho1 |
| +Ca²⁺ only | Hxk1 | Dbp3 | |

With this approach, proteins interacting with Dcp2p under each condition in comparison with a non-stressed control were identified, and indeed stress-specific subsets of proteins were detected (Table 1). We did not identify unique hit upon Na⁺ treatment. Interestingly, among the proteins detected specifically after glucose starvation we found Pby1p (**P-body associated protein 1**), which was previously identified to co-localize with P-bodies under glucose depletion (Sweet et al., 2007). Pby1p was implicated to be involved in DNA replication and repair, but it turned out that the $\Delta pby1$ mutant used in this study was actually wild-type for PBY1 and deleted for *mms4* (Olmezer et al., 2015). However, it was unclear if Pby1p is a *bona fide* P-body component or a stress-specific auxiliary protein. We confirmed the localization of Pby1p-GFP to P-bodies upon glucose starvation by microscopy. Importantly, no significant co-localization was observed upon the two osmotic stressors, indicating Pby1p as a stress-dependent P-body constituent rather than universal component (Figure 1).

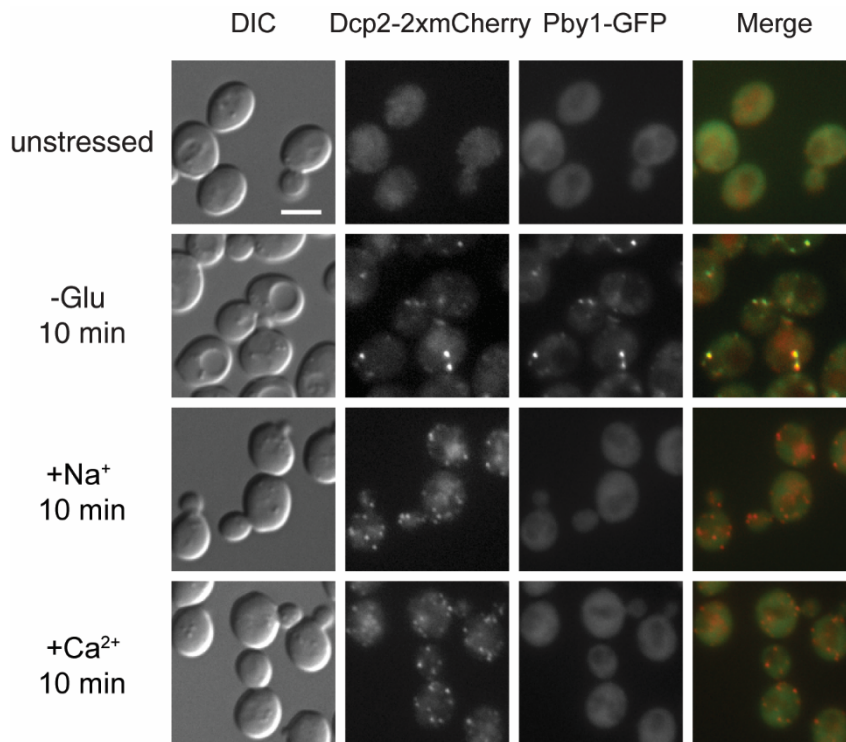


Figure. 1. Pby1p is an auxiliary P-body component.

Fluorescence images of P-bodies and Pby1p under glucose starvation or mild osmotic stress with Na^+ or Ca^{2+} . Cells expressing Dcp2p-2xmCherry and Pby1p-GFP were first grown in YPD media to mid-log phase and shifted to glucose-free YP media or YPD media containing 0.5 M NaCl or 0.2 M CaCl_2 for 10 min. Scale bars, 5 μm .

Loss of Pby1p reduces the protein level of Dcp2p without inhibiting P-body formation

To investigate the function of Pby1p, we first asked whether Pby1p was important for the P-body assembly. However, in the absence of Pby1p, P-body formation was not inhibited independent of the stressor (Figure 2A), excluding an indispensable role of Pby1p in P-body assembly. Even though P-body assembly appeared to be normal, we noticed a decrease in signal intensity of our P-body marker Dcp2p-GFP, in particular under glucose starvation (Figure 2A). Either Dcp2p was not efficiently recruited to the P-body or Dcp2p was downregulated in the $\Delta pby1$ strain. The latter possibility appeared to be correct, as the Dcp2p-GFP protein levels were drastically reduced in $\Delta pby1$ cells compared to wild-type cells. This effect was specific for Dcp2p because the protein level of two other P-body components, the helicase Dhh1p and the scaffold Pat1p, remained unaffected (Figure 2B). Thus, Pby1p may be involved in the regulation of Dcp2p stability in particular under glucose starvation.

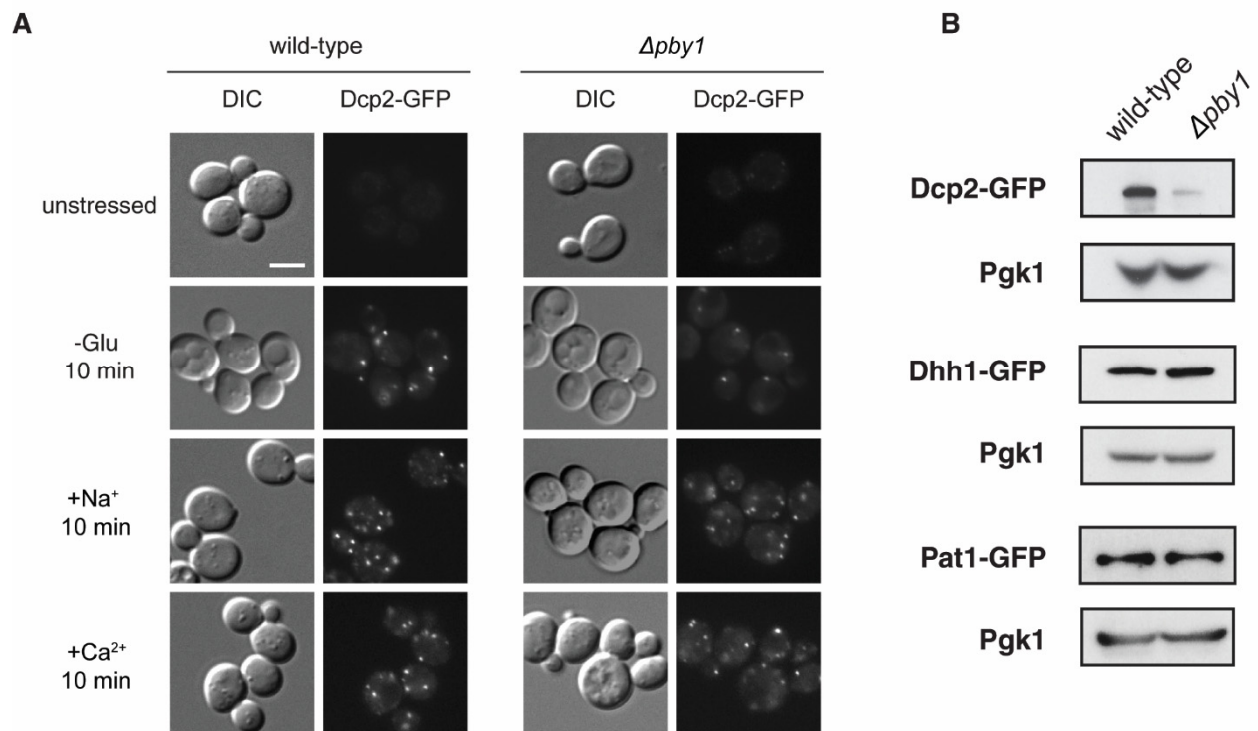


Figure 2. Dcp2p level but not P-body induction is repressed in $\Delta pby1$.

(A) Fluorescence images of P-bodies in wild-type and $\Delta pby1$ cells under glucose starvation, mild osmotic stress with Na⁺ or Ca²⁺. Scale bars, 5 μ m. (B) Western blot analysis of Dcp2p-GFP, Dhh1p-GFP and Pat1p-GFP in wild-type and $\Delta pby1$ cells. Pgk1p was used as a loading control. Anti-GFP and anti-Pgk1p antibodies were used for detection.

Pby1p possibly facilitates decay of P-body associated transcripts upon glucose deprivation

Since loss of Pby1p did not prevent P-body formation, we asked next whether Pby1p would be involved in the regulation of transcript turnover inside P-bodies. In a previous study, we characterized seven P-body associated transcripts under glucose depletion, one group (group I: *BSC1*, *TPI1*, *RLM1*) was decayed within P-bodies, while the other group (group II: *ATP11*, *ILM1*, *MRPL38*, *AIM2*) remained stable for at least 1 h after the stress (Wang et al., unpublished). To test our assumption, the stability of these seven mRNAs was analyzed with a non-invasive 4-TU pulse-chase RNA labeling technique followed by qRT-PCR in $\Delta pby1$. With this technique, we can specifically label RNA before stress application and determine its decay rate (Munchel et al., 2011). To distinguish whether loss of Pby1p affect P-body specific degradation (Xrn1p dependent), we also compared the mRNA half-life in $\Delta pby1$ with previously acquired data in wild-type and $\Delta xrn1$ (Fig. 3) (Wang et al., unpublished).

Interestingly, in the absence of Pby1p, degradation was delayed for group I transcripts *BSC1*, *RLM1* in contrast to wild-type, while deletion of the 5'-3' Xrn1p completely abolished decay (Figure 3). In addition, $\Delta pby1$ showed no significant change in mRNA decay rate for the

other group I transcripts *TPI1*, and group II mRNAs (*ATP11*, *ILM1*, *MRPL38* and *AIM2*). These observations imply Pby1p contributes to mRNA decay, and this role is specific to a subgroup of mRNAs.

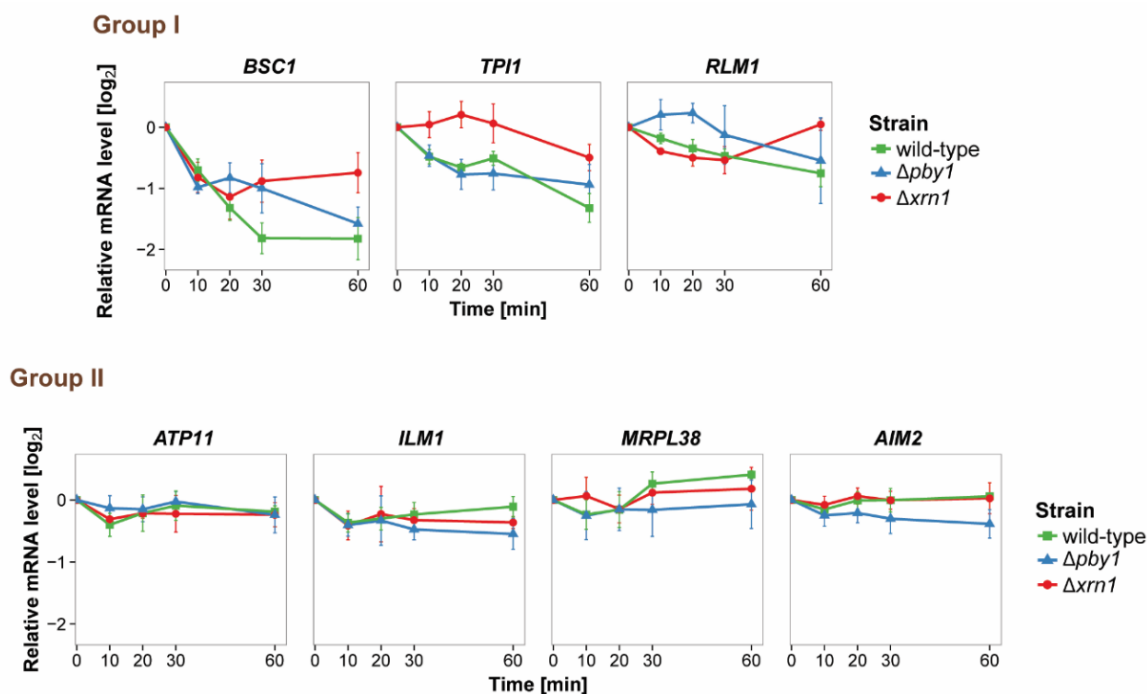


Figure 3. Degradation of P-body associated transcripts was slightly delayed in the absence of Pby1p.

The stability of 4TU labeled candidate mRNAs was determined by qRT-PCR in wild-type, $\Delta xrn1$ and $\Delta pby1$ at indicated time points following shift to glucose-depleted media. Transcription levels were normalized using *ACT1* mRNA as an endogenous reference. Group I: non-mitochondria-related candidates. Group II: mitochondria-related candidates. Data of wild-type and $\Delta xrn1$ was taken from previous results chapter. Error bars, \pm SEM.

Discussion and Outlook

In this study, Pby1p was identified by tandem purification followed by MS analysis as a glucose starvation P-body component. Loss of Pby1p did not significantly alter P-body assembly and morphology, indicating that Pby1p is not essential for P-body formation. In fact, most *bona fide* P-body constituents are not essential for P-body assembly. For example, P-body foci can still be induced in the absence of Dcp1p, Dhh1p or Xrn1p (Teixeira and Parker, 2007). Strikingly, Dcp2p protein levels were drastically reduced in $\Delta pby1$ cells, whereas Dhh1p and Pat1p remained unaffected. Previous study observed smaller P-bodies in $\Delta dcp2$ strain than wild-type strain upon glucose starvation (Teixeira and Parker, 2007), which suggests the remaining Dcp2p level in $\Delta pby1$ cells is sufficient to drive proper P-body formation in terms of morphology. However, whether $\Delta pby1$ shares phenotype similar with $\Delta dcp2$ remains to be established. The decapping enzyme is a dimer consists of Dcp1p and Dcp2p proteins that

directly interact with each other (Beelman et al., 1996; Sakuno et al., 2004; She et al., 2008). Although among the P-body components examined thus far, loss of Pby1p only affected Dcp2p abundance, it is still possible that other factors, in particular Dcp1p, are additionally co-regulated, since Dcp2p is required for Dcp1p accumulation in P-bodies (Teixeira and Parker, 2007).

In the absence of Pby1p, degradation of two P-body associated transcripts was slightly delayed, and there are three possible explanations for this observation. First, in eukaryotes, transcripts can be degraded in two alternative pathways: decapping-dependent 5' to 3' pathway or exosome mediated decay pathway (Balagopal et al., 2012; Garneau et al., 2007). However, how these two pathways are coordinated or regulated is not yet fully understood. Further experiments, for example by blocking one of the two pathways in $\Delta pby1$ strain, are necessary to address whether loss of Pby1p shifts the transcripts from being decayed via one pathway to the other, and thus affects the decay rate. The initial decapping step of the 5' to 3' decay pathway was shown to be co-translational in yeast, which takes place when transcripts are still bound by polysomes (Hu et al., 2009). The second possibility is that Pby1p is part of the decapping complex associated with polysomes, which can stabilize Dcp2p and ensure proper decapping. Loss of Pby1p renders decapping into a rate-limiting step in the 5' to 3' degradation, and in turn delay the general decay rate. Therefore, such role of Pby1p is independent from being present in P-bodies, which might be the reason why the level of Dcp2p is already downregulated in $\Delta pby1$ under normal growth condition where there is no significant P-body induction (Fig. 2A, 2B). To test this assumption, polysome profiling experiments can be performed to examine the association of Pby1p with polysomes. Third, it also well possible, that the alteration on degradation pattern in $\Delta pby1$ cells is achieved by affecting another thus far unknown factor and not through Dcp2p.

Since Pby1p does not appear to be a general P-body component, the next important questions are how Pby1p is recruited to P-bodies in a stress dependent manner and what is the role of Pby1p inside P-bodies. Previous studies have uncovered that Dcp2p and Pat1p contain phosphorylation sites, and their phosphorylation is important for P-body function and assembly, respectively (Ramachandran et al., 2011; Yoon et al., 2010). Interestingly, although the nonphosphorylatable variant of Dcp2p does not alter the P-body formation, Dcp2p is delocalized from P-bodies, indicating phosphorylation is required for the accumulation of Dcp2p itself in P-bodies (Yoon et al., 2010). We therefore hypothesized that Pby1p might undergo similar phosphorylation or other modification triggered by specific stress condition, like glucose starvation, which recruits it to P-bodies. Thus far, less is known regarding the function of Pby1p except the evidence of being localized in P-bodies under glucose starvation (Sweet et al., 2007). Therefore, additional studies should be done to find out the functional significance of Pby1p being associated with P-bodies.

Materials and Methods

Yeast strains and growth conditions

Standard genetic techniques were employed throughout (Sherman, 1991). All genetic modifications were carried out chromosomally. Chromosomal tagging and deletions were performed as described (Janke et al., 2004; Knop et al., 1999). For C-terminal tagging of Pby1p with GFP and Dcp2p with mCherry, the plasmids pYM26 (*kITRP1*) and pFA6a-3xmcherry (*hphNT1*) were used, respectively (Maeder et al., 2007). The plasmid pFA6a-natNT2 was employed for the construction of $\Delta pby1$ strains. Primers and strains used in this study are listed in Table S1 and S2, respectively. Unless otherwise noted, yeast cells were grown in YPD (1% yeast extract, 2% peptone, 2% dextrose) at 30°C. For glucose deprivation, cultures were further grown in YP media without dextrose for indicated times. For mild osmotic stress, the YPD growth medium was supplemented with 0.5 M NaCl or 0.2 M CaCl₂ for indicated times. Generally, yeast cells were harvested at mid-log phase with an OD₆₀₀ of 0.4-0.8.

HBH-purification

The HBH purification was carried out as previously described by Tagwerker and colleagues (Tagwerker et al., 2006) with minor modifications (Weidner et al., 2014). Cells expressing Dcp2-HBH were grown to mid-log phase, subjected to the corresponding stress and crosslinked with 1% formaldehyde for 2 min. Control cells were treated equally except for stress application. Cells were lysed in RIPA buffer (50 mM Tris-HCl pH 8.0, 150 mM NaCl, 1% NP-40, 0.5% sodium deoxycholate, 0.1% SDS, supplemented with protease inhibitors) using FastPrep (MP Biomedicals). Pull-downs were performed with streptavidin agarose beads (Thermo Fisher Scientific) in binding buffer (50 mM NaPi pH 8.0, 300 mM NaCl, 6 M GuHCl, 0.5% Tween-20). The beads were spun and followed by a series of washes with binding buffer supplemented with 0.1% octyl- β -glucoside, and 50 μ l of the solution was left in the tube after the final wash. To each tube, 0.5 μ l of 1 mg/ml Endoproteinase LysC (ELC) (Wako Chem) was added, and the tubes were placed at 37°C with shaking. After 2 h, 0.5 μ l of 1 mg/ml trypsin (Promega) was added and shake for another 2h, followed by adding a further 0.5 μ l of 1 mg/ml trypsin (Promega), and placed at 37°C overnight with shaking. The tubes were briefly spun down and the supernatant was collected. To stop digestion, TFA (trifluoroacetic acid) was added to final concentration of 1%. Samples were subject to mass spectrometric analysis using LC-MS/MS (Orbitrap) after desalting.

Live-cell imaging

For live-cell imaging, yeast cells were grown in YPD medium to mid-log phase. The cells were exposed to indicated stresses, spun down and taken up in HC-complete medium with corresponding stressors for imaging. Images were acquired with an AxioCam MRm camera mounted on an AxioPlan 2 fluorescence microscope using a Plan Apochromat 63x/NA1.40 objective and filters for eqFP611 and GFP. Axiovision software 4.8 was used to process images (Carl Zeiss).

Western Blotting

Cells expressing Dcp2p-GFP, Dhh1p-GFP and, Pat1p-GFP in wild-type and $\Delta pby1$ strains were grown to mid-log phase. The cells were harvested and lysed with glass beads in 150 μ l lysis buffer (20 mM Tris/HCl, pH 8.0, 5 mM EDTA) in the presence of 1 mM dithiothreitol (DTT) and protease inhibitors. The lysates were incubated at 65°C for 5 min, and unlysed cells subsequently were removed by centrifugation. The protein concentration was determined using the DC Protein Assay (Bio-Rad, Richmond, CA), and analyzed by SDS-PAGE and immunoblotting. The following antibodies were used for immunoblotting: anti-GFP (Torrey Pines Biolabs, Secaucus, NJ; 1: 5,000); anti-Pgk1p (Invitrogen #A-6457; 1: 1,000). Enhanced Chemiluminescence (ECL; GE Healthcare) was used for detection.

Pulse-chase labeling with 4TU and RNA purification and qRT-PCR

The pulse-chase labeling experiment was carried out as described previously (Zeiner et al., 2008). For the pulse, the yeast culture was grown in HC-Ura drop-out media supplemented with 2% dextrose, 0.1 mM uracil and 0.2 mM 4-thiouracil (Sigma-Aldrich) for 6 h. Yeast were spun down at 3,000 g for 2 min and resuspended in HC-Ura drop-out media containing 20 mM uracil (chase). Yeast cells were collected by centrifugation at the following time points: $t = 0$, 10, 20, 30, and 60 min. Cells were lysed followed by total RNA isolation using phenol-chloroform-isoamyl alcohol (125:24:1) (Sigma-Aldrich) as described (Schmitt et al., 1990). The RNA was then subjected to biotinylation and further purification according to Zeiner et al. (2008).

0.5-1 μ g of 4-TU labeled RNA or total RNA was reverse transcribed with the Transcriptor reverse transcriptase kit (Roche), oligo-dTs and random hexamers. The mRNA levels were analyzed by SYBR green incorporation using ABI StepOne Plus real-time PCR system (Applied Biosystems).

Table S1. List of primers used in this study.

| Primer ID | Designation | Sequence |
|-----------|------------------------|---|
| CW1155 | Pby1 S1_del_primer | TCTGACATTAATAAAATTCGGAAA CAATAAATAATTTCTTTTAAAG ATG CGTACGGCTGCAGGTCGAC |
| CW1156 | Pby1 S2_del_tag_primer | ATAATAACAGTATTTTAGGATGGTCTTTTTTTTTTTTTCATCGATGAATTCGAGCTCG |
| CW1157 | Pby1 S3_tag_primer | GACCCG AAC TTCGTAA AAGTCATTGATTACACTTCA AACGGTTGGCGTACGCTGCAGGTCGAC |
| CW1212 | PBY1_qPCR_forward | ACGGCCCTCACATTAACCTA |
| CW1213 | PBY1_qPCR_reverse | GAATCCTTATGTGCCCCCAA |

Table S2. List of strains used in this study.

| Strain ID | Designation | Genotype | Reference |
|-----------|-----------------------------|--|-----------------------|
| NY0-1 | ARF1 | MAT a ade2::ARF1::ADE2 arf1::HIS3 ura3 lys2 trp1 his3 leu2 | Yahara et al., 2001 |
| YAS2501 | Dcp2-HBH | MAT a ade2::ARF1::ADE2 arf1::HIS3 ura3 lys2 trp1 his3 leu2 DCP2::DCP2-HBH-kanMX4 | Weidner et al., 2014 |
| YAS1031A | Dcp2-GFP | MAT a ade2::ARF1::ADE2 arf1::HIS3 ura3 lys2 trp1 his3 leu2 DCP2::DCP2-yEGFP-kanMX4 | Kilchert et al., 2010 |
| YAS4163 | Dcp2-2mcherry | MAT a ade2::ARF1::ADE2 arf1::HIS3 ura3 lys2 trp1 his3 leu2 DCP2::DCP2-2xymcherry-hphNT1 | This study |
| YAS4459 | Dcp2-2mcherry Pby1-yeGFP | MAT a ade2::ARF1::ADE2 arf1::HIS3 ura3 lys2 trp1 his3 leu2 DCP2::DCP2-2xymcherry-hphNT1 PBY1::PBY1-yeGFP-kITRP1 | This study |
| YAS4466 | Dcp2-GFP Δpby1 | MAT a ade2::ARF1::ADE2 arf1::HIS3 ura3 lys2 trp1 his3 leu2 DCP2::DCP2-yEGFP-kanMX4 pby1::natNT2 | This study |
| YAS4967 | Dhh1-GFP Δpby1 | MAT a ade2::ARF1::ADE2 arf1::HIS3 ura3 lys2 trp1 his3 leu2 DCP2::DHH1-yEGFP-kanMX4 pby1::hphNT1 | This study |
| YAS4969 | Pat1-GFP Δpby1 | MAT a ade2::ARF1::ADE2 arf1::HIS3 ura3 lys2 trp1 his3 leu2 DCP2::PAT1-yEGFP-kanMX4 pby1::hphNT1 | This study |

4. FURTHER DISCUSSION AND OUTLOOK

The aim of this thesis was to gain a better understanding regarding the role of P-bodies in mRNA turnover, stress responses and P-body formation. To this end, we uncovered the mRNA content upon different stress conditions, their fates within P-bodies, and factors regulating P-body formation and P-body targeting.

It has been long hypothesized that one of the functional significance of P-body aggregates is to regulate the mRNA turnover in response to diverse stresses, since the aggregation of P-body monomers is largely triggered upon various stress conditions (Parker and Sheth, 2007). Additionally, the fact that the number, morphology and half-life of P-bodies vary depending on the particular stress (Kilchert et al., 2010), leads to the assumption that such regulation is stress-specific which is likely achieved by sequestering different transcript subsets in P-bodies. With the cCLAP technique we indeed identified common and stress-specific transcripts associating with P-bodies under three stress conditions, glucose deprivation as well as mild Na⁺ and Ca²⁺ osmotic stresses. In the following studies, we primarily focused on mRNAs specifically enriched in P-bodies upon glucose starvation. To extend our knowledge on the similarities and differences of P-bodies under various stresses, characterization of mRNAs from the osmotic stresses would be necessary in the future. Unlike harsh nutrient starvations, osmotic shocks are adaptable stresses, which cells can adapt by regulating the activity of the solute transporter and expression of genes involved in maintaining homeostasis (Albertyn et al., 1994; Chowdhury et al., 1992; Slaninova et al., 2000; Tamas et al., 1999). Accordingly, the assembly and disassembly of P-bodies was observed to occur within 30 minutes (Kilchert et al., 2010). In contrast, P-bodies induced upon glucose depletion persist as long as no glucose replenished. Therefore, it is reasonable to assume mRNAs decay and/or storage in P-bodies are different from non-adaptive stress conditions. Furthermore, although both Na⁺ and Ca²⁺ stressors alter the cellular osmotic pressure and induce P-bodies with similar appearance, Ca²⁺ has its special feature, since it's one of the most common signaling ions in the cell (Clapham, 2007). Strikingly, by GO analysis, we specifically found several Ca²⁺ specific GO term pathways, for example membrane invagination, which reflects the importance role of Ca²⁺ in the regulation of membrane trafficking (Micaroni, 2012). Moreover, in contrast to P-body induction upon glucose starvation and Na⁺, previous work in the lab has shown calmodulin is required for P-body formation under Ca²⁺ hyperosmotic condition (Kilchert et al., 2010). These evidences suggest in addition to be an osmotic stressor, Ca²⁺ and its signaling directly affect both P-body formation and RNA deposition into P-bodies. Therefore, additional experiments on Na⁺ and Ca²⁺ candidates would provide new insights on what and how mRNAs are fine-tuned inside P-bodies in response to two osmotic stress conditions, and how P-bodies are linked to Ca²⁺ signaling pathway.

P-bodies appear as spheres in cytoplasm and their size range from 40-100 nm in yeast, 100 to 300 nm in mammalian cells (Eystathioy et al., 2002; Kilchert et al., 2010; Yang

et al., 2004). Under normal growth conditions, P-bodies exist mostly in the form of monomers, and upon stress they aggregate into foci detectable by light microscopy (Decker et al., 2007). However, what size defines a functional P-body and whether its size directly correlates to its function remain poorly understood. aggregation of mRNA decay machinery into P-body foci does not appear to be a nonspecific process, but rather a direct response to cellular stress. As mentioned above, for example, calmodulin is required for the P-body formation specifically upon Ca^{2+} hyperosmotic stress (Kilchert et al., 2010), and loss of MAP kinase Hog1p, which is well known in osmoregulation, could block P-body aggregation under high salt conditions (Teixeira et al., 2005). P-body granules are conserved from yeast to mammals, it is believed the biological advantage of being assembled into granules is to control a subgroup of transcripts. Recent evidences showed that sequestration of transcripts into P-bodies could promote cell viability, growth and long term survival under particular conditions (Garmendia-Torres et al., 2014; Lavut and Raveh, 2012; Ramachandran et al., 2011). In contrast, several studies have suggested large P-body aggregates are not required for substantial mRNA decay in yeast and RNA-mediated gene silencing in fly (Decker et al., 2007; Eulalio et al., 2007b). However, to date, only a few mRNAs have been identified localizing in P-bodies, and only the fate of an artificial reporter transcript was examined in yeast lacking P-body aggregates (Decker et al., 2007). In this study, we have identified the mRNA components of P-bodies globally under different stress conditions. This result allows us to inspect on a global level the fates of transcripts in cells, which are defective in P-body assembly, and it could provide new insights in understanding the function of P-body forming aggregates in response to different stresses.

As mentioned previously, in comparison with P-bodies induced by glucose deprivation, P-bodies appeared to be smaller in size upon osmotic stresses (Kilchert et al., 2010). Interestingly, when glucose depletion and $\text{Ca}^{2+}/\text{Na}^{+}$ treatment were combined, only the multiple smaller P-bodies were present rather than a mixed population of small and large ones (Kilchert et al., 2010). This observation provides a condition, under which the fates and localization of glucose depletion specific candidates could be examined. Whether they are still localized inside these smaller P-bodies, and if yes, whether they are regulated in the same way as under glucose starvation alone would be important information that may reveal the relationship between the size and function of P-bodies.

Following validation of our glucose starvation candidate transcripts, we continued to measure their stabilities using a pulse-chase approach. Interestingly, we observed two major types of transcripts according to their fates. One type was subjected to degradation, while the other type was stabilized inside P-bodies. The existence of two distinct groups of transcripts points to the dual roles of P-bodies in both mRNA degradation and storage. However, one key question is whether the two functions happen in the same or separate compartments. As

discussed previously, we favor the dual roles are carried out by the same and perhaps the only P-body population within the cell. Supporting this, the P-body protein composition appears to be highly homogeneous throughout the cell (Kulkarni et al., 2010). Recent study in fly oocyte observed ribosomes and translational activators associated with the P-bodies at their edge, which suggests there is a distinct edge region of the P-body that is competent for translation whereas the core is a site of translational repression, and the translational regulation can be achieved by localizing transcripts between the core and edge of the P-bodies (Weil et al., 2012). Although in yeast the mechanism might not be the same, one possibility is the dual roles of storage and decay are differentiated by different zones within one P-body rather than two independent P-body subtypes. To solve this question the main obstacle is, to date, the absence of any reliable live-RNA imaging technique to study P-bodies, which would allow us to monitor the localization of several transcripts, including those being decayed and those being stored, simultaneously over time. We have shown that widely applied MS2 and U1A stem-loop system are prone to induce P-body formation and recruit transcripts to P-bodies non-selectively under normal growth condition, and a similar result has been reported by Parker's lab (Garcia and Parker, 2015). Hence, a method without changing the mRNA itself would be more appropriate for this purpose. Lately, small aptamer based detection techniques have been developed to visualize RNAs in real time (Dolgosheina et al., 2014; Paige et al., 2011). Although permeability seems to be a problem when applying such system into yeast cell, it is so far the method with least modifications on the endogenous mRNA, that can be applied for P-body localized transcript detection.

Within the mRNA group that is decayed in P-bodies, interestingly, P-body (Xrn1) specific degradation was initiated at different time points after stress induction, indicating the kinetics are transcript dependent as well. Various kinetics can be achieved by specific RBP binding to the mRNA which would temporarily stabilize the transcript and block decay initiation. To date, two core P-body components, Dcp2p and Pat1p were determined to be phosphorylated (Ramachandran et al., 2011; Yoon et al., 2010). Therefore, it would be possible, that those RBPs are subjected to post-translational modification, which serve as initiator for decay. Moreover, we have demonstrated Puf5p is involved in regulating both localization and degradation of *ATP11*. Although we could not identify a consensus Puf5p binding sequence within the transcript, Puf5p might still bind the transcript, which can be determined by approaches, like electrophoretic mobility shift assay (EMSA). Alternatively, Puf5p may function indirectly, and by taking advantage of RNA pull down experiments, potential interplayer(s) between Puf5p and *ATP11* could be discovered.

As discussed in previous chapters, we proposed that stored transcripts might return into translation pool at certain time points. Since SGs are frequently observed to dock and fuse with P-bodies, and they also share some common protein factors (Kedersha et al., 2005;

Stoecklin and Kedersha, 2013; Wilczynska et al., 2005), it is likely such re-arrangement occurs through SGs. Again, a reliable live mRNA imaging approach could be beneficial to test this hypothesis. Alternatively, a time course FISH-IF experiments with triple staining of P-bodies, SGs and transcripts can also be applied to address this issue. To further assess the role of SGs in the mRNA turnover driven by P-bodies, the stabilities of candidate mRNAs could be examined in yeast strains lacking SG formation, like $\Delta pub1$ and $\Delta pbp1$ (Buchan et al., 2008).

Consistent with previous data, the 3'UTR of our candidates contain key localization signals, that are required for proper P-body targeting, also affect their fates. However, the 3'UTR itself is not sufficient to drive the transcript to P-body indicating additional signals are present in the 5'UTR and/or coding sequence (CDS). To pinpoint these localization signals, RNA truncation constructs should be created to examine whether the P-body targeting is impaired.

In the second study, crosslinking HBH tandem affinity purifications using Dcp2p or Scd6p as bait proteins were applied to identify proteins that associate with P-bodies at ER membranes. Besides two proteins Bfr1 and Scp160 that are further addressed in this study, remaining candidate proteins also provide interesting implications that can be investigated in future studies (Table 4.1). Specifically, several identified proteins are involved in translation, such as Tef4p, Tif3p, Tif5p, Eap1p and Hef3p, implying a close physical link between translation and the P-body decay machinery, and similar observation has been reported in *Drosophila* (Weil et al., 2012). Localizing translation next to degradation might allow cell to rapidly regulate its gene expression. In support of this notion, in the previous study we found a group of stabilized mRNAs inside P-bodies which likely return into translation pool. In addition, we proposed that SGs might serve as intermediate granules that mediated the stored transcripts traveling back to translation, and interestingly, we indeed identified SG marker protein Pab1p in our screen. Since P-bodies localize in close proximity to the ER in yeast (Kilchert et al., 2010), it is also intriguing to uncover whether SGs link these two pools at ER physically and functionally. The homologs of the candidate protein Cdc48p was found in *Drosophila* and *C. elegans* are important to dissociate poly(Q) aggregating proteins (Higashiyama et al., 2002; Yamanaka et al., 2004). As many P-body and SG constituents contain Q/N rich regions (Reijns et al., 2008), one possibility could be Cdc48p facilitates the transition between P-body, SGs and polysomes through disruption of their Q/N rich interaction domains.

Table 4.1: Proteins identified through HBH purification found with Dcp2- and Scd6-HBH. Adapted from Weidner (2013).

| Gene Name | Description (Source: Proteome) | Found with both Dcp2- and Scd6-HBH | Found with Scd6-HBH | Found with Dcp2-HBH |
|---------------|--|------------------------------------|---------------------|---------------------|
| Dcp2 | mRNA decapping protein 2, a putative pyrophosphatase required with Dcp1p for mRNA decapping, suppresses the respiratory deficiency of a petite mutant | X | | |
| Xrn1 | KAR(-) enhancing mutation 1, a 5'-3' exonuclease for single-stranded RNA and DNA that degrades decapped mRNA, required for pseudohyphal and invasive growth, involved in the G1 to S phase transition | X | | |
| Pab1 | Poly(A) binding protein 1, a cytoplasmic and nuclear protein that is part of the 3'-end RNA-processing complex (cleavage factor I), involved in translation termination with Sup35p, has 4 RNA recognition (RRM) domains and functions in mRNA decay | X | | |
| Scd6 | Suppressor of clathrin deficiency, negatively regulates translation initiation, involved in mRNA decay, overproduction suppresses inviability exhibited by clathrin heavy chain (<i>chc1</i>) null mutant | X | | |
| Eap1 | Protein that inhibits <i>cap</i> -dependent translation, probable purine nucleotide-binding protein that associates with translation initiation factor eIF4E, also has an eIF4E-independent function in genetic stability | | X | |
| Dhh1 | DEAD-box helicase homolog 1, a putative RNA helicase required for normal sporulation, involved in glucose-starvation induced P body formation | X | | |
| <u>Scp160</u> | <i>S. cerevisiae</i> protein involved in the control of ploidy 160, acts in control of mitotic chromosome transmission and telomeric silencing, an effector for Gpa1p in the mating response pathway, contains 14 KH domains which are found in RNA-binding proteins | | X | |
| Edc3 | Enhancer of mRNA decapping 3, required for proper 5' to 3' degradation, and decapping, of cytoplasmic YRA1 pre-mRNA, enhances dcp1 and dcp2 mRNA decapping mutants | X | | |
| <u>Bfr1</u> | Protein that suppresses brefeldin A-induced lethality when overproduced, may be involved in mRNA metabolism | X | | |
| Pat1 | Protein associated with topoisomerase II, required for faithful chromosome transmission and normal translation initiation, involved in deadenylation-dependent mRNA decay, ethanol tolerance, and maintaining cell wall integrity | X | | |
| Cpr1 | Cyclophilin (peptidylprolyl cis-trans isomerase or PPIase) of the nucleus and cytoplasm that promotes meiotic gene expression, plays a role in the stress response, component of Set3p complex | X | | |
| Sbp1 | Single-stranded nucleic acid-binding protein 1, associated with small nucleolar RNAs (snoRNAs), involved in glucose starvation-induced translation repression and P body formation | | X | |
| Tef4 | Translation elongation factor EF-1gamma | X | | |
| Sti1 | Stress inducible 1, a stress-induced protein required for optimal growth at high and low temperature, TPR2A and DP2 domains mediate binding and signaling events associated with Hsp82p | X | | |
| Nam7 | Nuclear accommodation of mitochondria 7, a protein involved with Nmd2p and Upf3p in decay of mRNAs that contain premature nonsense codons | X | | |
| Yra1 | Yeast RNA annealing protein 1, a protein with RNA:RNA annealing activity, involved in mRNA packaging for export from the nucleus | | X | |
| Mpg1 | Mannose-1-phosphate guanyltransferase, GDP-mannose pyrophosphorylase | X | | |
| Not1 | Cell division cycle 39, a nuclear protein and component of the CCR4-Not complex that negatively affects basal transcription from many promoters also plays a role in decapping some mRNAs | | X | |
| Rps12 | Ribosomal protein S12 | | X | |
| Nog1 | Nucleolar G protein 1, a putative essential nucleolar GTP-binding protein, required for large ribosomal subunit biogenesis and export from the nucleolus | | | X |
| <u>Cdc48</u> | Cell division cycle 48, member of the AAA family of ATPases required for cell division and homotypic membrane fusion, component of the ubiquitin/proteasomal-dependent ER-associated degradation (ERAD) system | | | X |
| Vma13 | Vacuolar Membrane ATPase 13, subunit H of the V1 peripheral membrane domain of the vacuolar H(+)-ATPase (V-ATPase), required for V-ATPase activity | X | | |
| Hsp26 | Heat shock protein of 26 kDa, a chaperone that binds unfolded citrate synthase and rhodanese and is expressed during entry to stationary | X | | |

| | | | | |
|-------------|---|--|---|---|
| | phase and is induced by osmostress, may be required for resistance to ethanol and acetaldehyde | | | |
| Hsp12 | Heat shock protein of 12 kDa, induced by heat, osmotic stress, oxidative stress and in stationary phase, may be required for ethanol and acetaldehyde resistance | | X | |
| <i>Psp2</i> | High-copy suppressor of temperature-sensitive mutations in DNA polymerase alpha | | X | |
| Tif5 | Translation initiation factor eIF5, catalyzes hydrolysis of GTP on the 40S ribosomal subunit-initiation complex followed by joining to the 60S ribosomal subunit | | X | |
| <i>Tif3</i> | Translation initiation factor eIF4B, contains one RRM (RNA recognition motif) RNA-binding domain | | X | |
| Hta1 | Histone h two A 1, a chromatin binding protein that functions in chromatin related events | | | X |
| Atp1 | ATP synthase 1, alpha subunit of the F1 subunit of ATP synthase-mitochondrial respiratory complex V, three molecules are present in each F1 complex | | | X |
| Lsm5 | U6 snRNA-associated protein of the Sm-like group | | X | |
| Lsm2 | U6 snRNA-associated protein of the Sm-like group | | X | |
| Dcp1 | mRNA decapping 1, an mRNA decapping enzyme involved in mRNA turnover, plays a role in mediating proper translation termination via interaction with the Sup35p translation release factor | | X | |
| | <u>Underline</u> indicates ER localized proteins; proteins with RNA related abilities are shown in <i>italics</i> , and P-body proteins are shown in bold | | | |

Recent studies in both mammalian and yeast have revealed several factors promote or are required for P-body formation (Buchan et al., 2008; Zheng et al., 2008). In contrast, we showed that Bfr1p and Scp160p are involved in the inhibition of P-body formation under normal growth condition. Although loss of either Bfr1p or Scp160p both led to multiple Dcp2-positive foci without any stressor, proper P-body formation only occurs in $\Delta bfr1$ strain, while the Dcp2-positive foci in $\Delta scp160$ strain lack several core P-body constituents, indicating they might function at different levels. Bfr1p was identified as an RNA binding protein in a high-throughput study and shown to be an interacting partner of Scp160p (Hogan et al., 2008; Lang et al., 2001). It is well possible that there are other proteins binding to the transcripts together with Bfr1p to ensure correct P-body assembly, and are co-regulated by Scp160p. The potential candidates of such interactors could be Asc1p, Eap1p and Pab1p, that have been reported earlier to interact with both Bfr1p and Scp160p (Baum et al., 2004; Lang and Fridovich-Keil, 2000; Mendelsohn et al., 2003; Sezen et al., 2009). Interestingly, when *BFR1* or *SCP160* were deleted, P-body induction was uncoupled from translational attenuation suggesting Bfr1p and Scp160p are part of a signaling pathway, which would be required to link these two events. Therefore, further studies will not only uncover if the interacting proteins would act together with Scp160 and Bfr1 to prevent P-body formation and/or proper P-body assembly, but also provide us new insights in understanding P-body cellular signaling.

In the third part of this thesis, we identified a stress-specific P-body protein factor Pby1p following glucose depletion through HBH purification. In the absence of Pby1p the formation of P-body was not altered in both unstressed and three stress conditions, glucose starvation, Na⁺ and Ca²⁺ osmotic stresses. One explanation is that, to date, most factors that are essential for P-body formation and affecting its assembly are P-body components that

conserved across various stress conditions, such as Edc3p, Lsm4p and Pat1p (Buchan et al., 2008; Zheng et al., 2008). This might be important for cell to remodel or clearance of P-bodies in response to different or a combination of stresses. Thus far, Pby1p remains to be a rather uncharacterized protein except its P-body localization under glucose starvation (Sweet et al., 2007). Interestingly, our findings suggest Pby1p plays a role in regulating mRNA degradation inside P-bodies. However, the key question is if Pby1p would affect mRNA decay in a stress-dependent manner, future experimental work is necessary to address this issue. Moreover, loss of Pby1p significantly reduced Dcp2p level but not two other tested P-body proteins. Therefore, another open question would be to address whether Pby1p acts to stabilize decapping complex specifically.

5. APPENDIX

5.1 Additional Materials and Methods

Many of the materials and methods used in the lab are standardized and so a large part of this section has been taken from the dissertations of Cornelia Kilchert (Kilchert, 2010) and Julie Weidner (Weidner, 2013). Changes have only been made where necessary.

Media

| | |
|-------------|--|
| LB medium: | 10 g Bacto-tryptone (BD) 5 g Bacto yeast extract (BD) 10 g NaCl (Roth) dH ₂ O up to 1 l autoclaved the same day |
| LB agar: | 5 g Bacto-tryptone (BD) 2.5 g Bacto yeast extract (BD) 5 g NaCl (Roth) 10 g Bacto-agar (BD) dH ₂ O up to 500 ml autoclaved the same day |
| SOC medium: | 5 g yeast extract (BD) 20 g Bacto-peptone (BD) 20 g dextrose (Roth) 10 mM NaCl 2.5 mM KCl 10 mM MgSO ₄ dH ₂ O up to 1 l autoclaved the same day |
| YP-medium: | 1% Bacto yeast extract (BD) 2% Bacto-peptone (BD) dH ₂ O up to 1 l autoclaved the same day |

| | |
|---------------------------|---|
| YP agar: | 10 g Bacto-peptone (BD) 5 g Bacto yeast extract (BD) 10 g Bacto-agar (BD) dH ₂ O up to 450 ml autoclaved the same day 50 ml of 20% (w/v) glucose was added before plates were poured |
| 5-FOA plates: | 0.34 g Yeast Nitrogen Base without amino acids (BD) 0.05 g 5-fluoroorotic acid (Biovectra 1555) 1 g dextrose (Glucose-monohydrate, Roth 6780.2) 5 ml 10 x HC- complete selection mixture dH ₂ O up to 20 ml and filter sterilized into 25 ml warm (55°C) sterile agar (1 g in 25 ml H ₂ O) |
| 10x HC-selection mixture: | 0.2 mg/ml adenine hemi-sulfate 0.35 mg/ml uracil 0.8 mg/ml L-tryptophan 0.2 mg/ml L-histidine-HCl 0.8 mg/ml L-leucine 1.2 mg/ml L-lysine-HCl 0.2 mg/ml L-methionine 0.6 mg/ml L-tyrosine 0.8 mg/ml L-isoleucine 0.5 mg/ml L-phenylalanine 1.0 mg/ml L-glutamic acid 2.0 mg/ml L-threonine 1.0 mg/ml L-aspartic acid 1.0 mg/ml L-valine 2.0 mg/ml L-serine 1.0 mg/ml L-arginine-HCl autoclaved without the component to selected for |

| | |
|------------|--|
| 10x YNB: | 33.5 g Yeast Nitrogen Base w/o amino acids (BD) up to 500 ml with dH ₂ O wrapped in aluminum foil and autoclaved the same day |
| HC medium: | 800 ml dH ₂ O 100 ml 10 x HC-XX (without the component to select for) 100 ml 10 x YNB |
| HC plates: | hot sterile agar (10 g Bacto-agar (BD) dissolved in 350 ml) 50 ml 20% dextrose 50 ml 10 x YNB 50 ml 10 x HC selection mixture |

Commonly used solutions and buffers

Antibiotics

| | |
|--------------------|---|
| 1000 x ampicillin | 100 mg/ml in dH ₂ O, filter sterilized |
| 250 x kanamycin | 10 mg/ml in dH ₂ O, filter sterilized |
| 100 x G418 | 20 mg/ml geneticin in dH ₂ O, filter sterilized |
| 2000 x ClonNAT | 200 mg/ml nourseotricin in dH ₂ O, filter sterilized |
| 100 x hygromycin B | 50 mg/ml in dH ₂ O, filter sterilized |

Solutions

| | |
|----------------------------------|---|
| TE Buffer: | 10 mM Tris/HCl pH 7.5 1 mM EDTA |
| Carrier DNA for transformations: | 200 mg salmon sperm DNA (Sigma D1626) up to 100 ml with TE buffer, sterilized |
| 6x DNA loading buffer: | 0.25% bromophenol blue 0.25% xylene cyanol 30% glycerol |

| | |
|--------------------------|--|
| 50 x TAE-buffer | 2 M Tris/HAc pH 7.7 5 mM EDTA |
| 5 x Laemmli-buffer | 62.5 mM Tris/HCl pH 6.8 5% β -mercaptoethanol 10% glycerol 2% SDS 0.0025% bromophenolblue |
| 20 x TBS: | 60 g Tris/HCl pH 7.4 160 g NaCl 4 g KCl up to 1 l with dH ₂ O |
| TBST: | TBS with 0.1% Tween-20 |
| 20 x PBS: | 46.6 g Na ₂ HPO ₄ x 12 H ₂ O 4.2 g KH ₂ PO ₄ 175.2 g NaCl 44.8 g KCl up to 1 l with dH ₂ O |
| 50 x Denhardt's reagent: | 10 g Ficoll type 400 10 g BSA fraction V 10 g polyvinylpyrrolidone up to 1 l with dH ₂ O, filter sterilized and stored at -20°C |
| 20 x SSC: | 3 M NaCl 0.3 M Na-citrate/NaOH pH 7.0 |
| DEPC-H ₂ O: | 1 l H ₂ O 1 ml DEPC stirred for > 1 h, then autoclaved |

Web resources and tools

| Resource | URL | Application |
|---------------------------|---|--------------------------------|
| Entrez Pubmed | http://www.ncbi.nlm.nih.gov/sites/entrez?db=pubmed | Literature searches |
| SGD | http://www.yeastgenome.org/ | Genomic sequences; data mining |
| Proteome | https://portal.biobase-international.com/cgi-bin/portal/login.cgi | data mining |
| Euroscarf | http://web.uni-frankfurt.de/fb15/mikro/euroscarf/index.html | Plasmid sequences |
| YeastMine | http://yeastmine.yeastgenome.org/yeastmine/begin.do | GO term analysis |
| DAVID | https://david.ncifcrf.gov/ | GO term analysis |
| Primer3Plus | http:// http://bioinfo.ut.ee/primer3-0.4.0/primer3/input.htm | qPCR primer design |
| Manipulate a DNA sequence | http://www.vivo.colostate.edu/molkit/manip/ | Sequencing; primer design |
| NCBI Blast | http://blast.ncbi.nlm.nih.gov/Blast.cgi | Sequence Blast |
| Yeast GFP database | http://yeastgfp.yeastgenome.org/getOrf.php?orf=YOR239W | Yeast GFP fusion localization |
| ImageJ | http://rsb.info.nih.gov/ij/plugins/index.html | Image analysis |
| MEME Suite | http://meme-suite.org/ | RNA Motif search |
| Imaris | http://www.bitplane.com/imaris | Image analysis |

Additional methods**Determination of yeast cell density**

1 OD₆₀₀ corresponds to 1.5 x 10⁷ yeast cells per ml on the spectrophotometer Ultrospec 3100 pro (Amersham Biosciences). For measurements, cells were diluted to yield an OD₆₀₀ of no more than 0.7. Unless otherwise indicated, logarithmically growing cells were harvested at an OD₆₀₀ between 0.3 and 0.7.

Preparation of yeast total cell extract

15 ml of yeast culture were harvested, and the cells were resuspended in 150 µl 6 x Laemmli buffer. Approximately 120 µl of glass beads were added. After vigorous vortexing for 5 min, samples were incubated for 5 min at 65°C followed by an additional 1 min of vortexing. Cell debris and glass beads were sedimented (2 min at 10,000 x g), and the supernatant was

transferred to a fresh reaction tube. For subsequent analysis by SDS-PAGE and immunoblotting, 5 μ l of the lysate was loaded per lane.

For comparison of protein expression levels, Laemmli buffer was replaced by LowDTT lysis buffer. The lysates were normalized to equal total protein concentration using the Biorad DC protein assay used according to the manufacturer's protocol. Routinely, 20 μ g of total protein were loaded per lane.

6 x Laemmli buffer

62.5 mM Tris/HCl (pH 6.8)

5%-mercaptoethanol

10% glycerol

2% SDS

0.0025% bromophenol blue

LowDTT lysis buffer

20 mM Tris/HCl (pH 8.0)

5 mM EDTA

1 mM DTT

1 % SDS

Determination of protein concentration

Protein concentrations of detergent-free solutions were determined using the Biorad protein assay, which is based on the Bradford method (Bradford, 1976). Bovine gamma-globulin served as a protein standard. For detergent-containing solutions, the detergent-compatible Biorad DC protein assay was used, which is based on the Lowry method (Lowry et al., 1951). In this case, bovine serum albumin served as a standard. All measurements were performed according to the manufacturer's instructions.

Total RNA isolation

Total RNA was isolated from yeast essentially as described (Schmitt et al., 1990). Briefly, yeast cells were grown to logarithmic phase and 20 OD₆₀₀ were harvested. Cells were resuspended in 0.8 ml AE buffer, 80 μ l 20% SDS and 0.8 ml PCI were added, and the tube vortexed for 10 s. After incubation for 4 min at 65°C, tubes were chilled at -70°C for 30 s and then centrifuged (2 min, 10,000 x g, RT). The upper aqueous phase was transferred to a fresh tube and extracted with 400 μ l PCI and vortexed 10 s. After phase separation by centrifugation, the upper aqueous phase was again transferred to a fresh tube and 1/10 volume of 3 M NaAc (pH 5.2) was added. The RNA was precipitated with two volumes 100% EtOH at -20°C, washed with 70% EtOH, and the pellet resuspended in 200 μ l RNase-free water.

AE buffer

50mM NaAc pH 5.2

10mM EDTA

cCLAP (chemical Cross-Linking coupled to Affinity Purification)

The cCLAP was carried out according to Tagwerker, et al. (2006), Hafner et al., (2010), Weidner et al. (2014) and Kishore, et al. (2011) with modifications. Cells expressing Dcp2-HBH or Scd6-HBH were subject to the corresponding stress and crosslinked with 1% formaldehyde for 2 min at RT with gentle agitation. Control cells without any stress application were treated equally. The fixative was quenched for 5 min by the addition of 125 mM glycine. Cells were subsequently harvested (3,000 x g for 3 min at 4°C), washed in 50 ml ice-cold ddH₂O and sedimented by centrifugation (5 min at 3,000 x g). For lysate preparation, cells were first resuspended in 2 ml RIPA buffer (50 mM Tris-HCl pH 8.0, 150 mM NaCl, 1% NP-40, 0.5% sodium deoxycholate, 0.1% SDS, supplemented with protease inhibitors) per gram of yeast cell pellet. For each condition 15-20 L of yeast culture with an OD₆₀₀ 0.6-0.8 were used. Lysis was performed in a FastPrep machine (MP Biomedicals) for 4 x 45 s at 4°C. The lysates were cleared by a slow spin (1,300 x g for 10 min at 4°C). To dissolve large RNPs, the supernatants were treated with RNase T1 (Fermentas) to a final concentration of 50 U/ml at 22°C for 15 min. To perform the pull-down, the supernatant was further spun at 20,000 x g for 15 min at 4°C, and the resulting pellets were resuspended in approximately 10 ml binding buffer (50 mM NaPi pH 8.0, 300 mM NaCl, 6 M GuHCl, 0.5% Tween-20). 800 µl streptavidin agarose beads (Thermo Fisher Scientific) were added and the lysate was rotated for 2 h at RT. The slurry was washed three times with wash buffer (50 mM NaPi pH 8.0, 300 mM NaCl, 6 M GuHCl, 0.5% Tween-20, 0.5% NP-40), and three times with of PNK buffer (50 mM Tris HCl pH 7.5, 50 mM NaCl, 10 mM MgCl₂). After the final wash, the beads were resuspended in 1 bed volume of PNK buffer. The second RNase T1 digestion was performed on the beads with a final concentration of 1 U/µl. The sample was incubated at 22°C for 15 min, and placed on ice for 5 min. The beads were subsequently washed three times with PNK buffer. To dephosphorylate the RNA, the beads were resuspended in 1 bed volume of 1 x NEB buffer 3 (New England Biolabs) containing Calf intestinal alkaline phosphatase (New England Biolabs) at a final concentration of 0.5 U/µl. The reaction was incubated at 37°C with vigorous shaking for 10 min. Following the incubation, the beads were washed twice with PNK buffer and twice with PNK buffer containing 5 mM DTT (PNK-DTT). After the final wash, the beads were resuspended in 1 bed volume of PNK-DTT buffer. Radiolabeling of RNA was achieved by adding 0.5 µCi/µl γ-³²P-ATP (Hartmann analytic) and 1 U/µl T4 PNK (New England Biolabs). The samples were then incubated at 37°C for 30 min with vigorous shaking. Samples were further incubated for 5 min with 100 µM ATP. Beads were then washed five times with PNK buffer. To purify RNA, proteins were digested using 1.2 mg/ml proteinase K (Roche) in 2 x proteinase K buffer (100 mM Tris HCl pH 7.5, 200 mM NaCl, 2 mM EDTA, 1% SDS) for 30 min at 55°C. The RNA was subsequently isolated using phenol-chloroform-isoamyl alcohol (125:24:1) (Sigma-Aldrich) as described (Schmitt et al., 1990). Purified RNA was subjected to

3' and 5' adapter ligation according to Illumina's TruSeq Small RNA Library Prep Guide. After each adapter ligation step, a 15% PAGE was run to exclude free adapters and adapter dimers by size selection. RNAs were extracted from gels with a standard gel purification method (Nilsen, 2013). To eliminate the rRNA species, the RiboMinus transcriptome isolation kit (Invitrogen) was used according to the manufacturer's protocol. Reverse transcription using SuperScript III reverse transcriptase (Invitrogen), oligo-dT and random hexamer was subsequently performed. The cDNA libraries were generated by a final PCR amplification step with Illumina indexing primers.

Determination of nucleic acid concentration

The concentration of nucleic acids was determined using a spectrophotometer (Ultrospec 3100 *pro*, Amersham Biosciences) or NanoVue (GE Healthcare). The nucleic acids were diluted in dH₂O, and the absorption at 260 nm was determined. It was assumed that a unit of absorption at 260 nm corresponds to 50 µg/ml double-stranded DNA or 40 µg/ml single-stranded RNA.

Chromosomal manipulations of yeast cells

To delete or tag genes in yeast cells, or to place them under an exogenous promoter, PCR-generated cassettes were integrated into the genome as described previously (Gauss et al., 2005; Gueldener et al., 2002; Janke et al., 2004; Knop et al., 1999; Tagwerker et al., 2006). Briefly, preparative PCR was performed on template plasmids with primers bearing 45 bp 5' overhangs homologous to the desired target site in the yeast genome. The PCR-product was transformed directly into yeast cells without further purification. Cells were selected for with the corresponding auxotrophy or resistance marker, and correct integration was confirmed by analytical colony PCR. Wherever possible, expression of the appended tag was checked by immunoblotting on total yeast lysates. If required, the chromosomal manipulation was sequenced. In this case, a fragment containing the desired manipulation was amplified from genomic yeast DNA using the proof-reading Expand PCR system (Roche) and used as a template for the sequencing reaction.

Alleles were transferred into our preferred strain background by PCR-based allele replacement (Erdeniz et al., 1997) or integrated into the genomic locus using the pRS vector series (Sikorski and Hieter, 1989).

Preparation of genomic yeast DNA

Crude yeast DNA was obtained by rapid phenol/chloroform extraction (Hoffman and Winston, 1987). For this, 5 ml of yeast culture were grown to greater than 2 OD₆₀₀ units per ml. The cells were harvested and resuspended in 200 µl buffer A. Two hundred µl glass beads and

200 μ l PCI were added. After vigorous vortexing for 5 min, 200 μ l H₂O were added. Phase separation was accomplished by centrifugation (5 min, 10,000 x g). The aqueous phase was transferred to a fresh reaction tube and 1 ml 100% EtOH (RT) added to precipitate the DNA, which was pelleted by centrifugation for 5 min (16,000 x g). The resulting pellet was dried at 65°C for about 5 min and resuspended in 40 μ l H₂O. Routinely, 0.5 μ l genomic DNA were used per PCR reaction.

Buffer A

10 mM Tris/HCl pH 8.0

100 mM NaCl

1 mM EDTA

2% Triton X-100

1% SDS

Yeast transformations

Yeast cells were transformed by a highly efficient lithium acetate transformation method (Gietz et al., 1995). Cells were grown over night to early log phase. Five OD₆₀₀ of cells were harvested and washed once in sterile water. The cells were incubated for 5 min at 30°C in 100 mM LiAc. Subsequently, they were resuspended in 360 μ l transformation mix and vortexed for 1 min. A heat shock was employed for 15-40 min at 42°C, after which the cells were pelleted (5 s, 16,000 x g). The cell pellet was resuspended in 300 μ l sterile water and 150 μ l aliquots were plated on appropriate selection plates. If kanamycin or nourseothricin resistance cassettes were transformed, cells were first incubated in YPD for at least 3 h at RT before plating on the corresponding plates. Fast growing colonies were chosen for a second round of selection. Sometimes, replica plating was necessary to allow for the selection of stable transformants.

Transformation mix

240 μ l 50% (w/v) PEG (AMW 3,350)

36 μ l 1 M LiAc

50 μ l 2 mg/ml single-stranded salmon sperm DNA

5 μ l of PCR product or 0.25 μ l plasmid DNA, ad 360 μ l with H₂O

Analytical PCR of yeast colonies

Analytical PCR of yeast colonies was performed to confirm chromosomal manipulations of yeast cells. Generally, a forward primer binding 100-300 bp upstream of the desired integration event was combined with a reverse primer located on the integrated cassette, so that a product

of the correct size was only amplified if the integration had taken place. Single yeast colonies were picked with a pipette tip and incubated in 10 μ l 20 mM NaOH at 95°C for 5 min. Two μ l was then added to the PCR reaction mix. A typical reaction contained 18.4 μ l H₂O, 2.5 μ l 10 x reaction buffer, 1 μ l 10 mM dNTPs, 2 x 0.5 μ l 10 μ M oligonucleotide-primer, 0.15 μ l Taq DNA-polymerase (Roche). Usually, the annealing temperature was set at 53°C, and 1 min/kb was allowed for elongation. Generally, 35 cycles were used for amplification. Routinely, 20 μ l of the reaction were analyzed by agarose gel electrophoresis.

5.2 Abbreviations

| | |
|-------------------|---|
| A ₂₆₀ | absorbance at 260 nm |
| Ac | acetate |
| AP | alkaline phosphatase |
| APS | ammonium persulfate |
| ARE | AU-rich elements |
| ARF1 | ADP ribosylation factor 1 |
| ATP | adenosine-5'-triphosphate |
| bp | base pair |
| BSA | bovine serum albumin |
| cDNA | complementary DNA, generated by reverse transcription of RNA |
| <i>C. elegans</i> | <i>Caenorhabditis elegans</i> |
| CHX | cycloheximide |
| cCLAP | chemical Cross-Linking coupled to Affinity Purification |
| CLIP | cross-linking immunoprecipitation |
| DAPI | 4',6-Diamidino-2-phenylindole dihydrochloride |
| DEPC | diethyl pyrocarbonate |
| dH ₂ O | distilled water |
| DNA | deoxyribonucleic acid |
| DNase | DNA-hydrolyzing enzyme |
| dNTPs | deoxynucleotide triphosphates |
| DTT | dithiothreitol |
| ECL | enhanced chemoluminescence |
| <i>E. coli</i> | <i>Escherichia coli</i> |
| EDTA | ethylenediaminetetraacetic acid |
| eIF | eukaryotic translation initiation factors |
| ELC | endoproteinase Lys-C |
| EM | electron microscopy |
| EMSA | electrophoretic mobility shift assay |
| eqFP611 | Entacmaea quadricolor fluorescent protein, emission maximum at 611 nm |
| ER | endoplasmic reticulum |
| EtOH | ethanol |
| FISH | fluorescent in situ hybridization |
| FISH/IF | fluorescent in situ hybridization combined with immunofluorescence |
| FRAP | fluorescence recovery after photobleaching |
| g | gravitational acceleration constant |
| GAP | GTPase-activating protein |
| GDP | guanosine-5'-diphosphate |
| GEF | guanine nucleotide exchange factor |
| GFP | green fluorescent protein |
| GO | gene Ontology |
| GTP | guanosine-5'-triphosphate |
| GTPase | GTP hydrolyzing enzyme |
| h | hour |
| HBH | 6xHis-biotinylation sequence-6xHis |
| HEPES | N-[2-Hydroxyethyl]piperazine-N'-[2-ethanesulfonic acid] |
| HRP | horseradish peroxidase |
| iCLIP | individual-nucleotide resolution CLIP |
| IF | immunofluorescence |
| IP | immunoprecipitation |
| kb | kilo base |
| KH | K-homology |
| <i>K. lactis</i> | <i>Kluyveromyces lactis</i> |

| | |
|----------------------|---|
| LB | lysogeny broth |
| LC-MS | liquid chromatography coupled to mass spectrometry |
| MeOH | methanol |
| Min | minutes |
| miRNA | micro RNA |
| mRNA | messenger RNA |
| mRNP | messenger ribonucleoprotein |
| MS | mass spectrometry |
| MT | microtubule |
| MVBs | multivesicular bodies |
| MW | molecular weight |
| NaP _i | sodium phosphate buffer |
| Ni-NTA | Nickel-Nitrilo tetra-acetic acid agarose |
| NMD | nonsense-mediate decay |
| OD ₆₀₀ | optical density at 600 nm |
| PAGE | polyacrylamide gel electrophoresis |
| PAR-CLIP | Photoactivatable Ribonucleoside-Enhanced Crosslinking and Immunoprecipitation |
| P-bodies | processing body |
| PBS | phosphate buffered saline |
| PCA | principal component analysis |
| PCI | phenol:chloroform:isoamylalcohol |
| PCR | polymerase chain reaction |
| PEG | polyethylene glycol |
| PSMF | phenylmethylsulfonyl fluoride |
| qRT-PCR | quantitative reverse transcription followed by PCR |
| RBD | RNA-binding domain |
| RBP | RNA-binding protein |
| RIP | RNA Immunoprecipitation |
| RNA | ribonucleic acid |
| RNA-Seq | RNA sequencing |
| RNAi | RNA interference |
| RNase | RNA-hydrolyzing enzyme |
| rpm | revolutions per minute |
| RRM | RNA-recognition motif |
| RT | room temperature |
| <i>S. cerevisiae</i> | <i>Saccharomyces cerevisiae</i> |
| SDS | sodium dodecyl sulfate |
| SELEX | systematic evolution of ligands by exponential enrichment |
| SEM | standard error of the mean |
| SGs | stress granules |
| SRP | signal recognition particle |
| TBS | tris-buffered saline solution |
| TBST | tris-buffered saline solution + 0.1% tween-20 |
| TCA | trichloro acetic acid |
| TEMED | N,N,N',N'-Tetramethylethylenediamine |
| tRNA | transfer RNA |
| ts | temperature sensitive |
| UTR | untranslated region |
| WB | western blot |
| WT | wild-type |
| w/v | weight per volume |
| yeGFP | yeast codon-optimized GFP |
| YNB | yeast nitrogen base |
| 5-FOA | 5-fluoroorotic acid |

5.3 References

- Aizer, A., Brody, Y., Ler, L.W., Sonenberg, N., Singer, R.H., and Shav-Tal, Y. (2008). The dynamics of mammalian P body transport, assembly, and disassembly in vivo. *Molecular biology of the cell* *19*, 4154-4166.
- Aizer, A., Kalo, A., Kafri, P., Shraga, A., Ben-Yishay, R., Jacob, A., Kinor, N., and Shav-Tal, Y. (2014). Quantifying mRNA targeting to P-bodies in living human cells reveals their dual role in mRNA decay and storage. *Journal of cell science* *127*, 4443-4456.
- Alberti, S., Halfmann, R., King, O., Kapila, A., and Lindquist, S. (2009). A systematic survey identifies prions and illuminates sequence features of prionogenic proteins. *Cell* *137*, 146-158.
- Albertyn, J., Hohmann, S., and Prior, B.A. (1994). Characterization of the osmotic-stress response in *Saccharomyces cerevisiae*: osmotic stress and glucose repression regulate glycerol-3-phosphate dehydrogenase independently. *Current genetics* *25*, 12-18.
- Anders, S., Pyl, P.T., and Huber, W. (2015). HTSeq--a Python framework to work with high-throughput sequencing data. *Bioinformatics* *31*, 166-169.
- Anderson, P., and Kedersha, N. (2006). RNA granules. *The Journal of cell biology* *172*, 803-808.
- Anderson, P., and Kedersha, N. (2009). RNA granules: post-transcriptional and epigenetic modulators of gene expression. *Nature reviews Molecular cell biology* *10*, 430-436.
- Andreassi, C., and Riccio, A. (2009). To localize or not to localize: mRNA fate is in 3'UTR ends. *Trends in cell biology* *19*, 465-474.
- Andrei, M.A., Ingelfinger, D., Heintzmann, R., Achsel, T., Rivera-Pomar, R., and Luhrmann, R. (2005). A role for eIF4E and eIF4E-transporter in targeting mRNPs to mammalian processing bodies. *Rna* *11*, 717-727.
- Arribere, J.A., Doudna, J.A., and Gilbert, W.V. (2011). Reconsidering movement of eukaryotic mRNAs between polysomes and P bodies. *Molecular cell* *44*, 745-758.
- Ascano, M., Hafner, M., Cekan, P., Gerstberger, S., and Tuschl, T. (2012). Identification of RNA-protein interaction networks using PAR-CLIP. *Wiley interdisciplinary reviews RNA* *3*, 159-177.
- Ashe, M.P., De Long, S.K., and Sachs, A.B. (2000). Glucose depletion rapidly inhibits translation initiation in yeast. *Molecular biology of the cell* *11*, 833-848.
- Bailey, T.L., Boden, M., Buske, F.A., Frith, M., Grant, C.E., Clementi, L., Ren, J., Li, W.W., and Noble, W.S. (2009). MEME SUITE: tools for motif discovery and searching. *Nucleic Acids Res* *37*, W202-208.
- Baker, K.E., and Parker, R. (2004). Nonsense-mediated mRNA decay: terminating erroneous gene expression. *Current opinion in cell biology* *16*, 293-299.
- Balogopal, V., Fluch, L., and Nissan, T. (2012). Ways and means of eukaryotic mRNA decay. *Biochimica et biophysica acta* *1819*, 593-603.

- Balagopal, V., and Parker, R. (2009). Polysomes, P bodies and stress granules: states and fates of eukaryotic mRNAs. *Current opinion in cell biology* 21, 403-408.
- Bassell, G.J., and Warren, S.T. (2008). Fragile X syndrome: loss of local mRNA regulation alters synaptic development and function. *Neuron* 60, 201-214.
- Batish, M., van den Bogaard, P., Kramer, F.R., and Tyagi, S. (2012). Neuronal mRNAs travel singly into dendrites. *Proceedings of the National Academy of Sciences of the United States of America* 109, 4645-4650.
- Baum, S., Bittins, M., Frey, S., and Seedorf, M. (2004). Asc1p, a WD40-domain containing adaptor protein, is required for the interaction of the RNA-binding protein Scp160p with polysomes. *Biochem J* 380, 823-830.
- Beelman, C.A., Stevens, A., Caponigro, G., LaGrandeur, T.E., Hatfield, L., Fortner, D.M., and Parker, R. (1996). An essential component of the decapping enzyme required for normal rates of mRNA turnover. *Nature* 382, 642-646.
- Boeck, R., Lapeyre, B., Brown, C.E., and Sachs, A.B. (1998). Capped mRNA degradation intermediates accumulate in the yeast *spb8-2* mutant. *Molecular and cellular biology* 18, 5062-5072.
- Bolger, A.M., Lohse, M., and Usadel, B. (2014). Trimmomatic: a flexible trimmer for Illumina sequence data. *Bioinformatics* 30, 2114-2120.
- Bradford, M.M. (1976). A rapid and sensitive method for the quantitation of microgram quantities of protein utilizing the principle of protein-dye binding. *Analytical biochemistry* 72, 248-254.
- Brangwynne, C.P., Eckmann, C.R., Courson, D.S., Rybarska, A., Hoegge, C., Gharakhani, J., Julicher, F., and Hyman, A.A. (2009). Germline P granules are liquid droplets that localize by controlled dissolution/condensation. *Science* 324, 1729-1732.
- Bregues, M., Teixeira, D., and Parker, R. (2005). Movement of eukaryotic mRNAs between polysomes and cytoplasmic processing bodies. *Science* 310, 486-489.
- Buchan, J.R. (2014). mRNP granules. Assembly, function, and connections with disease. *RNA biology* 11, 1019-1030.
- Buchan, J.R., Kolaitis, R.M., Taylor, J.P., and Parker, R. (2013). Eukaryotic stress granules are cleared by autophagy and Cdc48/VCP function. *Cell* 153, 1461-1474.
- Buchan, J.R., Muhlrad, D., and Parker, R. (2008). P bodies promote stress granule assembly in *Saccharomyces cerevisiae*. *The Journal of cell biology* 183, 441-455.
- Buchan, J.R., Nissan, T., and Parker, R. (2010). Analyzing P-bodies and stress granules in *Saccharomyces cerevisiae*. *Methods in enzymology* 470, 619-640.
- Buchan, J.R., and Parker, R. (2009). Eukaryotic stress granules: the ins and outs of translation. *Molecular cell* 36, 932-941.
- Buchan, J.R., Yoon, J.H., and Parker, R. (2011). Stress-specific composition, assembly and kinetics of stress granules in *Saccharomyces cerevisiae*. *Journal of cell science* 124, 228-239.

- Burg, M.B., Ferraris, J.D., and Dmitrieva, N.I. (2007). Cellular response to hyperosmotic stresses. *Physiological reviews* *87*, 1441-1474.
- Cai, Y., and Futcher, B. (2013). Effects of the yeast RNA-binding protein Whi3 on the half-life and abundance of CLN3 mRNA and other targets. *PLoS one* *8*, e84630.
- Campbell, Z.T., Bhimsaria, D., Valley, C.T., Rodriguez-Martinez, J.A., Menichelli, E., Williamson, J.R., Ansari, A.Z., and Wickens, M. (2012). Cooperativity in RNA-protein interactions: global analysis of RNA binding specificity. *Cell reports* *1*, 570-581.
- Chan, S.P., and Slack, F.J. (2006). microRNA-mediated silencing inside P-bodies. *RNA Biol* *3*, 97-100.
- Chang, W., Zaarour, R.F., Reck-Peterson, S., Rinn, J., Singer, R.H., Snyder, M., Novick, P., and Mooseker, M.S. (2008). Myo2p, a class V myosin in budding yeast, associates with a large ribonucleic acid-protein complex that contains mRNAs and subunits of the RNA-processing body. *Rna* *14*, 491-502.
- Chen, C.Y., and Shyu, A.B. (2011). Mechanisms of deadenylation-dependent decay. *Wiley interdisciplinary reviews RNA* *2*, 167-183.
- Chen, C.Y., and Shyu, A.B. (2013). Deadenylation and P-bodies. *Advances in experimental medicine and biology* *768*, 183-195.
- Chen, L., Muhrad, D., Hauryliuk, V., Cheng, Z., Lim, M.K., Shyp, V., Parker, R., and Song, H. (2010). Structure of the Dom34-Hbs1 complex and implications for no-go decay. *Nature structural & molecular biology* *17*, 1233-1240.
- Cheong, C.G., and Hall, T.M. (2006). Engineering RNA sequence specificity of Pumilio repeats. *Proceedings of the National Academy of Sciences of the United States of America* *103*, 13635-13639.
- Chowdhury, A., and Tharun, S. (2009). Activation of decapping involves binding of the mRNA and facilitation of the post-binding steps by the Lsm1-7-Pat1 complex. *Rna* *15*, 1837-1848.
- Chowdhury, S., Smith, K.W., and Gustin, M.C. (1992). Osmotic stress and the yeast cytoskeleton: phenotype-specific suppression of an actin mutation. *The Journal of cell biology* *118*, 561-571.
- Chritton, J.J., and Wickens, M. (2010). Translational repression by PUF proteins in vitro. *Rna* *16*, 1217-1225.
- Chung, S., and Takizawa, P.A. (2011). In vivo visualization of RNA using the U1A-based tagged RNA system. *Methods Mol Biol* *714*, 221-235.
- Clapham, D.E. (2007). Calcium signaling. *Cell* *131*, 1047-1058.
- Coller, J., and Parker, R. (2005). General translational repression by activators of mRNA decapping. *Cell* *122*, 875-886.
- Condeelis, J., and Singer, R.H. (2005). How and why does beta-actin mRNA target? *Biology of the cell / under the auspices of the European Cell Biology Organization* *97*, 97-110.
- Cook, K.B., Hughes, T.R., and Morris, Q.D. (2015). High-throughput characterization of protein-RNA interactions. *Briefings in functional genomics* *14*, 74-89.

- Cougot, N., Babajko, S., and Seraphin, B. (2004). Cytoplasmic foci are sites of mRNA decay in human cells. *The Journal of cell biology* 165, 31-40.
- de Almeida, S.F., and Carmo-Fonseca, M. (2008). The CTD role in cotranscriptional RNA processing and surveillance. *FEBS letters* 582, 1971-1976.
- Decker, C.J., and Parker, R. (2002). mRNA decay enzymes: decappers conserved between yeast and mammals. *Proceedings of the National Academy of Sciences of the United States of America* 99, 12512-12514.
- Decker, C.J., and Parker, R. (2012). P-bodies and stress granules: possible roles in the control of translation and mRNA degradation. *Cold Spring Harbor perspectives in biology* 4, a012286.
- Decker, C.J., Teixeira, D., and Parker, R. (2007). Edc3p and a glutamine/asparagine-rich domain of Lsm4p function in processing body assembly in *Saccharomyces cerevisiae*. *The Journal of cell biology* 179, 437-449.
- Dolgosheina, E.V., Jeng, S.C., Panchapakesan, S.S., Cojocar, R., Chen, P.S., Wilson, P.D., Hawkins, N., Wiggins, P.A., and Unrau, P.J. (2014). RNA mango aptamer-fluorophore: a bright, high-affinity complex for RNA labeling and tracking. *ACS chemical biology* 9, 2412-2420.
- Doma, M.K., and Parker, R. (2006). Endonucleolytic cleavage of eukaryotic mRNAs with stalls in translation elongation. *Nature* 440, 561-564.
- Du, T.G., Jellbauer, S., Muller, M., Schmid, M., Niessing, D., and Jansen, R.P. (2008). Nuclear transit of the RNA-binding protein She2 is required for translational control of localized ASH1 mRNA. *EMBO reports* 9, 781-787.
- Ellington, A.D., and Szostak, J.W. (1990). In vitro selection of RNA molecules that bind specific ligands. *Nature* 346, 818-822.
- Erdeniz, N., Mortensen, U.H., and Rothstein, R. (1997). Cloning-free PCR-based allele replacement methods. *Genome research* 7, 1174-1183.
- Erickson, S.L., and Lykke-Andersen, J. (2011). Cytoplasmic mRNP granules at a glance. *Journal of cell science* 124, 293-297.
- Eulalio, A., Behm-Ansmant, I., and Izaurralde, E. (2007a). P bodies: at the crossroads of post-transcriptional pathways. *Nature reviews Molecular cell biology* 8, 9-22.
- Eulalio, A., Behm-Ansmant, I., Schweizer, D., and Izaurralde, E. (2007b). P-body formation is a consequence, not the cause, of RNA-mediated gene silencing. *Molecular and cellular biology* 27, 3970-3981.
- Eystathiou, T., Chan, E.K., Tenenbaum, S.A., Keene, J.D., Griffith, K., and Fritzer, M.J. (2002). A phosphorylated cytoplasmic autoantigen, GW182, associates with a unique population of human mRNAs within novel cytoplasmic speckles. *Molecular biology of the cell* 13, 1338-1351.
- Eystathiou, T., Jakymiw, A., Chan, E.K., Seraphin, B., Cougot, N., and Fritzer, M.J. (2003). The GW182 protein colocalizes with mRNA degradation associated proteins hDcp1 and hLsm4 in cytoplasmic GW bodies. *Rna* 9, 1171-1173.

- Ferraiuolo, M.A., Basak, S., Dostie, J., Murray, E.L., Schoenberg, D.R., and Sonenberg, N. (2005). A role for the eIF4E-binding protein 4E-T in P-body formation and mRNA decay. *The Journal of cell biology* *170*, 913-924.
- Frischmeyer, P.A., van Hoof, A., O'Donnell, K., Guerrerero, A.L., Parker, R., and Dietz, H.C. (2002). An mRNA surveillance mechanism that eliminates transcripts lacking termination codons. *Science* *295*, 2258-2261.
- Fromm, S.A., Truffault, V., Kamenz, J., Braun, J.E., Hoffmann, N.A., Izaurralde, E., and Sprangers, R. (2012). The structural basis of Edc3- and Scd6-mediated activation of the Dcp1:Dcp2 mRNA decapping complex. *The EMBO journal* *31*, 279-290.
- Gallo, C.M., Wang, J.T., Motegi, F., and Seydoux, G. (2010). Cytoplasmic partitioning of P granule components is not required to specify the germline in *C. elegans*. *Science* *330*, 1685-1689.
- Gandhi, R., Manzoor, M., and Hudak, K.A. (2008). Depurination of Brome mosaic virus RNA3 in vivo results in translation-dependent accelerated degradation of the viral RNA. *The Journal of biological chemistry* *283*, 32218-32228.
- Garcia, J.F., and Parker, R. (2015). MS2 coat proteins bound to yeast mRNAs block 5' to 3' degradation and trap mRNA decay products: implications for the localization of mRNAs by MS2-MCP system. *RNA* *21*, 1393-1395.
- Garmendia-Torres, C., Skupin, A., Michael, S.A., Ruusuvoori, P., Kuwada, N.J., Falconnet, D., Cary, G.A., Hansen, C., Wiggins, P.A., and Dudley, A.M. (2014). Unidirectional P-body transport during the yeast cell cycle. *PLoS one* *9*, e99428.
- Garneau, N.L., Wilusz, J., and Wilusz, C.J. (2007). The highways and byways of mRNA decay. *Nature reviews Molecular cell biology* *8*, 113-126.
- Garre, E., Romero-Santacreu, L., Barneo-Munoz, M., Miguel, A., Perez-Ortin, J.E., and Alepuz, P. (2013). Nonsense-mediated mRNA decay controls the changes in yeast ribosomal protein pre-mRNAs levels upon osmotic stress. *PLoS one* *8*, e61240.
- Gasch, A.P., Spellman, P.T., Kao, C.M., Carmel-Harel, O., Eisen, M.B., Storz, G., Botstein, D., and Brown, P.O. (2000). Genomic expression programs in the response of yeast cells to environmental changes. *Molecular biology of the cell* *11*, 4241-4257.
- Gasch, A.P., and Werner-Washburne, M. (2002). The genomics of yeast responses to environmental stress and starvation. *Functional & integrative genomics* *2*, 181-192.
- Gauss, R., Trautwein, M., Sommer, T., and Spang, A. (2005). New modules for the repeated internal and N-terminal epitope tagging of genes in *Saccharomyces cerevisiae*. *Yeast* *22*, 1-12.
- Gerber, A.P., Herschlag, D., and Brown, P.O. (2004). Extensive association of functionally and cytologically related mRNAs with Puf family RNA-binding proteins in yeast. *PLoS biology* *2*, E79.
- Gerstberger, S., Hafner, M., and Tuschl, T. (2013). Learning the language of post-transcriptional gene regulation. *Genome biology* *14*, 130.

- Gibbings, D.J., Ciaudo, C., Erhardt, M., and Voinnet, O. (2009). Multivesicular bodies associate with components of miRNA effector complexes and modulate miRNA activity. *Nature cell biology* *11*, 1143-1149.
- Gietz, R.D., Schiestl, R.H., Willems, A.R., and Woods, R.A. (1995). Studies on the transformation of intact yeast cells by the LiAc/SS-DNA/PEG procedure. *Yeast* *11*, 355-360.
- Gilks, N., Kedersha, N., Ayodele, M., Shen, L., Stoecklin, G., Dember, L.M., and Anderson, P. (2004). Stress granule assembly is mediated by prion-like aggregation of TIA-1. *Molecular biology of the cell* *15*, 5383-5398.
- Glisovic, T., Bachorik, J.L., Yong, J., and Dreyfuss, G. (2008). RNA-binding proteins and post-transcriptional gene regulation. *FEBS letters* *582*, 1977-1986.
- Goldstrohm, A.C., Hook, B.A., Seay, D.J., and Wickens, M. (2006). PUF proteins bind Pop2p to regulate messenger RNAs. *Nat Struct Mol Biol* *13*, 533-539.
- Gray, J.V., Petsko, G.A., Johnston, G.C., Ringe, D., Singer, R.A., and Werner-Washburne, M. (2004). "Sleeping beauty": quiescence in *Saccharomyces cerevisiae*. *Microbiology and molecular biology reviews* : MMBR *68*, 187-206.
- Grousl, T., Ivanov, P., Frydlova, I., Vasicova, P., Janda, F., Vojtova, J., Malinska, K., Malcova, I., Novakova, L., Janoskova, D., *et al.* (2009). Robust heat shock induces eIF2alpha-phosphorylation-independent assembly of stress granules containing eIF3 and 40S ribosomal subunits in budding yeast, *Saccharomyces cerevisiae*. *Journal of cell science* *122*, 2078-2088.
- Gruber, A.R., Fallmann, J., Kratochvill, F., Kovarik, P., and Hofacker, I.L. (2011). AREsite: a database for the comprehensive investigation of AU-rich elements. *Nucleic acids research* *39*, D66-69.
- Gueldener, U., Heinisch, J., Koehler, G.J., Voss, D., and Hegemann, J.H. (2002). A second set of loxP marker cassettes for Cre-mediated multiple gene knockouts in budding yeast. *Nucleic acids research* *30*, e23.
- Guil, S., Long, J.C., and Caceres, J.F. (2006). hnRNP A1 relocalization to the stress granules reflects a role in the stress response. *Molecular and cellular biology* *26*, 5744-5758.
- Hafner, M., Landthaler, M., Burger, L., Khorshid, M., Hausser, J., Berninger, P., Rothballer, A., Ascano, M., Jr., Jungkamp, A.C., Munschauer, M., *et al.* (2010). Transcriptome-wide identification of RNA-binding protein and microRNA target sites by PAR-CLIP. *Cell* *141*, 129-141.
- Harrison, P.M., and Gerstein, M. (2003). A method to assess compositional bias in biological sequences and its application to prion-like glutamine/asparagine-rich domains in eukaryotic proteomes. *Genome biology* *4*, R40.
- He, W., and Parker, R. (2001). The yeast cytoplasmic Lsm1/Pat1p complex protects mRNA 3' termini from partial degradation. *Genetics* *158*, 1445-1455.
- Hey, F., Czyzewicz, N., Jones, P., and Sablitzky, F. (2012a). DEF6, a novel substrate for the Tec kinase ITK, contains a glutamine-rich aggregation-prone region and forms cytoplasmic granules that co-localize with P-bodies. *J Biol Chem* *287*, 31073-31084.

Hey, F., Czyzewicz, N., Jones, P., and Sablitzky, F. (2012b). DEF6, a novel substrate for the Tec kinase ITK, contains a glutamine-rich aggregation-prone region and forms cytoplasmic granules that co-localize with P-bodies. *The Journal of biological chemistry* **287**, 31073-31084.

Higashiyama, H., Hirose, F., Yamaguchi, M., Inoue, Y.H., Fujikake, N., Matsukage, A., and Kakizuka, A. (2002). Identification of ter94, *Drosophila* VCP, as a modulator of polyglutamine-induced neurodegeneration. *Cell death and differentiation* **9**, 264-273.

Hillebrand, J., Barbee, S.A., and Ramaswami, M. (2007). P-body components, microRNA regulation, and synaptic plasticity. *TheScientificWorldJournal* **7**, 178-190.

Hocine, S., Raymond, P., Zenklusen, D., Chao, J.A., and Singer, R.H. (2013). Single-molecule analysis of gene expression using two-color RNA labeling in live yeast. *Nature methods* **10**, 119-121.

Hoffman, C.S., and Winston, F. (1987). A ten-minute DNA preparation from yeast efficiently releases autonomous plasmids for transformation of *Escherichia coli*. *Gene* **57**, 267-272.

Hogan, D.J., Riordan, D.P., Gerber, A.P., Herschlag, D., and Brown, P.O. (2008). Diverse RNA-binding proteins interact with functionally related sets of RNAs, suggesting an extensive regulatory system. *PLoS Biol* **6**, e255.

Hogan, G.J., Brown, P.O., and Herschlag, D. (2015). Evolutionary Conservation and Diversification of Puf RNA Binding Proteins and Their mRNA Targets. *PLoS Biol* **13**, e1002307.

Houseley, J., LaCava, J., and Tollervey, D. (2006). RNA-quality control by the exosome. *Nature reviews Molecular cell biology* **7**, 529-539.

Hoyle, N.P., Castelli, L.M., Campbell, S.G., Holmes, L.E., and Ashe, M.P. (2007). Stress-dependent relocalization of translationally primed mRNPs to cytoplasmic granules that are kinetically and spatially distinct from P-bodies. *The Journal of cell biology* **179**, 65-74.

Hu, W., Sweet, T.J., Chamnongpol, S., Baker, K.E., and Collier, J. (2009). Co-translational mRNA decay in *Saccharomyces cerevisiae*. *Nature* **461**, 225-229.

Ingelfinger, D., Arndt-Jovin, D.J., Luhrmann, R., and Achsel, T. (2002). The human LSm1-7 proteins colocalize with the mRNA-degrading enzymes Dcp1/2 and Xrn1 in distinct cytoplasmic foci. *Rna* **8**, 1489-1501.

Isken, O., and Maquat, L.E. (2008). The multiple lives of NMD factors: balancing roles in gene and genome regulation. *Nature reviews Genetics* **9**, 699-712.

Iwaki, A., and Izawa, S. (2012). Acidic stress induces the formation of P-bodies, but not stress granules, with mild attenuation of bulk translation in *Saccharomyces cerevisiae*. *The Biochemical journal* **446**, 225-233.

Jaglarz, M.K., Kloc, M., Jankowska, W., Szymanska, B., and Bilinski, S.M. (2011). Nuage morphogenesis becomes more complex: two translocation pathways and two forms of nuage coexist in *Drosophila* germline syncytia. *Cell Tissue Res* **344**, 169-181.

Janke, C., Magiera, M.M., Rathfelder, N., Taxis, C., Reber, S., Maekawa, H., Moreno-Borchart, A., Doenges, G., Schwob, E., Schiebel, E., *et al.* (2004). A versatile toolbox for PCR-based tagging of yeast genes: new fluorescent proteins, more markers and promoter substitution cassettes. *Yeast* **21**, 947-962.

- Jansen, R.P. (2001). mRNA localization: message on the move. *Nature reviews Molecular cell biology* 2, 247-256.
- Kedersha, N., Cho, M.R., Li, W., Yacono, P.W., Chen, S., Gilks, N., Golan, D.E., and Anderson, P. (2000). Dynamic shuttling of TIA-1 accompanies the recruitment of mRNA to mammalian stress granules. *The Journal of cell biology* 151, 1257-1268.
- Kedersha, N., Stoecklin, G., Ayodele, M., Yacono, P., Lykke-Andersen, J., Fritzler, M.J., Scheuner, D., Kaufman, R.J., Golan, D.E., and Anderson, P. (2005). Stress granules and processing bodies are dynamically linked sites of mRNP remodeling. *J Cell Biol* 169, 871-884.
- Kedersha, N.L., Gupta, M., Li, W., Miller, I., and Anderson, P. (1999). RNA-binding proteins TIA-1 and TIAR link the phosphorylation of eIF-2 alpha to the assembly of mammalian stress granules. *The Journal of cell biology* 147, 1431-1442.
- Keene, J.D. (2001). Ribonucleoprotein infrastructure regulating the flow of genetic information between the genome and the proteome. *Proceedings of the National Academy of Sciences of the United States of America* 98, 7018-7024.
- Kilchert, C., and Spang, A. (2011). Cotranslational transport of ABP140 mRNA to the distal pole of *S. cerevisiae*. *Embo J* 30, 3567-3580.
- Kilchert, C., Weidner, J., Prescianotto-Baschong, C., and Spang, A. (2010). Defects in the secretory pathway and high Ca²⁺ induce multiple P-bodies. *Molecular biology of the cell* 21, 2624-2638.
- Kim, V.N., Han, J., and Siomi, M.C. (2009). Biogenesis of small RNAs in animals. *Nature reviews Molecular cell biology* 10, 126-139.
- King, M.L., Messitt, T.J., and Mowry, K.L. (2005). Putting RNAs in the right place at the right time: RNA localization in the frog oocyte. *Biology of the cell / under the auspices of the European Cell Biology Organization* 97, 19-33.
- Kishore, S., Jaskiewicz, L., Burger, L., Hausser, J., Khorshid, M., and Zavolan, M. (2011). A quantitative analysis of CLIP methods for identifying binding sites of RNA-binding proteins. *Nature methods* 8, 559-564.
- Klosinska, M.M., Crutchfield, C.A., Bradley, P.H., Rabinowitz, J.D., and Broach, J.R. (2011). Yeast cells can access distinct quiescent states. *Genes & development* 25, 336-349.
- Knop, M., Siegers, K., Pereira, G., Zachariae, W., Winsor, B., Nasmyth, K., and Schiebel, E. (1999). Epitope tagging of yeast genes using a PCR-based strategy: more tags and improved practical routines. *Yeast* 15, 963-972.
- Konig, J., Zarnack, K., Rot, G., Curk, T., Kayikci, M., Zupan, B., Turner, D.J., Luscombe, N.M., and Ule, J. (2010). iCLIP reveals the function of hnRNP particles in splicing at individual nucleotide resolution. *Nature structural & molecular biology* 17, 909-915.
- Kuhn, U., and Wahle, E. (2004). Structure and function of poly(A) binding proteins. *Biochimica et biophysica acta* 1678, 67-84.
- Kulkarni, M., Ozgur, S., and Stoecklin, G. (2010). On track with P-bodies. *Biochemical Society transactions* 38, 242-251.

- Lang, B.D., and Fridovich-Keil, J.L. (2000). Scp160p, a multiple KH-domain protein, is a component of mRNP complexes in yeast. *Nucleic Acids Res* 28, 1576-1584.
- Lang, B.D., Li, A., Black-Brewster, H.D., and Fridovich-Keil, J.L. (2001). The brefeldin A resistance protein Bfr1p is a component of polyribosome-associated mRNP complexes in yeast. *Nucleic Acids Res* 29, 2567-2574.
- Langmead, B., Trapnell, C., Pop, M., and Salzberg, S.L. (2009). Ultrafast and memory-efficient alignment of short DNA sequences to the human genome. *Genome Biol* 10, R25.
- Lavut, A., and Raveh, D. (2012). Sequestration of highly expressed mRNAs in cytoplasmic granules, P-bodies, and stress granules enhances cell viability. *PLoS Genet* 8, e1002527.
- Lee, Y.S., Pressman, S., Andress, A.P., Kim, K., White, J.L., Cassidy, J.J., Li, X., Lubell, K., Lim do, H., Cho, I.S., *et al.* (2009). Silencing by small RNAs is linked to endosomal trafficking. *Nature cell biology* 11, 1150-1156.
- Li, X., Kazan, H., Lipshitz, H.D., and Morris, Q.D. (2014). Finding the target sites of RNA-binding proteins. *Wiley interdisciplinary reviews RNA* 5, 111-130.
- Ling, S.H., Decker, C.J., Walsh, M.A., She, M., Parker, R., and Song, H. (2008). Crystal structure of human Edc3 and its functional implications. *Molecular and cellular biology* 28, 5965-5976.
- Ling, Y.H., Wong, C.C., Li, K.W., Chan, K.M., Boukamp, P., and Liu, W.K. (2014a). CCHCR1 interacts with EDC4, suggesting its localization in P-bodies. *Experimental cell research* 327, 12-23.
- Ling, Y.H., Wong, C.C., Li, K.W., Chan, K.M., Boukamp, P., and Liu, W.K. (2014b). CCHCR1 interacts with EDC4, suggesting its localization in P-bodies. *Exp Cell Res* 327, 12-23.
- Liu, J., Rivas, F.V., Wohlschlegel, J., Yates, J.R., 3rd, Parker, R., and Hannon, G.J. (2005a). A role for the P-body component GW182 in microRNA function. *Nature cell biology* 7, 1261-1266.
- Liu, J., Valencia-Sanchez, M.A., Hannon, G.J., and Parker, R. (2005b). MicroRNA-dependent localization of targeted mRNAs to mammalian P-bodies. *Nature cell biology* 7, 719-723.
- Loschi, M., Leishman, C.C., Berardone, N., and Boccaccio, G.L. (2009). Dynein and kinesin regulate stress-granule and P-body dynamics. *Journal of cell science* 122, 3973-3982.
- Lowry, O.H., Rosebrough, N.J., Farr, A.L., and Randall, R.J. (1951). Protein measurement with the Folin phenol reagent. *The Journal of biological chemistry* 193, 265-275.
- Lunde, B.M., Moore, C., and Varani, G. (2007). RNA-binding proteins: modular design for efficient function. *Nature reviews Molecular cell biology* 8, 479-490.
- Maeder, C.I., Hink, M.A., Kinkhabwala, A., Mayr, R., Bastiaens, P.I., and Knop, M. (2007). Spatial regulation of Fus3 MAP kinase activity through a reaction-diffusion mechanism in yeast pheromone signalling. *Nature cell biology* 9, 1319-1326.
- Mager, W.H., and Ferreira, P.M. (1993). Stress response of yeast. *The Biochemical journal* 290 (Pt 1), 1-13.

- Martin, K.C., and Ephrussi, A. (2009). mRNA localization: gene expression in the spatial dimension. *Cell* 136, 719-730.
- Masliyah, G., Barraud, P., and Allain, F.H. (2013). RNA recognition by double-stranded RNA binding domains: a matter of shape and sequence. *Cellular and molecular life sciences : CMLS* 70, 1875-1895.
- Maxon, M.E., and Herskowitz, I. (2001). Ash1p is a site-specific DNA-binding protein that actively represses transcription. *Proceedings of the National Academy of Sciences of the United States of America* 98, 1495-1500.
- Mazzoni, C., D'Addario, I., and Falcone, C. (2007). The C-terminus of the yeast Lsm4p is required for the association to P-bodies. *FEBS letters* 581, 4836-4840.
- Mendelsohn, B.A., Li, A.M., Vargas, C.A., Riehn, K., Watson, A., and Fridovich-Keil, J.L. (2003). Genetic and biochemical interactions between SCP160 and EAP1 in yeast. *Nucleic Acids Res* 31, 5838-5847.
- Micaroni, M. (2012). Calcium around the Golgi apparatus: implications for intracellular membrane trafficking. *Advances in experimental medicine and biology* 740, 439-460.
- Middleton, S.A., and Kim, J. (2014). NoFold: RNA structure clustering without folding or alignment. *Rna* 20, 1671-1683.
- Mili, S., and Steitz, J.A. (2004). Evidence for reassociation of RNA-binding proteins after cell lysis: implications for the interpretation of immunoprecipitation analyses. *Rna* 10, 1692-1694.
- Miller, C., Schwalb, B., Maier, K., Schulz, D., Dumcke, S., Zacher, B., Mayer, A., Sydow, J., Marciniowski, L., Dolken, L., *et al.* (2011). Dynamic transcriptome analysis measures rates of mRNA synthesis and decay in yeast. *Mol Syst Biol* 7, 458.
- Mitchell, S.F., Jain, S., She, M., and Parker, R. (2013). Global analysis of yeast mRNPs. *Nature structural & molecular biology* 20, 127-133.
- Munchel, S.E., Shultzaberger, R.K., Takizawa, N., and Weis, K. (2011). Dynamic profiling of mRNA turnover reveals gene-specific and system-wide regulation of mRNA decay. *Molecular biology of the cell* 22, 2787-2795.
- Neu-Yilik, G., and Kulozik, A.E. (2008). NMD: multitasking between mRNA surveillance and modulation of gene expression. *Advances in genetics* 62, 185-243.
- Olmezer, G., Klein, D., and Rass, U. (2015). DNA repair defects ascribed to pby1 are caused by disruption of Holliday junction resolvase Mus81-Mms4. *DNA repair* 33, 17-23.
- Otterstedt, K., Larsson, C., Bill, R.M., Stahlberg, A., Boles, E., Hohmann, S., and Gustafsson, L. (2004). Switching the mode of metabolism in the yeast *Saccharomyces cerevisiae*. *EMBO reports* 5, 532-537.
- Paige, J.S., Wu, K.Y., and Jaffrey, S.R. (2011). RNA mimics of green fluorescent protein. *Science* 333, 642-646.
- Parenteau, J., Durand, M., Veronneau, S., Lacombe, A.A., Morin, G., Guerin, V., Cecez, B., Gervais-Bird, J., Koh, C.S., Brunelle, D., *et al.* (2008). Deletion of many yeast introns reveals a minority of genes that require splicing for function. *Molecular biology of the cell* 19, 1932-1941.

- Parker, R., and Sheth, U. (2007). P bodies and the control of mRNA translation and degradation. *Molecular cell* 25, 635-646.
- Parker, R., and Song, H. (2004). The enzymes and control of eukaryotic mRNA turnover. *Nature structural & molecular biology* 11, 121-127.
- Pilkington, G.R., and Parker, R. (2008). Pat1 contains distinct functional domains that promote P-body assembly and activation of decapping. *Molecular and cellular biology* 28, 1298-1312.
- Rajyaguru, P., She, M., and Parker, R. (2012). Scd6 targets eIF4G to repress translation: RGG motif proteins as a class of eIF4G-binding proteins. *Molecular cell* 45, 244-254.
- Ramachandran, V., Shah, K.H., and Herman, P.K. (2011). The cAMP-dependent protein kinase signaling pathway is a key regulator of P body foci formation. *Molecular cell* 43, 973-981.
- Ray, D., Kazan, H., Chan, E.T., Pena Castillo, L., Chaudhry, S., Talukder, S., Blencowe, B.J., Morris, Q., and Hughes, T.R. (2009). Rapid and systematic analysis of the RNA recognition specificities of RNA-binding proteins. *Nature biotechnology* 27, 667-670.
- Reijns, M.A., Alexander, R.D., Spiller, M.P., and Beggs, J.D. (2008). A role for Q/N-rich aggregation-prone regions in P-body localization. *Journal of cell science* 121, 2463-2472.
- Rikhvanov, E.G., Romanova, N.V., and Chernoff, Y.O. (2007). Chaperone effects on prion and nonprion aggregates. *Prion* 1, 217-222.
- Ritz, A.M., Trautwein, M., Grassinger, F., and Spang, A. (2014). The prion-like domain in the exomer-dependent cargo Pin2 serves as a trans-Golgi retention motif. *Cell reports* 7, 249-260.
- Robinson, M.D., McCarthy, D.J., and Smyth, G.K. (2010). edgeR: a Bioconductor package for differential expression analysis of digital gene expression data. *Bioinformatics* 26, 139-140.
- Romero-Santacreu, L., Moreno, J., Perez-Ortin, J.E., and Alepuz, P. (2009). Specific and global regulation of mRNA stability during osmotic stress in *Saccharomyces cerevisiae*. *Rna* 15, 1110-1120.
- Sakuno, T., Araki, Y., Ohya, Y., Kofuji, S., Takahashi, S., Hoshino, S., and Katada, T. (2004). Decapping reaction of mRNA requires Dcp1 in fission yeast: its characterization in different species from yeast to human. *Journal of biochemistry* 136, 805-812.
- Scherrer, T., Mittal, N., Janga, S.C., and Gerber, A.P. (2010). A screen for RNA-binding proteins in yeast indicates dual functions for many enzymes. *PloS one* 5, e15499.
- Schmitt, M.E., Brown, T.A., and Trumpower, B.L. (1990). A rapid and simple method for preparation of RNA from *Saccharomyces cerevisiae*. *Nucleic Acids Res* 18, 3091-3092.
- Schuller, C., Brewster, J.L., Alexander, M.R., Gustin, M.C., and Ruis, H. (1994). The HOG pathway controls osmotic regulation of transcription via the stress response element (STRE) of the *Saccharomyces cerevisiae* CTT1 gene. *The EMBO journal* 13, 4382-4389.
- Schwartz, D.C., and Parker, R. (2000). mRNA decapping in yeast requires dissociation of the cap binding protein, eukaryotic translation initiation factor 4E. *Molecular and cellular biology* 20, 7933-7942.

- Sen, G.L., and Blau, H.M. (2005). Argonaute 2/RISC resides in sites of mammalian mRNA decay known as cytoplasmic bodies. *Nature cell biology* 7, 633-636.
- Serman, A., Le Roy, F., Aigueperse, C., Kress, M., Dautry, F., and Weil, D. (2007). GW body disassembly triggered by siRNAs independently of their silencing activity. *Nucleic acids research* 35, 4715-4727.
- Sezen, B., Seedorf, M., and Schiebel, E. (2009). The SESA network links duplication of the yeast centrosome with the protein translation machinery. *Genes Dev* 23, 1559-1570.
- Shah, K.H., Zhang, B., Ramachandran, V., and Herman, P.K. (2013). Processing body and stress granule assembly occur by independent and differentially regulated pathways in *Saccharomyces cerevisiae*. *Genetics* 193, 109-123.
- She, M., Decker, C.J., Svergun, D.I., Round, A., Chen, N., Muhlrads, D., Parker, R., and Song, H. (2008). Structural basis of dcp2 recognition and activation by dcp1. *Molecular cell* 29, 337-349.
- Sherman, F. (1991). Getting started with yeast. *Methods Enzymol* 194, 3-21.
- Sheth, U., and Parker, R. (2003). Decapping and decay of messenger RNA occur in cytoplasmic processing bodies. *Science* 300, 805-808.
- Sheth, U., and Parker, R. (2006). Targeting of aberrant mRNAs to cytoplasmic processing bodies. *Cell* 125, 1095-1109.
- Sikorski, R.S., and Hieter, P. (1989). A system of shuttle vectors and yeast host strains designed for efficient manipulation of DNA in *Saccharomyces cerevisiae*. *Genetics* 122, 19-27.
- Simpson, C.E., Lui, J., Kershaw, C.J., Sims, P.F., and Ashe, M.P. (2014). mRNA localization to P-bodies in yeast is bi-phasic with many mRNAs captured in a late Bfr1p-dependent wave. *Journal of cell science* 127, 1254-1262.
- Slaninova, I., Sestak, S., Svoboda, A., and Farkas, V. (2000). Cell wall and cytoskeleton reorganization as the response to hyperosmotic shock in *Saccharomyces cerevisiae*. *Archives of microbiology* 173, 245-252.
- Snee, M.J., and Macdonald, P.M. (2009). Dynamic organization and plasticity of sponge bodies. *Developmental dynamics: an official publication of the American Association of Anatomists* 238, 918-930.
- Souquere, S., Mollet, S., Kress, M., Dautry, F., Pierron, G., and Weil, D. (2009). Unravelling the ultrastructure of stress granules and associated P-bodies in human cells. *Journal of cell science* 122, 3619-3626.
- Steffens, A., Jaegle, B., Tresch, A., Hulskamp, M., and Jakoby, M. (2014). Processing-body movement in *Arabidopsis* depends on an interaction between myosins and DECAPPING PROTEIN1. *Plant physiology* 164, 1879-1892.
- Steiger, M., Carr-Schmid, A., Schwartz, D.C., Kiledjian, M., and Parker, R. (2003). Analysis of recombinant yeast decapping enzyme. *Rna* 9, 231-238.
- Stoecklin, G., and Anderson, P. (2007). In a tight spot: ARE-mRNAs at processing bodies. *Genes & development* 21, 627-631.

Stoecklin, G., and Kedersha, N. (2013). Relationship of GW/P-bodies with stress granules. *Advances in experimental medicine and biology* 768, 197-211.

Stoecklin, G., Stubbs, T., Kedersha, N., Wax, S., Rigby, W.F., Blackwell, T.K., and Anderson, P. (2004). MK2-induced tristetraprolin:14-3-3 complexes prevent stress granule association and ARE-mRNA decay. *The EMBO journal* 23, 1313-1324.

Storici, F., and Resnick, M.A. (2006). The delitto perfetto approach to in vivo site-directed mutagenesis and chromosome rearrangements with synthetic oligonucleotides in yeast. *Methods Enzymol* 409, 329-345.

Stracka, D., Jozefczuk, S., Rudroff, F., Sauer, U., and Hall, M.N. (2014). Nitrogen source activates TOR (target of rapamycin) complex 1 via glutamine and independently of Gtr/Rag proteins. *The Journal of biological chemistry* 289, 25010-25020.

Suk, K., Choi, J., Suzuki, Y., Ozturk, S.B., Mellor, J.C., Wong, K.H., MacKay, J.L., Gregory, R.I., and Roth, F.P. (2011). Reconstitution of human RNA interference in budding yeast. *Nucleic Acids Res* 39, e43.

Sun, M., Schwalb, B., Pirkl, N., Maier, K.C., Schenk, A., Failmezger, H., Tresch, A., and Cramer, P. (2013). Global analysis of eukaryotic mRNA degradation reveals Xrn1-dependent buffering of transcript levels. *Molecular cell* 52, 52-62.

Sweet, T.J., Boyer, B., Hu, W., Baker, K.E., and Coller, J. (2007). Microtubule disruption stimulates P-body formation. *Rna* 13, 493-502.

Tagwerker, C., Flick, K., Cui, M., Guerrero, C., Dou, Y., Auer, B., Baldi, P., Huang, L., and Kaiser, P. (2006). A tandem affinity tag for two-step purification under fully denaturing conditions: application in ubiquitin profiling and protein complex identification combined with in vivocross-linking. *Mol Cell Proteomics* 5, 737-748.

Takizawa, P.A., Sil, A., Swedlow, J.R., Herskowitz, I., and Vale, R.D. (1997). Actin-dependent localization of an RNA encoding a cell-fate determinant in yeast. *Nature* 389, 90-93.

Tamas, M.J., Luyten, K., Sutherland, F.C., Hernandez, A., Albertyn, J., Valadi, H., Li, H., Prior, B.A., Kilian, S.G., Ramos, J., *et al.* (1999). Fps1p controls the accumulation and release of the compatible solute glycerol in yeast osmoregulation. *Molecular microbiology* 31, 1087-1104.

Tanaka, T. (2001). Chromatin Immunoprecipitation in Budding Yeast. In *Mapping Protein/DNA Interactions by Cross-Linking* (Paris).

Teixeira, D., and Parker, R. (2007). Analysis of P-body assembly in *Saccharomyces cerevisiae*. *Molecular biology of the cell* 18, 2274-2287.

Teixeira, D., Sheth, U., Valencia-Sanchez, M.A., Brengues, M., and Parker, R. (2005). Processing bodies require RNA for assembly and contain nontranslating mRNAs. *RNA* 11, 371-382.

Tenenbaum, S.A., Carson, C.C., Lager, P.J., and Keene, J.D. (2000). Identifying mRNA subsets in messenger ribonucleoprotein complexes by using cDNA arrays. *Proceedings of the National Academy of Sciences of the United States of America* 97, 14085-14090.

- Tharun, S., He, W., Mayes, A.E., Lennertz, P., Beggs, J.D., and Parker, R. (2000). Yeast Sm-like proteins function in mRNA decapping and decay. *Nature* *404*, 515-518.
- Tharun, S., and Parker, R. (2001). Targeting an mRNA for decapping: displacement of translation factors and association of the Lsm1p-7p complex on deadenylated yeast mRNAs. *Molecular cell* *8*, 1075-1083.
- Tsvetanova, N.G., Klass, D.M., Salzman, J., and Brown, P.O. (2010). Proteome-wide search reveals unexpected RNA-binding proteins in *Saccharomyces cerevisiae*. *PLoS one* *5*.
- Tucker, M., Valencia-Sanchez, M.A., Staples, R.R., Chen, J., Denis, C.L., and Parker, R. (2001). The transcription factor associated Ccr4 and Caf1 proteins are components of the major cytoplasmic mRNA deadenylase in *Saccharomyces cerevisiae*. *Cell* *104*, 377-386.
- Uesono, Y., and Toh, E.A. (2002). Transient inhibition of translation initiation by osmotic stress. *The Journal of biological chemistry* *277*, 13848-13855.
- Ule, J., Jensen, K.B., Ruggiu, M., Mele, A., Ule, A., and Darnell, R.B. (2003). CLIP identifies Nova-regulated RNA networks in the brain. *Science* *302*, 1212-1215.
- Updike, D., and Strome, S. (2010). P granule assembly and function in *Caenorhabditis elegans* germ cells. *Journal of andrology* *31*, 53-60.
- van Dijk, E., Cougot, N., Meyer, S., Babajko, S., Wahle, E., and Seraphin, B. (2002). Human Dcp2: a catalytically active mRNA decapping enzyme located in specific cytoplasmic structures. *The EMBO journal* *21*, 6915-6924.
- van Hoof, A., Frischmeyer, P.A., Dietz, H.C., and Parker, R. (2002). Exosome-mediated recognition and degradation of mRNAs lacking a termination codon. *Science* *295*, 2262-2264.
- Voronina, E., Seydoux, G., Sassone-Corsi, P., and Nagamori, I. (2011). RNA granules in germ cells. *Cold Spring Harbor perspectives in biology* *3*.
- Vuppalanchi, D., Coleman, J., Yoo, S., Merianda, T.T., Yadhati, A.G., Hossain, J., Blesch, A., Willis, D.E., and Twiss, J.L. (2010). Conserved 3'-untranslated region sequences direct subcellular localization of chaperone protein mRNAs in neurons. *The Journal of biological chemistry* *285*, 18025-18038.
- Walters, R.W., Shumilin, I.A., Yoon, J.H., Minor, W., and Parker, R. (2014). Edc3 function in yeast and mammals is modulated by interaction with NAD-related compounds. *G3* *4*, 613-622.
- Wang, Y., Liu, C.L., Storey, J.D., Tibshirani, R.J., Herschlag, D., and Brown, P.O. (2002). Precision and functional specificity in mRNA decay. *Proceedings of the National Academy of Sciences of the United States of America* *99*, 5860-5865.
- Weidner, J., Wang, C., Prescianotto-Baschong, C., Estrada, A.F., and Spang, A. (2014). The polysome-associated proteins Scp160 and Bfr1 prevent P body formation under normal growth conditions. *J Cell Sci* *127*, 1992-2004.
- Weil, T.T., Parton, R.M., Herpers, B., Soetaert, J., Veenendaal, T., Xanthakis, D., Dobbie, I.M., Halstead, J.M., Hayashi, R., Rabouille, C., *et al.* (2012). *Drosophila* patterning is established by differential association of mRNAs with P bodies. *Nat Cell Biol* *14*, 1305-1313.
- Wickens, M., Bernstein, D.S., Kimble, J., and Parker, R. (2002). A PUF family portrait: 3'UTR regulation as a way of life. *Trends in genetics : TIG* *18*, 150-157.

Wiederhold, K., and Passmore, L.A. (2010). Cytoplasmic deadenylation: regulation of mRNA fate. *Biochemical Society transactions* **38**, 1531-1536.

Wilczynska, A., Aigueperse, C., Kress, M., Dautry, F., and Weil, D. (2005). The translational regulator CPEB1 provides a link between dcp1 bodies and stress granules. *Journal of cell science* **118**, 981-992.

Wilinski, D., Qiu, C., Lapointe, C.P., Nevil, M., Campbell, Z.T., Tanaka Hall, T.M., and Wickens, M. (2015). RNA regulatory networks diversified through curvature of the PUF protein scaffold. *Nat Commun* **6**, 8213.

Will, C.L., and Luhrmann, R. (2011). Spliceosome structure and function. *Cold Spring Harbor perspectives in biology* **3**.

Wilsch-Brauninger, M., Schwarz, H., and Nusslein-Volhard, C. (1997). A sponge-like structure involved in the association and transport of maternal products during *Drosophila* oogenesis. *The Journal of cell biology* **139**, 817-829.

Wu, J., Zhang, N., Hayes, A., Panoutsopoulou, K., and Oliver, S.G. (2004). Global analysis of nutrient control of gene expression in *Saccharomyces cerevisiae* during growth and starvation. *Proceedings of the National Academy of Sciences of the United States of America* **101**, 3148-3153.

Yamanaka, K., Okubo, Y., Suzaki, T., and Ogura, T. (2004). Analysis of the two p97/VCP/Cdc48p proteins of *Caenorhabditis elegans* and their suppression of polyglutamine-induced protein aggregation. *Journal of structural biology* **146**, 242-250.

Yang, Z., Jakymiw, A., Wood, M.R., Eystathiou, T., Rubin, R.L., Fritzler, M.J., and Chan, E.K. (2004). GW182 is critical for the stability of GW bodies expressed during the cell cycle and cell proliferation. *Journal of cell science* **117**, 5567-5578.

Yoon, J.H., Choi, E.J., and Parker, R. (2010). Dcp2 phosphorylation by Ste20 modulates stress granule assembly and mRNA decay in *Saccharomyces cerevisiae*. *The Journal of cell biology* **189**, 813-827.

Yoshimoto, H., Saltsman, K., Gasch, A.P., Li, H.X., Ogawa, N., Botstein, D., Brown, P.O., and Cyert, M.S. (2002). Genome-wide analysis of gene expression regulated by the calcineurin/Crz1p signaling pathway in *Saccharomyces cerevisiae*. *The Journal of biological chemistry* **277**, 31079-31088.

Zayat, V., Balcerak, A., Korczynski, J., Trebinska, A., Wysocki, J., Sarnowska, E., Chmielarczyk, M., Macech, E., Konopinski, R., Dziembowska, M., *et al.* (2015). HAX-1: a novel p-body protein. *DNA and cell biology* **34**, 43-54.

Zeiner, G.M., Cleary, M.D., Fouts, A.E., Meiring, C.D., Mocarski, E.S., and Boothroyd, J.C. (2008). RNA analysis by biosynthetic tagging using 4-thiouracil and uracil phosphoribosyltransferase. *Methods in molecular biology* **419**, 135-146.

Zeitelhofer, M., Karra, D., Macchi, P., Tolino, M., Thomas, S., Schwarz, M., Kiebler, M., and Dahm, R. (2008). Dynamic interaction between P-bodies and transport ribonucleoprotein particles in dendrites of mature hippocampal neurons. *The Journal of neuroscience : the official journal of the Society for Neuroscience* **28**, 7555-7562.

Zenklusen, D., Larson, D.R., and Singer, R.H. (2008). Single-RNA counting reveals alternative modes of gene expression in yeast. *Nat Struct Mol Biol* *15*, 1263-1271.

Zenklusen, D., Wells, A.L., Condeelis, J.S., and Singer, R.H. (2007). Imaging real-time gene expression in living yeast. *CSH Protoc* *2007*, pdb prot4870.

Zheng, D., Ezzeddine, N., Chen, C.Y., Zhu, W., He, X., and Shyu, A.B. (2008). Deadenylation is prerequisite for P-body formation and mRNA decay in mammalian cells. *The Journal of cell biology* *182*, 89-101.

5.4 Acknowledgments

First and foremost, I would like to thank my supervisor Prof. Anne Spang for giving me the opportunity to conduct my PhD in her lab. I am very grateful for her guidance and support that I received throughout the years.

I am also very grateful to the members of my thesis committee, Prof. Ralf Jansen and Prof. Mihaela Zavolan for their time and valuable suggestions.

I would like to acknowledge our collaborators Prof. Niko Beerenwinkel and Fabian Schmich for the great computational support for my project.

I want to thank Julie Weidner and Cornelia Kilchert for introducing me into the RNA field, for their valuable advice, and for developing methods which laid the foundations for my work.

For the critical and careful reading of my thesis and manuscript, I am very grateful to Thomas Gross.

Besides those mentioned above, I wish to express my thanks to all present and past members of the Spang lab for all the help, discussions, ideas, and extra-lab activities: Benjamin Abitbol, Karin Ackema, Florian Baier, Ivana Bratic Hench, Carla Cadena del Castillo, Melanie Diefenbacher, Alejandra Fernandez Belmonte, Alejandro Fernandez-Estrada, Thomas Gross, Stefan Hümmer, Martina Huranova, Cornelia Kilchert, Heidi Mergentaler, Gopinath Muruganandam, Maria Podinovskaya, Sabine Probst, Uli Rockenbauch, Alicia Siliezar, Jachen Solinger, Timo Stahl, Julia Stevens, Claudia Stohrer, Diego Stohrer, Akshay Subramanian and Lukas Thiel and Kiril Tishinov. I feel very privileged working with these talented scientists.

Also, I would like to express my gratitude to the people working on the technical, administrative staff of the 5th floor and core facilities of the Biozentrum, in particular the imaging core facility and quantitative genomics facility for all the supports.

Special thank goes to “Fellowship for Excellence” for funding my PhD study.

Last but not least, a very big thank goes to my family and friends for being patient, for always understanding, and for supporting me through these years. Without them I would not have been able to accomplish any of this.

5.5 Curriculum Vitae

CONGWEI WANG

Date of birth: 24.09.1986

Nationality: Chinese

Address: Steinengraben 2, 4051 Basel, Switzerland

Email: congwei.wang@unibas.ch

EDUCATION

2011 – 2016 Ph.D. in Cell Biology | Focal area Growth and Development

Biozentrum, University of Basel, Basel, Switzerland

2009 – 2010 M.Sc. in Molecular Biology | International Max Planck Research school (IMPRS)

University of Goettingen, Goettingen, Germany

2007 – 2008 Exchange student | The Interfaculty Institute of Biochemistry (IFIB)

University of Tuebingen, Tuebingen, Germany

2004 – 2008 B.Sc. Bioscience | College of Life Science

Capital Normal University, Beijing, China

FURTHER TRAINING AND WORKSHOPS

2016 Applied Statistics using R

University Hospital of Basel, Basel, Switzerland

2014 qPCR Essentials Training

Biozentrum, Basel, Switzerland

2013 Next Generation Sequencing Workshop

EMBL-EBI, Hinxton, UK

FELLOWSHIPS AND HONORS

2011 - 2015 Fellowships for Excellence by Werner Siemens-Foundation

2013 ALLBIO Bioinformatics Travel Bursary Grant

2009 – 2010 Stipend of the Excellence Foundation for the Promotion of the Max Planck Society

2007 – 2008 Stipend of DAAD International Study and Training Partnerships (ISAP)

PUBLICATIONS

Wang, C., Schmich, F., Beerenwinkel, N., Weidner, J., and Spang, A. (2016). To be, or not to be: Context-dependent deposition and regulation of mRNAs in P-bodies. *Submitted*.

Weidner, J., Wang, C., Prescianotto-Baschong, C., Estrada, A.F., and Spang, A. (2014). The polysome-associated proteins Scp160 and Bfr1 prevent P body formation under normal growth conditions. *J Cell Sci* 127, 1992-2004.

Burmann, B.M., Wang, C., and Hiller, S. (2013). Conformation and dynamics of the periplasmic membrane-protein-chaperone complexes OmpX-Skp and tOmpA-Skp. *Nature structural & molecular biology* 20, 1265-1272.